UNIVERSITAT DE BARCELONA

Explaining and reducing variability of distribution coefficients of radionuclides in soils: improvement of input data for radiological assessments

Josep Oriol Ramírez Guinart

EXPLAINING AND REDUCING VARIABILITY OF DISTRIBUTION COEFFICIENTS OF RADIONUCLIDES IN SOILS: IMPROVEMENT OF INPUT DATA FOR RADIOLOGICAL ASSESSMENTS

Josep Oriol Ramírez Guinart

UNIVERSITAT DE BARCELONA

Programa de doctorat

Química Analítica del Medi Ambient i la Pol·lució

Tesi Doctoral

EXPLAINING AND REDUCING VARIABILITY OF DISTRIBUTION COEFFICIENTS OF RADIONUCLIDES IN SOILS: IMPROVEMENT OF INPUT DATA FOR RADIOLOGICAL ASSESSMENTS

Memòria presentada per:

Josep Oriol Ramírez Guinart

Direcció:

Dr. Miquel Vidal Espinar

Catedràtic del Departament d'Enginyeria Química i Química Analítica, Secció de Química Analítica, de la Universitat de Barcelona

Dra. Anna Rigol Parera

Professora Titular del Departament d'Enginyeria Química i Química Analítica, Secció de Química Analítica, de la Universitat de Barcelona

El Dr. Miquel Vidal Espinar, Catedràtic, i la Dra. Anna Rigol Parera, Professora Titular, del Departament d'Enginyeria Química i Química Analítica, Secció de Química Analítica, de la Universitat de Barcelona,

FAN CONSTAR

que el present treball d'investigació que porta per títol:

EXPLAINING AND REDUCING VARIABILITY OF DISTRIBUTION COEFFICIENTS OF RADIONUCLIDES IN SOILS: IMPROVEMENT OF INPUT DATA FOR RADIOLOGICAL ASSESSMENTS

ha estat realitat sota la seva direcció per en Josep Oriol Ramírez Guinart per optar al Títol de Doctor per la Universitat de Barcelona.

Barcelona, maig de 2017

Dr. Miquel Vidal Espinar Dra. Anna Rigol Parera

"Choose life.
Choose a job. Choose a career.
Choose a family. Choose a big television.
Choose washing machines, cars, compact disc players, and electrical tin can openers.
Choose good health, low cholesterol and dental insurance.
Choose fixed-interest mortgage repayments.
Choose a starter home. Choose your friends.
Choose leisure wear and matching luggage.
Choose a three piece suite on hire purchase in a range of fabrics.
Choose DIY and wondering who you are on a Sunday morning.
Choose sitting on that couch watching mind-numbing spirit-crushing game shows, stuffing junk food into your mouth.
Choose rotting away at the end of it all, pishing your last in a miserable home, nothing more than an embarrassment to the selfish, fucked-up brats you have spawned to replace yourself.
Choose your future. Choose life . . . "

Renton's speech in Trainspotting (1996)

"Choose life.
Choose Facebook, Twitter, Instagram and hope that someone, somewhere cares.
Choose looking up old flames, wishing you'd done it all differently.
And choose watching history repeat itself.
Choose your future.
Choose reality TV, slut shaming, revenge porn.
Choose a zero hour contract, a two hour journey to work.
And choose the same for your kids, only worse, and smother the pain with an unknown dose of an unknown drug made in somebody's kitchen.
And then… take a deep breath.
You're an addict, so be addicted.
Just be addicted to something else.
Choose the ones you love.
Choose your future.
Choose life."

Renton's speech in T2: Trainspotting (2017)

"El esfuerzo inútil conduce a la melancolía."

José Ortega y Gasset

TABLE OF CONTENTS

CHAPTER 1. INTRODUCTION

1.1 ENVIRONMENTAL RADIOACTIVITY

1.1.1 Radioactivity and related concepts

Radioactivity is the emission of radiation originating from a nuclear reaction or as a result of the spontaneous decay of nuclei that are unstable due to a neutron to proton ratio (N:Z) higher or lower than the value corresponding to the band of nuclear stability. For light elements the stable nuclides present N = Z, whereas for heavier elements the N:Z ratio tends to 1.5. **Figure 1.1** shows the band of nuclear stability (in black) as well as the most likely types of nuclear processes by which unstable atomic nuclei disintegrate according to their N:Z ratio to reach a more stable state, termed as radioactivity decay.

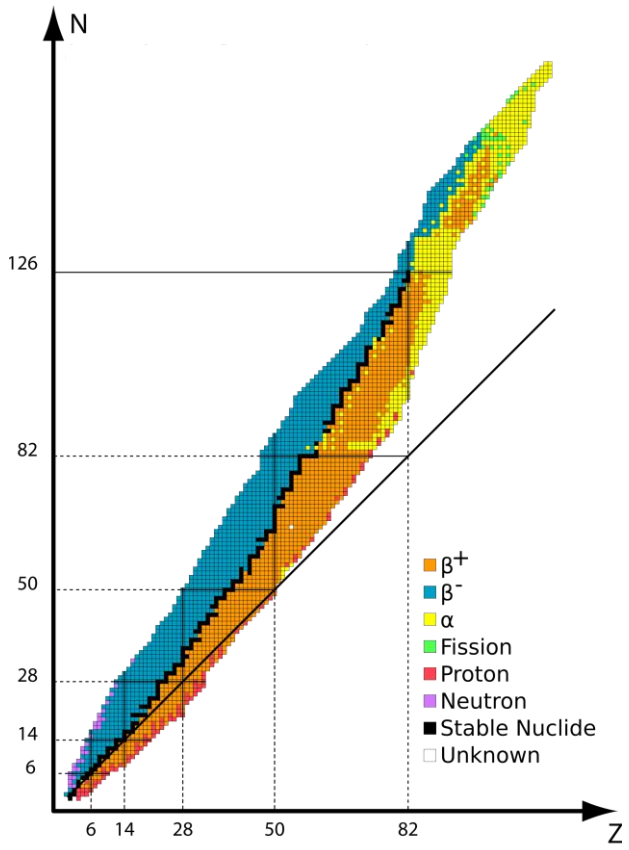

Figure 1.1 *Radioactive decay processes leading to nuclear stability (Chemistry Libretext, 2017).*

Radioactive decay entails the emission of elementary particles with high kinetic energy or photons with very short wavelength. This emission can originate directly from the nucleus (*e.g.,* alpha particles, beta particles, neutrons or gamma-ray photons), or from the atomic electron shells within which the nucleus resides (*e.g.,*

Auger electrons and X-ray photons). Isotopes undergoing radioactive decay are called radioisotopes or radionuclides (RNs). Most RNs do not decay directly to a stable state, but rather undergo a series of decays (decay chain or cascade) until eventually a stable isotope is reached. Isotopes among a decay chain are referred to by their relationship to previous or subsequent decay stages. The RN that undergoes decay is called parent isotope, whereas the formed one is called daughter isotope. The term progeny accounts for all the daughter nuclides that are generated from a parent radioisotope through a decay chain.

The particles and photons emitted by RNs when disintegrate are known as ionising radiations since cause ionisation of atoms and molecules of the matter they interact with. **Figure 1.2** shows the penetrating power of the different types of ionising radiations described thereupon.

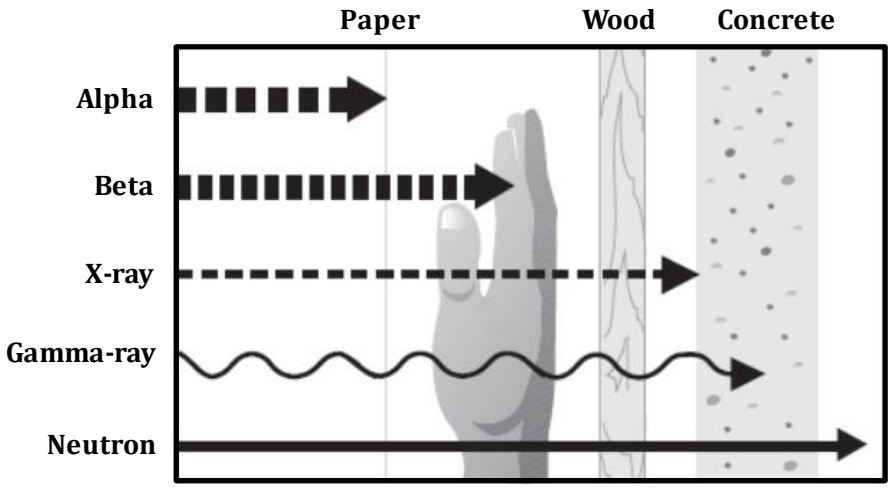

Figure 1.2 *Penetrating power of main ionising radiations (From NUREG, 2000).*

Alpha radiation (α) consists of the emission of $^{4}_{2}$He nucleus by isotopes with a large excess of protons. Due to their nature (heavy and charged), when emitted α-particles interact with matter release a high amount of energy of per unit of decay track length, *i.e.*, they present a high linear energy transfer (LET). Consequently, α-particles possess a high specific ionisation power whereas their decay tracks are very short (*e.g.*, few centimetres of air or a sheet of paper is enough to stop α-particles).

Beta radiation (β) can occur in nucleus with excess of protons or neutrons, either by a neutron decay into a proton (β-minus) or *vice-versa* (β-plus), depending upon which process would lead to the most stable nucleus, as depicted in **Figure 1.3**. In β-minus decay, a neutron splits into a proton, an electron and an antineutrino (a particle lacking of charge and mass). While the new proton is retained in the nuclei, the electron and ν particles are emitted. In β-plus decay, a proton is split into a neutron, a positron, which is considered the antiparticle of the electron, and a neutrino (ν). In this case, the new neutron is retained in the nuclei, whereas the positron and ν particles are emitted. In comparison with α-particles, the emitted β-particles (positron and electron) have lower LET as a consequence of their lower charge and mass, which results in a lower specific ionisation power but higher decay tracks (higher penetration power through matter), being necessary some millimetres of heavy materials to stop them.

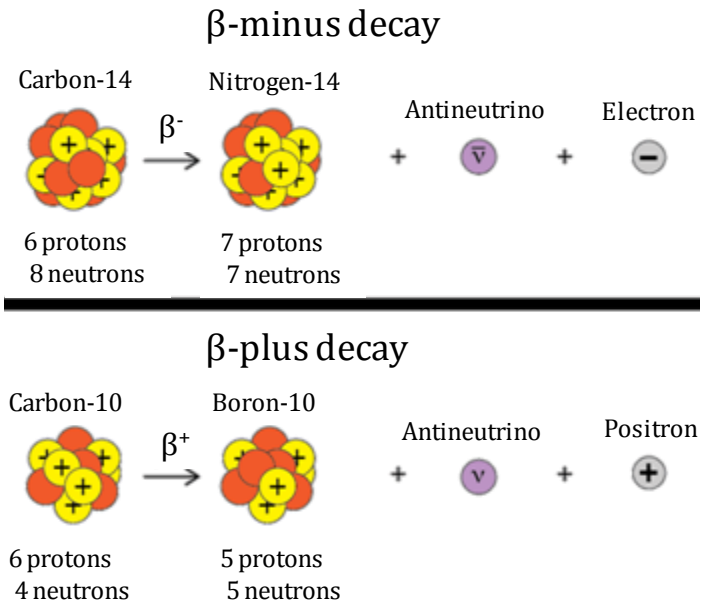

Figure 1.3 *Examples of beta-minus and beta-plus disintegration reactions undergone by ^{14}C and ^{10}C radioisotopes.*

The emission of α and β particles during the radioactive decay usually provokes a promotion of the nucleus of the RN atoms to excited states. The exited nuclei are very unstable and tend to undergo relaxing processes to reach a more stable state. The most common relaxing mechanism to release the excess of energy is a nuclear transition that entails the emission of electromagnetic radiation with extremely high

frequency, called gamma-rays (γ). Due to the electromagnetic nature of γ-rays (lack of mass and charge) they have a much more penetrating power than α and β particles, being necessary many centimetres of heavy materials like lead or many meters of concrete to attenuate them, whereas the specific ionisation of γ-rays is much lower than those of α and β particles due to their low LET. When nuclear transitions of excited atoms are prohibited, the alternative relaxing mechanism is based on a process by which the excess of energy is transferred from the nucleus to the electron shell, called internal conversion. As a consequence of this energy transfer, electrons close to the nucleus (high-energy electrons) may be emitted (Auger electrons) and the generated holes are subsequently filled by electrons from an upper orbital, which also involves the emission of high-frequency photons (X-rays). Although X-rays are less energetic (lower frequency) than γ-rays, they can also penetrate through most of the organs and tissues of living organisms.

Those RNs with excess of protons may also disintegrate by electron capture alternatively to β-plus, a process in which a proton is transformed into a neutron by absorbing an electron of an inner atomic (K or L) shell. The generated electron vacant is replaced by electrons from outer shells, which cause the emission of characteristic X-rays. Following electron capture, the daughter nuclides are frequently in an excited state and nuclear de-excitation takes place either by emitting γ-rays or by undergoing internal conversion with the subsequent emission of Auger electrons and/or X-rays.

Finally, isotopes of elements with atomic masses greater than 92 (heavy nuclides) may undergo spontaneous nuclear fission, that is nucleus breakdown into two nearly equal fragments (lighter nuclei called fission-products) along with the emission of free neutrons and the release of a large amount of energy. Because neutrons are uncharged particles, they are barely attenuated when interact with matter and thus, are more penetrating than alpha, beta and even gamma radiation, but they are stopped by materials rich in hydrogen bounds such as water. Neutrons are indirect ionising radiation since they may be eventually absorbed by certain nuclei, which, in turn, cause their excitement and subsequent gamma radiation emission.

The radioactivity decay, regardless of the type, is a random phenomenon devoid of any external influence (*e.g.*, temperature, pressure, etc.). The probability of a certain radionuclide (RN) to decay is only proportional to the time interval contemplated.

The constant of proportionality, called decay constant (λ), is specific for each RN and accounts for the probability of a given nucleus undergoing a spontaneous nuclear transition to decay per unit of time ($[\lambda] = s^{-1}$). The decay rate of a certain RN is a first order decay process, which means it follows an exponential decay pattern and the temporary evolution of the RN atoms is described by the fundamental radioactive decay law:

$$N_{(t)} = N_{(0)}\, e^{-\lambda t} \qquad [1.1]$$

where

$N_{(t)}$ is the number of RN atoms at time t ($t > 0$).

$N_{(0)}$ is the number of RN atoms at $t = 0$.

The time required to decrease the number of atoms for a given RN by half, due to a radioactive decay process, is referred as the RN half-life ($t_{1/2}$) and it is directly related to the decay constant by the expression $t_{1/2} = \ln 2/\lambda$. Depending on the RN, the $t_{1/2}$ constant can vary from a small fraction of a second (short-lived RNs, such as ^{220}Rn) to millions of years (long-lived RNs, such as ^{232}Th). The RN mean-life (τ) corresponds to the mean amount of time required for RN atoms to decay which is also related to the decay constant by the expression $\tau = 1/\lambda$.

In view that it does not exist a practical method to measure the number of RN atoms, the RN activity (A), a magnitude defined as the average number of disintegrations of RN atoms per unit of time and easier to measure, is taken as a reference. For a group of RN atoms (N) with a decay constant (λ), the activity corresponds to: $A = \lambda N$, and thus, Eq. 1.1 can be rearranged as follows:

$$A_{(t)} = A_{(0)}\, e^{-\lambda t} \qquad [1.2]$$

The activity in a radioactive sample can be determined by measuring the particles and/or photons emitted by RN atoms when disintegrate, and its unit in the International System is the Becquerel (Bq), which corresponds to one disintegration per second (dps). When the activity is very high it is also used the former unit Curie (C_i), which corresponds to the activity of 1g of ^{226}Ra isotope ($1\ C_i = 3.7 \times 10^{10}$ Bq).

1.1.2 Environmental background radiation

Radioactivity is present on Earth since its formation and thus, ionising radiation has been always in the environment. At present, the majority of background radioactivity occurs naturally, *e.g.* RNs are present in minerals of rocks and soils, water sources and living organisms, whereas a small fraction comes from man-made elements and human activities. Although environmental radioactivity varies only within narrow limits in most places on Earth, there are some localities with large variances in natural background namely due to abnormally high concentrations of radioactive minerals in surface soils, or certain places where environmental background can be enhanced or changed over time due to natural processes and/or human activities.

1.1.2.1 Natural radioactivity sources

Natural radioactivity originates from extraterrestrial sources as well as from RNs in the Earth's crust and atmosphere. On the one hand, Earth's outer atmosphere is continually bombarded by cosmic radiation consisting of fast moving particles that exist in space (Shabazi-Gahrouei et al., 2013). Cosmic radiation is attenuated as they pass through the atmosphere due to the interaction with particles present on it, which makes that the cosmic radiation levels on Earth vary a lot depending on the altitude. On the other, naturally occurring radioisotopes present on Earth include three major categories: primordial RNs, secondary RNs and cosmogenic RNs. Primordial RNs are a group of radioisotopes that have existed since before the Earth creation. Currently, only those whose half-life is comparable to the age of universe are present on Earth. These RNs are estimated to be around 32 RNs. Apart from these, the vast majority of naturally occurring RNs are originated from radioactive decay of the primordial RNs (secondary RNs). Most of them results from the so-called four natural decay series, that is, they are the progeny of the primordial RNs ^{232}Th, ^{237}Np, ^{235}U and ^{238}U. Finally, cosmogenic RNs relate to a number of 22 radioisotopes of a series of elements (H, Be, C, F, Na, Mg, Si, P, S, Cl, Ar, and I) that exist on the surface of the Earth and in the atmosphere due to the interaction of cosmic rays with atmospheric nuclei (Thorne, 2003).

1.1.2.2 Anthropogenic radioactivity sources

Mankind has learnt to artificially create RNs and to use them for a wide variety of purposes in medical, commercial and industrial activities. For instance, RNs are used in medical diagnosis and treatment (nuclear medicine), research at different disciplines such as biomedical, genetics or pharmaceutical, weapon creation, devices production, agriculture, industrial processes control or energy generation (nuclear energy) (Martin and Thomas, 1990; NUREG, 2000). Besides the generation and application of artificially created RNs, some industrial practices involving natural resources, such as water treatment, coal and geothermal energy production, mining activities, oil and gas production, phosphate industry or nuclear fuel production, tend to concentrate naturally occurring RNs, which lead to the so-called technologically enhanced naturally occurring radioactive materials (TENORM), that can easily enhance the radiation receiving people from natural RNs.

Anthropogenic sources of radioactivity generally do not significantly contribute to total environmental background and can be controlled more readily than most natural ones. However, these sources can vary greatly, much more than naturally sources do, as a result of voluntary actions and, particularly, when accidents happen. Consequently, most people receive relatively small amount of radiation coming from anthropogenic sources, whereas a few ones may get many thousands times the amount they receive from natural sources, for instance due to medical diagnosis and therapy or due to exposure to areas affected by fallout from past nuclear explosions and nuclear disasters.

1.1.3 Management and disposal of radioactive wastes

Radioactive waste is an unavoidable by-product when nuclear technologies are used for electricity production and for beneficial practices in medicine, agriculture, research and industry. Some radioactive waste may contain high amounts of RNs and, thus, may have significant levels of radiotoxicity. Moreover, RNs occurring in some radioactive waste may have long half-lives, which entails that the time scale for the radioactivity of such waste to decrease to levels that are considered non-hazardous (clearance level) will be of several thousands of years. Thus, the management and

disposal of radioactive waste is one of the most challenging environmental problems, difficult to solve, which requires the isolation of radioactive waste in the environment so as to kept it away from living organisms until it may not pose unacceptable risks.

When the radioactivity of the waste is above a certain threshold, the waste requires special disposal methods. Standards and approaches have been developed for a safe preparation of the radioactive waste for its eventual disposal (IAEA, 1992; IAEA, 2001; IAEA, 2002). Thus, once radioactive waste is generated; it undergoes a number of management treatment steps to transform it into a safe, stable and manageable form suitable for transport, storage and disposal.

Radioactive waste must be characterised to gain knowledge of its physical, chemical and radiological properties to identify appropriate safety requirements and potential treatment options, and to ensure compliance with accepted storage and disposal criteria. According to the waste characteristics, a series of treatment and conditioning activities are performed, which may include waste classification, volume reduction, partial RN removal from the waste, and often changes on its physical and chemical composition. Treated radioactive waste are then encapsulated or solidified in cement, bitumen or glass to facilitate handling and transport to storage facilities, as well as to slow the release of RNs from the disposed waste package into the environment. The storage requirements depend on the type of waste and may be a short term storage to allow for radioactive decay or a long term storage until the waste can be safely transferred to a suitable disposal site (IAEA, 2014a).

The appropriate disposal option and the extent of isolation and containment needed depend on the properties of the waste and the time period the waste remains radioactive. To this end, despite the physical and chemical heterogeneity in radioactive waste forms and characteristics, radioactive waste is divided into different categories according to the activity level and the half-life of the RNs present on it (IAEA, 2009) and disposal strategies are proposed on the basis of each radioactive waste category (IAEA, 2011). **Figure 1.4** summarises the different radioactive waste types contemplated and related final disposal requirements.

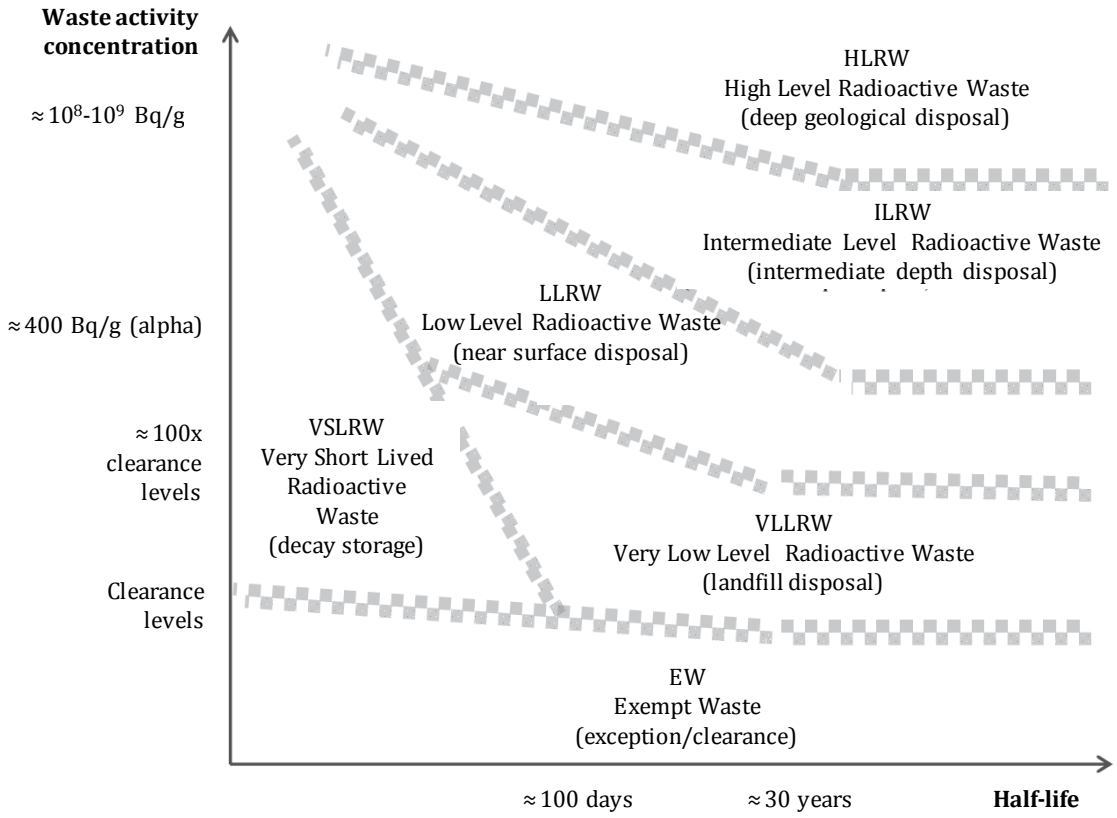

Figure 1.4 *Conceptual illustration of the waste classification scheme. Adapted from IAEA (2009).*

Among the different radioactive waste types, those whose radioactivity concentration is 100 times higher than the clearance level (the concentration activity to consider a waste as non-radioactive or exempt due to the low radiotoxicity) caused by long-lived RNs ($t_{1/2}$ > 30 years) (*i.e.*, namely, low intermediate and high level radioactive waste) require special facilities for their disposal over relevant periods of time.

- Low Level Radioactive Waste requires robust isolation and containment for periods of up to a few hundred years, and it can be disposed in engineered near surface facilities.

- Intermediate level radioactive waste requires disposal at greater depths, of the order of tens of meters to few hundred meters because of the quantity of alpha emitting long-lived RNs that it may contain.

- High level radioactive waste (HLRW) is of special concern since it may contain large amounts of long-lived RNs and high levels of activity concentration (10^4-10^6 TBq m^{-3}), thus requiring the design of suitable disposal facilities. There is an international agreement about their disposal in deep, stable geological formations, usually several hundred meters or more below the surface, that ensure its long-term isolation by means of a system of multiple engineered and natural (geosphere) barriers, known as the deep geological repository (DGR) concept (IAEA, 1990).

Despite the advances achieved for the safety disposal of radioactive waste, the management of HLRW is still challenging because DGR facilities are not yet available in all countries that generate them. In the meantime, HLRW are stored temporarily in storage buildings that provide radiation shielding or directly in the nuclear power plants. This situation may pose a threat to the environment and human health because under certain circumstances, such as in case of nuclear accident, significant releases of RNs can occur. According to this, it is crucial to be able to foresee the risk that could be arisen from an eventual contamination episode. To this end, among a series of different issues that will be explained in further sections, it is essential to have information of the composition of HLRW, *i.e*, an inventory of the different RNs occurring in such waste, which often is derived from the composition of the spent nuclear fuel (SNF). Although the composition of SNF varies according to the degree of burn-up, on average, the main species expected to be found are those depicted in **Figure 1.5**.

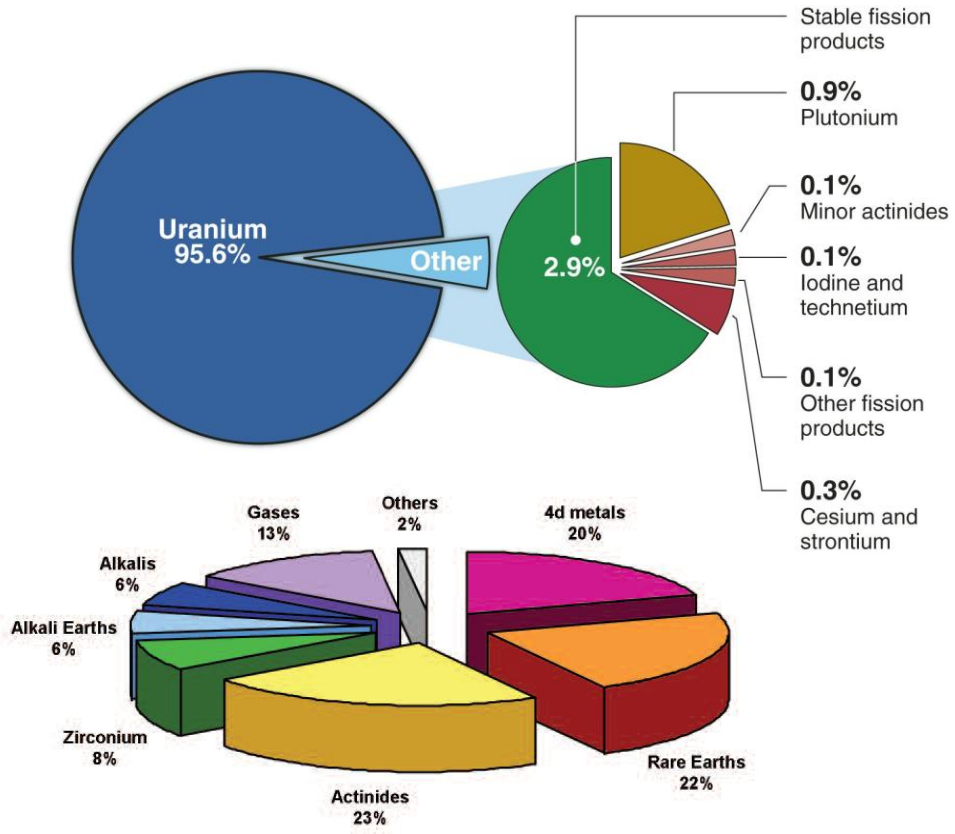

Figure 1.5 *Average composition of moderate burn-up spent nuclear fuel (up) and element families proportions of the major types of fission products and transuranium elements sorted by family of elements (down). Adapted from Buck et al. (2004).*

Most of the SNF corresponds to depleted U, whereas the rest is a mixture of a great number of fission products (*e.g.*, ^{90}Sr, ^{129}I, ^{131}I, ^{137}Cs, ^{151}Sm, etc.) and transuranium elements (*e.g.*, ^{239}Pu, ^{237}Np, ^{243}Am), being the actinides and the rare earths those that account for a great percentage of the total species present in SNF (once excluded U species) (Buck et al., 2004). Despite the small proportion of fission products and, specially, of actinides, these RNs are specially relevant because they are responsible for the majority of the radiotoxicity and decay-derived heat in the short-term and the long-term, respectively (IPFM, 2011). According to this, it is of special importance to study the behaviour of actinide and lanthanides RNs in the environement, an issue covered in the present Thesis by means of a systematic study of the interaction with soils of two RNs representative for both families of elements.

1.2 RADIOLOGICAL DOSE AND RISK

1.2.1 The concept of radiological dose

Radiological dose is a measure of the energy deposited by ionising radiation in a target material. The act or condition of being subject to ionising radiation is termed as (radioactive) exposure. A radiological dose assessment calculates the amount of radiation energy that might be absorbed by a potentially exposed individual as a result of a specific exposure (ICRP, 2007).

Radiological dose to humans can be external or internal depending on whether the radiation source is located outside the body or within the body, respectively. External dose occurs due to exposure to RNs deposited on the body surface or to irradiation from RNs present in the environment, whereas internal dose occurs due to the ingestion, inhalation or cutaneous perfusion of RNs. As explained in section 1.1.1, alpha and beta particles have high ionising power but low penetrating power. In contrast, gamma-rays have very low ionising power but extremely high penetrating power. Therefore, external dose is primarily a concern for gamma radiation, since it is very unlikely that α - emitter and β-emitter RNs may enter directly in contact with living organisms' surface. Instead, internal dose is a concern for alpha and beta radiation, which may cause serious cell damage in internal parts of the body, as well as for gamma radiation, which may cause ionisations that damage tissues and DNA to the entire body of organisms. Besides this, doses caused by medical, occupational and public exposure are frequently distinguished.

The radiological dose can be localised to specific organs or distributed across the whole body. Consequently, radiological dose is measured and expressed in different units depending on the purpose. Absorbed dose describes the total amount of energy absorbed by an object or person and its unit is J kg^{-1}, termed as Gray (Gy). **Figure 1.6** shows, as an example, the average contributions of different radiation sources to absorbed dose of citizen in the USA (NCRP, 2009).

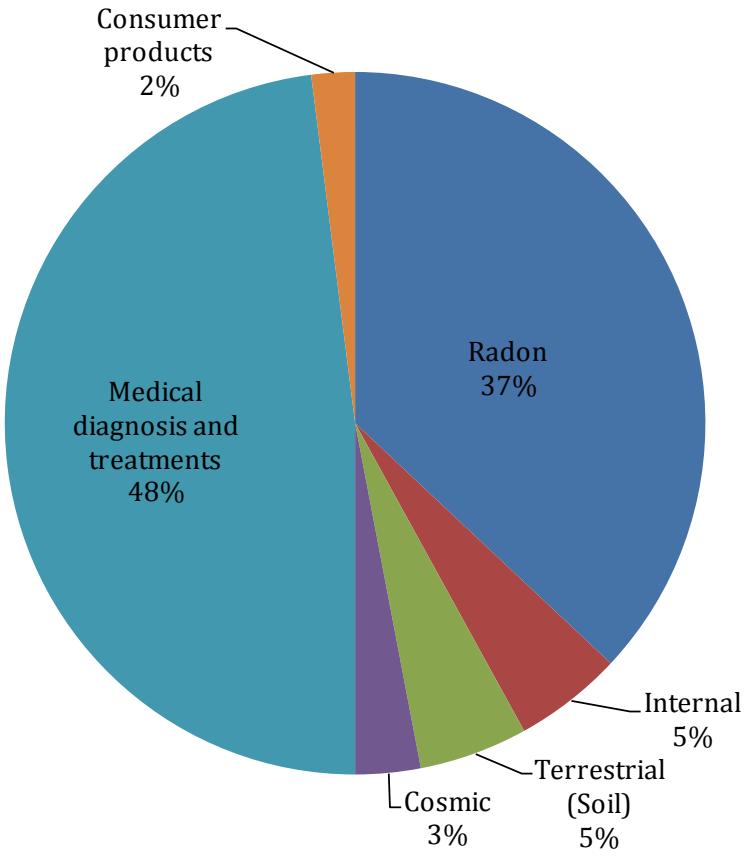

Figure 1.6 *Absorbed dose from ionising radiation exposure to the public (NCRP, 2009).*

On average, around half of the dose absorbed by individuals is due to natural radiation sources and half of it to man-made ones. The natural sources contributing to human dose may vary depending on the individuals' location (as explained before natural background radiation levels can largely vary from place to place) and on their habits, since they determine in a great extent the exposure level to them. However, most of the dose caused by natural radiation sources generally comes from exposure to radon, a gas originated from the Earth's crust that emanates from the ground, which is accumulated in buildings and eventually inhaled by humans, and to a much lesser extent from cosmic radiation and RNs present both in our internal body (*e.g.*, ^{40}K) and in the ground. Regarding radiological dose to humans due to anthropogenic radiation sources, the vast majority is caused due to medical exposure and a small fraction due to consumption, usage or manipulation of manufactured products that contain natural RNs. The contribution to the radiological dose to human due to industrial and occupational exposure is on average negligible (usually < 0.1% of dose).

On the other hand, two types of doses, equivalent dose and effective dose, are also defined to contemplate the risk arisen from radiological exposure. Equivalent dose is a measure of the biological damage to living tissue resulting from exposure. It is defined as the absorbed dose delivered by a given radiation type and its unit is Sievert (Sv). Radiation weighting factors are used to take into account different radiation effects and risks for the same energy absorption, depending on the radiation type (alpha, beta and gamma rays). Whereas effective dose, also expressed in Sv, represents the stochastic health risk to the whole body, which is the probability of detrimental effects. It is defined as the sum of the equivalent doses for the different tissues, each one multiplied by the appropriate tissue weighting factor, and accounts for the existing differences among tissues regarding their sensibility to radiation. Values of effective dose from any type of radiation and mode of exposure can be compared straightforwardly (ICRP, 2007).

1.2.2 Biological and health effects of radiation: from radiological dose to risk

The biological effects caused by exposure to ionising radiation are well understood. The detrimental effects of ionising radiation include the inducement of cancer (carcinogenesis), mutations in cells (mutagenesis) and birth defects (teratogenesis). Because radiation affects different people in different ways, it is not possible to say what dose is going to be fatal (UNSCEAR, 2000). In general, the amount and duration of radiation exposure affects the severity or type of health effect. The higher the radiation dose, the sooner the effects of radiation will appear, and the higher the probability of death (EPA, 1994, NRC, 2006).

Although there are no data to establish a firm link between cancer and low doses (below about 100 mSv) and despite knowing that low doses spread out over a long period would not cause an immediate problem and the effects, if any, would occur at the cell level, radiation protection guidelines traditionally are predicated on a linear dose response, which assumes that the harmful effects of radiation are linearly related to the dose and that there is no threshold dose. That is, radiological risk estimates are typically based on a model that assumes there is no level below which radiological doses are safe, which is considered to be conservative since it ignores the

potentially beneficial effects of the body's repair mechanisms and, thus, overestimates the effects of ionising radiation at low doses (Maurice, 2005).

Risk is defined as the probability of injury, disease or death from exposure to a hazard. Radiological risk generally refers to all excess cancers caused by radiation exposure (incidence risk or morbidity) or only excess fatal cancers (mortality risk or death) and it can be expressed in many ways. It can be stated in relative terms such as a ratio or percent of the risk in one exposure group to another or as the excess relative risk, that is, the difference between the observed relative risk and that expected in the absence of an effect. Risk can also be couched in absolute terms as the excess of number of occurrences of an effect above the number expected in the absence of exposure to other unnatural causes. Radiological dose can be converted to carcinogenic risk by applying radionuclide-specific dose-to-risk conversion coefficients to the effective dose that are identified by organisations, such as the International Commission on Radiological Protection (ICRP) and the United Nations Scientific Committee on the Effects of Atomic Radiation (UNSCEAR). These coefficients are the result of epidemiological studies and basic research throughout the world collected, assessed and assembled as radiation risks (Kim et al., 2016).

It is commonly accepted that efforts should be undertaken at all times to keep radiological doses “as low as reasonably achievable”, which is referred to as the ALARA principle or requirement. According to this, ICRP recommends specific regulatory standards for radiation protection, such as maximum permissible dose, based on radiation risks scientifically assessed, which take into consideration societal demands, ethics, and past experience in application of standards (ICRP, 2007). In turn, ICRP’s recommendations are incorporated in the international Basic Safety Standards of the International Atomic Energy Agency (IAEA) (IAEA, 2014b), as well as in national regulations of various countries, aiming at establishing recommended dose limits for both workers and the general public for different types of activities, towards ensuring a secure radiation environment in society by setting dose limitation requirements.

1.3 RADIOLOGICAL RISK ASSESSMENT

Radiological risk assessment accounts for the quantitative process of estimating the consequences to the environment and humans of the presence and/or release of RNs to the biosphere that probably may cause detrimental health effects over the lifetime of an exposed individual. Radiological risk assessment is divided into probabilistic risk assessment, where the risk is derived from a probabilistic analysis considering the occurring probability and consequences of a radioactive contamination event; real-time risk assessment, which aims at providing an input for emergence response through predicting risk and providing support for emergency response managers before accident releases, and over-event; and past accident consequence assessment, which entails the performance of risk assessment studies through retracing the transport of radioactive material for the historical releases (Rentai, 2011).

1.3.1 Requirements and applications of radiological risk assessments

Radiological risk assessment is an important tool used as a part of the decision-making process required by national regulators regarding nuclear-related activities. For instance, risk assessment is used for the performance of safety analysis of existing and planned nuclear facilities, which are compulsory and aim to predict the potential environmental impact arisen from their normal operation or in case of nuclear disaster.

When a radioactive contamination episode occurs, intervention objectives and actions are established according to the appropriate management and cleanup requirements that are based on the potential radiological risk (ITRC, 2002; ITRC, 2008). That is, remediation and decontamination strategies are planned on radiological risk basis to ensure that doses to future site users will be low enough, which involves making the proper actions (*e.g.*, do nothing, capping in place, excavation, burial, landfill, establishment of exclusion zones or control of radioactivity level in food stuffs). Besides this, radiological risk assessments are also used to set a series of preventive actions to ensure that radiation exposures are kept at safe and acceptable levels. Among these, operational controls such as time limitations and access controls to areas with relevant radiation levels, personal

protective equipment or radioactive waste requirements, as well as the proper design and operation of facilities devoted to radioactive waste treatment, storage and disposal, are crucial to ensure protection of workers and general public in the time during operation and in the post-closure of nuclear facilities. On the other, radiological assessments are widely used to estimate the effect arisen from radiological doses not only occurring at or near the time of the assessment, but also those expected to possibly occur in the future or occurred in the past, which include to estimate the effects of projected routine and accidental releases of RNs from nuclear facilities and the radiological dose reconstruction caused by past events. A particularly important use of radiological assessment is the rapid forecasting of doses resulted from nuclear disasters (Raskob et al., 2015). To this end, the potential accidents must be identified ahead of time and most of the information of radioactivity exposure pathways and target populations must be known in advance in order to enable the rapid identification and communication of potential risk to the public and thus, to manage a crisis situation efficiently. Finally, risk assessment is essential in addressing the uncertainty (sensitivity analyses) associated with key site parameters or to decide whether the available knowledge is enough to make reliable decisions or not (EPA, 2001).

The reliably determination of the adverse effects for humans, caused by the presence or release of RNs in the biosphere, requires that the radiological risk assessments covers all aspects, from the source term (radioactive release or contamination start point) to the estimation of the dose. To this end, it is essential to have quality data regarding a great variety of factors. This includes, for instance, to have suitable information related to the physical and chemical characteristics of the radioactive source material (*e.g.*, volume and containment of this material, specific RNs present, their chemical and physical form, their concentration, etc.); the configuration and location of the contaminated area (*e.g.*, distribution of the contamination, hydrologic and geologic characteristics of the contaminated area, meteorological conditions, population density around the affected site, etc.); and the exposure scenarios (*e.g.*, which target individuals, public and workers may be exposed; the nature of the workers' activities; the way by which members of the general public may be radiological exposed during remediation and following closure of the site; the potential future uses of the site; the possible environmental pathways and exposure

pathways, etc.). According to this, the assessment of the overall radiological risk for human health arisen from contamination events is a complex issue that implies to take into consideration the specific RNs released; their transport, bioaccumulation, and uptake by humans; and the doses resulting from the uptakes and exposure, as shown in **Figure 1.7**.

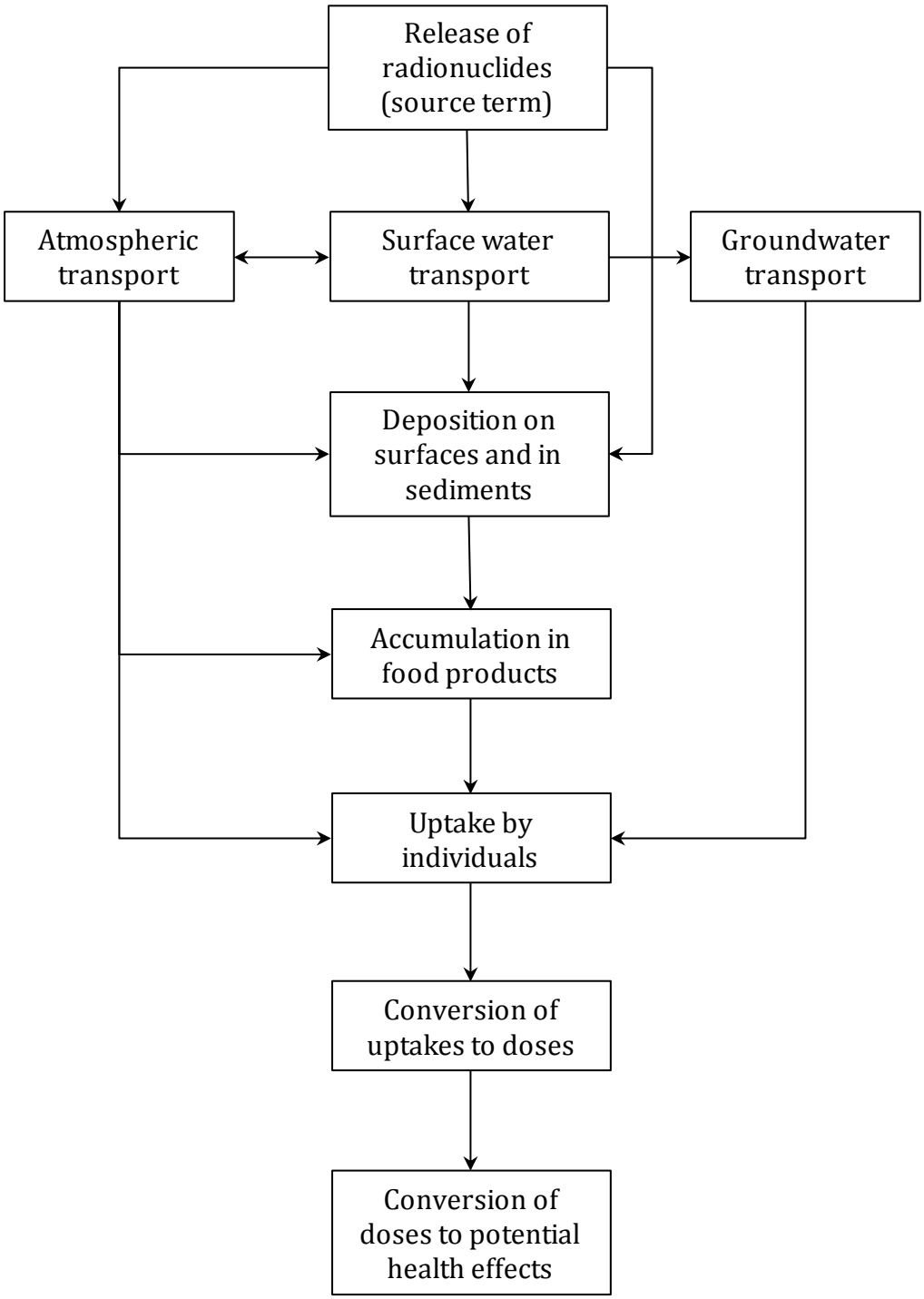

Figure 1.7 *Major steps in radiological assessment. Adapted from NCRP, 1984.*

In order to reliably estimate radiological doses to human and subsequent risk arisen from a contamination episode, it is crucial to be able to characterise and quantify the RNs released to the biosphere and, on the other, to assess the fate and transport of released RNs among the different environmental compartments According to the scope of the present Thesis, it is given special relevance to this latter issue and, particularly, to the analysis of the interaction and transport processes occurring in the terrestrial ecosystem, as it will be explained in following sections.

1.3.2 Environmental and exposure pathways analysis used to calculate radiological dose in risk assessment

The biosphere is commonly defined as the region of the Earth's surface and its atmosphere integrating all living beings and their relationships, including their interaction with the surroundings (Porteous, 2008; Vernadsky, 1998). The biosphere comprises the regolith, hydrological and subsurface hydrogeological systems, biota (including humans), and the overlying atmosphere. For the sake of simplicity, the biosphere is often divided into atmospheric, aquatic and terrestrial ecosystems according to where the communities of organisms are placed.

Any route of transport by which a RN can travel from its release site to human populations, including air, food chain, and water, is called environmental pathway. On the other hand, an exposure pathway refers to the way a person can come into contact with a hazardous substance. There are three basic exposure pathways: inhalation, ingestion, or direct contact. Human exposure may entail very simple environmental pathways, for instance, external exposure from airborne RNs transported to the surface or vicinity of the target individual directly by air, or from much more complex pathways, such as internal exposure from drinking milk from cows that ate grass contaminated with deposited RNs. Therefore, it is likely that some environmental pathways may cross between the different ecosystems. For example, water from a river containing radioactive materials may be used for irrigation of crops, thereby entering the terrestrial ecosystem. Similarly, radioactive materials sorbed onto soil may be washed off into a river, pass through an estuary, and eventually be incorporated in the ocean, thereby involving all four ecosystems. As an

example, **Figure 1.8** schematically shows the environmental pathways analysis considered to assess the risk derived from a soil radioactive contamination.

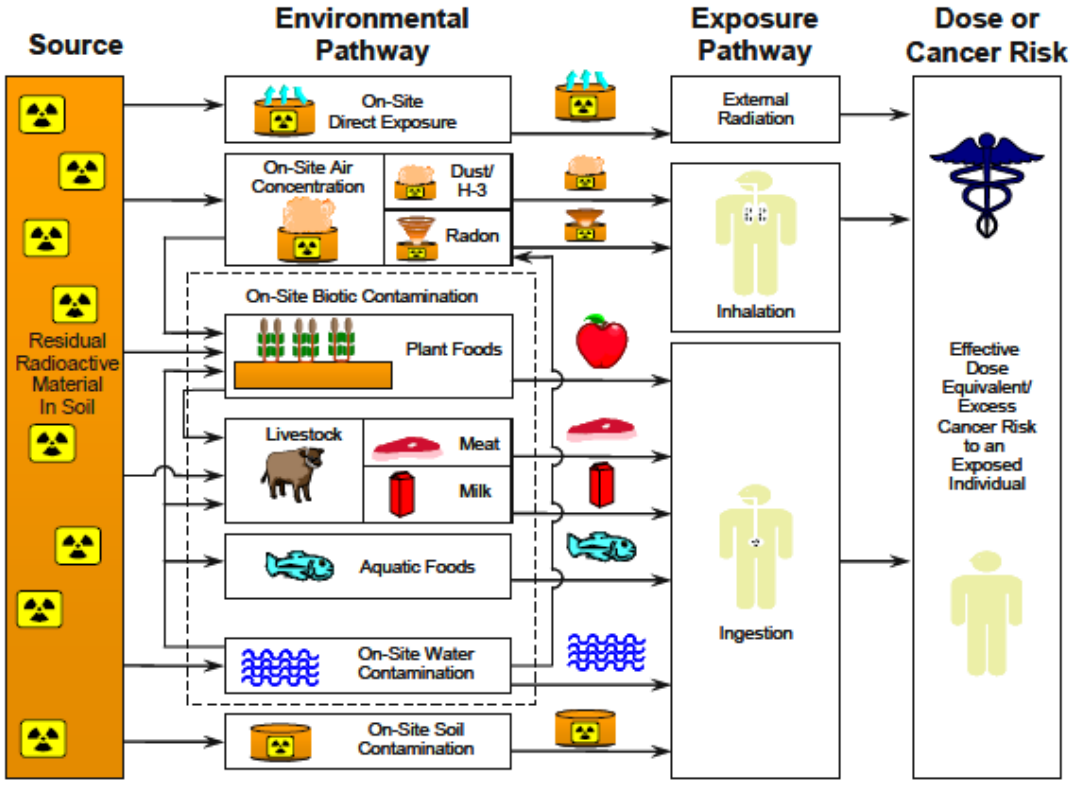

Figure 1.8 *Schematic diagram to analyse the radiological exposure pathways causing risk to humans. From Yu et al. (2001).*

As can be seen in the scheme, a large number of processes and complex interactions occur in the biosphere which requires having an interdisciplinary knowledge to elucidate which ones significantly influence the transport and accumulation of RNs in the environment, and thus, that must be taken into account in the assessment. Due to this complexity and because data of certain key parameters related to the fate and transport of RNs are frequently sparse, or even unavailable, radiological risk assessment in most cases is performed my means of using models.

Ecosystems are frequently divided into different non-living (abiotic) systems (*e.g.*, air, water and solid material) and living systems (biotic) systems (*e.g.*, flora and fauna including man), called environmental compartments or components to enable the analysis of the processes and equilibria taking place along an environmental pathway (Duursma and Carroll, 1996). There are different kinds of processes acting in the

biosphere that are important for the fate and transport of RNs and, eventually, for the human exposure to radiation. On the one hand, transport processes (*e.g.,* convection, deposition, interception, etc.) whereby elements and substances are transported from one point to another in an ecosystem can have a large effect on where RNs end up or if they are transported out of the examined ecosystem. These type of processes determines in a great extent the pool of RNs present in a given environmental compartment arisen from a given contamination episode. On the other, chemical, mechanical and physical processes that influence the state of RNs present in a given environmental compartment are essential to determine their transport and bioavailability in the aftermath of a radioactive contamination. Among these, the chemical reactions governing the RN speciation as well as the sorption/desorption processes of RN species in porous media such as soils and sediments, are of paramount importance. These processes, determine in a great extent whether a given RN may be barely mobile, for instance because of being tightly bound to solid particles, or may be easily dissolved and transported by water, as well as whether it can be taken up by organisms or not. As it will be explained in following sections, the sorption and desorption of RNs soils are relevant processes to be parameterised in risk assessment since they play a key role in the introduction of RNs into the food-chain and contamination of water sources, which are two main environmental pathways leading to human exposure to RNs.

1.3.3 Considerations of radiological risk assessments involving the terrestrial ecosystem

The terrestrial ecosystem is the most important concerning the potential radiological exposure and risk to humans, not only because human beings reside within this ecosystem, but also because a significant portion of human food comes also from terrestrial sources. Radioactive materials can enter the terrestrial ecosystem in a variety of ways, from the atmosphere through deposition, from water used for irrigation, or from soil contaminated by ground water or deposited RNs. Some exposure pathways are direct (*e.g.*, inhalation, transpiration, external irradiation from airborne materials, and external irradiation from radioactive materials contained within buildings or storage tanks) and, thus, radiation doses from these sources can

be estimated straightforwardly for instance from atmospheric diffusion calculations, shielding calculations and knowledge of occupancy factors or inhalation rates. Conversely, other exposure pathways relevant in the terrestrial ecosystems, such as consumption of contaminated water and food-stuff are much more complex to evaluate since different transport processes may lead to the accumulation of RNs in a certain environmental medium, which makes that the concentration of RNs may be much higher in some terrestrial compartments than that in air or water at the point of release (NUREG, 1983). The principal processes leading to RN accumulation in the terrestrial ecosystem are schematically summarised in **Figure 1.9**.

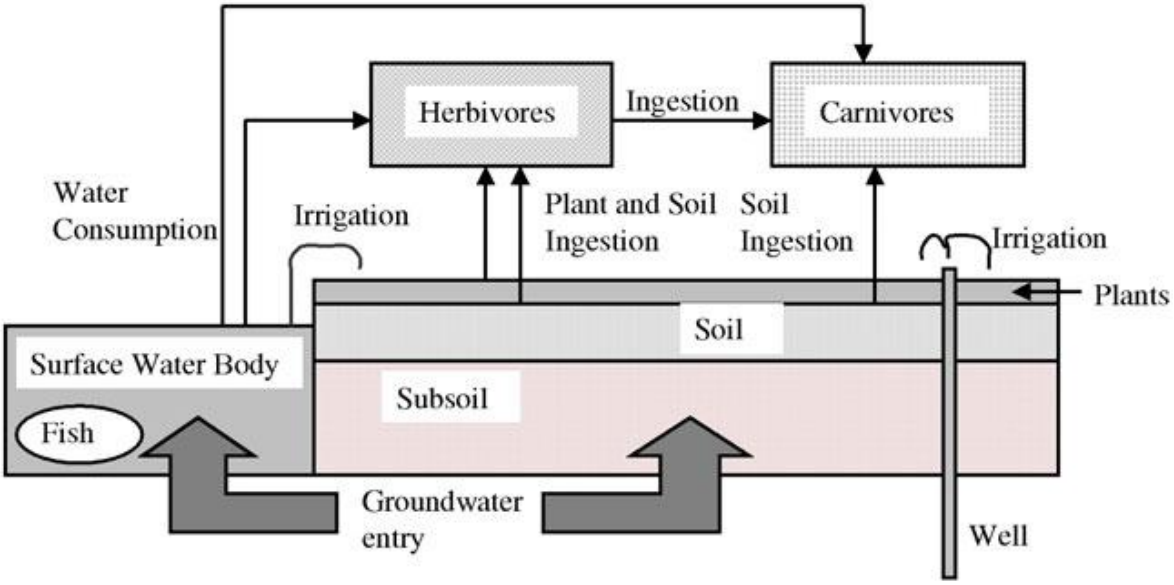

Figure 1.9 *RN transfers leading to accumulation in a temperate terrestrial ecosystem. From Thorne et al. (2002).*

RNs may enter the soil from surface deposits (dry and wet atmospheric deposition) and with irrigation water and subsequently a fraction may be lost from soil surface, by runoff, and from the rooting zone, by infiltration into deeper soil strata and by radioactive decay. Besides, a fraction of RNs may be accumulated in soils, transferred from the soil to plants and introduced into the food chain. Herbivore animals may be contaminated through the consumption of plants, soil and drinking water containing RNs and, in turn, carnivores animals through the consumption of contaminated herbivores and drinking water (Thorne et al., 2002). As a result of this series of processes radioactive materials may be incorporated in vegetal products as well as in animal products such as meat, milk and eggs, which are eventually consumed by humans. Because of this, it is of primary importance to estimate the long-term

radioactive contamination of food crops and animal feeds. To this end, the estimation not only of the RN concentration in the soil layer equivalent to the depth of plant root penetration, but also the RN mobility and bioavailability in this environmental compartment is of principal interest (NUREG, 1983).

There are several mechanisms that can result in the contamination of vegetation by radioactive materials, which in turn, are influenced by numerous biophysical and biochemical processes. In brief, external surface contamination in vegetation occurs as a result of aerial deposition and surface adsorption of radioactive materials, which namely involves physical processes, and it is the primary mechanism for contamination of food and feed crops by short-lived RNs when there is a continuing source of effluent release. On the other hand, internal contamination of plants occurs primarily from biological uptake of RNs from the soil solution through roots. Plant uptake of RNs from soils is regulated by biological and chemical mechanisms related to plant physiology (*e.g.*, plant species and internal RN translocation) and RN availability in soils. Among the latter ones, the physical and chemical form of a RNs as well as the soil characteristics can have a profound effect on the RN retention in soil, its mobility, its bioavailability and, thus, on its eventual uptake by plants.

1.3.4 Modelling transport of RNs between and within environmental compartments to assess radiological risk

Conceptual biosphere models are commonly used as an approach to schematically represent what is happening in nature. In such models, the different environmental compartments or components (model objects) of the studied scenario are usually represented with boxes that are interlinked with arrows indicating the interaction and processes (*e.g.*, reactions, equilibriums, energy or mass transfers, etc.) occurring among them. The conceptual model is frequently accompanied with a phenomenological Interaction Matrix (IM) to help in the understanding of the system dynamics (Velasco et al., 2006). The IM approach is used to identify important phenomena based on analysis of the interactions (*i.e.*, relationships and dependencies) between the biosphere components contemplated in the system under study aiming at providing a clear way of ensuring that each of the interactions can be

'mapped' into the assessment model, for instance to assess the radiological dose or risk to human. As models are merely representations of reality, any simplification and assumption inherent in their construction, implementation, and execution must be examined carefully through uncertainty and sensibility analysis of the results obtained when applying the model for a given purpose (Hinton et al., 2013; IAEA, 1989). As an example, **Figure 1.10** shows the conceptual model proposed by Liu and Cohen (2014) which summarises the environmental compartments and processes considered to analyse the RN transport pathways in the biosphere.

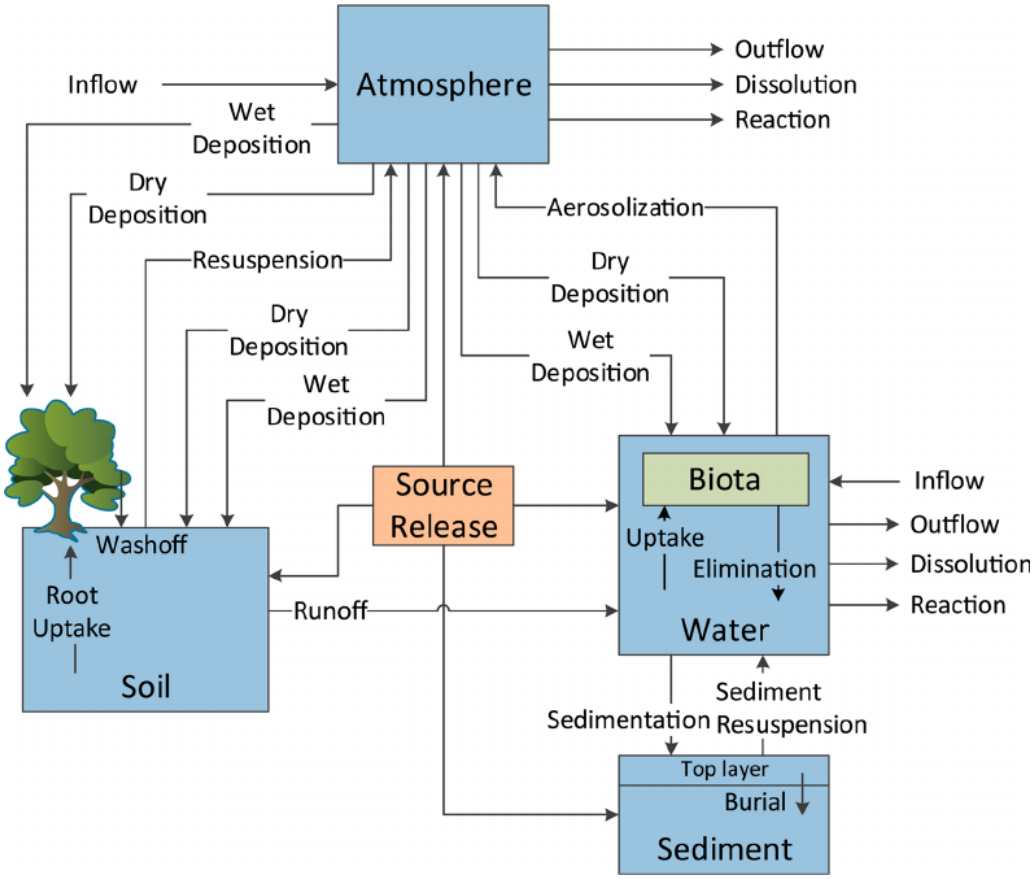

Figure 1.10 *Environmental compartments and intermedia transport processes in a multimedia environment conceptual model. From Liu and Cohen (2014).*

Once identified the key parts in a given system, mathematical models made of combinations of equations and parameters, usually formulated in computer codes, are extensively used to perform risk assessments. Such models are quantitative approximations of the processes that affect the transfer of radioactive substances in the environment. It does not exist a universal model that could be applied to assess

any risk arisen from all the existing or future scenarios. Instead, risk assessments models are created, or just adapted, to ensure that they fit for purpose. The main purposes of risk assessment models include to contribute to public confidence or to confidence of policy makers and scientific community, to guide research priorities, to demonstrate compliance with regulatory requirements, to help in regulatory development, to guide site selection and approval of later stages in repository development for radioactive waste disposal, to optimise a radioactive waste management system, or just to be a proof of concept (IAEA, 2003).

The model's complexity varies depending on the nature of the assessment question and the degree of resolution required to answer it. The more complex a model is, the more realistic may become, that is, the model may be a representation closer to the reality. However, the number of parameters required as input data increases with increasing its complexity, and thus, complex models have lower applicability than simple ones. Therefore, there is always a trade-off between developing models as realistic as possible and keeping them as useful as possible. Besides this, another important issue is the grade of flexibility of risk assessments models. Models developed aiming at performing site-specific assessments may succeed in trustworthy reproducing a certain scenario but may lack of versatility and, consequently, they may fail to assess the risk in other scenarios due to their low extrapolation capability. Currently, there are many several models and tools available devoted to assess the radiological dose and risk arisen from a great variety of contamination scenarios, exposure types and target individuals or group, such as RESRAD and TSD-DOSE (Argonne, USA), SimER and ReCLAIM (UK National Nuclear Laboratory, UK), SAFRAN (Facilia, Sweden) or ERICA (Center for Ecology and Hydrology, UK).

1.4 INTERACTION OF RNs IN SOILS

RNs in solution are likely transported to other environmental compartments and incorporated to the food chain and, thus, become potential contributors to human internal dose. Conversely, high RN affinity for binding and retention in the upper layers of soils may reduce their mobility which can lead to an enhancement of the external dose. As mentioned before, soil may act as a relevant sink of RNs in the terrestrial ecosystem and play a key role in the subsequent transfer to other environmental compartments and in the RN introduction into the food chain. In light of this, the study of the RN-soil interactions, *i.e.*, the elucidation of the mechanisms controlling how a RN is bound to solid phases and the estimation of RN incorporation and retention in the solid matrix, are crucial in radiological risk assessments involving terrestrial compartments. The examination and understanding of RN-soil interaction (*i.e.*, sorption degree and reversibility) is a rather complex issue since partition of dissolved RN ions between liquid and solid phases is controlled by numerous geochemical processes, with different relevancy in the overall RN-soil interaction according to the characteristics of the RN and of the system (soil and aqueous solution) under study.

1.4.1 Geochemical processes involved in the RN-soil interaction

Sorption is a generic term used to describe the partitioning of aqueous phase constituents (*e.g.*, RNs species) to a solid phase medium (*e.g.*, soil solid matrix) that results from a series of geochemical processes, namely adsorption/desorption, dissolution/precipitation and absorption. **Figure 1.11** depicts some of the processes occurring at the solid-water interfaces leading to RN sorption. Without extensive testing or the use of spectroscopic or microscopic techniques, it is not possible to know if a RN is sorbed onto the surface of a solid by inner- or outer- sphere complex formation, sorbed into the structure of a solid or precipitated as a three-dimensional molecular structure on the surface of the soil (EPA, 1999a; Selim and Sparks, 2010). Thereupon, the most relevant geochemical processes leading to RN sorption in soils, as well as those occurring in aqueous phase affecting the availability of soil sorption sites and the affinity between them and RN species are described.

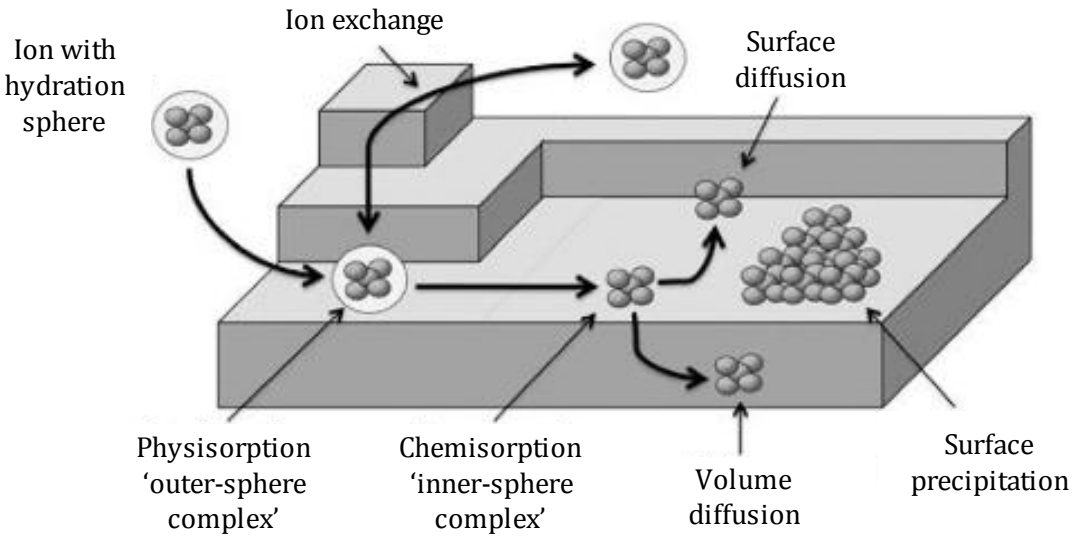

Figure 1.11 *Basic processes at solid-water interfaces. In: Neumann (2012) (adapted from Manceau et al. (2002)).*

1.4.1.1 Adsorption and desorption

Adsorption is the net accumulation of matter in two-dimensional molecular arrangements at the interface between a solid phase and an aqueous-solution phase (Kabata-Pendias, 2010). Adsorption is likely to be the key process controlling RN sorption in soils in areas where there is chemical equilibrium, such as in areas far from the point source (EPA, 1999a). RN adsorption can take place via two mechanisms:

- Formation of an inner-sphere surface complex by means of either ionic or covalent bonding, which lies within the Stern Layer (*i.e.*, the adsorbed ion is in direct contact with the surface of soil particles).

- Formation of outer-sphere surface complex exclusively through ionic bonding, which reside in the Guoy Layer extending from the surface into the surrounding liquid (*i.e.*, there is, at least, one water molecule between the soil surface and the adsorbed ion) (Hiemenz, 1997).

Generally, the relative affinity of cations to sorb will increase with its tendency to form inner-sphere surface complexes, which in turn increases with a higher ionic potential of a cation. Therefore, rankings of RN proneness to interact by inner-sphere

adsorption process follow the well-known periodic table trends related to charge to radii ratio, albeit for transition metal cations the electron configuration also plays an important role. It should also be noted that the adsorption of RNs to soil may be totally to partially reversible. For instance, as the concentration of a dissolved RN declines in solution in response to some change in geochemistry (*e.g.*, due to pH variations in groundwater), some of the adsorbed RNs will be released to the aqueous phase. The opposite process leading to the release of species adsorbed in the solid matrix to the aqueous phase is generally termed as desorption (EPA, 1999a).

One of the most common adsorption reactions in soils is ion exchange, described as the interaction occurring when a charged solid matrix attracts oppositely charged solution species close enough to its surface to form electrostatic bonds involving the replacement of one ionic species between the solid phase and the aqueous solution in contact (NUREG, 1981). Thus, ion exchange occurs when a previously sorbed ion of weaker affinity is exchanged by the soil solid phase for an ion in aqueous solution. Most metals in aqueous solution exist as charged ions and, thus, RNs of metal species adsorb primarily in response to electrostatic attraction. Besides this, most soils have net negative surface charges originated from the substitution of a lower valence cation for a higher valence cation in the soil mineral structure (permanent charge), as well as from the presence of surface functional groups in soil phases such as aluminium, iron, and manganese oxide solids or organic matter (variable charge). According to this, most of ion exchange interactions occur with cations in solution. Although in soils there are many cation species simultaneously competing for available soil surface exchange sites of different nature and contrasting affinity for them, the cation exchange capacity (CEC) of soils (an operational soil property defined elsewhere, for instance in Burt (2004)) is frequently used as a measure of the overall capacity of soils to bind positively charged species.

1.4.1.2 Precipitation/dissolution

The precipitation reaction of dissolved species is a special case of the complexation reaction in which the complex formed by two or more aqueous species is a solid. Another process related to RN sorption in soils is surface precipitation and co-

precipitation, which is defined as the three-dimensional growth of a solid phase containing the target RN on a mineral surface (Neumann, 2012). Surface precipitation of RNs occurs when the RN concentration in a given aqueous phase exceeds its solubility limit. The solubility limit of a given species is highly dependent on the chemistry of the aqueous phase and, thus, if the system chemistry changes, especially in terms of pH and/or redox state, the individual species concentrations may change due to precipitation/dissolution processes. RN sorption through surface precipitation is particularly important for multivalent RNs (*e.g.*, Pu, U and Am) in the case of soil/groundwater systems where there is chemical nonequilibrium (*e.g.*, at a point source or where high RN concentrations, or steep pH or redox gradients exists). In contrast, it is not expected to be a dominant sorption reaction in the far-field because the RN activity concentrations are not likely to be high enough (Sposito, 2016). On the other, co-precipitation is the simultaneous inclusion or adsorption of a species in a precipitate formed by other species, generally major components in the system. Therefore, RN can be scavenged in a precipitate, by means of a co-precipitation process, under at RN concentration much lower than the solubility limit (NUREG, 1981).

1.4.1.3 Absorption

Absorption process is limited to the special cases in which the RNs becomes integrated into the mineral structure, such as Cs into illitic minerals (Kim et al., 1996), RNs occurring as oxyanions species, like U, into iron oxide minerals (Duff et al., 2002), or RNs occurring as divalent and trivalent cations into iron and manganese oxyhydroxide minerals (Morse et al. 1993). Such process results from the progressively incorporation of an ion previously sorbed in the soil surface into the mineral structure by volume diffusion or crystal growth (Neumann, 2012). With respect to RN retention, the distinct property of an absorbed RN is that it is strongly bound by the solid phase, requiring structure bonds to be broken prior to it being released into the aqueous phase. Therefore, absorption cannot be considered a reversible interaction process and such fact should be taken into account when examining the RN-soil interaction over time.

1.4.1.4 Other aqueous phase processes affecting RN sorption in soils

Notwithstanding the relevancy of the sorption processes described in previous sections for the incorporation of RNs in soils, there are other processes occurring in aqueous solution which are also crucial for the fate of RNs occurring in water sources since they determine in a great extent the availability of soluble RNs to participate in the different sorption reactions.

Complexation/hydrolysis reactions

A complex is said to form whenever a molecular unit, such as an ion, acts as a central group to attract and form a close association with other atoms or molecules (Sposito, 2016). Ionic species in solution, such as RNs, react with others also in solution to form a complex if there is a large increase in stability. Most of the complexes likely to form in solution are metals occurring as cationic species combining typically with anions and neutral species, termed ligands or complexant. The most common inorganic ligands present in soil solution sorted by decreasing affinity to form complexes with many RNs are HCO_3^-/CO_3^{2-}, SO_4^{2-}, PO_4^{3-} and Cl^- (Stumm and Morgan, 2012). Besides inorganic anions, there can be a large number of dissolved, low molecular weight small chain humate substances of organic origin (*e.g.*, humic and fulvic acids, etc.) present in groundwater, that when occurring at significant concentration may dominate the speciation of most cationic RNs since lead to the formation of extremely stable RN-humate complexes.

Complexation reactions in solution involving RNs are paramount concerning the RN-soil interaction since they can enhance, partially inhibit or completely suppress the sorption processes previously explained. Complexation of RNs with most inorganic ligands usually results in lowering the RN potential for sorption in soils and increasing its solubility, both of which can enhance RN mobility (Wang et al., 2011). Conversely, certain RNs are more retained by soils when form complexes with high-molecular weight humate ligands that are readily bond to the soil matrix (Xu et al., 2014). Finally, hydrolysis reactions are a specialised type of complex formation in aqueous phase in which the hydroxyl (OH^-) anion act as a ligand. The hydrolysis of cationic

RNs is important because hydrolysed species are more readily adsorbed by soil surfaces than the corresponding free species do (NUREG, 1981).

Colloid formation

Another aqueous process that may affect the availability of soluble species to interact with soil sorption sites is the formation of submicron size entities by means of combining atoms or molecules of soluble RNs with themselves (*i.e.*, colloids) or with molecules of other species (*e.g.*, aggregated humate compounds, metal oxide particles or even suspended clay particles), the latter case often designated as 'pseudo colloid'.

Colloids behave intermediately between small soluble and larger suspended particulates and may have negative net surface charge. Colloids usually exhibit a smaller charge/surface area ratio and are thus less chemically reactive (Moulin and Ouzounian, 1992). When soluble RNs form colloids they are less prone to participate in sorption reactions with soil solid phases because of size exclusion or electrostatic repulsions, which enhances their transport in water compared to the corresponding RN free species. For instance, highly charged metal ions such as Pu, Th, U, Zr and to a lesser extent Am, Cm, Sb and Ru are believed to commonly migrate as colloids under certain conditions (NUREG, 1981).

1.4.2 Characteristics of the soil-water system affecting RN sorption

The characteristics of the soil system determine which geochemical processes are responsible for the RN-soil interaction since they affect the soil surface reactivity (*i.e.*, availability and accessibility of pool of sorption sites) as well as the RN speciation and affinity for sorption sites. It is essential to identify the soil characteristics involved in the RN sorption processes as well as to understand the way how they can affect the RN-soil interaction in order to be able to foresee the behaviour of a given RN in different scenarios. Such issue is not easy because for the same RN the relationships between most of the relevant soil characteristics and the geochemical processes involved in its interaction with soils are not univariant, but often imply simultaneous processes contributing oppositely to RN incorporation in the soil matrix or affect

differently when other conditions and/or other characteristics of the system change, as it is explained hereinafter.

1.4.2.1 Soil pH

In many natural systems, the extent of RN sorbs to soils is controlled by the electrostatic surface charge of soil particles. As mentioned before, there is a fraction of the total surface charge in soils that results from functional groups of certain mineral and organic matter phases. The magnitude and polarity of such surface charge contribution changes with a number of factors, including pH. As the pH increases, soil surface becomes increasingly more negatively charged, especially those of mineral particles, which favours adsorption of RNs present as dissolved cations (*e.g.*, species of Sr, Cd or Ni). Thus, cation adsorption is greatest at high (basic) pH and decreases with decreasing pH (EPA, 1999a). In contrast, at decreasing pH soil particles surface becomes more positively charged, which favours adsorption of RNs occurring as anions (*e.g.*, species of Tc, I or As). Thus, anion adsorption is greatest at acid pH and decreases with increasing pH.

Besides changes in the surface reactivity, pH also affects directly the speciation of dissolved RNs, not only due to obvious effect on hydrolysis reactions, but also because it controls the formation of soluble complexes, more or less reactive, with organic and inorganic ligands. Such effect on complex formation results from two factors, one related to the complex stability and formation rate (*i.e.*, complexation and dissociation constants are pH-dependent), and one related to the solubility and, thus, availability of potential ligands (*i.e.*, changes in pH may entail dissolution of soil phases or precipitation of aqueous species causing an increase or decrease of ligand concentration in solution, respectively).

Finally, system pH affect the solubility/precipitation of RNs as well as, directly or indirectly, the desorption of RNs adsorbed at soil surface. Generally, solubility of cationic RNs decreases when increasing pH, thus enhancing surface precipitation. On the other, decreasing pH may increase RN desorption (*e.g.*, at acid pH, protons may displace cationic RNs adsorbed by cation exchange) or may cause the dissolution of solid phases providing sorption sites for RN and, thus, the solubilisation of RNs (*e.g.*,

lanthanides and actinides tend to sorb to carbonate minerals, which get progressively dissolved at acid pH).

1.4.2.2 Soil-solution Eh (Oxidation-Reduction conditions)

System Eh determines the oxidation state of RNs, which in turn has profound effects on the affinity of redox sensitive RNs for sorption sites. Whereas the sorption of certain RNs is not redox sensitive, RN sorption in soils may increase as the oxidation state of the RN decreases (*i.e.*, under reducing conditions), such is the case of Tc, Se, Pu, Np or U (Kaplan et al., 2016; Sharmasarkar and Vance, 2002), albeit there are few exceptions such as the case of I or As. Moreover, at reducing conditions certain elements present in the soil matrix may undergo redox reactions resulting in dissolution of certain soil phases and release of ligands to the aqueous phase. Such phenomenon may have a strong influence on RN sorption in different manners. If the solubilised phases were a pool of potential sorption sites of RNs, such is the case of Mn and Fe oxides, RNs will be desorbed. Besides, the concomitant release of ligands may either form complexes with soluble RNs and, thus, decrease their affinity for soil solid phases (*e.g.*, release of carbonates and complexation with lanthanides and actinides RNs) or, on the contrary, cause RN precipitation (*e.g.*, sulphides (HS^-) accumulation in solution and precipitation of many transition metals, including Cr, Cd, Am, Cm, and Eu (EPA, 1999b)).

1.4.2.3 Aqueous phase composition

A typical natural water source can easily contain 100 to 200 different soluble species, many of them are alkali and alkaline earth metal cations, inorganic ligands and organic compounds. The type and concentration of inorganic and organic ligands in the aqueous phase is one of the most relevant factors for RN sorption since, as stated in section 1.4.1.4, the presence of certain ligands may enhance either RN dissolution or precipitation reactions, thus affecting their sorption in the solid phase. Apart from this, the presence of proton donor/acceptors will determine in a great extent the pH of the soil-solution system, unless a given soil presents a significant buffer capacity, which in turn governs most of the geochemical processes responsible for RN sorption

in soils (see section 1.4.2.1). As well as that, the presence of major cations in solution may also influence the soil interaction of those cationic RNs interacting with the soil solid phase namely by means of ion exchange. Since major cations can compete for available sorption sites, the increase in ionic strength and, especially the increase in chemical analogue cation concentration, may imply a decrease in RN soil sorption. For instance, that is the case of Sr^{2+} that sorbs to soils in a lesser extent when high concentrations of dissolved Ca^{2+} and Mg^{2+} are present (Gil-García et al., 2008). Finally, the ionic strength of soil solution can also indirectly influence RN sorption in soils since it determines the solubility and/or solid-phase stability of other species (*e.g.*, organic and inorganic ligands) that interact with RNs, *i.e.*, affect both the ability of ligands to form soluble RN complexes and the affinity that RN complex may have for the soil solid phase (Ye et al., 2014; Zavarin et al., 2005). In further section 1.4.2.5 is described the relationship between RN soil sorption and organic ligands, pH and ionic strength characteristics.

1.4.2.4 Soil mineralogy and texture

Soil mineral particles often play a key role in RN sorption. They comprise clay minerals, oxides, sesquioxides and hydrous oxides of minerals.

Clay minerals are hydrous aluminium phyllosilicates with a small particle size originated from other forms of silicates. There are two major types of clay minerals found in soils, 2:1 and 1:1 phyllosilicates.. The unit cell of the 2:1 phyllosilicate type is built from two silica tetrahedral layers, surrounding an aluminium octahedral layer. Only weak van der Waals forces exist between two units so that water, and hydrated cations can readily enter the interlayer regions and react with the inner surface, often being immobilised. This also causes the ability of some 2:1 phyllosilicates (*e.g.* smectite and vermiculite) to expand in contact with water. The unit cell of 1:1 phyllosilicate type is composed of one silica tetrahedral layer bonded to an aluminium octahedral sheet and the unit cells in 1:1 type are hydrogen bonded together providing no interlayer regions. Thus, neither water nor cations can enter between sheets (Bergaya and Lagaly, 2013). Expanding clay minerals have much higher total surface area, because of the existence of external and internal surface

area, as well as a much greater CEC than the non-expanding clay type and, thus, have a much greater propensity for immobilising cationic RNs (Brown, 1998).

A very important factor influencing RN sorption processes in soils is the fact that clay particles can get negatively charged, which favours the interaction of cationic species. Such negative charge is formed via two main mechanisms. On the one hand, the weakly tight proton of the hydroxyl groups that exist on the edges and on the outer layers of clay minerals can be replaced by other cations. This is a pH-dependent process, that increases when increasing pH. The second process is the creation of negative charges as a result of isomorphous ion replacement in the clay mineral structure, that is, substitutions of Si(IV) by Al(III) and of Al(III) by Mg(II) or Fe(II) in tetrahedral sheets. This process is pH-independent and, therefore, quite persistent.

Besides clay minerals, the oxides and hydrous oxides of iron and aluminium are commonly found in soils in several mineralogical forms (*e.g.*, hematite, goethite, gibbsite and bohemite) and manganese oxides are also found in moderately high amounts in some soils. These minerals may exist as positive, neutral or negatively charged particles depending on pH and, thus, they present a pH-dependent ability to sorb RNs.

Finally, soil texture is an operational classification related with the particle size and defined as the relative proportion of clay (<0.002 mm), silt (0.002-0.05 mm) and sand (0.05-2 mm) mineral particles. Clayey soils, rich in finer particles, present much higher specific surface srea (SSA) than sandy soils, rich in coarser particles, thus being more prone to sorb large amounts of RNs.

1.4.2.5 Soil organic matter fraction

Soil organic matter (SOM) is the second main component of the soil solid fraction and includes high molecular weight organic materials such as polysaccharides and proteins; simpler substances such as sugars, amino acids, and other small molecules; and humic substances (Stevenson, 1992). Humic substances, which accounts for approximately 85-90% of the total organic carbon in soils, are formed as a result of decay and transformation of plant residues and other unaltered material. They are of

major importance from the standpoint of sorption properties. Humic substances consist of a heterogeneous mixture of compounds for which no single structural formula can be attributed. Despite this fact, substantial evidence exists that humic materials consist of a skeleton of alkyl/aromatic units cross-linked mainly by oxygen and nitrogen groups with the major functional groups being carboxylic acid, phenolic and alcoholic hydroxyls, ketone and quinone groups (Schulten, 1991). Humic substances are operationally divided into fulvic acids (soluble in water at acid and basic pH), humic acids (soluble at basic pH) and humin (insoluble at any pH). Humic acids have larger average molecular masses than fulvic acids, are less mobile in soils than fulvic acids and are strongly sorbed by clay minerals. Fulvic acids have more alkyl groups than humic acids and their aromatic core is not so matured. Humic substances may occur as part of solid organic matter particles or bound to silicate surface in clay minerals via several mechanisms (*e.g.*, Al^{3+}, Fe^{2+}, Ca^{2+} and Mg^{2+} bridges, van der Waals forces, hydrogen bondings or adsorption by association with hydrous oxides), forming mineral coatings.

The existence of humic substances in soils strongly influences sorption of RNs. Humic and fulvic acids have a large content of oxygen-containing functional group (*e.g.,* carboxylic -COOH, phenolic -OH and carbonylic -C=O groups) which makes that they can exist in a dissociated, negatively charged form. Humic substances play a key role as ligands with high ability to form stable complexes with cationic RNs. Depending on their solubility and stability in the solid phase, which is highly affected by pH and ionic strength conditions, humic substances can efficiently sorb RNs through ternary-surface complexes or, in contrast, solubilise them by forming soluble, non-reactive humate complexes. It seems that at basic pH values, cationic RN sorption into solid mineral phases may be decreased, for certain RNs, in soils with high humic substance content, namely because a fraction of this organic phase is solubilised and subsequently forms stable, negatively charged complexes with RN species in solution that do not interact with the solid phase due to electrostatic repulsions. Conversely, at acid pH values, a lower fraction of humic substances is solubilised and the fraction remaining in the solid phase has a surface more negatively charged than mineral phases, which makes that sorption of cationic RNs increases in soils containing high humic substance content. On the other, for the same pH scenario and soil humic substance content and composition, cationic RNs sorption in soils increases when

increasing high ionic strength, which is attributed to an increase of the solid-phase stability of humic substances (Pathak and Choppin, 2007; Ye et al., 2014).

1.5 THE SOLID-LIQUID DISTRIBUTION COEFFICIENT (K_D) CONCEPT

The partitioning of RNs between solid and liquid soil phases largely affects the RN mobility and bioavailability in soils. Partitioning of RNs is often quantified by an empirical parameter, the solid-liquid distribution coefficient (K_d),which is defined as the ratio of activity concentration of RN sorbed on a specified solid phase (C_{solid}) to the RN activity concentration in a specified liquid phase (C_{liquid}) in equilibrium with the former. Thus, K_d has unit of volume per unit mass (*e.g.* L kg^{-1}) (ICRU, 2001):

$$K_d = \frac{C_{solid}}{C_{liquid}} \qquad [1.3]$$

The use of K_d constitutes the simplest sorption model available. In principle, it does not give information about the sorption mechanisms governing the phase partitioning of the target species. A K_d measured for an ionic species is not meaningful in the general sense but it is specific to the soil system tested, that is, it is valid only to describe the partitioning of species between the solid and aqueous phases, for the particular soil sample and aqueous chemical conditions (*e.g.*, target species concentration, solution composition, temperature) in which K_d is measured (Bethke and Brady, 2000). K_d parameter of most RNs varies over various orders of magnitude among different soils, mainly due to differences in those soil and solution characteristics controlling the geochemical processes involved in the RN-soil interaction, as described in previous section 1.4.2. Besides this, depending on the methods used to characterise the solid and liquid phase, different K_d values may be obtained that express partitioning between different pools and, thus, representative of different scenarios.

1.5.1 Uses of K_d of RNs in soils

Soil K_d values are frequently used to relate the concentrations of RNs in contaminated soils with those in soil solution in order to assess radiological risk arisen from different radioactive contamination scenarios. For instance, in the Biosphere Model (SKB, Sweden) the RN retention in the regolith is modelled using element specific K_d values to assess the long-term RN transport and accumulation in the biosphere in the frame of the performance of radioactive waste repositories(SKB, 2013). Another

example of use of the K_d in risk assessment models is the CROM tool (CIEMAT, Spain), which uses K_d values to assess RN concentration in waters resulting from an irrigation process of soils contaminated with RNs due to continuous planned releases (CIEMAT, 2007). Finally, the SYMBIOSE modelling platform (IRSN, France) also uses K_d values of RNs in two soil models (*i.e.*, simple soil model and vadose soil model) to estimate the proportion of RN that exists in the interstitial solution of contaminated soils and, thus, that can be carried away by infiltrating water in order to evaluate the transfer of the bio-available pool of RNs between soil layers (*e.g.*, surface layer, root layer and underlying layer) (Simon-Cornu et al., 2015; Sy et al., 2016).

On the other hand, the K_d parameter, apart from being a descriptor of the partitioning between solid and liquid phases of a given pollutant, implicitly relates to other transport and transfer parameters. Consequently, K_d values of RN in soils are used directly, or indirectly, to estimate a wide range of different transport processes of RNs, such as the velocity of dissolved RNs and diffusion transport through soils, the vertical mobility of RNs inside a soil column, or the RN plant root-uptake. Risk assessment models frequently use a series of parameters to model uptake of RNs by different types of biota, among which the soil-to-plant concentration ratio (CR), is frequently used to calculate RN soil-to-plant transfer. Based on the assumption that plants primarily take up RNs from the porewater phase, the RN soil-to-plant transfer can be indirectly estimated by means of the K_d parameter. That is the case of the terrestrial component of the Radioactive Waste Management Directorate (RWMD model (Quintessa, UK) (Walke et al., 2013) and the PRISM Food Chain Model (Food Standards Agency, UK) (Throne et al., 2004), which instead of using measured CR values of RNs, use the soil K_d value, the affinity for plants to take-up an element from the soil solution to the edible component of the plant (δ), the water-filled porosity (θ) and the bulk density (ρ_b) (kg/m^3) of the soil, to calculate CR values, as follows:

$$CR = \frac{\delta}{(\theta + \rho_b K_d)} \qquad [1.4]$$

Moreover, the transport of RNs in the soil system can be described by the advection-dispersion equation, which uses the retardation factor (R_f) to characterise the delay of RN transport compared to the transport of water. The R_f (unitless) is defined as the ratio between the velocity of water (V_p) and the velocity of the RN (V_c), through a

controlled volume. When the RN interacts with the soil solid phase, the R_f is then greater than 1. To predict the effects of retardation, sorption processes must be described in quantitative terms and the K_d parameter provides such a quantitative estimate. Under saturation conditions, the K_d can be related to R_f by means of using the soil bulk density (ρ_b) and its effective porosity (n_e), as follows:

$$R_f = 1 + \frac{\rho_b}{n_e K_d} \qquad [1.5]$$

According to the existing relationship between the K_d and R_f parameters, K_d values are also commonly used in transport models for reactive RNs for risk assessment purposes. For instance, the abovementioned RWMD biosphere and PRISM models, also use K_d values to represent the retardation of RNs in their transport between and out of the two soil compartments (topsoil and subsoil) contemplated for agricultural ecosystems (Stansby and Thorne, 2000). Besides, in the RESRAD family of codes (Argonne National Laboratory, USA), K_d values are used in the components regarding ingestion pathways to estimate the leaching of RNs from the surface of contaminated soils and further transport in the unsaturated zone (vadose zone) and saturated zone (groundwater), aiming at knowing whether RNs may leach out more quickly (due to low K_d) in the surface soil, and hence the RNs concentration in the unsaturated zone may be higher (Yu et al., 2001). Finally, the CIEMAT soil-plant model (CIEMAT, Spain) uses time-dependent soil K_d values that vary according to the water table moves, to calculate rate constants aiming to estimate RN migration up and down in a multi-layered soil column (Pérez-Sánchez and Thorne, 2014).

As explained above, there are a number of manners that soil K_d values are used in specific codes and tools of radiological risk assessments involving the terrestrial ecosystem. Therefore, modellers need to understand not only the mathematics associated with the K_d construction, but also the biogeochemistry that this parameter us attempting to describe, since K_d values are expected to vary according to the processes that are being modelled. They have also to take into consideration the propagation of the K_d assumptions and constraints on the new parameters calculated.

1.5.2 Assumptions and constraints of the K_d concept

As explained before, K_d values of RNs in soils are extensively used. This is in part because of the ease of some experimental methods to measure this parameter, which will be explained in the following section, and due to the simplicity of the K_d model. However, the simplistic K_d model is based on several theoretical assumptions, extensively discussed for instance in EPA, (1999a) or IAEA, (2010), some of which may jeopardise the suitability of the K_d parameter to quantify RN sorption and/or transport in certain scenarios. In summary, the K_d model namely assumes that:

- only trace amounts of contaminants exist in aqueous and solid phases,
- all sorption sites are accessible and have equal binding energies,
- linear relationships exist between RN solid and liquid concentrations, *i.e.*, sorption is independent of the RN concentration in the aqueous phase,
- equilibrium conditions exist between solid and liquid phases,
- reversible sorption reactions take place, *i.e.*, equally rapid sorption and desorption kinetics are assumed.

Several of these assumptions are likely to be violated in the common protocols used to measure K_d values or to be further disregarded when RN sorption and/or transport in a system is parameterised in models by means of using K_d values. For instance, in the estimation of K_d values from naturally occurring stable isotopes at concentrations higher than trace amounts, not only the first assumption is already violated, but also those related to sorption sites homogeneity and to linear sorption might be. Depending on the experimental conditions applied, other processes than reversible sorption might be included in the quantification of K_d values (*e.g.* due to the effects of precipitation or matrix diffusion). Moreover, the fraction of RN incorporated in the solid phase may become fixed and, thus, no longer participate in the partitioning between the solid and liquid phases due to sorption dynamics, which relates to changes with time of RN speciation in the solid phase (*i.e.*, ageing processes) or, in contrast, it may become more labile due to progressive dissolution, degradation or transformation of certain soil phases of the soil. Therefore, unless the sorption

dynamics of the studied system is negligible and its integrity is assured, the assumptions of sorption reversibility and/or equilibrium will not be respected.

Besides the conceptual uncertainties related to the assumptions of the simplistic K_d model, there are several types of variations and uncertainties associated with the implementation of the K_d model/concept both at spatial and at temporal scale. On the one hand, the upscaling from site-specific samples or laboratory tests to landscape level introduces uncertainties regarding representativeness. The assigned distribution coefficients are assumed to represent the average values of the entire model compartment, and it is assumed that these 'effective' K_d or 'best estimate' values describe the sorption at a macro scale level by weighting out all the processes. However, since RN sorption is governed by a series of characteristics of the soil and the aqueous solution (see section 1.4.2) and soils and water sources in a given area may present rather contrasting properties, the sorption of a given RN, and thus, its K_d values in soils may vary significantly. According to this, the variation in K_d values used to assess the interaction of a given RN in the area under study should account for the variation in the chemical environments among the possible contamination source points. On the other hand, the overall variation assigned to K_d values should also account for the long-term landscape evolution that will change the environmental conditions over time, *i.e.*, the dynamics of the sorption processes in relation to the modelled temporal resolution should be also described by K_d values to properly estimate RN mobility.

1.5.3 Experimental approaches to quantify K_d

The K_d parameter can be determined by means of a great variety of methods. Depending on the method used, different geochemical processes controlling RN-soil interaction (section 1.4.1) may be captured or the system studied may move away from the conditions in which assumptions implied in the K_d concept are respected. The wide range of methods used for making K_d measurements and the use of operational definitions and their associated assumptions makes that the K_d values for a RN-soil combination may differ significantly according to the method applied. Consequently, the method used may be one of the main sources of K_d variability that

should be evaluated when possible. The different methodological approaches to quantify K_d values can be grouped into three general categories: *in-situ*, dispersed or batch and compacted or column (EPA, 1999).

1.5.3.1 In-situ method

The *in situ* method is based on the quantification of K_d values as the ratio of the concentration levels of the target element determined in the contact solution (*e.g.,* run-off soil solution; groundwaters) and in the solid particles of the soil sample (*i.e.*, once the liquid phase, or porewater, has been removed from the bulk matrix of the soil), collected directly at field (EPA, 1999).

Since *in situ* K_d values are determined directly using quasi-undisturbed field soil samples and contact solutions, the main advantages of this approach are that representative solution composition and solid phase mineralogy can be used, if required, for further modelling and, on the other, that a true equilibrium between the solid and the liquid phases may have been attained. On the other, the disadvantages of the *in situ* method are less apparent but nonetheless appreciable. Depending on the method used to determine the RN concentration in the solid soil matrix (*e.g.*, by means of total or pseudo-total digestion of the sample), this approach may lead to K_d values determined by including fraction of RN not reversibly bound to the soil matrix and, thus, not available for exchange with the liquid phase. Therefore, *in situ* values may be higher than those derived from methods aiming at estimating reversible K_d. Besides this, with the *in situ* method it is not possible to distinguish between sorption and precipitation of the target element in the matrix of the environmental sample. Since some transport and risk assessment models treat sorption and precipitation processes differently, which require that K_d values only account for the element sorption processes, the use of *in-situ* K_d data for this purpose is unsuitable since it may overestimate the element-soil interaction. Finally, the *in situ* method is not cost-effective, which makes its application to be very limited, and thus, the number of available *in-situ* K_d data of RNs in soils are scarce. This scarcity of *in situ* K_d data jeopardise their use to assess the interaction of RNs in other scenarios than those already studied.

1.5.3.2 Disperse or batch method

In the batch method dispersed soil samples are mixed with contact solutions during a given period of time. It represents the most widely applied approach to estimate the K_d values for a given RN in soils. In this type of test, a known amount of unconsolidated or disaggregated, clean soil sample, is put in contact with a volume of an aqueous solution spiked with the target RN. "Clean" refers to an initial RN activity concentration in the solid sample which is negligible compared with the sorbed activity concentration after contact with the solution. After shaking the mixture for a short period of time, from hours to few days, the solid and liquid phases of the resulting suspension are separated and K_d values are calculated as the ratio of the RN concentration determined in both phases.

Quantification of the K_d may be affected by experimental conditions, such as temperature, filtration of the resulting solution, contact time, and L/M ratios, albeit K_d variability due to experimental conditions is normally much lower than those arising from RN and solid phase characteristics. Because of the operational nature of this method, recommendations on experimental conditions are often given by international guidelines (ASTM, 2003; ASTM, 2010; OECD, 2000) to facilitate comparability of the results and representativeness of the K_d data measured. For instance, it is recommended to use contact times long enough to achieve sorption equilibrium, which should be checked in advance; to keep L/M ratios in batch sorption tests between 10:1 and 50:1 L/kg, which are not fully representative for soils at field; and, when possible, to use contact solutions with a composition (*e.g.*, ionic strength, pH, presence and concentration of ligands and/or other species, etc.) as similar as possible to that of the liquid sources expected to cause the radioactive soil contamination (*e.g.*, using solutions sampled at field or synthetic solutions prepared by mimicking the composition of real ones).

The batch method also has the added benefit that the assumptions of "reversibility" and "steady-state" of the K_d measurements can be demonstrated. Moreover, batch sorption tests are particularly useful for doing inexpensive, relatively convenient, series of K_d measurements in which a given characteristic of the soil system, potentially impacting K_d values, (*e.g.*, pH of soil/solution suspension, ionic strength, redox potential, concentration of organic or inorganic ligands, etc.) is kept reasonably

constant or, in the other way around, is intentionally varied under controlled conditions, in order to develop an understanding of RN sorption mechanisms.

Besides batch sorption tests are often completed with tests aiming at predicting processes related to the remobilisation of RNs from contaminated soils, the so-called batch desorption tests. Such methods consist in performing a leaching test to soil samples containing the target RN, such as soils affected by past contamination episodes or soils intentionally spiked (*e.g.*, sorption test soil residues). According to which scenario wants to be reproduced and, thus, to which RN remobilisation process wants to be assessed, extractant solutions of different composition are applied.

K_d values gathered in soils from desorption tests tend to be higher than those obtained when sorption tests are applied, even when the same experimental conditions (*i.e.*, same contact solution, contact time, L/M ratio, etc.) are used in both types of test. The differences between sorption and desorption K_d values can be taken as representative for the effect of sorption dynamics (see section 1.5.2), which is RN dependent and tends to increase as the time elapsed since the RN was incorporated to the studied soil increases. With the exception of those RNs with a high sorption K_d (*e.g.*, over 10^4 L/kg), it is relevant to estimate how much higher the desorption K_d would be, as this may be of major significance for risk assessment exercises.

1.5.3.4 Compacted or column methods

The column method entails the study of a solution containing the target RN as it flows through soil samples. In this case, K_d values can be derived from the diffusion-based mass transport pattern of a RN in undisturbed soil cores or compacted soils. The approach takes into account the retardation of the RN due to interactions with soil particles. Mass transport experiments are used to simulate the migration of RNs through soils under saturated and/or unsaturated conditions. They allow observation of RNs migration rates without significant solid particle alteration caused by grinding, as in batch experiments, and often produce results more representative of the field conditions than those obtained by the batch method.

Mass transport experiments are usually carried out with columns. Experimental setup includes a reservoir to the column, a cylindrical holder to contain the crushed or intact soil sample being tested, and a sample collector for the column effluent. Several operational problems with column experiments have been identified, such as homogeneity of column packing, potential short-circuit effects, and residence time required for experimentation (ANL, 2015). Besides these experimental complications, the associated equipment costs, time constraints and variability of the obtained data limit the use of this approach. Thus, alike the case of *in situ* K_d data of RNs in soils, scarce K_d data derived from mass transport experiments in soils are available.

1.5.4 Alternatives to single site-specific K_d data through modelling sorption of RNs in soils

The large variation in the reported K_d values are ultimately caused by differences in environmental, chemical and physical conditions (indicating both spatial and temporal variation in soils) as well as by differences in experimental methods. According to this, in order to perform reliable risk assessments, models may be feed with an enormous number of site-specific K_d values as input data, which in the vast majority of cases are not available. To overcome this problem, different models are currently in use to predict K_d values by means of describing RN sorption as a function of the soil characteristics governing the RN-soil interaction mechanisms. These models can be divided in three groups, multisurface models, parametric or empirical regression models, and probabilistic models.

1.5.4.1 Multisurface models

Multisurface models, also termed assemblage models, consider the soil as a set of independent reactive surfaces (*e.g.*, organic matter, both solid and dissolved, (hydr)oxides or clay), and combine several submodels to describe RN sorption onto each one. The speciation calculations are performed with geochemical programs, such as ECOSAT (Weng et al., 2001), WHAM (Tipping et al., 2003), or ORCHESTRA (Schröder et al., 2005). A surface complexation model is used to describe sorption on (hydr)oxides, while sorption on clay minerals is usually modelled with an ion

exchange approach. In turn, sorption on organic matter is modelled with models, such as the NIC(C)A-Donnan model (Kinniburgh et al., 1999) or Model VI (Tipping, 1998), that assume two types of sites (typically associated with carboxylic and phenolic groups) on which protons and RN species compete for binding (specific sorption) together with non-specific electrostatic sorption (Tipping, 1998).

Many research has shown that multisurface models can be successfully used simulating pollutant sorption, specially metals, in a variety of environments, from pristine soils (Weng et al., 2001; Gustafsson et al., 2003) to strongly contaminated soils (Dijkstra et al., 2004; Khai et al., 2008). Although multisurface models are conceptually attractive, because of their complicated nature, they require extensive input information, often not available in more routine research, which jeopardises the applicability of this approach. Moreover, assumptions are required to define the reactivity of surfaces compared with model constituents, for instance, the active fraction of organic matter or the surface area of oxyhydroxides. Only a few studies have compared experimentally determined solid–liquid distribution of metals in soils with predictions of mechanistic models (Weng et al., 2002; Tipping et al., 2003; Schröder et al., 2005; MacDonald and Hendershot, 2006). It is often found that the experimental and predicted solid–liquid distributions differ considerably. Unless more validation exercises for real soil systems is carried out, prediction of metal partitioning with multisurface models seems still unreliable at present.

1.5.4.2 Parametric models

Another practical conceptual model for sorption is called the parametric K_d model. The K_d value in this model varies as a function of empirically derived relationships with independent parameters of the liquid and solid phases. Thus, from a practical point of view, it is preferable that only routinely measured soil properties (*e.g.* pH, percentage of organic carbon) are included in the model. Most of these models take the form of a multivariate, linear relations between K_d and soil properties (Sauvé et al., 2000; Sheppard, 2011). Statistical methods commonly used to derive quantitative predictor equations include standard linear or nonlinear regressions, stepwise regression, and adaptive, learning networks (Gil-García et al., 2011a; SKB, 2009). It is

critical that parametric models are used to calculate K_d values for systems only within the range of the independent variables used to create the model.

Parametric models may be devoid of causality and therefore provide no certain information on the mechanism by which the RN partitioned to the solid phase, unless they are developed by taking into consideration parameters known to be specifically controlling the soil interaction of the target RN, *i.e.*, related to its sorption mechanisms. For example, the statistical analyses may suggest a very strong relationship between pH and the K_d term, when the actual sorption process may be controlled by iron oxide adsorption. Because pH and the surface charge of iron oxides are covariant, a statistical relationship could be calculated, suggesting that sorption is solely caused by pH. Up to now mechanistic parametric models have been successfully constructed only for a few RNs presenting a barely complex and thoroughly studied sorption behaviour, such is the case of Sr or Cs (Gil-García, et a., 2011a and 2011b).

The main advantage of parametric models is that they are more robust than a site-specific K_d value, which is representative only for a set of conditions, and removes the burden of determining new K_d values for each environmental condition. As well as that, an advantage over the multisurface models is that parametric models, due to their lower complexity, are usually calibrated on a larger number of soils and, thus, they have more applicability and representativeness.

1.5.4.3 Probabilistic models

The probabilistic model is based on using K_d compilations or data bases to statistically derive discrete conservative and most likely K_d values or functions describing the overall variability of K_d values. Such approach has been used since the 80s, when K_d compilations were developed in the frame of national nuclear waste disposal or site decommissioning programs aiming at providing input data for modelling RN mobility in the environment (Hakanen and Holtta, 1992; SKB, 1991; Stenhouse, 1994; Thibault et al., 1990). Currently, this is an approach widely applied to estimate radiological risk in terrestrial ecosystems, especially for screening assessments required in preliminary stages of radioactive waste facilities planning

and development. For instance, several radiological risk assessment tools and models, such as RESRAD (Argonne, USA) or Biosphere Model (SKB, Sweden), use the K_d data summarised in international compilations (IAEA, 2010), either by directly selecting the mean and minimum K_d values provided for a large number of RNs to assess the best estimate and conservative K_d data, respectively, or by also taking into account the associated variability, provided as geometric standard deviation (GSD) values, to construct statistical distribution functions and derive confidence intervals at desired significance levels (Simon-Cornu et al., 2015).

Since data compilations are gathered from a great variety of soils and solutions with contrasting properties and by applying different methods, the statistically derived K_d values encompass a wide range of scenarios. Thus, one advantage of this approach is its high applicability. In contrast, due to the high heterogeneity of data sources, K_d values in compilations for most RNs tend to have a large variability, which makes that the derived statistical values have a related high uncertainty. Therefore the derived statistical K_d values are suitable only for screening purposes, unless data variability is somehow decreased, for instance, by creating K_d data sets for different soil types on the basis of the soil characteristics expected to control the target RN sorption in soils (see section 1.4.2) (IAEA, 2010).

Some risk assessment models require probability distribution functions (PDF) instead of discrete values in order to express parameter uncertainty and to enable the performance of sensibility analysis (EPA, 2001). Such type of risk assessment K_d input data can be derived with this approach. Whereas PDFs of K_d were satisfactorily obtained for freshwater sediments, the obtaining of PDFs of soil K_d data suitable for risk assessment purposes up to know has remained as a challenge (IAEA, 2010). Part of the present Thesis is dedicated to explore this latter issue.

1.6 REFERENCES

Aldaba, D., Rigol, A., Vidal, M., 2010. Diffusion experiments for estimating radiocesium and radiostrontium sorption in unsaturated soils from Spain: Comparison with batch sorption data. J. Hazard. Mater. 181, 1072.

ANL, 2001. Report ANL/EAD-4 User's Manual for RESRAD Version 6. Argonne National Laboratory, USA.

ANL, 2015. ANL/EVS/TM-14/4 Data collection handbook to support modeling impacts of radioactive material in soil and building structures. Argonne National Laboratory, USA.

ASTM, 2003. ASTM D4646-03 Standard Test Method for 24-h Batch-type Measurement of Contaminant Sorption by Soils and Sediments. American Society for Testing and Materials, USA.

ASTM, 2010. ASTM C1733–10 Standard Test Method for Distribution Coefficients of Inorganic Species by the Batch Method. American Society for Testing and Materials, USA.

Baes III, C. F., Garten Jr, C. T., Taylor, F. G., Witherspoon, J. P., 1986. Report ORNL-6146 - The long-term problems of contaminated lands: sources, impacts and countermeasures. Oak Ridge National Laboratory, USA.

Bergaya, F., Lagaly, G., 2013. Handbook of clay science, 2nd Ed. Amsterdam, The Netherlands: Elsevier.

Bethke, C. M., Brady, P. V., 2000. How the K_d approach undermines ground water cleanup. Ground Water 38 (3), 435-443.

Brown, G., 1998. The structures and chemistry of soil clay minerals. The chemistry of soil constituents. New York, USA: John Wiley and Sons, Inc.

Buck, E. C., Hanson, B. D., McNamara, B. K., 2004. The geochemical behaviour of Tc, Np and Pu in spent nuclear fuel in an oxidizing environment. In: Gieré, R., Stille, P. (eds) *Energy, Waste, and the Environment: a Geochemical Perspective*. The Geological Society of London Special Publication 236, 65-88.

Burt, R., 2004. Soil survey laboratory methods manual. Investigation report No 42, Version 4.0, Natural Resources Conservation Service, USDA, Washington, USA.

Chemistry Libretexts, 2017. https://chem.libretexts.org/Core/Physical_and_Theoretical_Chemistry/Nuclear_Chemistry/Nuclear_Stability_and_Magic_Numbers. Accessed 04-24-17.

CIEMAT, 2007. Modelos implementados en el código CROM (Código de cRiba para la evaluaciÓn de iMpacto). Colección Documentos CIEMAT. Robles, B., Suáñez, A., Mora, J. C., Cancio, D., Editiorial CIEMAT, Spain.

Degryse F., Smolders, E., Parker, D. R., 2009. Partitioning of metals (Cd, Co, Cu, Ni, Pb, Zn) in soils: concepts, methodologies, prediction and applications – a review. European Journal of Soil Science 60: 590-612.

Dijkstra, J. J., Meeussen, J. C. L., Comans, R. N. J., 2004. Leaching of heavy metals from contaminated soils: an experimental and modeling study. Environ. Sci. Technol. 38, 4390-4395.

Duff, M.C., Coughlin, J. U., 2002. Uranium co-precipitation with iron oxide minerals. Geochim. Cosmochim. Acta 66 (2002) 3533-3547.

Duursma, E., K., Carroll, J., 1996. Environmental compartments: Equilibria and assessment of processes between air, water, sediments and biota. 1st Ed. Springer, Germany.

EPA, 1994. EPA Report 402-R-93-076 - Estimating radiogenic cancer risks. Environmental Protection Agency, USA.

EPA, 1999a. EPA 402-R-99-004A Understanding variation in partition coefficient, K_d, values. Volume I: The Kd model, methods of measurement, and application of chemical reaction codes, U. S. Environmental Protection Agency, USA.

EPA, 1999b. EPA 402-R-99-004A Understanding Variation in Partition Coefficient, Kd, Values. Volume II: Review of Geochemistry and Available Kd Values for Cadmium, Cesium, Chromium, Lead, Plutonium, Radon, Strontium, Thorium, Tritium (3H), and Uranium, U. S. Environmental Protection Agency, USA.

EPA, 2001. EPA 540-R-02-002 - Risk assessment guidance for superfund: volume III - Part A, Process for conducting probabilistic risk assessment, U. S. Environmental Protection Agency, USA.

EPA, 2008. EPA Technical Report 402-R-05-008 – Technologically enhanced naturally occurring radioactive materials from uranium mining. Volume 2: Investigation of potential health, geographic, and environmental issues of abandoned uranium mines. U. S. Environmental Protection Agency, USA.

Gil-García, C., Rigol, A., Rauret, G., Vidal, M., 2008. Radionuclide sorption-desorption pattern in soils from Spain. Appl. Radiat. Isotopes 66, 126-138.

Gil-García, C.J., Rigol, A., Vidal, M., 2011a. The use of hard- and soft- modeling to predict radiostrontium solid-liquid distribution coefficients in soils. Chemosphere 85, 1400-1405.

Gil-García, C.J., Rigol, A., Vidal, M., 2011b. Comparison of mechanistic and PLS-based regression models to predict radiocaesium distribution coefficients in soils. J. Hazard. Mater. 197, 11-18.

Gustafsson, J. P., Pechova, P., Berggren, D., 2003. Modeling metal binding to soils: the role of natural organic matter. Environ. Sci. Technol. 37, 2767-2774.

Hakanen, M., and Holtta, R., 1992. Technical Report YJT-92-14 - Review of Sorption and Diffusivity Parameters for TVO-92. Nuclear Waste Commission of Finnish Power Companies, Finland.

Hiemenz, P.C., Rajagopalan, R., 1997. Principles of Colloid and Surface Chemistry, Marcel Dekker, Inc., USA.

Hinton, T.G., Garnier-Laplace, J., Vandenhove, H., Dowdall, M., Adam-Guillermin, C., Alonzo, F., Barnett, C., Beaugelin-Seiller, K., Beresford, N.A., Bradshaw, C., Brown, J., Eyrolle, F., Fevrier, L., Gariel, J.C., Gilbin, R., Hertel-Aas, T., Horemans, N., Howard, B.J., Ikaheimonen, T., Mora, J.C., Oughton, D., Real, A., Salbu, B., Simon-Cornu, M., Steiner, M., Sweeck, L., Vives i Batlle, J., 2013. An invitation to contribute to a strategic research agenda in radioecology. J. Environ. Radioactiv. 115, 73-82.

IAEA, 1989. Evaluating the reliability of predictions made using environmental transfer models. In: IAEA (Ed.), Safety Series 100, International Atomic Energy Agency, Austria.

IAEA, 1990. IAEA-TECDOC-563 - Siting, design and construction of a deep geological repository for the disposal of high level and alpha bearing wastes. International Atomic Energy Agency, Austria.

IAEA, 1992. IAEA-TECDOC-655 - Treatment and conditions of radioactive solid wastes.

IAEA, 2001. TRS-402 - Handling and Processing of Radioactive Waste from Nuclear applications. International Atomic Energy Agency, Austria.

IAEA, 2002. IAEA-TECDOC-1325 - Management of low and intermediate radioactive wastes with regard to their chemical toxicity. International Atomic Energy Agency, Austria.

IAEA, 2003. Report IAEA-BIOMASS-6 - "Reference Biospheres" for solid radioactive waste disposal. International Atomic Energy Agency, Austria.

IAEA, 2009. IAEA Safety Standards Series No. GSD-1 - Classification of radioactive waste. General Safety Guide. International Atomic Energy Agency, Austria.

IAEA, 2010. TRS-472 Handbook of Parameter Values for the Prediction of Radionuclide Transfer in Terrestrial and Freshwater Environments. International Atomic Energy Agency, Austria.

IAEA, 2011. IAEA Safety Standards Series No. SSR-5 - Disposal of radioactive waste. Specific safety requirements. International Atomic Energy Agency, Austria.

IAEA, 2014a. IAEA Bulletin 55-3 - Step-by-step: life cycle radioactive waste management. IAEA Division of Nuclear Fuel Cycle and Waste Technology, International Atomic Energy Agency, Austria.

IAEA, 2014b. IAEA Safety Standards Series No. GSR Part3 - Radiation protection and safety of radiation sources: international basic safety standards. International Atomic Energy Agency, Austria.

ICRP, 2007. ICRP Publication 103 - The 2007 recommendations of the International Commission on Radiological Protection. Ann. ICRP 37 (2-4).

ICRU, 2001. ICRU Report 65 - Quantities, Units and Terms in radioecology. International Commission on Radiation Units and Measurements, Journal of the ICRU 1.

ITRC, 2002. Technical and Regulatory Document - Determining Cleanup Goals at Radioactively Contaminated Sites: Case Studies The Interstate Technology and Regulatory Council Radionuclides Team, USA.

ITRC, 2008. Technical/Regulatory Guidance - Decontamination and Decommissioning of Radiologically Contaminated Facilities. The Interstate Technology and Regulatory Council Radionuclides Team, USA.

Kim, S., Min, B. I., Park, K., Yang, B. M., Suh, K. S., 2016. The system of radiation dose assessment and dose conversion coefficients on the ICRP and FGR. J. Radiat. Prot. Res. 41 (4), 424-435.

Kim, Y., Cygan, R.T., Kirkpatrick, R.J., 1996. 133Cs NMR and XPS investigation of cesium adsorbed on clay minerals and related phases. Geochim. Cosmochim. Acta 60, 1041–1052.

Liu, H. H., Cohen, Y., 2014. Multimedia environmental, distribution of engineered nanomaterials. Environ. Sci. Technol. 48, 3281-3292.

Kabata-Pendias, A., 2010. Trace Elements in Soils and Plants, CRC Press, Boca Raton, USA.

Kaplan, D.I., 2016. SRNL-STI-2016-00267 - Geochemical Data Package for Performance Assessment and Composite Analysis at the Savannah River Site - Supplemental Radionuclides. Savannah River National Laboratory, USA.

Khai, N. M., Öborn, I., Hillier, S., Gustafsson, J. P., 2008. MOdeling of metal binding in tropical Aerisols and Fluvisols treated with biosolids and wastewater. Chemosphere 70, 1338-1346.

Kinniburgh, D.G., van Riemsdijk, W.H., Koopal, L.K., Borkovec, M., Benedetti, M.F., Avena, M.J., 1999. Ion binding to natural organic matter: competition, heterogeneity, stoichiometry and thermodynamic consistency. Colloids Surface A 151, 147–166.

Kowe, R., Norris, S., 2012. Representation of the biosphere in post-closure assessments for the UK geological disposal programme. Mineral. Mag. 76 (8), 3217-3223.

MacDonald, J.D., Hendershot, W.H., 2006. Modelling trace metal partitioning in forest floors of northern soils near metal smelters. Environ. Pollut. 143, 228–240.

Manceau, A., Marcus, M. A., Tamura, N., 2002. Quantitative speciation of heavy metals in soils and sediments by synchrotron X-ray techniques. In: Fenter, P. A., Rivers, M. L., Sturcio, N. C., Sutton, S. R., *Applications of Synchrotron Radiation in Low-temperature Geochemistry and Environmental Science,* Rev. Mineral. Geochem. 49, 341-428.

Maurice, M. D., 2005. Dose-effect relationship and estimation of the cancirogenic effects of low doses or ionizing radiation: the joint report of the académie des sciences (Paris) and of the académie nationale de médecine. Int. J. Radiation Oncology Biol. Phys. 63 (2), 317-319.

Morse, J. W., Arakaki, T., 1993. Adsorption and coprecipitation of divalent metals with mackinawite (FES). Geochim. Cosmochim. Acta 57, 3635-3640.

Moulin, V., Ouzounian, G., 1992. Role of colloids and humic substances in the transport of radioelements through the geosphere. Appl. Geochem. Suppl. Issue (1), 179-186.

NCRP, 1984. Report 76 - Radiological assessment: Predicting the transport, bioaccumulation, and uptake by man of radionuclides released to the environment. National Council on Radiation Protection and Measurements, USA.

NCRP, 2009. NCRP Report No. 160 - Ionizing radiation Exposure of the Population of the United States. National Council on Radiation Protection and Measurements, USA.

Neumann, T., 2012. Fundamentals of aquatic chemistry relevant to radionuclide behaviour in the environment. In: Poinssot, C., Geckeis, H. (Eds.), *Woodhead Publishing Series in Energy: Number 42 - Radionuclide behaviour in the natural environment: Science, implications and lessons for the nuclear industry* (pp. 13-43), Cambridge, UK: Woodhead.

NRC, 2006. Health risks from exposure to low levels of ionizing radiation. BEIR VII Report, Phase II. Washington, USA: National Academy Press.

NUREG, 1981. NUREG/CR-1322 report - Critical Review: Radionuclide transport, sediment transport, and water quality mathematical modelling; and radionuclide adsorption/desorption mechanisms. U.S. Nuclear Regulatory Commission, USA.

NUREG, 1983. NUREG/CR-3332 ORNL-5968 report - Radiological assessment: a textbook on environmental dose analysis. U.S. Nuclear Regulatory Commission, USA.

NUREG, 2000. BR-0217 - The regulation and use of radioisotopes in today's world. U. S. Nuclear Regulatory Commission, USA.

Ochs, M., Lothenbach, B., Wanner, H., Sato, H., Yui, M., 2001. An integrated sorption-diffusion model for the calculation of consistent distribution and diffusion coefficients in compacted bentonite. J. Contam. Hydrol. 47, 283.

OECD, 2000. Guideline for the testing of chemicals: Adsorption-desorption using a batch equilibrium method, Guideline 106. Organisation for Economic Cooperation and Development, France.

Pathak, P.N., Choppin, G.R., 2007. Sorption of Am^{3+} cations on suspended silicate: effects of pH, ionic strength, complexing anions, humic acids and metal ions. J. Radioanal. Nucl. Ch., 274 (3), 517-523.

Pérez-Sánchez, D., Thorne, M. C., 2014. An investigation into the upward transport of uranium-series radionuclides in soils and uptakes by plants. J. Radiol. Prot. 34, 545-573.

Porteous, A., 2008. Dictionary of environmental science and technology. 4th ed. Chichester, UK: Wiley.

Raskob, W., Schneider, T., Gering, F., Charron, S., Zhelezniak, M., Andronopoulos, S., Heriard-Dubreuil, G., Camps, J., 2015. PREPARE: innovative integrated tools and platforms for radiological emergency preparedness and post-accident in Europe. Radiat. Prot. Dosim. 164 (1–2), 170-174.

Rentai, Y., 2011. Atmospheric dispersion radioactive material in radiological risk and emergency response. J. Nucl. Sci. Technol. 1, 7-11.

Sauvé, S., Hendershot, W., Allen, H.E., 2000. Solid–solution partitioning of metals in contaminated soils: Dependence on pH, total metal burden, and organic matter. Environ. Sci. Technol. 34, 1125–1131.

Schröder, T.J., Hiemstra, T., Vink, J.P.M., van der Zee, S., 2005. Modeling of the solid–solution partitioning of heavy metals and arsenic in embanked flood plain soils of the rivers Rhine and Meuse. Environ. Sci. Technol. 39, 7176–7184.

Schulten, H. R., Plage, B., Schnitzer, M., 1991. A chemical structure for humic substances. Naturwissenschaften 78, 311-312.

Selim, H.M., Sparks, D.L., 2010. Heavy Metals Release in Soils. Boca Raton, USA: CRC Press.

Sharmasarkar, S., Vance, G., F., 2002. Selenite-selenate sorption in surface coal mine environment. Adv. Environ. Res. 7, 87-95.

Sheppard, S.C., 2011. Robust Prediction of Kd from Soil Properties for Environmental Assessment. Hum. Ecol. Risk Assess. 17(1), 263-279.

Simon-Cornu, M., Beaugelin-Seiller, K., Boyer, P., Calmon, P., Garcia-Sanchez, L., Mourlon, C., Nicoulaud, V., Sy, M., Gonze, M. A., 2015. Evaluating variability and uncertainty in radiological impact assessment using SYMBIOSE. J. Environ. Radioactiv. 139, 91-102.

SKB, 1991. Technical Report 91-50 - Concentrations of Particulate Matter and Humic Substances in Deep Groundwaters and Estimated Effects on the Adsorption and Transport of Radionuclides, Allard, B., Karlsson, F., and Neretnieks, I., Swedish Nuclear Fuel and Waste Management Co., Sweden.

SKB, 2009. Report R-09-27 - Solid/liquid Partition Coefficients (Kd) for Selected Soils and Sediments at Forsmark and Laxemar-Simpevarp, Sheppard, S., Long, J., Sanipelli, B., Sohlenius, G., Swedish Nuclear Fuel and Waste Management Co., Sweden.

SKB, 2013a. Report R-13-1 – Kd and CR used for transport calculations in the biosphere in SR-PSU. Tröjbom, M., Grolander, S., Rensfeldt, V., Nordén, S., Swedish Nuclear Fuel and Waste Management Co., Sweden.

SKB, 2013b. Report R-13-6 - The Biosphere model for radionuclide transport and dose assessment in SR-PSU. Saetre, P., Nordén, S., Keesmann, S., Ekström, P.A., Swedish Nuclear Fuel and Waste Management Co., Sweden.

Sposito, G., 2016. The Chemistry of Soils, New York: Oxford University Press.

Stansby, S.J., Thorne, M.C., 2000. AEA Technology Report AEAT/R/ENV/0296 - Generic Biosphere Modelling: Final Report to United Kingdom Nirex Limited, UK.

Stenhouse, M. J., 1994. Technical Report NTB 93-06 - Sorption Databases for Crystalline, Marl and Bentonite for Performance Assessment. NAGRA, Switzerland.

Stevenson, F. J., 1992. Humus Chemistry. Genesis, Composition and Reactions. New York, USA: Wiley.

Stumm, W., Morgan, J. J. , 2012. Aquatic Chemistry, Chemical Equilibria and Rates in Natural Waters, New York, USA: John Wiley & Sons, Inc.

Sy, M., Gonze, M. A., Métivier, J. M., Nicoulaud-Gouin, V., Simon-Cornu, M., 2016. Uncertainty analysis in post-accident risk assessment models: application to the Fukushima accident. Annals of Nuclear Energy 93, 94-106.

Thibault, D. H., Shepard, M. I., and Smith, P. A., 1990. AECL- 10125 - A Critical Compilation and Review of Default Soil Solid/Liquid Partition Coefficients, Kd, for Use in Environmental Assessments. Atomic Energy Canada Ltd., Canada.

Thorne, M. C., Kelly, M., Rees, J. H., Sánchez-Friera, P., Calvez, M., 2002. A model for evaluating radiological impacts on organisms other than man for use in post-

closure assessments of geological repositories for radioactive waste. J. Radiol. Prot. 22, 249-277.

Thorne, M. C., 2003. Background Radiation: Natural and Man Made. J. Radiol. Prot. 23, 29-42.

Thorne, M., Maul, P., Robinson, P., 2004. Report QRS-1198A-1 - The PRISM food chain modelling software: model structures for PRISM 2.0. Food Standards Agency, UK.

Tipping, E. 1998. Humic ion-binding model VI: an improved description of the interactions of protons and metal ions with humic substances. Aquat. Geochem. 4, 3–48.

Tipping, E., Rieuwerts, J., Pan, G., Ashmore, M.R., Lofts, S., Hill, M.T.R., Farago, M.E., Thornton, I., 2003. The solid–solution partitioning of heavy metals (Cu, Zn, Cd, Pb) in upland soils of England and Wales. Environ. Pollut. 125, 213–225.

UNSCEAR, 2000. Sources and Effects of Ionizing Radiation. Vol. II Effects, United Nations Scientific Committee on the Effects of Atomic Radiation. United Nations, USA.

Velasco, H.R., Ayub, J.J., Belli, M., Sansone, U., 2006. Interaction matrices as a first step toward a general model of radionuclide cycling: application to the 137Cs behavior in a grassland ecosystem. J. Radioanal. Nucl. Ch. 268, 503–509.

Vernadsky, V., 1998. The biosphere. New York: Copernicus.

Walke, R., Thorne, M., Limer, L., 2013. AMEC Report 18025/TR/002 - RWMD Biosphere Assessment Model: Terrestrial Component. AMEC Nuclear UK Limited, UK.

Wang, Y. Q., Fan, Q. H., Li, P., Zheng, X. B., Xu, J. Z., Jin, Y. R., Wu, W. S., 2011. The sorption of Eu(III) in calcareous soil: effect of pH, ionic strength, temperature, foreign ions and humic acid.

Wang, T. H., Li, M. H., Teng, S. P., 2009. Bridging the Gap between Batch and Column Experiments: A Case Study of Cesium Adsorption on Granite. J. Hazard. Mater. 161, 409–415.

Weng, L.P., Temminghoff, E.J.M., van Riemsdijk, W.H. 2001. Contribution of individual sorbents to the control of heavy metal activity in sandy soil. Environ. Sci. Technol. 35, 4436–4443.

Weng, L.P., Temminghoff, E.J.M., Lofts, S., Tipping, E., van Riemsdijk, W.H., 2002. Complexation with dissolved organic matter and solubility control of heavy metals in a sandy soil. Environ. Sci. Technol. 36, 4804–4810.

Xu, C., Athon, M., Ho, Y. F., Chang, H. S., Zhang, S., Kaplan, D., Schwehr, K., DiDonato, N., Hatcher, P. G., Santschi, P. H., 2014. Plutonium immobilization and re-mobilization by soil mineral and organic matter in the far-field of the Savannah River Site, USA, Environ. Sci. Techno. 48, 3186-3195.

Ye, Y., Chen, Z., Montavon, G., Jin, Q., Guo, Z., Wu, W., 2014. Surface complexation modeling of Eu(III) adsorption on silica in the presence of fulvic acid. Sci. China. Chem. 57 (9), 1276-1282.

Zavarin, M., Roberts, S. K., Hakem, N., Sawvel, A., M., Kersting, A., B., 2005. Eu(III), Sm(III), Np(V), Pu(V), and Pu(IV) sorption to calcite. Radiochim. Acta 9, 93-102.

CHAPTER 2. MOTIVATION AND OBJECTIVES

The assessment of the potential radiological risk for the human health and the environment that a radioactive contamination episode may entail is one of the most concerning issues in the current society, due to the increasing amounts of radioactive waste resulting from the proliferation of the nuclear industry and other activities. Such assessment is performed by taking into account a large number of environmental components, processes and interactions occurring in a given contamination scenario and governing the transport of radionuclides from the source point of contamination to a potential target individual. In those radioactive contamination episodes in which the terrestrial ecosystem may be affected, one of the key processes to be described, in order to properly assess the potential human exposure to radioactivity, is the partitioning of released radionuclides between water sources and soils in a given contaminated area, since it controls in a great extent radionuclide transport to non-contaminated areas and subsequent introduction into the food chain. Such process can be estimated with the solid-liquid distribution coefficient (K_d), which is a highly operational parameter that for a given radionuclide may remarkably vary depending on the soil-solution system characteristics.

In light of this, **the aim of this thesis is the development of strategies to provide reliable solid-liquid distribution coefficients (K_d) of radionuclides in soils as input data for models devoted to assess the radiological risk that could be arisen from radioactive contamination episodes involving the terrestrial ecosystem.** To reach this goal, two different approaches aiming at reducing and explaining the variability of this parameter and based on the knowledge of the specific radionuclide-soil interaction behaviour, are explored.

On the one hand, despite being paramount elements in the field of radioactive waste management and nuclear safety, there is limited knowledge regarding the interaction in soils of trivalent actinides and lanthanides, such as americium (Am) and samarium (Sm), respectively. Due to the scarce and highly variable soil K_d data available in the literature for these elements, and the unclear conclusions about their sorption mechanisms and the soil properties involved, the proposal of reliable K_d data for risk assessment purposes is seriously jeopardised. According to this, the present thesis is focused on **the examination of the main factors controlling the interaction of**

trivalent actinides and lanthanides in soils, which leads to the following specific objectives:

- To study the sorption and desorption behaviour of Am and Sm radioisotopes in a collection of soils with contrasting properties.
- To identify the soil-solution system characteristics involved in the interaction processes of Am and Sm and to develop parametric models for the prediction of K_d values of these elements in soils.
- To check the analogy between Am and Sm interaction in soils to demonstrate the suitability of using K_d data of trivalent lanthanides (stable isotopes and radioisotopes) to foresee the soil interaction of trivalent actinides and *vice versa*.
- To evaluate the dependency of Sm interaction in soils as a function of its concentration.

On the other hand, due to the lack of site-specific K_d data, radiological risk is frequently assessed with models using, as input data, generic soil K_d values of radionuclides. Such generic K_d data (single values or functions) most of times are statistically derived from compilations in which K_d values may range within several orders of magnitude as a result of contrasting sorption behaviour among the soil-solution systems involved. This fact leads to a high uncertainty in the description or prediction of radionuclide soil-to-solution partitioning in the contamination scenario under assessment. According to this, the present thesis is also committed to **the development of a strategy to derive probabilistic K_d data from compilations with low uncertainty and suitable to perform reliable risk assessments.** To this end, three radionuclides, Cs, U and Am, have been used as case studies, and the following specific objectives are drawn:

- To construct an updated and critically reviewed compilation of K_d data of radionuclides in soils to be used for the development of probabilistic K_d models.

- To evaluate the most suitable criteria to create group K_d values according to soil characteristics (*e.g.*, pH, texture, organic matter content, etc.) and factors related to the experimental approach applied (*e.g.*, sorption *vs.* desorption test or effect of sorption dynamics) for the quantification of the K_d governing the radionuclide-soil interaction.

- To propose cumulative distribution functions of K_d values for different soil groups created according to the developed and optimised K_d grouping criteria.

- To check the viability of using K_d data gathered from geological materials other than soils (analogue material approach) and for elements chemically analogue to the target element (chemical analogue approach) to enhance datasets containing insufficient entries of the target element and to derive reliable probabilistic K_d data.

CHAPTER 3. ASSESSING THE INTERACTION OF TRIVALENT ACTINIDES AND LANTHANIDES IN SOILS

3.1 INTRODUCTION

Large amounts of waste containing radionuclides (RN) are generated every year and its production is expected to increase in the future because of the nuclear energy proliferation. Up to now, uncontrolled releases of large quantities of RNs to the biosphere have already occurred due to many reasons, for instance, nuclear weapon tests, military nuclear accidents (*e.g.* Palomares, Spain, 1966; Thule, Greenland, 1968), nuclear power plants disasters (*e.g.* Three Mile Island, U.S., 1979; Chernobyl, Ukraine, 1986; Fukushima, Japan, 2011) or incidents during the nuclear fuel reprocessing and radioactive waste management (*e.g.* Tomks, Russia, 1993; Tokaimura, Japan, 1999) (Sovacool, 2010). Safe waste management systems are crucial given that radioactive waste represents a potential hazard to the environment and human health, especially the high level radioactive waste (HLRW) rich in long-lived RNs. Although considerable progress has already been achieved in the safe disposal of radioactive waste towards its isolation for a period of time long enough to diminish the potential radiological risk that could be derived from an eventual human exposure (NAGRA, 1988; NEA, 2000; NEA, 2008; OECD/NEA, 1995), accidents during the radioactive waste management or the release of RNs from HLRW to deep groundwater in the long-term could lead to the incorporation of significant amounts of RNs into the biosphere. Besides this, also a small fraction of the RNs produced in nuclear power plants and fuel-cycle facilities is released in airborne and liquid form to the environment during their normal operation (OECD/NEA, 2003). Therefore, the potential emission of RNs into the environment should always be considered.

Since radioactive releases may imply a negative impact to the environment and human health, it is essential that the risk derived from contamination episodes can be assessed within decision support systems. For this reason, the development of reliable risk assessment tools and platforms (*e.g.* DCAL, RESRAD, ERICA, RODOS, SYMBIOSE, etc.) aiming to properly estimate the radiological dose arisen from radiation exposure, or to foresee the potential hazard that could be derived from an eventual radiological contamination, has become a key issue in radioecology (IAEA, 2001). Radioactive risk assessment is based on the parameterisation and quantification of the processes governing the fate and transport of RNs among ecosystems and the subsequent transfer to the food web and human beings, as well as

on the determination of the main exposure pathways for a given individual. In the specific case of terrestrial ecosystems, the performance of radiological risk assessments often implies the development and application of reactive transport models for porous media, which require reliable input data for those parameters that describe the behaviour of RNs in the target matrices (IAEA, 2001). Given that soils play a key role in governing the transfer of RNs to other environmental compartments and to the food chain, it is essential that the interaction of RNs in soils be parameterised in order to assess radiological risk in scenarios involving terrestrial ecosystems (IAEA, 2009). In this context, the solid-liquid distribution coefficient (K_d) of RNs in soils is a parameter frequently used in risk assessment models since it gives information on the extent to which RNs are sorbed and retained in the soil matrices, and thus, it allows foreseeing the RN mobility to bordering water sources (*e.g.*, due to soil weathering processes and RN migration to groundwater) or its potential availability and uptake by plants present in the affected soils (EPA, 1999; IAEA, 1994). However, soils are heterogeneous materials with contrasting physicochemical properties and capacities to sorb RNs. Consequently, K_d values for a given element can range within several orders of magnitude depending on the soil studied (IAEA, 1994; IAEA, 2009). In that case, unless site-specific K_d data are available, representative for the field conditions to be assessed, the proposal of a single K_d value as input data for models cannot be used as a scientifically based option, since the intrinsic K_d variability may jeopardise its suitability for risk assessment purposes. Therefore, for a given element not only it is important to quantify its sorption and desorption degree in soils through determining K_d values, but also a further step must be taken towards identifying the factors affecting and controlling its soil interaction in order to be able to foresee RN sorption in other soil-solution system conditions by means of predicting K_d values.

3.1.1 Radiological concern regarding soil contamination with trivalent actinides and lanthanides radionuclides

While the interaction mechanisms in soils have been ascertained for a limited number of RNs, such as radiocaesium, radiostrontium or uranium (Gil-García et al., 2009a; Vandenhove et al., 2009), less is known about other families of elements the radioisotopes of which can be found at relevant amounts in the radioactive waste, some of them presenting a very high radiotoxicity for the environment and human health both in the short- and long-term. For instance, there are scarce sorption data of lanthanides and transuranic actinides as well as there is a lack of knowledge regarding their interaction mechanisms in soils (Gil-García et al., 2009b). Among these, americium (Am) and samarium (Sm), a trivalent actinide (Ac(III)) and lanthanide (Ln(III)) element, respectively, are of special concern in the radioactive waste management and nuclear safety fields.

Am is a radioactive transuranic element artificially originated in nuclear reactors due to decay of Pu isotopes and subsequent neutron capture (see Figure 3.1). Am is one of the so-called minor actinides, a family of elements named after being present in the spent nuclear fuel (SNF) in much lesser amounts than U and Pu. The longest-lived and most prevalent Am radioisotopes in nuclear waste are the alpha emitters ^{241}Am ($t_{1/2}$ = 432.2 years) and ^{243}Am ($t_{1/2}$ = 7370 years), which pose a high risk to the environment due to their high radiotoxicity, and are among the top five radioisotopes contributing the most to bulk radioactivity and heat of the SNF in the period of time comprised between 300 and 20,000 years after fuel burn-up (National Research Council, 1999). On the other, significant amounts of radioactive and stable isotopes of Sm are produced as a result of ^{235}U nuclear fission during nuclear fuel burn-up and the neutron capture processes occurring in the subsequent SNF cooling period (GRS, 2012; Magill et al., 2003). Consequently, Sm radioisotopes can be found in radioactive waste, especially at higher levels in those resulting from SNF reprocessing (GRS, 2012; IAEA, 2004). Among all Sm radioisotopes, the medium-lived beta emitter ^{151}Sm ($t_{1/2}$ = 90 years) is of paramount importance when analysing nuclear waste disposal safety, since in surface repositories containing low and intermediate level radioactive waste (LILRW) Sm is expected to be one of the main contributors to the external dose

in the stint comprised between 100 and 500 years after closure of these nuclear facilities (Rego et al., 2011; SKB, 1997).

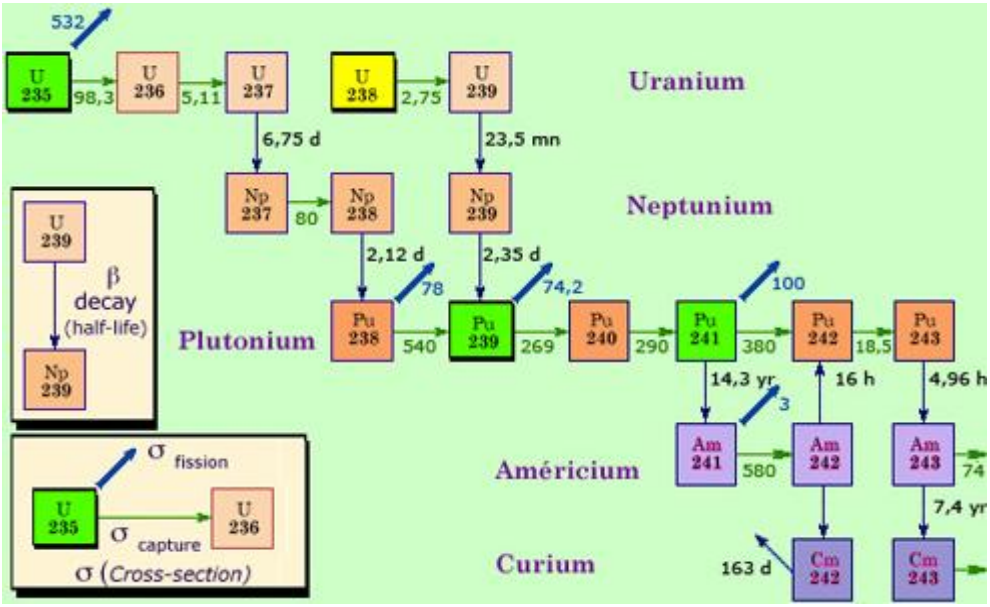

Figure 3.1 *Generation of minor actinides from ^{235}U present in nuclear fuel. From IN2P3, 2017.*

Despite the relevancy of these elements, the sorption and desorption pattern in soils has not yet been fully clarified for Am and Sm because soil interaction data of these elements and, specifically, K_d values, are scarce and affected by a high degree of variability, which makes impossible to foresee the Am and Sm interaction in soils (Gil-García et al., 2009b). Conversely, much is known regarding the interaction of Ac(III) and Ln(III), such as Am or Eu, with pure mineral phases much simpler than soils (*e.g.* silica, pyrite, granite or clay minerals). There are evidences that the interaction of Ac(III) and Ln(III) with pure mineral phases appears to be namely controlled by the formation of surface complexes with iron and manganese oxides, phyllosilicates and carbonates minerals or with the organic matter coatings present in some mineral particles (Fan et al., 2010; McCarthy et al., 1998; Pavlotskaya et al., 2003; Takahashi et al., 1998; Tanaka and Muraoka, 1999; Ye et al., 2014). Besides this, it is known that speciation in solution of Ac(III) and Ln(III) elements is highly pH-dependent and involves hydrolysis and complexation reactions with organic and inorganic ligands, such as fulvic/humic acids and carbonate ions (Das et al., 2009; Ho Lee et al., 2011; Lujaniene et al., 2007; Pathak and Choppin, 2007).

As explained in Chapter 1, soils are complex matrices containing several of the abovementioned phases interacting with Ac(III) and Ln(III) elements. Taking into account that the RN-soil interaction is dominated by multiple, interlinked geochemical processes dominating the RN aqueous speciation and affinity for sorption sites that are highly dependent on the soil properties (*e.g.*, pH, organic matter nature and solubility or mineralogy), it is difficult to foresee the overall interaction of Ac(III) and Ln(III) elements, such as Am or Sm, in a given soil as the sum of the individual contribution of each soil constituent and, thus, studies in soils must be undertaken. The use of univariate and multivariate analyses might provide valuable information to deal with the complexity of Am and Sm interaction with soils and to help in the identification of the key soil factors controlling their sorption in soils, or even the elucidation of the sorption processes or mechanisms involved (EPA, 1999). Both approaches have been successfully applied in previous environmental studies, either to describe the sorption of radionuclides in soils (Gil-García et al., 2011a and 2011b; Ishikawa et al., 2009; Sheppard, 2011), or to predict radionuclide soil-to-plant transfer (Rigol et al., 2008). One of the main goals of the present Thesis is to study the interaction of Am and Sm radioisotopes, represented here by ^{241}Am and ^{151}Sm, in a collection of soils with contrasting properties so as to obtain a global sorption-desorption pattern in soils, to identify the soil properties governing the Am and Sm sorption behaviour and, if possible, to develop and validate models capable to successfully predict Am and Sm K_d values in soils just by using soil properties.

Furthermore, Ac(III) and Ln(III) elements are frequently considered as chemical analogues due to their similar chemical properties, such as ionic radii, coordination number and oxidation state. In fact, stable Ln(III) isotopes, like those of Eu or Sm, have been used as surrogates of radioisotopes of Ac(III) relevant in the context of radioactive waste management, including curium (Cm) and americium (Am), to study their interaction with matrices such as engineered barrier materials, rocks and clay minerals (Krauskopf, 1986; McCarthy et al., 1998; SKB, 1995 and 1997). Although a few studies have tested the similarity between Ac(III) and Ln(III) elements in terms of their sorption in geological materials (*e.g.* Lee et al., 2006), there have been no quantitative studies that have tested the suitability of using Ln(III) as chemical analogues of Ac(III), and *vice versa*, for interaction studies in soils. Therefore, in the present Thesis the analogy between Am and Sm regarding their sorption-desorption

behaviour in soils is also studied with the aim of demonstrating the suitability of using indistinctly Ln(III) or Ac(III) sorption data to foresee the interaction in soils of radioisotopes of both families.

3.1.2 Soil contamination scenarios with high loads of lanthanides: the role of concentration

Sm, along with the rest of lanthanides, have unique physico-chemical properties and have recently become key elements in agriculture and industrial activities like metallurgy, electronics or materials synthesis (Awual et al., 2013). The increasing relevancy and use of these elements have led to an enhancement of the Sm anthropogenic input in the environment due to the intensive exploitation of mines rich in lanthanide elements (Jinxia et al., 2010; Li et al., 2013; Liang et al., 2014), the discharge of effluents and wastes enriched with these elements (Ali, 2014; He et al., 2010) and the extensive application of fertilisers as plant growth promoters in land fields (Cao et al., 2001; Pang et al., 2001; Tyler, 2004; Zhang et al., 2000). The anthropogenic contribution of lanthanide elements in some cases is so high that there are evidences of contamination of watersheds and soils affected by lanthanides discharges, which has arisen special concern about the potential harmful implications that could be derived for non-human biota and human health (Ali, 2014; Humsa and Srivastava, 2015; Jinxia et al., 2010; Li et al., 2013; Zhao et al., 2017; Zhu et al., 1997).

Previous studies evidenced that the sorption and retention in clay minerals and soils of different Ln(III), such as La, Pr, Gd or Lu, were highly dependent on their concentration in solution (Galunin et al., 2009 and 2010; Jones, 1997; Zhu et al., 1993). Although Am and Sm RNs are expected to be present at low concentrations in the liquid sources that could potentially enter in contact with soils, such as leaks or spills of radioactive liquid waste or leachates coming from solid waste, it is feasible that elements that could behave similarly to Am or Sm, *i.e.* stable isotopes of other Ac(III) and Ln(III) elements, may be present in much higher concentrations. In that case the assumption of linear sorption of Am and Sm in soils would be no longer plausible and thus, sorption isotherms models representative for wider

concentrations ranges would be necessary to properly describe and foresee the effect of concentration in the interaction of Am and Sm.

There is a large extent of literature available aiming at studying the distribution and abundance of lanthanides either in natural waters (Elbaz-Poulichet and Depuy, 1999; Gimeno-Serrano et al., 2000; He et al., 2010; Migaszewski et al., 2014; Wood et al., 2006) or in solid environmental materials such as sediments or soils (Cheng et al., 2012; Hu et al., 2006; Liang et al., 2014; Wang and Liang, 2015; Zhu et al., 2002; Zhu et al., 2012), whereas only few works dedicated to deeply study the effect of geochemical factors on the interaction of lanthanides in soils or sediments can be found (Cao et al., 2000; Cao et al., 2001; Li et al., 2000 and 2001; Shan et al., 2002; Wang et al., 2011; Wetje et al., 2002), none of them dealing with the study of the combined effect of soil properties and concentration dependency on the interaction with soils of Ln(III) or Ac(III) elements. According to this, the present Thesis is also devoted to study the sorption-desorption behaviour of Sm in a set of soil samples with contrasting edaphic properties as a function of Sm concentration. The goal is not only to provide Sm sorption isotherms models for different soil-types, but also to explain the role of Sm concentration on the interaction of this element in soils in terms of the soil phases and sorption mechanisms involved, in order to enable the extrapolation of the isotherm sorption models, constructed here for a group of soils, to other scenarios.

3.2 MATERIALS AND METHODS

3.2.1 Soil samples and sample characterization

A total of thirty soil samples with contrasting characteristics were selected from an already existing soil collection of our research group. Most of them were natural and agricultural soils integrated within the Spanish radioactive monitoring network, collected in a sampling campaign carried out in a previous work (Gil-García et al., 2008). Additionally, with the aim of having a set of soils with edaphic properties as much contrasted as possible, some peat soils originated from wet meadows of Ukraine, Belarus and United Kingdom were also included.

All soil samples were taken from the surface layer (0-10 cm), air-dried, sieved through a 2 mm mesh, homogenised with a roller table and stored in plastic bottles until analyses. An extensive physico-chemical characterisation of the samples was carried out. cation exchange capacity (CEC) was determined as the sum of exchangeable bases plus the exchangeable acidity obtained by displacement with $BaCl_2$-triethanolamine solution buffered at pH 8.2 (Burt, 2004). Lost on ignition content (LOI) content was determined as the loss of soil weight by heating 2 g of each soil sample at 450°C for 16 h in a muffle furnace. Organic carbon content (C_{org}) was determined in the samples pre-treated with 2 mol L^{-1} HCl to eliminate carbonates by Thermo EA 1108 elemental analyser (ThermoScientific, Italy) using tin capsules and V_2O_5 as additive (ISO, 1995). The carbonate content ($CaCO_3$) was determined by using the calcimeter Bernard method (Muller and Gastner, 1971). Particle size distribution (Clay% and Sand%) was also determined by the pipette method (Burt, 2004) and specific surface area of soils was determined by the BET method (BET), consisting of N_2 adsorption after degasification at 100°C (Fagerlund, 1973). Finally, the iron and manganese amorphous contents (Fe_{amorph} and Mn_{amorph}) were quantified by means of ascorbate extraction (Kotska and Luther, 1994), whereas the content of aluminium amorphous content (Al_{amorph}) was determined by extraction with oxalic acid under darkness (Carter and Gregorich, 2006). **Table 3.1** shows the main characteristics of the soil samples, with wide ranges of values for most variables, thus confirming that the selected soil samples represent varying soil scenarios.

In addition, supernatant solutions were obtained by equilibrating each soil sample with deionised water under the same conditions (solid-to-liquid ratio and contact time) as those applied in the sorption tests (see following Section 3.2.2.1) and were also characterised in terms of: pH, dissolved organic carbon (DOC), dissolved inorganic carbon (DIC) and concentration of major cations (Ca, Mg, K and Na).

DOC content was determined by catalytic oxidation combustion of supernatant solutions at 680°C using the Total Organic Carbon analyser Shimadzu TOC-5000A with nondispersive infrared sensor (Shimadzu, Japan), with a previous acidification with HCl to pH 3 to remove carbonates in solution. DIC content was calculated as the difference between the Total Carbon content, determined as DOC but without the acidification step, and the DOC content.

The concentration of major cations was determined by inductively coupled plasma optical emission spectrometry (ICP-OES) (Thermo-Jarrell Ash 25 and Perkin Elmer Optima 3200 RL, USA). The following emission lines were used (nm): Ca: 315.887 and 317.933, Mg: 279.077 and 285.213, K: 766.490, and Na: 330.237. The detection limits of ICP-OES were 0.1 mg L^{-1} for Ca and Mg, 1 mg L^{-1} for K, and 5 mg L^{-1} for Na. **Table 3.2** summarises the characterisation data gathered from the soil supernatant solutions.

Table 3.1 Soil characteristics concerning soil solid phases.

Soil Sample	Clay (%wt)	Sand (%wt)	$CaCO_3$ (%wt)	C_{org} (%wt)	LOI (%wt)	Al_{amorph} (mg kg^{-1})	Fe_{amorph} (mg kg^{-1})	Mn_{amorph} (mg kg^{-1})	CEC ($cmol_c$ kg^{-1})	BET (m^2 g^{-1})
ANDCOR	18.3	39.1	2	9.3	19	2725	465	85	54.2	4.5
ASCO	16.9	18.5	38	0.2	1.6	504	407	87	40.8	11
BAD1	19.4	50.2	2	0.9	2.8	493	581	168	22.0	8.7
CABRIL	20.0	57.5	2	1.4	6.0	477	371	415	19.3	9.5
ENUSA	10.9	64.2	6	3.2	5.2	1880	3160	504	19.6	0.9
GRACOR	19.3	34.5	2	0.8	5.9	440	182	78	28.6	11
TRILLO	24.4	23.2	43	1.9	4.9	322	64	31	30.4	15
BILBAO	21.0	42.5	3	4.1	6.5	397	2247	4018	41.6	14
DELTA2	33.5	12.2	51	7.7	23	230	2966	330	87.3	6.5
FONCOR	13.1	59.8	2	8.4	17	1687	1508	330	43.0	1.8
GARROÑA	27.9	15.0	43	2.2	6.9	73	77	120	32.7	9.9
LEON	26.6	31.8	5	7.0	15	268	2618	1706	46.1	1.9
MALAGA	49.9	4.3	12	0.9	4.9	160	136	405	28.5	47
OVI01	18.9	41.3	3	9.4	20	377	4515	390	44.3	1.8
TEN1	15.5	54.6	2	0.6	3.7	783	127	2073	64.2	30

Table 3.1 Soil characteristics concerning soil solid phases (Cont'd).

Soil Sample	Clay (%wt)	Sand (%wt)	$CaCO_3$ (%wt)	C_{org} (%wt)	LOI (%wt)	Al_{amorph} (mg kg^{-1})	Fe_{amorph} (mg kg^{-1})	Mn_{amorph} (mg kg^{-1})	CEC ($cmol_c$ kg^{-1})	BET (m^2 g^{-1})
VAN1	6.2	85.6	5	0.3	1.4	138	238	150	25.3	22
ZORITA	20.8	41.0	40	1.0	5.3	118	56	199	27.1	14
MATEIKI	7.8	66.2	0.8	9.4	26	280	4552	583	55.0	0.4
REDSTONE	7.6	46.4	1.3	9.3	46	584	4421	114	60.2	1.1
DUBLIN	1.3	20.7	1.6	39	78	167	10640	1443	140	0.6
DELTA1	29.3	41.2	29	6.3	15	702	10091	366	65.2	0.6
VAN2	22.2	30.4	29	1.7	5.3	2138	459	110	35.6	23
ALMERIA	10.6	54.4	2	1.6	3.6	404	1013	204	23.4	2.0
GOLOSO	9.8	73.4	4	3.9	5.9	325	138	336	72.4	0.7
FROCOR2	14.5	62.2	5	6.3	12	1390	1015	61	48.1	1.2
UPV	18.9	24.4	17	0.8	2.6	183	56	11	21.5	11
AYUD	34.1	20.6	19	1.7	6.4	665	205	76	49.7	31
UIAR	3.0	46.0	0.2	27	46	1732	6502	556	90.0	0.5
KOM	1.1	20.0	0.5	41	70	481	19668	393	114	0.8
BRA	2.0	35.0	2	32	55	1027	12358	598	103	0.6

Table 3.2 Characteristics of soil supernatant solutions.

Soil Sample	pH	DIC (mg L^{-1})	DOC (mg L^{-1})	Ca (mg L^{-1})	Mg (mg L^{-1})	K (mg L^{-1})	Na (mg L^{-1})
ANDCOR	4.9	1	78	4	9	3	2.8
ASCO	8.4	5	5	134	4	5	0.7
BAD1	7.7	15	11	44	13	4	1.4
CABRIL	6.4	3	10	5	3	2	1.1
ENUSA	6.5	5	14	32	2	2	0.4
GRACOR	5.9	1	9	29	5	2	2.8
TRILLO	7.9	23	12	76	5	6	0.2
BILBAO	7.0	8	14	39	3	8	1.2
DELTA2	8.0	32	39	79	17	5	93
FONCOR	6.4	7	41	53	9	4	3.6
GAROÑA	7.6	28	20	93	5	12	0.9
LEON	6.4	19	72	63	5	1	2.3
MALAGA	8.0	22	10	68	10	10	3.2
OVI01	5.2	11	250	55	4	3	2.1
TEN1	9.9	18	18	7	2	9	74
VAN1	9.9	6	4	75	3	1	1.4
ZORITA	8.5	11	7	80	2	3	0.3
MATEIKI	6.2	7	94	62	4	1	5.2
RED STONE	3.9	5	180	6	4	7	2.0
DUBLIN	5.7	29	290	54	9	6	4.4
DELTA1	5.2	2	230	69	12	7	5.2
VAN2	7.6	139	1	81	3	2	2.0
ALMERIA	5.5	1	15	24	3	3	0.8
GOLOSO	5.9	1	14	36	3	3	0.3
FROCOR2	5.6	5	67	8	13	10	18
UPV	7.0	73	1	444	5	5	0.6
AYUD	7.4	138	8	71	14	7	1.7
UIAR	5.8	11	180	68	7	2	4.8
KOM	5.7	12	187	70	8	5	4.0
BRA	5.7	12	175	72	13	3	2.5

3.2.2 Quantification of soil interaction parameters

3.2.2.1 Batch sorption and desorption tests

A series of batch sorption and desorption tests were applied following the procedure summarised in **Figure 3.2** in order to estimate the interaction of Am and Sm in soils. On the one hand, ^{241}Am and ^{151}Sm radiotracers were used to evaluate the capacity of soils to sorb these elements at concentrations relevant for radioactive level and, on the other, stable Sm was used to perform a series of tests at varying initial Sm concentration. The sorption test consisted in mixing each soil sample with double-deionised water at a solid-to-liquid ratio of 1 g/25 ml in 80 mL polypropylene centrifuge tubes and the suspensions were shaken for 16 h using an end-over-end shaker at 60 rpm. Afterwards, each resulting suspension was spiked with a volume of a solution containing the target element to have a known initial concentration in solution (C_i), 10^5 Bq L^{-1} for the case of radiotracers and between 10^{-2} meq L^{-1} and 10 meq L^{-1} for stable Sm. The spiking radiotracer solutions were prepared from ^{241}Am and ^{151}Sm stock solutions (Eckert&Ziegler, Germany), whereas stable Sm solutions were directly prepared from $Sm(NO_3)_3$ 99.9% pure salt (Sigma-Aldrich, Germany). The spiked suspensions were equilibrated again for 24 h, the final suspensions were centrifuged (12880 *g*, 30 min, 10°C) using a Beckman J2-HS centrifuge with a rotor JA14 (Beckman, Ireland), the supernatant solutions were decanted off, filtered through 0.45 µm nylon syringe filters, transferred to 20 mL polyethylene vials and stored at 4°C until analysis.

For ^{241}Am sorption tests were applied to 20 soil samples by duplicate, whereas for ^{151}Sm sorption tests were applied by triplicate to a total of 30 soils including the 20 soils used for Am. It was checked that the relative error between K_d values gathered from replicates was always lower than 10%. Finally, sorption tests were applied to 5 soil samples selected from those used in the experiments with radiotracers at varying initial concentration of stable Sm (a minimum of 9 concentrations comprised between 10^{-2} and 10 meq L^{-1} were tested).

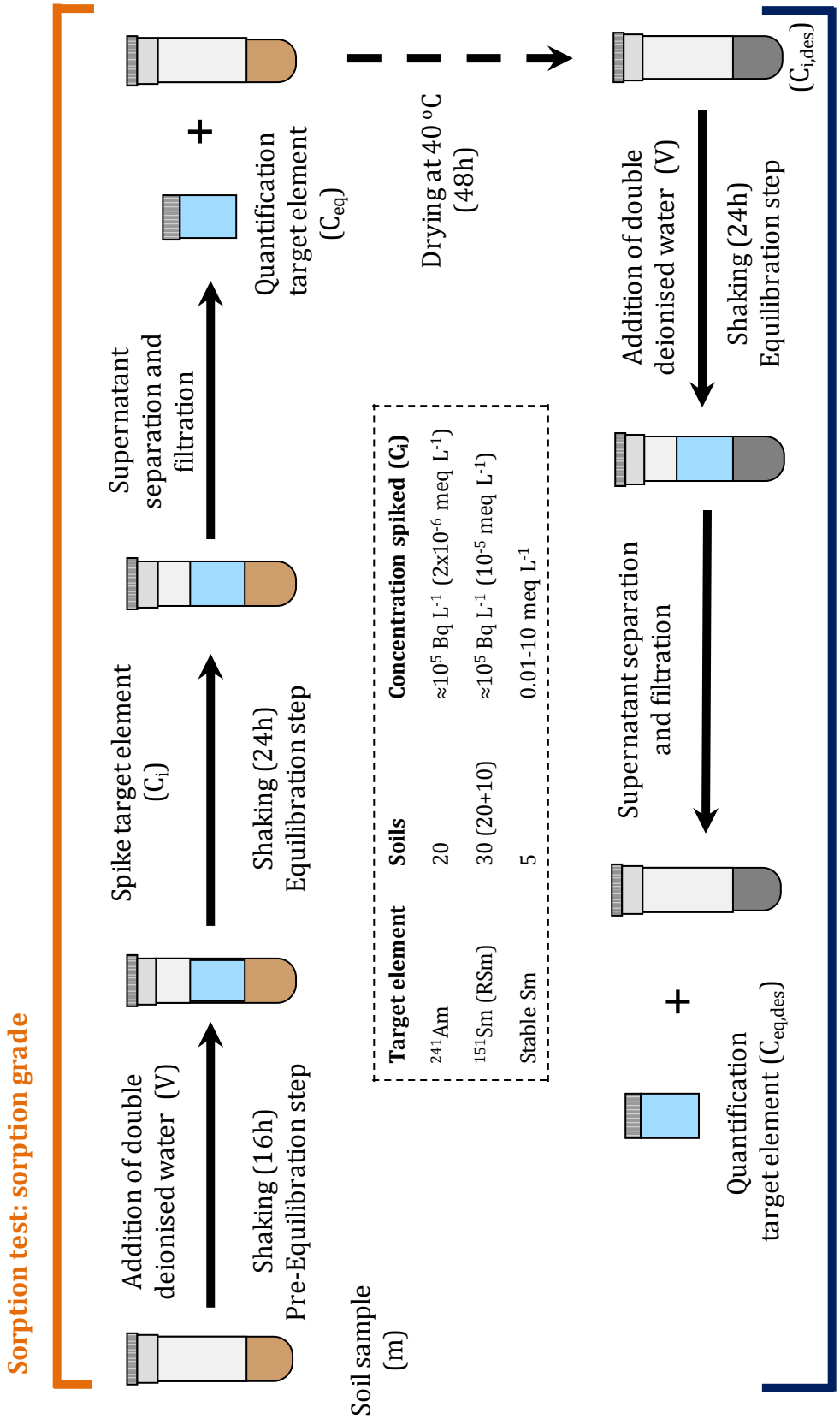

Figure 3.2 *Scheme of batch sorption and desorption tests.*

The sorption reversibility of the target elements in each soil sample was evaluated by applying a desorption test to the soil residues originated from the previous batch sorption experiments. To this end, soil residues were firstly dried at 40°C for 48 h to simulate the aging process that occurs at field scenarios and, subsequently, a single extraction was carried out under the same experimental conditions as those of the sorption test, *i.e.* same equilibration time (24 h), solid-to-liquid ratio (1 g/25 mL) and contact solution (double deionised water). The obtained supernatant solutions were centrifuged, decanted-off, filtered through 0.45 μm, transferred to 20 mL polyethylene vials and stored at 4ºC until analysis. For radiotracers, the desorption test was applied to one of the sorption residues of each soil sample, whereas for stable Sm it was applied to a selection of four sorption residues corresponding to four initial Sm concentrations.

Moreover, for each soil sample a blank assay was also carried out in parallel following the sorption and desorption procedure explained above, but without spiking with the solution containing the target element. Aliquots of the supernatant solutions resulting from the sorption blank assays were used to obtain a series of characterisation data, as explained before. Additionally, aliquots of both sorption and desorption blank assays were also used as measurement blanks for the proper quantification of the target elements.

3.2.2.2 Fractionation of stable Sm sorbed in soils

Consecutive extractions were applied to the soils contaminated with stable Sm originated in the previous sorption experiments in order to distinguish the following sorbed Sm fractions:

- F1: 0.01 mol L^{-1} $CaCl_2$; electrostatically weakly bound (Houba et al., 2000).
- F2: 0.43 mol L^{-1} CH_3COOH; sensitive to acidification processes *(e.g*., bound to carbonates) (Quevauviller et al., 1997).
- F3: 0.1 mol L^{-1} NaOH; bound to labile organic matter (*e.g.*, humic and fulvic acids) (Shand et al., 1994),;
- Residue: bound to non-soluble organic matter and/or mineral phases (*e.g.*, humin or clay minerals).

Two soil sorption residues corresponding to low and high loads of stable Sm (C_i approximately 0.06 meq L^{-1} and 6 meq L^{-1}, respectively) were selected for each soil sample. The extractions were performed by mixing 1 g of soil sorption residue with 40 mL of extract solution and shaking the mixture in an end-oven-end for 16 h at room temperature. Afterwards, the soil suspensions were centrifuged and the supernatant solutions were decanted-off, filtered through 0.45 µm nylon syringe filters, placed in plastic vials, diluted with 1% HNO_3 and stored at 4ºC until their analysis.

3.2.2.3 Analytical measurements of target elements

Determination of ^{241}Am activity concentration in liquid samples derived from the sorption and desorption experiments

20 mL aliquots were placed in polyethylene vials and the ^{241}Am gamma emission at 59 keV was measured in triplicate with the solid scintillation detector Wizard^2 Automatic gamma counter (Perkin Elmer, USA), equipped with a well-type 3.5-inch NaI (Tl activated) crystal. The counting window (40-80 keV) and measurement time (20 min) were set to obtain a relative standard deviation lower than 3% between measurement replicates.

Determination of ^{151}Sm activity concentration in samples derived from the sorption and desorption experiments

2 mL aliquots of each filtered supernatant solution were mixed with 18 mL of OptiPhase HiSafe 3 scintillation cocktail (Perkin Elmer, USA) in 20 mL capacity high-density polyethylene vials. The vials were stored in the dark for 2 h prior to analysis to avoid photoluminescence, and the ^{151}Sm beta emission, with a maximum energy of 77 keV (99.1%), was measured by liquid scintillation counting (LSC) in triplicate using a Wallac 1550 Tri-Carb (Packard, USA). The counting window (0.5 to 150 keV) and measurement time (30 min) were set to ensure a relative standard deviation lower than 2% between measurement replicates. Aliquots of the corresponding blank sorption and desorption assays were used as ^{151}Sm measurement blanks to establish the contribution of background activity in each case by analysing them following the

above measurement procedure. Since measurement of ^{151}Sm activity by LSC is influenced by matrix effects, thus causing a loss of counting efficiency (eff) (*i.e.* the so-called quenching phenomenon), which depends on the composition of the supernatant solutions, the ^{151}Sm activity measurements were corrected by the counting efficiency in each case. This was accomplished by spiking aliquots of supernatant solutions gathered from the blank sorption assays with a known amount of the ^{151}Sm solution and measuring the ^{151}Sm activity following the above measurement procedure. A quenching curve was then constructed by correlating the ^{151}Sm counting efficiency (eff = measured activity / spiked activity $\times$ 100) with a tSIE (Transformed Spectral Index of the External Standard) quenching parameter provided by the LSC counter for each measurement of the spiked supernatant solutions. Finally, the constructed quenching curve ($eff = -6.4 \times 10^{-6}\ tSIE^2 + 4.4 \times 10^{-3}\ tSIE - 1.2 \times 10^{-1}$) was used to calculate the counting efficiency in each of the previously measured sorption and desorption supernatant solutions by interpolating the corresponding tSIE value in the quenching curve, and the ^{151}Sm activities measured in the sorption and desorption supernatants were corrected according to their counting efficiencies.

Determination of stable Sm concentration in samples derived from sorption, desorption and fractionation tests

The Sm concentration in the different supernatant liquids was determined by inductively coupled plasma optical emission spectroscopy (ICP-OES) at a wavelength of 359.3 nm, using a Thermo-Jarrell Ash 25 and Perkin Elmer Optima 3200 RL (Perkin Elmer, USA).

For Sm concentrations lower than the ICP-OES quantification limit (30 $\mu g\ L^{-1}$), Sm concentrations were obtained from measurements of the ^{147}Sm isotope by inductively coupled plasma mass spectrometry (ICP-MS), using a Perkin Elmer Elan-6000 (Perkin Elmer, USA). The Sm quantification limit for ICP-MS was 10 $ng\ L^{-1}$.

3.2.2.4 Calculation of sorption and desorption parameters

The solid-liquid distribution coefficients of the sorption process, K_d, that correspond to the ratio between the target element concentration sorbed in the soil (C_{sorb}) and the concentration remaining in the liquid phase after the sorption process (C_{eq}) were calculated for the target elements as follows:

$$K_d\ (L\ kg^{-1}) = \frac{C_{sorb}}{C_{eq}} = \frac{(C_i - C_{eq})\ \frac{V}{m}}{C_{eq}} \qquad [3.1]$$

where

V is the liquid phase volume.

m is the soil sample dry weight.

C_i is the initial concentration in the liquid phase.

Besides, sorption percentages, S (%), were calculated as follows:

$$S\ (\%) = \frac{(C_i - C_{eq})}{C_i} \times 100 \qquad [3.2]$$

The solid-liquid distribution coefficients of the desorption process, $K_{d,des}$, which correspond to the ratio between the element concentration remaining in the soil after the desorption process ($C_{sorb,des}$) and the Sm concentration desorbed from the soil to the liquid phase ($C_{eq,des}$) were calculated with the following equation:

$$K_{d,des}\ (L\ kg^{-1}) = \frac{C_{sorb,des}}{C_{eq,des}} = \frac{C_{i,des} - C_{eq,des} \times \frac{V}{m}}{C_{eq,des}} \qquad [3.3]$$

where

$C_{i,des}$ is C_{sorb} corrected by the amount of target element present in the residual volume of solution after the sorption experiment incorporated to the solid phase after drying (V_{res}):

$$C_{i,des} = C_{sorb} + C_{eq} \times \frac{V_{res}}{m} \qquad [3.4]$$

Besides, desorption percentages D (%) were calculated as follows:

$$D\ (\%) = \frac{C_{eq,des} \times V}{C_{i,des} \times m} \times 100 \qquad [3.5]$$

3.2.2.5 Construction and fitting of sorption isotherms

With the aim of evaluating the changes in the Sm sorption capacity of the tested soils as a function of Sm concentration, sorption isotherms were constructed by plotting C_{sorb} *vs.* C_{eq} and K_d *vs.* C_{sorb} data obtained at the concentration range assayed. Moreover, the C_{sorb} *vs.* C_{eq} isotherms were fitted with Freundlich, Langmuir and linear sorption models.

The Freundlich model has been extensively applied to describe the sorption behaviour of contaminants of different nature in environmental samples (Echevarría et al., 1998; Milinovic, et al., 2015, Venegas et al., 2015). It is considered appropriate for describing both multilayer sorption (unlimited number of surface sorption sites) and sorption on heterogeneous surfaces (sites of different affinity for a given contaminant). The Freundlich isotherm equation is defined as follows:

$$C_{sorb} = K_f \times C_{eq}^{\ N} \qquad [3.6]$$

where

C_{sorb} is the contaminant sorbed concentration.

C_{eq} is the contaminant concentration in solution after the sorption process.

K_f is the Freundlich constant which describes the contaminant partitioning between the solid and liquid phases at a given contaminant concentration.

N is the Freundlich exponent which describes the site heterogeneity.

As N decreases, the isotherm indicates the presence of higher affinity sites for the contaminant at the lowest concentration range. Values of $N > 1$ in the context of inorganic contaminants, as the case of Sm, might indicate inhibition of the contaminant sorption at the lowest concentrations due to competing processes (*e.g.* complexation with a ligand in solution; presence of competitive cations) (Hinz, 2001).

If N = 1, the Freundlich isotherm corresponds to a linear sorption model and the constant contaminant partitioning between the solid and liquid phases can be described as follows:

$$C_{sorb} = K_{d,\,linear} \times C_{eq} \qquad [3.7]$$

The Langmuir sorption model assumes that the contaminant sorption takes place in a monolayer of homogeneous sorption sites with the same affinity for the contaminant, that the number of surface sorption sites are limited and can get saturated and that no interaction between sorbed species occurs. Despite the aforementioned assumptions, this model has been considered appropriate to fit sorption data for certain contaminant-geological material combinations (Jones, 1997; Do, 1998; Echevarría et al., 1998; Galunin et al., 2010).

The Langmuir isotherm model is described by the following rquation:

$$C_{sorb} = \frac{b \times K \times C_{eq}}{1 + K \times C_{eq}} \qquad [3.8]$$

where

b denotes the maximum capacity of a sorbent material to sorb a contaminant.

K is the contaminant-sorbent bonding energy.

Regardless of the best model describing each Sm sorption isotherm, the C_{sorb} *vs* C_{eq} data corresponding to the Sm low concentration region were also fitted to the linear sorption model (Eq. 3.7) to obtain K_d values related to linear Sm sorption in the studied soils ($K_{d,linear}$).

The Curve Fitting Tool (cftool), an interactive environment for fitting curves to one-dimensional data, which is included in the mathematical software Matlab R2009A (The Mathworks, Inc., 2009), was used to fit the experimental sorption isotherms to the above mentioned sorption models. The fitting coefficients were constrained as positive values, with confidence limits ≥95%, using non-linear least squares fitting with the Trust-region algorithm option.

3.2.3 Statistical analysis and construction of K_d prediction models

In order to gain knowledge regarding which soil properties are more relevant in the ^{241}Am and ^{151}Sm (hereinafter Am and RSm, respectively) sorption in soils and, thus, responsible for the K_d variability, statistical analyses of the sorption and soil characterisation data were performed on the basis of univariate and multivariate approaches.

3.2.3.1. Data pre-treatment

Before applying the statistical analyses, soil property data that were below the quantification limit, such as the $CaCO_3$ content of some soils, were set to one-half of the established limit of quantification of the analytical method used for its determination, as recommended by Reid and Spencer (2009). Subsequently, the Kolmogorov-Smirnov test was applied to check the distribution followed by the considered variables (soil properties), which demonstrated that soil characterisation (with the logical exception of pH) data as well as Am and RSm K_d values were log-normally distributed ($p < 0.05$). Consequently, as recommended by Sheppard (2011), all data were log-transformed. In addition to this, for the multivariate analysis based on soil latent variables, all data were also autoscaled, *i.e.* mean centred and scaled to variance equal to 1, to give all variables the same weight.

3.2.3.2. Linear regressions analysis with soil variables

The soil properties more relevant in terms of Am and RSm sorption in soils were firstly identified with univariate linear regression (ULR). Then, a stepwise multiple linear regression (MLR) analysis was carried out by combining two or more noncovariant soil properties that yielded a better correlation with K_d values in order to propose MLR models to predict K_d (Am) and K_d (RSm) values.

An internal validation following the leave-one-out cross-validation (LOOCV) method was done to examine the prediction capability of the best MLR significance at $p = 0.05$. In short, LOOCV consisted in calibrating the K_d prediction model (in this case the MLR model) by excluding the data corresponding to one soil sample and predicting the K_d

value of the excluded soil. The "leave-one-out" exercise was repeated until all soil samples were excluded once from the model and externally predicted. Then, to have an indicator of the goodness of prediction the root-mean-square error of cross-validation (RMSECV) was calculated as follows:

$$RMSECV = \sqrt{\frac{\sum_{i=1}^{n}\left(log\ K_{d,exp}^{i} - log\ K_{d,CVpred}^{i}\right)^{2}}{n}} \quad [3.9]$$

where

$log\ K_{d,exp}^{i}$ are the experimental log K_d values.

$log\ K_{d,CVpred}^{i}$ are the log K_d values predicted with the MLR model by means of the LOOCV method.

n is the number of soil samples.

3.2.3.3. Multivariate regression analysis based on latent variables

Complementary to the ULR analysis, Principal Component Analyses (PCA) were performed to visually explore the existing relationships between the soil properties and K_d values of Am and RSm, whereas Partial Least Square Regression (PLS) was used to determine the relative importance of each soil property in the prediction of K_d values of both Am and RSm as well as to construct a multivariate model to predict K_d values of these two elements.

Principal Component Analysis

PCA transforms a multivariate data array into a new data set in which the new variables, Principal Components (PC), are calculated from linear combinations of the original variables, being each PC orthonormal and explaining maximum variance since no information is repeated. Consequently, a low dimension space composed by a reduced set of PCs that synthesise all the information from the original matrix is obtained. Each PC is formed by loadings and scores, related to the importance of each

original variable and to the weight of each sample in a given PC, respectively (Esbensen, 2004).

To perform the PCA analyses data matrices in which each row corresponded to a soil sample and each column corresponded to a variable (soil properties and K_d values) were constructed (*i.e.* 20×18, for Am; 30×18, for RSm). The optimal number of PCs necessary to perform the PCA (dimension of the PCA model) is ascertained by selecting that model leading to the lowest RMSECV when a LOOCV is performed (Rigol et al., 2008). Besides, the loading values in the PC1 were checked In order to identify the soil properties with less relevance in the model, and thus, eligible to be rejected to simplify and optimise the PCA model. Whereas, the scores influence plot was also checked to detect possible outlier soil samples, *i.e.* samples with large values of Residuals (Q), Hotelling (T^2) or both statistics, that may distort the model and hidden the structure of the rest of the data.

Once the PCA model was optimised, the final loading plots in the PCs space were analysed to single out the existing relationships between K_d variable and the rest of soil properties, whereas the score plot permitted to detect possible sample clusters, which allowed to examine whether soils were grouped by the model according to their similar properties or not.

Partial Least Squares Regression analysis

PLS is a multivariate regression method that builds a model for predictive purposes in a low-dimensional space formed by Latent Variables (LV). Each LV is constructed by linear combination of a set of predictor variables (X) covarying optimally with the predicted property (Y). Thus, LVs are obtained from the maximum amount of variance described by the samples that better correlates with Y.

PLS can be used to determine which variables are more important at predicting Y property by checking certain indexes such as the Variable Importance in Projection (VIP) index. Since PLS only evaluate the variance that can be used to separate samples on the basis of a target property, it can be applied to do calibration models in a low-dimension space and the regression coefficient matrix derived can be subsequently

applied to predict Y values from new samples for which X data is available (Esbensen, 2004).

Here, the same data matrices previously created for PCA analyses were also used to perform PLS regressions. The optimal number of significant latent variables (LV), *i.e.* the PLS model dimension, was firstly ascertained in each case by selecting those LVs that led to a model with the lowest RMSECV (see Eq. 3.9) when performing a cross-validation by means of the leave-one-out method. Once the PLS-based models dimensions were established, the relevance of each soil property in the constructed models was identified by checking the variable importance in projection (VIP) index values. Irrelevant soil properties, *i.e.* those with VIP index values < 1 were rejected from the data matrices in order to simplify and optimise the PLS-based models. Each data matrix was then refined, and the final PLS-based models were finally built with the remaining soil properties and their prediction capabilities were evaluated by leave-one-out cross-validation.

3.2.3.4. External validation of MLR and PLS-based prediction models of K_d (RSm)

To further demonstrate the capacity of the MLR and PLS models to predict K_d (RSm) values, an external validation was also performed. To this end, the sorption and characterisation data gathered from the 30 soil samples were split into two sets: a calibration set containing the data gathered from the 20 soil samples also used to determine K_d (Am) value and a test set consisting of data gathered from the 10 extra soil samples used for RSm.

To perform the external validation, new MLR and PLS models were constructed using only the calibration set data (hereinafter MLR_EV and PLS_EV, respectively). In order to ensure that the calibration dataset was representative and suitable for performing the external validation, the MLR_EV and PLS_EV models were compared in terms of K_d (RSm) variance captured, goodness of fit (RMSECV) and model composition (variable coefficients in the MLR equation and variable VIP values in the case of the PLS-based model) to those previously developed with the overall dataset.

Once the suitability of the calibration set was confirmed, the external validation was accomplished by using the MLR_EV and PLS_EV models to predict the K_d (RSm) values of the test set. The prediction capability of the models was evaluated by calculating the root-mean-square error of prediction (RMSEP) as follows:

$$\text{RMSEP}=\sqrt{\frac{\sum_{i=1}^{n}\left(log\ K_{d,exp}^{i}-log\ K_{d,EVpred}^{i}\right)^{2}}{n}} \qquad [3.10]$$

where

$log\ K_{d,exp}^{i}$ are the experimental log K_d values of the test set.

$log\ K_{d,EVpred}^{i}$ are the log K_d values predicted with the corresponding MLR_EV and PLS_EV models.

n is the number of soil samples of the test set.

3.3 RESULTS AND DISCUSSION

3.3.1 Sorption and desorption pattern of Am and RSm in soils

Table 3.3 and **Table 3.4** summarise the sorption and desorption data derived from the batch experiments for Am and for RSm, respectively. The overall geometric mean (GM) of K_d values were 1.95×10^4 L kg^{-1} for Am and 6.1×10^3 L kg^{-1} for RSm, one order of magnitude higher than respective best estimate K_d values in reported compilations (IAEA, 2009), evidencing that the soils analysed have a high capacity to sorb both RNs. Although the individual sorption K_d (Am) and K_d (Sm) values were generally high (>10^3 L kg^{-1}), K_d values varied within a wide range in the soils examined, covering several orders of magnitude (Am: $K_{d,min}$ = 1.6 $\times10^3$ L kg^{-1} (DUBLIN soil), $K_{d,max}$ = 2.8×10^5 L kg^{-1} (VAN1 soil); RSm: $K_{d,min}$ = 5.4×10^2 L kg^{-1} (RED STONE soil), $K_{d,max}$ = 2.8×10^5 L kg^{-1} (ASCO soil)).

Due to the K_d large variability observed for Am and RSm, the proposal of a unique K_d best estimate value to describe the partitioning of this element in soils should be dismissed as a suitable approach. Unlike previous reports, in the present study K_d data variability must solely be attributed to the variability in soil properties and their effect on Am and RSm speciation, as a unique and controlled methodology was applied in all soils to obtain the K_d data. Therefore, this dataset can be worthy to clearly identify those soil properties controlling the Am and RSm sorption in soils and to suggest soil factors to group soils and decrease their K_d data variability, leading to the proposal of more reliable K_d data for risk assessment purposes.

A preliminary exploratory data analysis indicated that those soils with basic pH and/or high carbonate content seemed to have a high capacity to sorb Am and RSm, whereas these elements were less sorbed in soils with high organic matter (OM) content. However, no clear trends were observed, and thus, statistical analyses were required to further explore the soil properties most relevant to their sorption. This issue is extensively discussed in following Section 3.3.2.

Table 3.3 Sorption and desorption parameters of ^{241}Am in the soils studied.

Soil sample	K_d (L kg^{-1})	$K_{d,des}$ (L kg^{-1})	D (%)
ANDCOR	2000	4400	0.5
ASCO	105000	73000	0.1
BAD1	8300	3000	0.4
CABRIL	9200	23800	0.2
ENUSA	6500	14800	0.2
GRACOR	43400	26800	0.1
TRILLO	176000	11000	0.1
BILBAO	73000	6000	0.1
DELTA2	76000	11400	0.1
FONCOR	9500	60000	0.4
GAROÑA	24500	4200	0.2
LEON	6400	41000	0.6
MALAGA	72000	3700	0.1
OVI01	2800	6700	0.7
TEN1	11400	24500	0.4
VAN1	280000	21600	0.1
ZORITA	180000	45000	0.1
MATEIKI	6500	5900	0.4
RED STONE	8500	2000	1.2
DUBLIN	1600	2300	1.1

Table 3.4 Sorption and desorption parameters of RSm in the soils studied.

Soil sample	K_d (L kg^{-1})	$K_{d,des}$ (L kg^{-1})	D (%)	Soil sample	K_d (L kg^{-1})	$K_{d,des}$ (L kg^{-1})	D (%)
ANDCOR	1600	4600	0.6	VAN1	28000	10000	0.4
ASCO	280000	160000	<0.1	ZORITA	30000	18000	0.1
BAD1	7000	17500	0.1	MATEIKI	2000	38000	<0.1
CABRIL	5600	22000	0.1	RED STONE	520	1300	1.9
ENUSA	6100	4400	0.6	DUBLIN	2200	6700	0.4
GRACOR	41000	27000	<0.1	DELTA1	1900	5400	0.5
TRILLO	4000	6200	0.4	VAN2	49000	23000	0.1
BILBAO	12000	18000	0.1	ALMERIA	2300	11000	<0.2
DELTA2	26000	27000	0.1	GOLOSO	2000	8300	0.3
FONCOR	2100	4900	0.5	FROCOR2	1900	7400	0.4
GARROÑA	7900	9500	0.3	UPV	8200	13000	0.2
LEON	2600	2000	1.8	AYUD	39000	17000	0.2
MALAGA	23000	25000	0.1	UIAR	2600	6400	0.4
OVI01	940	3600	0.7	KOM	6500	19000	0.2
TEN1	3300	6600	0.4	BRA	2900	8200	0.4

Regarding the desorption data, the $K_{d,des}$ values were always higher than 10^3 L kg^{-1} for both elements in all soils. This fact, along with the extremely low D % values (< 1.2%, for Am and < 1.9%, for RSm), suggests that the Am and RSm were strongly and very irreversibly sorbed in all soils, which agrees with conclusions drawn by other authors (Lujaniene et al., 2002; Pavlotskaya et al, 2003). Besides this, the GM values (1.1×10^4 L kg^{-1} for both elements) were not significantly different ($p < 0.05$) than the GMs of sorption K_d values, showing that in general no ageing effects occurred during the drying process.

The sorption and desorption pattern obtained here for Am and RSm points to a remarkably retention of these elements in the soils and conditions tested. Therefore, it can be said that soils entering in contact with liquid sources contaminated with Am and RSm may act as natural barriers limiting the spreading from the contamination source point in the short-term since most of the Am and RSm could be incorporated and retained into the soil matrices.

3.3.2 Influence of soil properties in Am and RSm sorption in soils

3.3.2.1 Elucidation of soil phases and sorption mechanisms responsible for the Am and RSm interaction in soils

The examination of the correlations between soil properties data and K_d values permits to identify those soil components governing Am and RSm sorption in soils. **Table 3.5** and **Table 3.6** show the correlation matrix obtained from the ULR analyses performed for the case of Am and RSm, respectively. A few soil properties highly correlated with K_d (Am) and K_d (RSm). The most relevant to explain the K_d data variability were: specific surface area (BET), supernatant pH, carbonate content ($CaCO_3$), amorphous iron content (Fe_{amorph}), and those properties related to soil OM content (LOI, C_{org} and DOC).

Table 3.5 Pearson coefficients (r) of ULRs obtained from soil properties and K_d (Am) log-log correlations (n = 20).

Variable	K_d (Am)	Clay	Sand	$CaCO_3$	C_{org}	LOI	Al_{amorph}	Fe_{amorph}	Mn_{amorph}	CEC	BET	pH	DIC	DOC	Ca	Mg	K	Na
K_d (Am)		0.39	-0.25	0.67*	-0.67*	-0.64*	-0.46	-0.61*	-0.32	-0.37	0.70*	0.68*	0.12	-0.77*	0.48*	-0.18	0.13	-0.22
Clay	0.39		-0.40	0.49*	-0.37	-0.39	-0.03	-0.50*	-0.18	-0.45	0.58*	0.24	0.07	-0.42	0.08	0.15	0.13	-0.02
Sand	-0.25	-0.40		-0.57*	0.02	-0.06	0.43	0.20	0.11	-0.20	-0.33	-0.12	-0.48*	0.04	-0.37	-0.54*	-0.58*	-0.13
$CaCO_3$	0.67*	0.49*	-0.57*		-0.36	-0.37	-0.45	-0.49*	-0.37	-0.17	0.46	0.51*	0.44	-0.46	0.58*	0.08	0.32	-0.24
C_{org}	-0.67*	-0.37	0.02	-0.36		0.95*	0.16	0.74*	0.32	0.63*	-0.78*	-0.73*	0.15	0.90*	-0.15	0.36	0.02	0.22
LOI	-0.64*	-0.39	-0.06	-0.37	0.95*		0.08	0.69*	0.24	0.72*	-0.75*	-0.75*	0.11	0.92*	-0.21	0.37	0.05	0.33
Al_{amorph}	-0.46	-0.03	0.43	-0.45	0.16	0.08		0.25	-0.02	-0.03	-0.26	-0.38	-0.57*	0.14	-0.59*	-0.03	-0.15	0.06
Fe_{amorph}	-0.61*	-0.50*	0.20	-0.49*	0.74*	0.69*	0.25		0.48*	0.53*	-0.82*	-0.60*	0.01	0.73*	-0.04	0.18	-0.18	0.26
Mn_{amorph}	-0.32	-0.18	0.11	-0.37	0.32	0.24	-0.02	0.48*		0.34	-0.19	0.03	0.29	0.27	-0.06	-0.19	0.07	0.41
CEC	-0.37	-0.45	-0.20	-0.17	0.63*	0.72*	-0.03	0.53*	0.34		-0.41	-0.25	0.31	0.71*	-0.04	0.35	0.31	0.64*
BET	0.70*	0.58*	-0.33	0.46	-0.78*	-0.75*	-0.26	-0.82*	-0.19	-0.41		0.71*	0.09	-0.77*	0.05	-0.08	0.33	-0.01
pH	0.68*	0.24	-0.12	0.51*	-0.73*	-0.75*	-0.38	-0.60*	0.03	-0.25	0.71*		0.40	-0.73*	0.40	-0.20	0.17	0.11
DIC	0.12	0.07	-0.48*	0.44	0.15	0.11	-0.57*	0.01	0.29	0.31	0.09	0.40		0.13	0.50*	0.27	0.52*	0.21
DOC	-0.77*	-0.42	0.04	-0.46	0.90*	0.92*	0.14	0.73*	0.27	0.71*	-0.77*	-0.73*	0.13		-0.22	0.30	0.02	0.33
Ca	0.48*	0.08	-0.37	0.58*	-0.15	-0.21	-0.59*	-0.04	-0.06	-0.04	0.05	0.40	0.50*	-0.22		0.19	0.03	-0.21
Mg	-0.18	0.15	-0.54*	0.08	0.36	0.37	-0.03	0.18	-0.19	0.35	-0.08	-0.20	0.27	0.30	0.19		0.22	0.35
K	0.13	0.13	-0.58*	0.32	0.02	0.05	-0.15	-0.18	0.07	0.31	0.33	0.17	0.52*	0.02	0.03	0.22		0.15
Na	-0.22	-0.02	-0.13	-0.24	0.22	0.33	0.06	0.26	0.41	0.64*	-0.01	0.11	0.21	0.33	-0.21	0.35	0.15	

*Significant correlations at $p < 0.05$.

Table 3.6 Pearson coefficients (r) of ULRs obtained from soil properties and K_d (RSm) log-log correlations (n = 30).

Variable	K_d (RSm)	Clay	Sand	$CaCO_3$	C_{org}	LOI	Al_{amorph}	Fe_{amorph}	Mn_{amorph}	CEC	BET	pH	DIC	DOC	Ca	Mg	K	Na
K_d (RSm)		0.34	-0.41*	0.55*	-0.65*	-0.58*	-0.22	-0.46*	-0.25	-0.34	0.68*	0.63*	0.31	-0.71*	0.44*	-0.08	-0.04	-0.14
Clay	0.34		-0.22	0.66*	-0.59*	-0.58*	-0.13	-0.59*	-0.27	-0.58*	0.63*	0.26	0.11	-0.49*	0.00	-0.02	0.14	-0.07
Sand	-0.41*	-0.22		-0.42*	0.04	-0.06	0.38*	0.14	0.11	-0.11	-0.38*	-0.12	-0.50*	0.09	-0.40*	-0.41*	-0.45*	-0.10
$CaCO_3$	0.55*	0.66*	-0.42*		-0.50*	-0.49*	-0.34	-0.52*	-0.41*	-0.33	0.53*	0.45*	0.37	-0.52*	0.42*	0.03	0.28	-0.21
C_{org}	-0.65*	-0.59*	0.04	-0.50*		0.95*	0.28	0.79*	0.38*	0.75*	-0.78*	-0.64*	-0.02	0.84*	-0.10	0.43*	0.03	0.29
LOI	-0.58*	-0.58*	-0.06	-0.49*	0.95*		0.22	0.77*	0.36	0.79*	-0.71*	-0.64*	0.01	0.86*	-0.14	0.45*	0.05	0.39*
Al_{amorph}	-0.22	-0.13	0.38*	-0.34	0.28	0.22		0.33	0.01	0.16	-0.27	-0.25	-0.18	0.18	-0.43*	0.13	-0.13	0.20
Fe_{amorph}	-0.46	-0.59*	0.14	-0.52*	0.79*	0.77*	0.33		0.52*	0.62*	-0.77*	-0.50*	-0.14	0.78*	-0.06	0.31	-0.10	0.36
Mn_{amorph}	-0.25	-0.27	0.11	-0.41*	0.38*	0.36	0.01	0.52*		0.40*	-0.28	-0.01	-0.10	0.45*	-0.18	-0.15	-0.06	0.33
CEC	-0.34	-0.58*	-0.11	-0.33	0.75*	0.79*	0.16	0.62*	0.40*		-0.54*	-0.28	0.09	0.71*	-0.02	0.43*	0.23	0.52*
BET	0.68*	0.63*	-0.38*	0.53*	-0.78*	-0.71*	-0.27	-0.77*	-0.28	-0.54*		0.62*	0.38*	-0.76*	0.09	-0.18	0.17	-0.08
pH	0.63*	0.26	-0.12	0.45*	-0.64*	-0.64*	-0.25	-0.50*	-0.01	-0.28	0.62*		0.43*	-0.61*	0.42*	-0.28	0.10	-0.03
DIC	0.31	0.11	-0.50*	0.37	-0.02	0.01	-0.18	-0.14	-0.10	0.09	0.38*	0.43*		-0.26	0.51*	0.21	0.25	0.12
DOC	-0.71*	-0.49*	0.09	-0.52*	0.84*	0.86*	0.18	0.78*	0.45*	0.71*	-0.76*	-0.61*	-0.26		-0.27	0.40*	0.11	0.40*
Ca	0.44*	0.00	-0.40*	0.42*	-0.10	-0.14	-0.43*	-0.06	-0.18	-0.02	0.09	0.42*	0.51*	-0.27		0.14	-0.03	-0.26
Mg	-0.08	-0.02	-0.41*	0.03	0.43*	0.45*	0.13	0.31	-0.15	0.43*	-0.18	-0.28	0.21	0.40*	0.14		0.35	0.42*
K	-0.04	0.14	-0.45*	0.28	0.03	0.05	-0.13	-0.10	-0.06	0.23	0.17	0.10	0.25	0.11	-0.03	0.35		0.22
Na	-0.14	-0.07	-0.10	-0.21	0.29	0.39*	0.20	0.36	0.33	0.52*	-0.08	-0.03	0.12	0.40*	-0.26	0.42*	0.22	

*Significant correlations at $p < 0.05$.

The K_d *vs.* BET correlation had a high and positive regression coefficient (Am: r = 0.70; RSm: r = 0.68), thus indicating that a higher Am and RSm sorption took place in those soils with smaller particle size, and thus, with higher surface area. This finding, in conjunction with the non-significant correlations ($p > 0.05$) of K_d values with CEC and most of the major cations in solution (Mg, K and Na) as well as the weak correlation between K_d values and Ca (Am: r = 0.48; RSm: r = 0.44), suggests that the interaction of Am and RSm with soils was controlled by surface complexation reactions whereas cationic exchange mechanisms played a minor role.

Besides, K_d (Am) and K_d (RSm) values were strongly and positively correlated to pH (Am: r = 0.67; RSm: r = 0.63) within the pH range defined by the soils under study (3.9 - 9.9) denoting that basic-pH soils had a much higher capacity to sorb Am and RSm than the acid ones. This pH-dependency of Am and RSm sorption is in agreement with previous works in which the interaction of Ln(III) and Ac(III), such as Eu and Am, was investigated in mineral phases such as silica (Pathak and Choppin, 2007; Righetto et al., 1991; Ye et al., 2014), granite (Jin et al., 2014; Kitamura et al., 1999), pyrite (Das et al., 2009) or clays (Ho Lee et al., 2011; Schott et al., 2012; Takahashi et al., 1998) as a function of pH. In these works it was observed that the Eu/Am sorption continuously increased from negligible values to over 95% by increasing the pH within the 4-10 pH range, with a sharply sorption increase at pH between 5-7 depending on the material tested. Taking into account that Ln(III) and Ac(III) speciation in this pH range in the absence of dissolved humic acids (HA) is dominated by cationic species, such as X^{3+}, $X(OH)^{2+}$ and $X(OH)_2^{+}$, where X corresponds to any Ln(III) and Ac(III) element (Choppin, 2007; Lujaniene et al., 2007), this sorption behaviour was attributed to a progressively deprotonation of certain functional groups leading to a higher net negatively surface charge, and thus, to a higher capacity to form surface complexes with the cationic Eu/Am species.

It is worth noting that when TEN1 soil sample, which had lower Am and RSm K_d values (1.1×10^4 L kg^{-1} and 3.3×10^3 L kg^{-1}, respectively) than that expected from its extremely basic pH (9.9) (compare for instance with VAN; pH = 9.9, K_d (Am) = 2.8×10^5 L kg^{-1}, K_d (RSm) = 2.8×10^4 L kg^{-1} or ZORITA; pH = 8.5, K_d (Am) = 1.8×10^5 L kg^{-1}, K_d (RSm) = 3.0×10^4 L kg^{-1}), was excluded from the regression, the correlations between Am and RSm K_d data and pH remarkably

improved (Am: r = 0.80; RSm: r = 0.74), which in turn implied that pH was the soil property among all those considered in the present study that better explained the K_d variability.

Several researchers (Choppin, 2007; Lujaniene et al., 2007; Pathak and Choppin, 2007) have reported that at pH values higher than 8.5 and in the presence of carbonates in solution, the formation of anionic Ln/Ac-carbonate complexes (*e.g.*, $Am(CO_3)_2^-$ and $Am(CO_3)_3^{3-}$) takes place, being especially significant at pH close to 10. According to this, a feasible hypothesis for the particular behaviour of the TEN1 soil would be that due to its very basic pH (pH >> 8.5) and its relative high DIC value (an indicator of the amount of carbonate in solution), the formation of the aforementioned anionic Am and RSm species was much higher than in other soil samples with same pH but lower DIC content (VAN1), or with similar DIC content but much lower pH (ZORITA). Therefore, the Am and RSm affinity for TEN1 soil would be much lower due to electrostatic repulsions between the negatively charged soil surface and the Am/RSm anionic species (Degueldre et al., 1994) present at this pH, resulting in K_d values one order of magnitude lower than those expected.

Previous studies had already found an empirical relationship between pH and K_d (Am) values in soils. For instance, Roussel-Debet (2005) succeeded in developing a parametric K_d model ($K_d = 189\ pH^2 - 1526\ pH + 3222$) from a set of 6 French agricultural soils, *i.e.* loamy soils with relative low OM content and with pH from slightly acid to slightly basic, which could capture 94% of the K_d (Am) data variability, much more than that of the ULR found here and thus, with a higher prediction capability. However, it is worth noting that the Roussel-Debet model failed in predicting the K_d (Am) values of the soil samples studied here, denoting that its applicability is reduced to scenarios dealing with soils similar to those used to develop the model, as already mentioned by the author (Roussel-Debet, 2005). This finding confirms the relevance of pH in the interaction of Am, but also reveals that it is necessary to contemplate a large number of soils with contrasting properties so as to develop K_d (Am) and K_d (RSm) prediction models to be reliably extrapolated for screening purposes to different scenarios.

Regarding the rest of relevant soil properties, K_d (Am) and K_d (RSm) values were strongly and positively correlated with $CaCO_3$ (r = 0.67 and r = 0.54, respectively),

indicating that Am and RSm were sorbed in a greater extent in calcareous soils. Some researchers have pointed to a extremely high affinity of certain carbonate minerals, such as calcite and specially aragonite, for the hydrated, cationic species of lanthanides and actinides (Sutton, 2009), as evidenced by the extremely high K_d (Am) values (within the range 10^5 - 10^6 L kg^{-1}) reported in the literature for calcite-rich materials (Higgo and Rees, 1986; Shanbhag and Morse, 1981).

On the other hand, the strong and negative correlation between DOC and K_d of both elements (Am: r = -0.77; RSm: r = -0.71) indicated that those soils with higher concentrations of soluble organic compounds exhibited a lower capacity to sorb Am and Sm. To date, studies aiming at examining the sorption of lanthanides and actinides in minerals indicate that Ac/Ln-humate complexes may be relevant in the presence of soluble organic compounds (humic and fulvic acids) in the pH range within 4 - 8 (Ho Lee et al., 2011; Jin et al., 2014; Riguetto et al., 1991; Ye et al., 2014). As a result of deprotonated carboxylic groups present in the humate compounds, these Ac/Ln-humate complexes have a net negative charge and, consequently, they remain in solution due to electrostatic repulsions with the negatively charged mineral surface. Moreover, C_{org} and LOI were also strongly and negatively correlated with K_d (Am) values (r = -0.67 and r = -0.64, respectively) and with K_d (RSm) values (r = -0.66 and r = -0.58, respectively), which may indicate that soils with higher OM fraction in the solid phase presented less capacity to sorb Am and RSm. This finding disagrees with previous works that suggested that Ac(III) and Ln(III) have a high affinity for organic matter compounds. Special care must be taken when the effect of soil properties are analysed univariately, since the existence of more than two variables covarying among them may lead to wrong interpretations of the ULRs. That is the case of C_{org}, LOI and DOC variables, that not only are highly correlated with K_d (Am) and K_d (RSm), but also among them. Therefore, since high and positive correlations existed between DOC and C_{org} (r = 0.90) and between DOC and LOI contents (r = 0.92), the strong and negative correlation of Am and RSm K_d values with C_{org} and LOI parameters in fact can be attributed to the above described role of DOC. Consequently, the sorption of Am and RSm in soils with high OM content seems to be governed by the soluble organic matter fraction, which modifies the Am/Sm speciation and suppresses the interaction with the soil matrix rather than by the sorption sites originated from the OM remaining in the soil solid matrix. In addition to

this, the key role that DOC plays in the Am interaction in soils was already found in a previous study where a geochemical model that takes into account the influence of the humic substances in the Am speciation in solution and in the Am interaction with the soil matrix (WHAM; *Windermere Humic Aqueous Model*) was developed to predict K_d (Am) values in acid soils. Although the WHAM capability to predict K_d (Am) values in soils under acidic conditions is out of discussion, its complexity and the fact that it has been tested only in acid soils may restrict to other types of soil, as above stated for the parametric K_d (Am) model proposed by Roussel-Debet (2005).

Finally, moderate and negative correlations were also observed between K_d data and Fe_{amorph} (Am: r = -0.61; RSm: r = -0.46), indicating that Am and RSm were less sorbed in those soils with higher amorphous iron content. This pattern agreed with the fact that the presence of soluble Fe colloids has been reported to enhance the migration of transuranic elements in soils (Moulin and Ouzounian, 1992; Novikov et al., 2011). Thus, the negative correlation observed can be explained by the fact that amorphous metal oxides may form negatively charged colloids, capable to chelate the cationic Am and Sm species, which remain in solution due to the existing electrostatic repulsions with the negatively charged soil surface.

3.3.2.2 Exploratory analysis of K_d and soil characterisation data with PCA: the case of Am

The application of PCA to the matrix dataset led to a model consisting in two PCs that explained around 60% of the data variability. Some soil variables (sand, DIC and K) presented very low loadings (< 0.1 in absolute value) in the first PC (see **Figure 3.3**), which suggested that their relevance in the PCA model was very low and, thus, their removal was examined in order to avoid distortions and to simply the PCA model. The optimised PCA model consisted in three PCs, all of them with eigenvalues higher than 1, which means that all PCs significantly contributed to explain a 73% of the total data variance (PC1, 47%; PC2, 15%; PC3 11%).

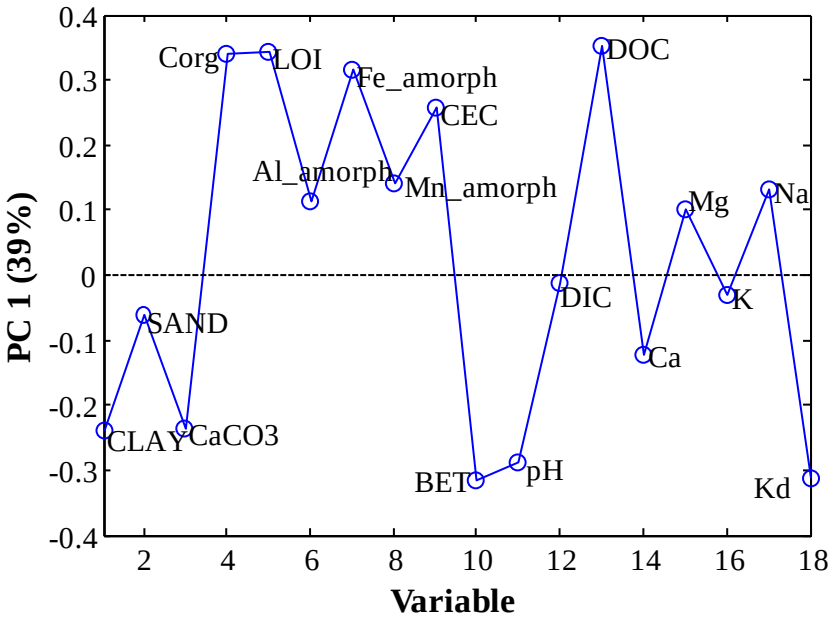

Figure 3.3 *Variable loadings in PC1 of PCA model constructed with all variables.*

A further step forward optimising the PCA model was taken by means of checking the scores influence plot of the simplified PCA model (**Figure 3.4**) aiming at identifying outlier soil samples. As can be seen, TEN1 soil sample presented a statistically unusual Hotelling (T^2) value, indicating that due its soil properties this soil was considered by the model as an extreme sample which may distort the model. This finding is consistent with that already observed in the ULR analysis, which evidenced that the inclusion of TEN1 soil data worsened the ULR between pH and K_d values. Thus, the removal of TEN1 soil data from the model was also evaluated. However, the structure of the PCA model, *i. e.,* the loadings and scores of the relevant PCs in the model, did not change when it was constructed without data of TEN1 soil sample. Consequently, the inclusion of TEN1in the final PCA was eventually accepted. The variables with the highest absolute values of loadings in the PC1, and thus most relevant in the model to explain data relationships, were variables related to the organic matter content (DOC, C_{org} and LOI), iron amorphous content (Fe_{amorph}), clay, specific surface area (BET), supernatant pH and K_d.

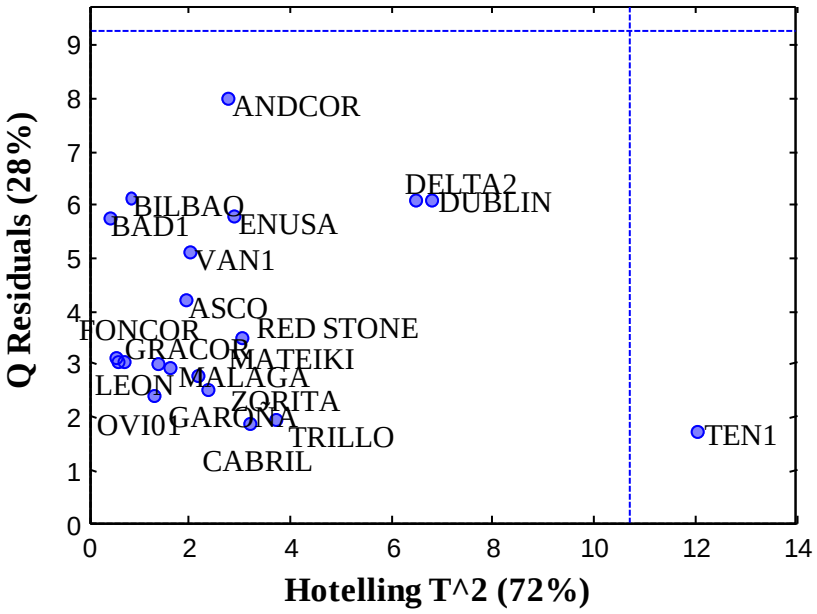

Figure 3.4 *Influence plot of the simplified PCA model.*

In order to identify which soil variables were more correlated with K_d (Am), the PC1-PC2 and PC1-PC3 loading plots (**Figure 3.5**) were examined. Considering the variable vectors formed by linking the origin (0,0) point with the variable position in a given two PCs-space loading plot and by checking the angle between two variable vectors, the correlation between two variables can be ascertained. Two variable vectors forming an angle of 0° means that these two variables are highly, positively correlated; whereas if they form an angle of 180° means that they are highly, negatively correlated. Thus, from the PC1-PC2 plot (**Figure 3.5 A**) it can be deduced that a high, positive correlation existed between K_d and pH, whereas moderate, positive correlations between K_d, BET and $CaCO_3$ variables were also evidenced. Besides, in the PC1-PC3 space (**Figure 3.5 B**) an angle close to 180° between the K_d vector and the vectors of DOC and Fe_{amorph} variables indicated a negative correlation between K_d and these variables whereas an angle close to 0° between K_d and clay vectors indicated a positive correlation between K_d (Am) and clay.

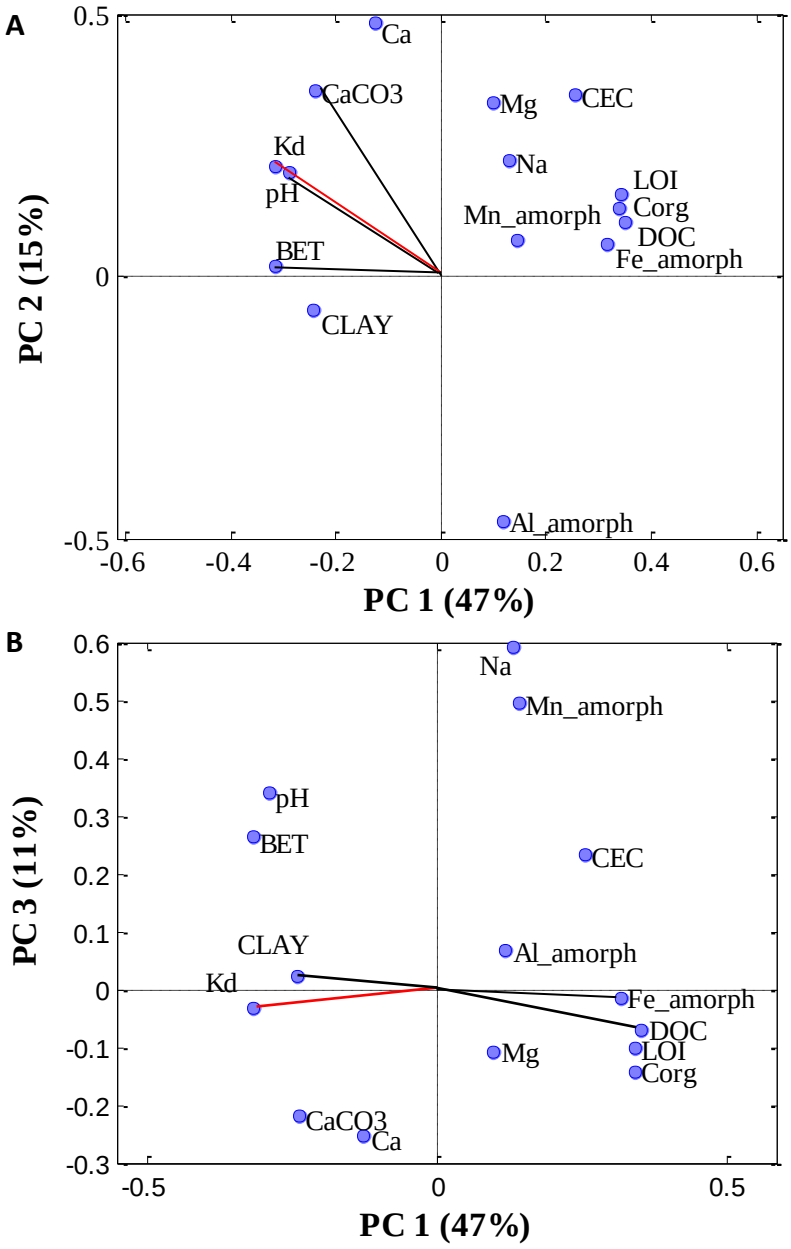

Figure 3.5 *Data exploration with Principal Component Analysis. (A) Loadings plot of PC1-PC2 space; (B) Loadings plot of PC1-PC3 space.*

With the exception of the correlation with clay, these results agreed with findings obtained in the previous ULR analysis and were consistent with the Am sorption mechanisms previously described (section 3.3.2.1). Finally, no sample clusters in the scores plot in the PC1-PC2 space were noticed, thus confirming that soils were not grouped according to their properties and had contrasted edaphic properties.

3.3.2.3 Multivariate analysis to predict K_d (Am) and K_d (RSm) values from soil properties

Considering that the K_d (Am) and K_d (RSm) variability described by ULRs was lower than 60% (with the exception of that with pH), and that more than one non covariant soil properties affected the K_d (Am) and K_d (RSm) values, two approaches based on multivariate regression, MLR and PLS, were explored to develop Am and RSm prediction parametric models.

Multiple Linear Regression models

A few MLR models with two variables (6 for Am and 2 for RSm) succeeded in explaining higher variance than any ULR, whereas MLR models constructed by combining three or more variables did not lead to any significant correlation ($p > 0.05$). **Table 3.7** summarises the equations of the significant MLRs ($p < 0.05$).

For both elements, the MLRs obtained by combining pH and BET variables were those that explained a higher K_d (Am) and K_d (RSm) variability (73% and 76%, respectively). Although BET was not among the two soil properties that individually were more correlated with K_d data, the lack of covariance between BET and pH implied that, when combined, these soil properties were the most efficient to explain the K_d data variability. Besides this, the BET_pH MLR model is consistent with the sorption mechanisms proposed from the ULR analysis since it suggests that Am and RSm are sorbed in a greater extent in those soils presenting higher surface area and when sorption occurs at basic pH conditions.

It should be noted that the combination of the two variables that individually were most correlated with K_d data, *i. e.* pH and DOC, led to a non-significant MLR ($p > 0.05$) for Am, whereas for RSm this combination led to the second best MLR in terms of K_d (RSm) variance captured. Albeit explaining less variance than the BET_pH MLR, other relevant MLRs in the case of Am that can be used alternatively in case that the BET and/or pH of the soil under assessment is not available are, on the one hand, that resulting from the combination of DOC and $CaCO_3$, which was also consistent with the above described Ln(III)/Ac(III) sorption mechanisms in soils since it includes soil properties that inhibit (DOC) and enhance ($CaCO_3$) Am sorption in soils, and, on the other, those MLRs combining $CaCO_3$ with C_{org} and LOI variables that results from the

existing covariance between DOC, C_{org} and LOI variables. Despite knowing that the C_{org}, LOI based MLRs models do not capture the sorption mechanisms and soil phases directly involved in the Am interaction as the DOC-based does, the MLRs constructed with C_{org} and LOI may be good alternatives to estimate K_d (Am) values since these variables are more often available than DOC in routine soil analyses.

Regarding the prediction capability of the proposed MLR models, when the cross-validation exercises (LOOCV) were performed, it was evidenced that the predicted log K_d values and the experimental ones were highly correlated ($r > 0.68$), and the average errors associated to the log K_d predicted values (RMSECV values) were always lower than 0.5 log units (see **Table 3.7**). These figures indicate that the different MLR models were robust and capable to predict the order of magnitude of K_d (Am) and K_d (RSm) values, which is a significant improvement with respect to the inherent K_d variability observed in the experimental data (around 3 log units) in our test of soils.

End-users must be warned before making use of the MLR models that it should be avoided the extrapolation to scenarios not covered in the MLRs (*i.e.*, their application aiming to predicting K_d (Am) and K_d (RSm) values in soils whose properties are not encompassed in the variable ranges used to the MLR models construction). Moreover, it is important to point that the MLR models including the pH variable were developed excluding the TEN1 soil data. Therefore, especial care must be taken when applying these MLR models to predict K_d (Am) and K_d (RSm) values, even for screening purposes, in the particular scenario involving a soil with extremely basic pH ($pH >> 8.5$) and high DIC content since the predicted K_d data values may be systematically overestimated (up to 0.8 log units).

Table 3.7 MLR models for log K_d (Am) and log K_d (RSm) prediction. Values in brackets correspond to the standard error of the MLR parameters at $p < 0.05$.

MLRs without OM-related soil properties	n	r	Variance explained (%)	Cross-validation	
				RMSECV	r
log K_d (Am) = 2.2 (0.5) + 0.5 (0.2) log BET + 0.25 (0.08) pH	19	0.85	73*	0.43	0.79
log K_d (Am) = 3.6 (1.0) - 0.4 (0.2) log Fe_{amorph} + 0.26 (0.09) pH	19	0.83	69*	0.46	0.74
log K_d (Am) = 3.5 (0.2) + 0.6 (0.2) log BET + 0.5 (0.2) log $CaCO_3$	20	0.80	64	0.47	0.68
log K_d (RSm) = 2.3 (0.3) + 0.4 (0.1) log BET + 0.20 (0.05) pH	29	0.87	76*	0.40	0.75

MLRs with OM-related soil properties	n	r	Variance explained (%)	Cross-validation	
				RMSECV	r
log K_d (Am) = 5.0 (0.3) - 0.7 (0.2) log DOC + 0.5 (0.2) log $CaCO_3$	20	0.85	72	0.41	0.79
log K_d (Am) = 4.1 (0.2) - 0.6 (0.2) log C_{org} + 0.6 (0.2) log $CaCO_3$	20	0.81	66	0.45	0.74
log K_d (Am) = 4.5 (0.3) - 0.7 (0.2) log LOI + 0.6 (0.2) log $CaCO_3$	20	0.79	63	0.48	0.76
log K_d (RSm) = 2.7 (0.5) - 0.3 (0.1) log DOC + 0.22 (0.06) pH	29	0.83	69*	0.44	0.70

*TEN1 soil data were excluded from all correlations involving pH variable.

Partial Least Square Regression - based models

As a second approach, PLS regression was applied to construct models using all of the soil characterisation data available (soil samples and properties). The PLS-based models constructed with all data consisted in one LV that could explain around 69% and 52% of the K_d (Am) and K_d (RSm) variability, respectively.

The examination of the VIP index values revealed that several soil properties (clay, sand, Mn_{amorph}, CEC, DIC, Mg, K and Na) were not relevant in the prediction of K_d (Am) in soils since presented VIP values < 1, whereas in the K_d (RSm) prediction model, apart from the latter variables, Al_{amorph} variable was also not relevant. Consequently, data of these soil properties were removed from the corresponding data matrix in order to calibrate much simpler models.

The optimised PLS-based model for Am did not significantly change since the K_d (Am) variance explained only increased up to 70% and it was still composed just by one LV. In contrast, the resulting model for RSm improved substantially since it explained around 72% of the K_d (RSm) variability with 4 LVs. In both cases the K_d variance explained in the PLS-based model was similar to that of the best MLR models.

Regarding the prediction capability of PLS-based models, strong correlations between predicted and experimental log K_d values (Am: r = 0.76; RSm: r = 0.70) were observed alike the case of MLR models, indicating the robustness of the models. Besides, the RMSECV obtained for K_d (Am) (0.44 log units) and K_d (RSm) (0.46 log units), despite being slightly higher than those obtained in the MLR models, indicated that the PLS-based models were also capable to predict the order of magnitude of K_d (Am) and K_d (RSm) values in soils.

External validation of K_d prediction models for RSm

An external validation (EV) of the best MLR and PLS-based K_d (RSm) prediction models was performed according to that explained in section 3.2.3.4. To this end, a reduced calibration set, consisting in the data of 20 soils, was used to construct again the BET-pH MLR and the PLS-based models for RSm, hereinafter referred to as BET-pH MLR_EV and PLS_EV, respectively.

The equation of the BET-pH MLR_EV model ($\log K_d$ (RSm) = 2.2 (0.3) + 0.4 (0.1) log BET + 0.18 (0.05) pH) did not statistically differ from that deduced from the overall dataset model (see **Table 3.7**). Regarding the PLS_EV model, the VIP index values pattern, and thus the relevancy of soil properties in K_d (RSm) prediction, was also comparable to that previously constructed with the overall dataset model. According to these results, it was confirmed that the calibration set used to construct the BET-pH MLR_EV and PLS_EV models was representative for the overall dataset and, consequently, that it was suitable to perform the external validation. Furthermore, the K_d (RSm) variance explained by the EV models and their RMSECV were also similar to those previously obtained for the overall dataset models (see **Figure 3.6**), which confirms the robustness and suitability of the BET-pH MLR_EV and PLS_EV models to predict K_d (RSm) values.

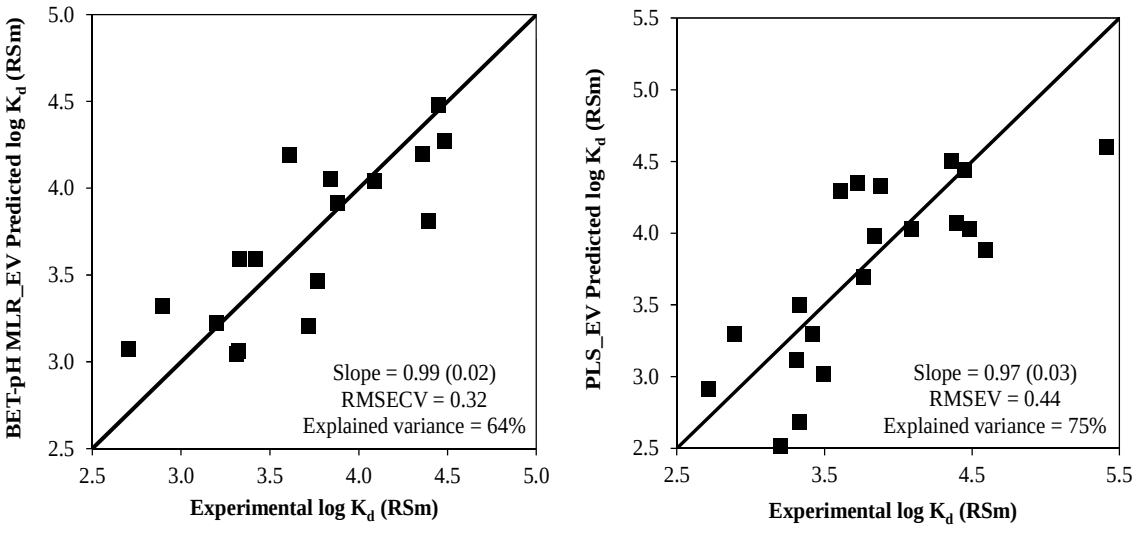

Figure 3.6 *Calibration of K_d (RSm) prediction models for external validation. Plots of predicted by cross-validation vs. experimental log K_d (RSm) values in soils of the calibration set. Solid line represents ideal Experimental log K_d (RSm) = Predicted log K_d (RSm) relationship.*

When K_d (RSm) values of the test set were predicted by means of the EV models, the regressions obtained between the experimental and predicted K_d (RSm) data (depicted in **Figure 3.7**) presented slopes close to unit, intercepts close to zero and high correlation coefficients, especially in the case of the BET-pH MLR_EV model. This demonstrated the absence of bias of the EV models developed.

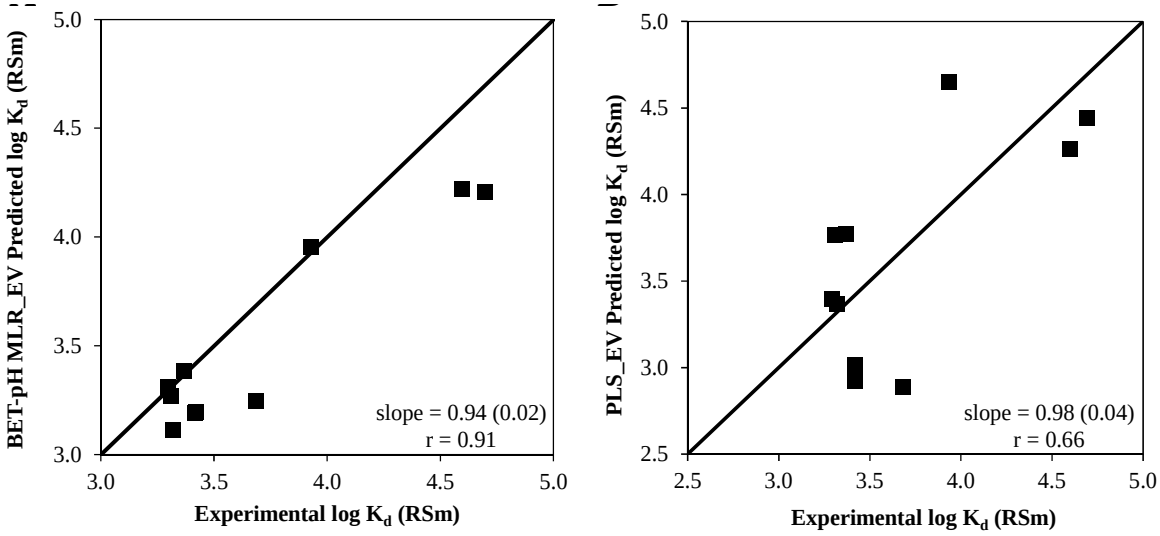

Figure 3.7 *Performance of K_d (RSm) external prediction models. Plots of externally predicted vs. experimental K_d (RSm) values for the test set. Solid line represents ideal Experimental log K_d (RSm) = Predicted log K_d (RSm) relationship.*

So as to ease the examination of the prediction capability of the developed EV models, **Figure 3.8** compares the experimental K_d (RSm) values and those predicted with the BET_pH MLR_EV and the PLS-EV models for the test set. The BET-pH MLR_EV model succeeded in predicting the K_d (RSm) values since a very low average prediction error was obtained (RMSEP = 0.20 log units) and, the experimental and predicted K_d values overlapped for all the soils tested. On the other hand, although the PLS_EV predicted K_d (RSm) values of certain soils, such as UPV or KOM, did not overlap with the experimental data, in general, the PLS-EV model was capable to predict the order of magnitude of K_d (RSm) values since the RMSEP was of 0.50 log units.

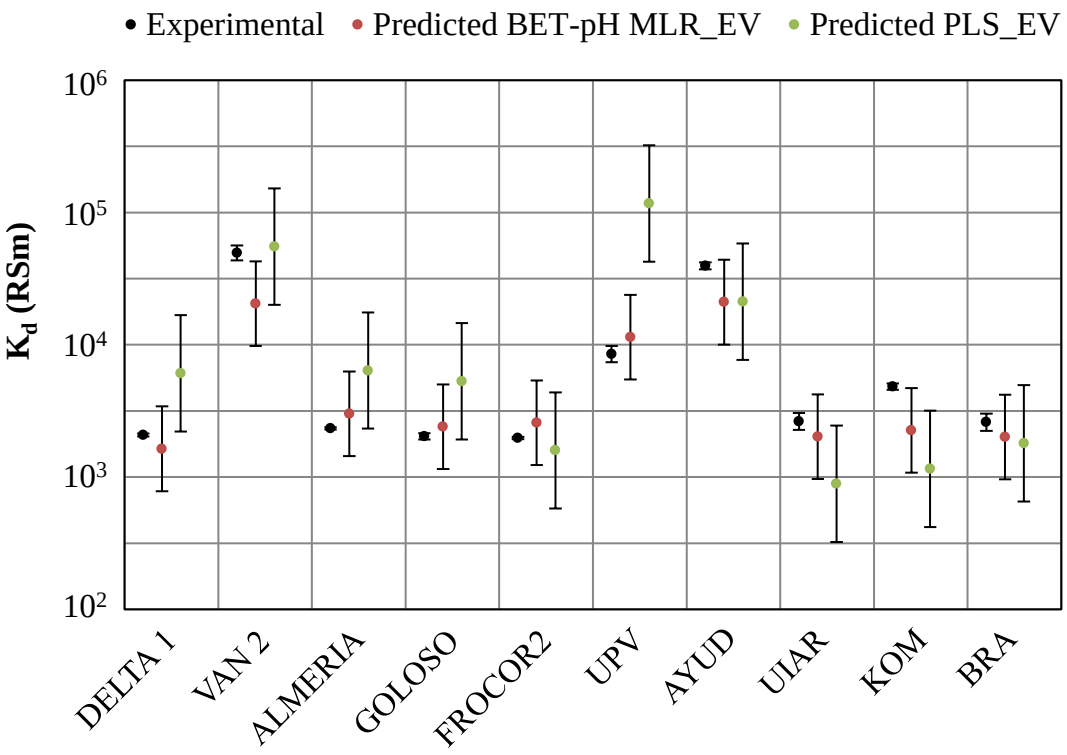

Figure 3.8 *External validations of K_d (RSm) prediction models. Bars correspond to the prediction error of the corresponding model.*

To select a MLR or PLs model is a difficult choice. Latent variable modelling, such as PLS regression, despite being more complex is often favoured over linear regression modelling for predictive purposes when it cannot be guaranteed that the variables used are non covariant, like is the case of a few soil properties used here (Wold et al., 2001). However, the external validation exercise demonstrated that both the MLR and the PLS-based models succeeded in reliably predicting K_d (RSm) values in soils, and even evidenced that the MLR had a better performance since it led to a lower prediction error. Therefore, it may be suggested to use the MLR model due to its simplicity, as only pH and BET data of the soil under assessment are required.

3.3.3 Analogy between Am and RSm interaction in soils

3.3.3.1 Quantitative analysis: comparison of K_d (Am) and K_d (RSm) data

In a first attempt to test the suitability of considering Ln(III) and Ac(III) elements as chemical analogues to determine sorption-desorption parameters in soils of these two families, the K_d (Am) and K_d (RSm) data gathered for the 20 soil in common were statistically compared. The regression between log K_d (RSm) and log K_d (Am) data (depicted in **Figure 3.9**) showed that K_d values of both elements were strongly correlated but K_d (Am) data were slightly higher than K_d (RSm) data ($p < 0.05$).

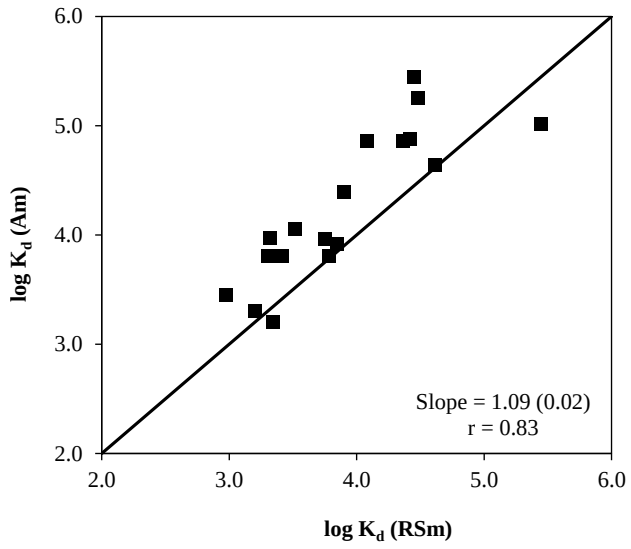

Figure 3.9 *Correlation between log K_d (RSm) and log K_d (Am) values. Solid line represents the ideal log K_d (Am) = log K_d (RSm) relationship.*

Besides the similarity between the Am and RSm sorption data obtained, both elements also presented a similar pattern for desorption data, *i.e.*, $K_{d,des}$ values were generally higher than the K_d values, and desorbed percentages of both elements were always lower than 2% (see **Table 3.3** and **Table 3.4**). These results suggest that the two elements are closely comparable with respect to their sorption-desorption behaviour in soils.

3.3.3.2 Qualitative analysis: comparison of soil properties governing Am and RSm sorption in soils

The same soil properties were found to be affecting in the same way the sorption in soils of Am and RSm since non-significant differences (at $p = 0.05$) existed between the ULRs that correlate soil properties and K_d values of both elements (see **Table 3.8**), which denotes that their interaction is governed by similar sorption mechanisms and involving the same soil fractions, *i.e.* surface complexation on negatively charged sorption sites, enhanced at higher pH, soil BET and soil $CaCO_3$ content, and inhibited by dissolved organic matter. These results confirms the analogy between Am and RSm with respect to their interaction with soils.

Table 3.8 Comparison of ULRs between soil properties and K_d values for RSm and Am. Values in brackets indicate standard error of the log-log correlation parameters at $p = 0.05$.

Variable	Interception		Slope		Variance explained (%)	
	RSm	Am	RSm	Am	RSm	Am
*pH	1.8 (0.3)	1.6 (0.5)	0.31 (0.05)	0.39 (0.07)	60	64
log DOC	4.7 (0.2)	5.6 (0.3)	-0.6 (0.1)	-0.9 (0.2)	51	59
log BET	3.4 (0.1)	3.7 (0.2)	0.6 (0.1)	0.8 (0.2)	47	49
log C_{org}	4.1 (0.1)	4.6 (0.1)	-0.7 (0.1)	-0.8 (0.2)	43	45
log LOI	4.5 (0.2)	5.2 (0.3)	-0.7 (0.2)	-1.0 (0.3)	34	41
log $CaCO_3$	3.4 (0.1)	3.7 (0.2)	0.5 (0.2)	0.8 (0.2)	30	45

*TEN1 data were excluded from the ULR.

This analogy is also evidenced when analysing which soil properties and phases are crucial to develop different models to predict K_d values of Am and RSm. On the one hand, the best MLR for both elements consisted in the combination of the same soil properties (BET and pH) which led again to comparable equations (non-significantly different at $p = 0.05$). On the other, the pattern of variables' relevance in the PLS-based models (Fe_{amorph} < LOI < C_{org} < pH < $CaCO_3$ < BET < DOC), apart from being in line with that observed by ULR and MLR analyses, was almost identical for both elements as shown in **Figure 3.10**.

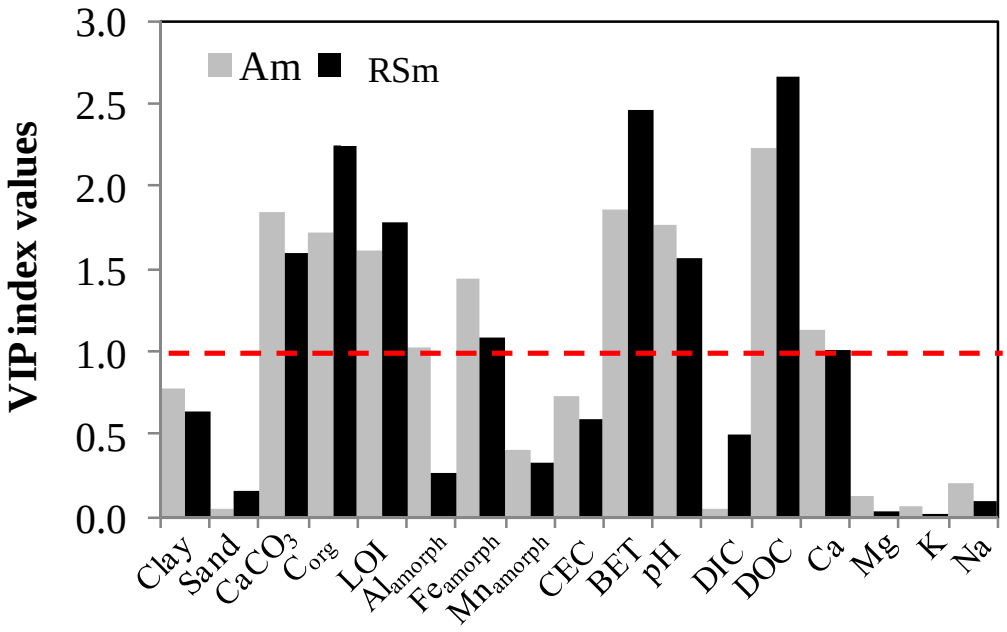

Figure 3.10 *VIP index values from the PLS-based model constructed for RSm, in which the red dotted line represents the VIP threshold value (1.0) for the relevant variables in the model.*

These results suggest that the same soil properties can be used to predict soil K_d values of both elements, even in multivariate models based on soil latent variables.

3.3.3.3 Indistinct prediction of Am and RSm interaction in soils from soil properties

As a final test to check the soil-interaction analogy between RSm and Am, which can anticipate the feasibility of indistinctly using Ln(III) and Ac(III) sorption data for predictive purposes, the BET-pH MLR and PLS models previously constructed with Am data (Am models) were applied to predict K_d (RSm) values of the soils of the test set previously used for the external validation of RSm prediction models (see section 3.3.2.3). In **Figure 3.11** the experimental K_d (RSm) values are compared with those predicted with Am models and also with the RSm models.

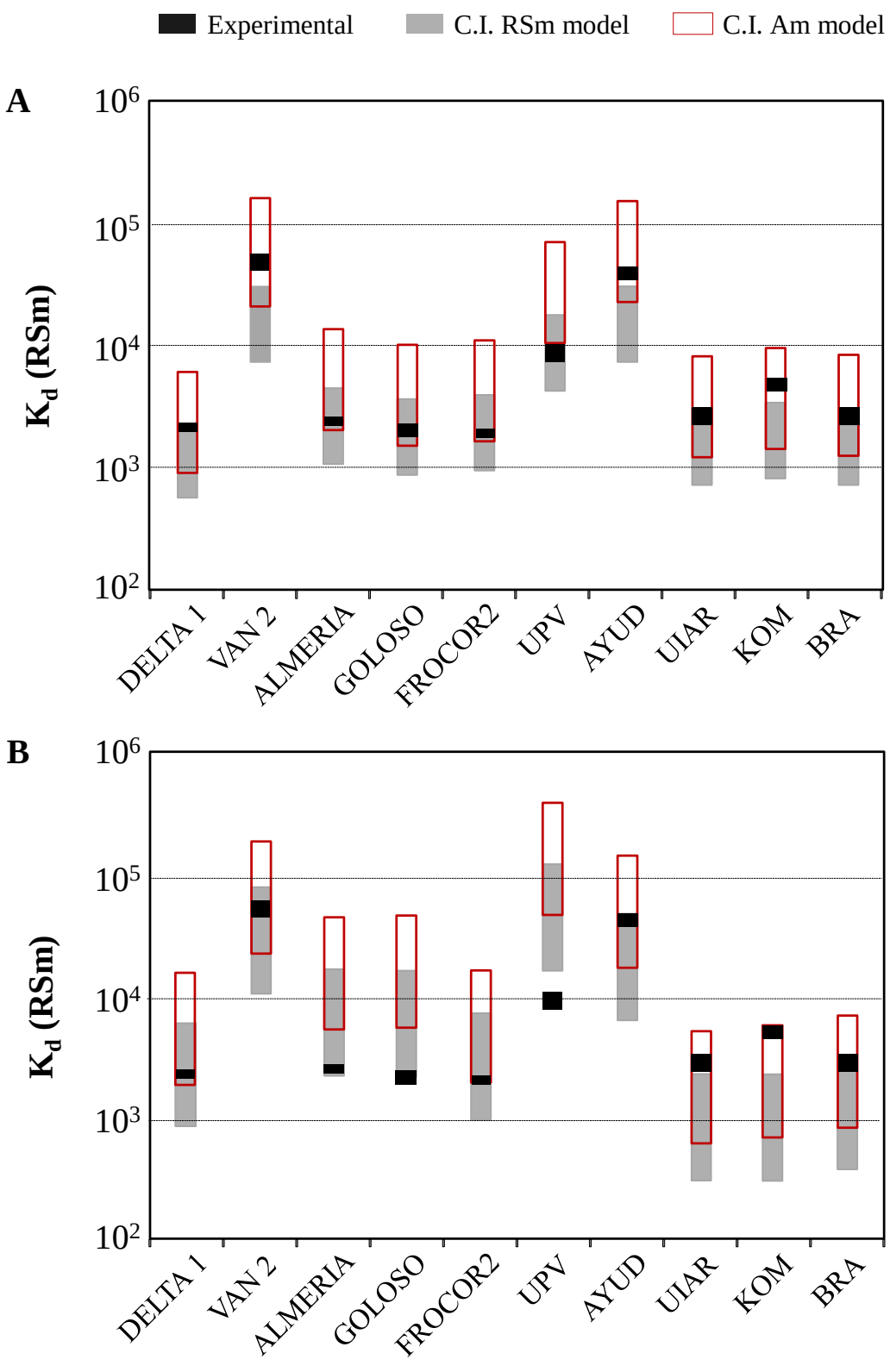

Figure 3.11 *Comparison of experimental and externally predicted K_d (RSm) values with models calibrated with RSm and with Am data: (A) Prediction with BET_pH MLR models; (B) Prediction with PLS-based models. C.I.: confidence interval of predicted K_d (RSm) values calculated as the log K_d ± RMSECV.*

The application of the MLR (**Figure 3.11 A**) and PLS (**Figure 3.11 B**) models calibrated with Am data (Am models) led to K_d (RSm) systematically higher than those predicted with models calibrated with RSm data. However, the average prediction errors obtained when applying the Am models (RMSEP = 0.26 and 0.60 log units with the BET-pH_MLR and with the PLS model, respectively) were comparable to those obtained with models calibrated with RSm data (RSm_EV models), showing that in general the Am models succeeded in predicting the K_d (RSm) values within an order of magnitude range. These results clearly indicate that the interaction of RSm in soils could be assessed from the soil properties regardless of the element (Am or RSm) used to calibrate the models.

3.3.4 Influence of Sm concentration on Sm sorption-desorption behaviour in soils

3.3.4.1 Sm sorption isotherms

Figure 3.12 shows the Sm sorption isotherms (C_{sorb} *vs.* C_{eq} and K_d *vs.* C_{sorb}) constructed for the five soils analysed. Nearly linear-shaped C_{sorb} *vs.* C_{eq} isotherms were obtained for DELTA2 and DUBLIN soils, showing constant Sm sorption capacity irrespective of the initial Sm concentration in solution, and thus, that no saturation of sorption sites occurred. However, although both DELTA2 and DUBLIN sorption isotherms display almost constant K_d (Sm) values in the entire Sm concentration range tested, it seems that K_d (Sm) values were slightly lower at small Sm loads, suggesting that Sm might be affected by competing processes such as the formation of soluble chelates with dissolved organic matter or the favoured sorption of competitive cationic species in solution with a higher concentration than that of Sm.

Regarding ANDCOR, ASCO and CABRIL soils, the curve-shaped C_{sorb} *vs.* C_{eq} isotherms evidenced that the Sm sorption in these soils was strongly influenced by the Sm concentration in solution. For these soils, the slope of the C_{sorb} *vs.* C_{eq} isotherm decreased when increasing the Sm concentration and a pseudoplateau was reached at the high Sm concentration region, which might indicate either a saturation of the Sm sorption sites or the presence of sorption sites of contrasting affinity for Sm.

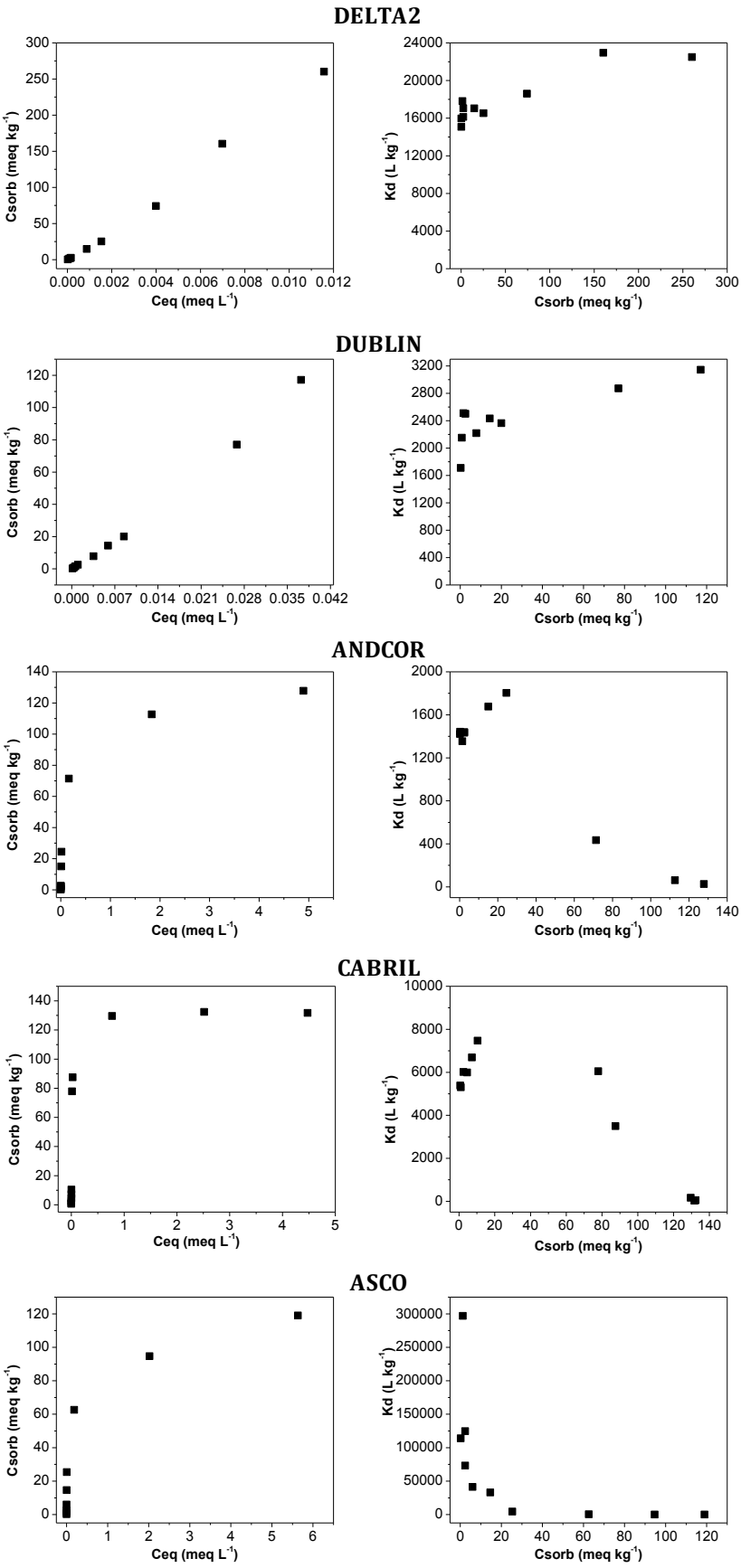

Figure 3.12 *Sorption isotherms of Sm in analysed soils: C_{sorb} vs. C_{eq} and K_d vs. C_{sorb} plots.*

Examination of the K_d *vs.* C_{sorb} isotherms, as suggested by Hinz (2001), also permits to observe a relatively constant partitioning at the lowest Sm concentration range ($C_i < 0.6$ meq L^{-1}, related to $C_{sorb} < 20$ meq kg^{-1}) for ANDCOR and CABRIL soils followed by a linear decrease in K_d (Sm) values at higher Sm loads. These sorption patterns can be associated with Langmuir-type sorption behaviour as well as they suggest the existence of sorption sites with similar affinity for Sm that get saturated when increasing the Sm loads into these soils. Conversely, K_d *vs.* C_{sorb} isotherm of ASCO showed an initial sharply decrease in Sm sorption at low concentrations followed by constant K_d values at $C_i > 0.6$ meq L^{-1}. This sorption pattern might hint that Sm was sorbed into sites with much higher affinity at small Sm loads than at large Sm loads, which can be associated with Freundlich-type sorption behaviour.

3.3.4.2 Sm-soil interaction at varying Sm concentration

Table 3.9 summarises sorption and desorption parameters gathered from the five soils at four levels of Sm concentration. At the lowest Sm concentration tested, all soils showed a high Sm sorption capacity, with K_d (Sm) values always $>10^3$ L kg^{-1} and sorption percentages (S) close to 100%. At this Sm concentration level, in all cases, the Sm concentration remaining in solution after the sorption process (C_{eq}) did not exceed the maximum Sm concentration permitted in drinking water ($4.8\ 10^{-4}$ meq L^{-1}) proposed by Mọikin, (1993). Therefore, it seems as if soils act as a natural barrier remediating liquid sources containing small Sm amounts ($C_i < 10^{-2}$ meq L^{-1}).

When higher concentration of Sm was added to the soils, the K_d (Sm) remained almost constant for DELTA2 and DUBLIN, but for ANDCOR, CABRIL and ASCO soils, K_d (Sm) values dropped several orders of magnitude and sorption percentages plummeted to around 50% when the largest Sm load was added. Such sorption parameter values indicated that, at these high concentrations, Sm sorption occurs at low-affinity sites. Therefore, for this type of soils, a single value of K_d(Sm) cannot be used for risk assessment purposes, but the most appropriate value depending on the Sm concentration released in the contamination event.

Table 3.9 Values of sorption and desorption parameters of Sm in the tested soils.

Soil sample	Sorption				Desorption				$K_{d,des}/K_d$ ratio
	C_i (meq L^{-1})	C_{eq} (meq L^{-1})	K_d (L kg^{-1})	S (%)	$C_{i,des}$ (meq kg^{-1})	$C_{eq,des}$ (meq L^{-1})	$K_{d,des}$ (L kg^{-1})	D (%)	
ANDCOR	0.01	1.9×10^{-4}	1400	98.2	0.28	1.1×10^{-4}	2600	0.8	1.8
	0.1	1.7×10^{-3}	1400	98.2	2.5	8.8×10^{-4}	2800	0.7	1.9
	2.9	0.16	400	94.3	71	0.018	3800	0.5	8.8
	9.8	4.9	26	50.2	128	0.097	1300	1.6	50
CABRIL	0.03	1.3×10^{-4}	5400	99.5	0.71	8×10^{-5}	8900	0.3	1.6
	0.3	1.1×10^{-3}	6700	99.6	7.3	9×10^{-4}	8100	0.3	1.2
	3.1	0.013	6000	99.6	78	0.0034	23000	0.1	3.8
	9.6	4.5	29	53.4	132	0.071	1800	1.4	62
ASCO	0.05	4.1×10^{-6}	300000	>99.9	1.2	< lq	-	-	-
	0.2	1.4×10^{-4}	41000	99.9	6.0	9.3×10^{-5}	64000	0.04	1.6
	2.7	0.19	340	93.0	63	0.0019	21000	0.1	63
	10.3	5.6	21	45.6	119	0.019	6200	0.4	300
DELTA2	0.01	1.8×10^{-5}	16000	99.8	0.28	1.6×10^{-5}	18000	0.1	1.1
	0.1	1.5×10^{-4}	16000	99.8	2.5	1.3×10^{-4}	19000	0.1	1.2
	2.9	4×10^{-3}	19000	99.9	74	0.0042	18000	0.1	1.0
	9.9	0.01	22000	99.9	260	0.0098	27000	0.1	1.2
DUBLIN	0.03	3.5×10^{-4}	2200	98.7	0.75	1.7×10^{-4}	4300	0.7	2.0
	0.3	3.5×10^{-3}	2200	98.7	7.8	1.5×10^{-4}	5400	0.5	2.4
	2.7	0.027	2900	99.0	77	0.017	4500	0.6	1.6
	9.4	0.068	3400	99.4	233	0.051	5300	0.5	1.6

With respect to the desorption parameters, $K_{d,des}$ values were always >10^3 L kg^{-1} and the desorption percentages (D %) were extremely low (<2%) suggesting that, after the drying process, most of the Sm incorporated into these soils was irreversibly sorbed regardless of the soil properties or the amount of Sm previously sorbed in soils. In addition, the $K_{d,des}/K_d$ ratio was constant and close to 1 in all the Sm concentration tested for DELTA2 and DUBLIN soils, whereas for ANDCOR, CABRIL and ASCO soils the $K_{d,des}/K_d$ factor increased up to values from tens to hundreds when increasing the Sm concentration. These sorption-desorption pattern suggests that, after the drying process, $K_{d,des}$ values are closer among scenarios, and become less dependent on the initial Sm concentration. However, in spite of the high irreversibility of Sm sorption in soils, for the highest levels of soil contamination, the Sm concentration that might reach the solution after the desorption process ($C_{eq,des}$) exceeded the maximum Sm concentration permitted in drinking water (4.8 10^{-4} meq L^{-1}), entailing a risk for living beings.

3.3.4.3 Proposal of Sm sorption data for different environmental contamination scenarios

The incorporation of Sm in soils and its retention by the soil solid matrix have been demonstrated to be heavily influenced by the amount of Sm released to a given soil and by the soil properties. Therefore, in order to reliably assess the interaction of Sm in varying contamination scenarios (both in terms of Sm loads and type of soil) sorption models describing the Sm sorption as a function of its concentration, for different soil-types, are needed. **Table 3.10** summarises the parameters derived from the best fitting of the sorption isotherms constructed for the contrasting soils tested here.

On the one hand, sorption data at the lowest Sm concentration range tested were fitted to a linear model and the derived $K_{d,linear}$ (Sm) values are provided as appropriate K_d (Sm) best estimates to assess risk for soil contamination episodes with small loads of Sm. On the other, Freundlich or Langmuir isotherms (see section 3.2.2.5) are also provided for the assessment of soil contamination episodes with liquid sources containing higher Sm concentrations.

T**able 3.10** Sorption parameters (confidence range, $p = 0.05$) derived from fitting Sm sorption isotherms to Freundlich, Langmuir and linear equations. $K_{d,linear}$ (L kg^{-1}); K (L meq^{-1}); b (meq kg^{-1}); K_f ($meq^{(1-N)}$ L^N kg^{-1}); and N (dimensionless).

Soil sample	Sorption models
DELTA2	$K_{d,linear}$[a] = 17000 (80) ; R^2 = 0.99
	Freundlich: K_f = 37000 (15000), N = 1.1 (0.1); R^2 = 0.99
DUBLIN	$K_{d,linear}$[a] = 2400 (40); R^2 = 0.99
	Freundlich: K_f = 6000 (1000), N = 1.2 (0.1); R^2 = 0.99
ANDCOR	$K_{d,linear}$[a] = 1400 (20); R^2 = 0.99
	Langmuir: K = 10 (4), b = 124 (13); R^2 = 0.99
CABRIL	$K_{d,linear}$[a] = 5900 (100) ; R^2 = 0.99
	Langmuir: K = 90 (17), b = 132 (5); R^2 = 0.99
ASCO	$K_{d,linear}$[a] = 260000 (75000) ; R^2 = 0.92
	Freundlich: K_f = 81 (15), N = 0.23 (0.05); R^2 = 0.99

[a] Linear model at $C_i < 0.1$ meq L^{-1} for ASCO, at $C_i < 0.2$ meq L^{-1} for ANDCOR, CABRIL, DELTA2 and DUBLIN.

As expected, the sorption isotherms of DELTA2 and DUBLIN soils were perfectly described with a Freundlich model with *N* value close to 1, which means that there was not saturation of the sorption sites and that all sites presented similar affinity for Sm (pseudo-linear sorption behaviour). However, the N value slightly higher than 1, especially in the case of DUBLIN soil, suggested that Sm sorption was slightly lowered at small Sm loads. Taking into account the high content of dissolved organic matter of these soils (see DOC values in **Table 3.2**), such Sm sorption behaviour at low Sm concentrations can result from the formation of stable, negatively charged Sm-humate complexes that remains in solutions as previously explained in section 3.3.2.1.

The Freundlich model was also the most appropriate for describing the Sm sorption isotherm of ASCO soil. The *N* value (much lower than 1) indicates Sm sorption at sites of varying affinity, which suggest that the decrease in the ASCO capacity to sorb Sm at high Sm concentrations is due to the saturation of the available high-affinity sites. The presence of high-affinity sites in this soil was already deduced from the K_d *vs.* C_{sorb} representation in **Figure 3.12**, since there was a sharply decrease in Sm sorption at low concentrations followed by constant K_d values at higher concentrations.

Conversely, the Langmuir model was appropriate to describe the Sm sorption behaviour for ANDCOR and CABRIL soils. These soils presented a limited number of sorption sites (around 120-130 meq Sm per kg) with relatively constant and low affinity for Sm. The Sm sorption sites available in ANDCOR soil seems to be of much lower bonding energy than those present in the rest of soils.

3.3.4.4 Comparison of K_d values for stable Sm and ^{151}Sm

A much smaller load of Sm is expected in soils due to the impact of radioactive liquid wastes than in contamination episodes of stable Sm isotopes. Thus, the $K_{d,linear}$ (Sm) derived at the lowest concentration range (**Table 3.10**) and the $K_{d,des}$ (Sm) data obtained at the lowest Sm concentration assayed (**Table 3.9**) were compared with the sorption-desorption K_d data previously obtained for the ^{151}Sm radioisotope in the same soil samples (see Section 3.3.1, **Table 3.4**), as can be seen in **Figure 3.13**. The two series of data were highly correlated (r = 0.98) and the paired-tests revealed that no significant differences existed between the two series of data (p<0.05).

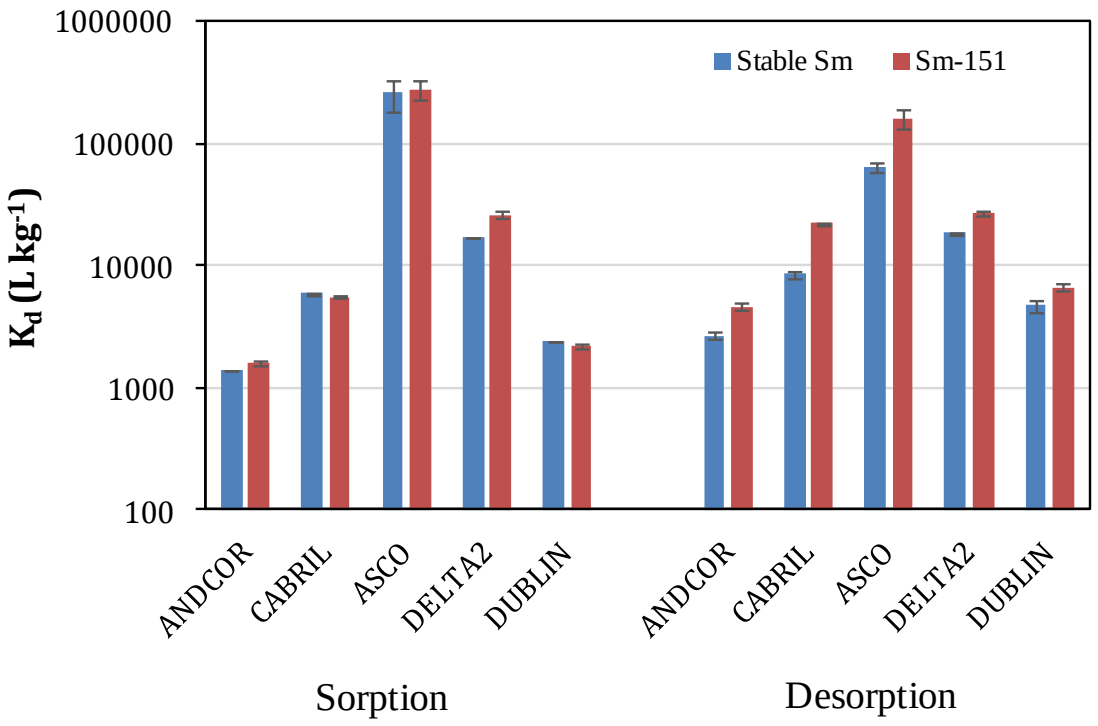

Figure 3.13 *Comparison of K_d values of stable Sm at low initial concentrations and ^{151}Sm obtained in the tested soils. Error bars for K_d values of ^{151}Sm correspond to standard deviation of replicates (n= 3) and, for stable Sm, to the confidence range of $K_{d,linear}$ (p = 0.05).*

From these results, it was demonstrated that the capacity of different types of soils to retain Sm radioisotopes or low concentrations of stable Sm was similar, and thus, the data gathered here can also be suitable to assess the risk derived from radioactive releases to the environment involving Sm radioisotopes.

3.3.4.5 Examination of soil characteristics responsible for Sm sorption in soils as a function of Sm concentration

The contrasting sorption behaviour observed among soils demand to go one step further in explaining the relationship between the concentration-dependent capacity to sorb Sm of the tested soils and the sorption mechanisms responsible for such soil-Sm interaction behaviour, to assess the Sm interaction in other scenarios. **Figure 3.14** shows the Sm fractionation obtained with the sequential extraction procedure applied to the soil residues coming from the sorption experiments performed at low and high Sm concentrations (0.06 and 6 meq L^{-1}, respectively). Although the sequential extraction approach is highly operational, it provides approximate information about the soil phases involved in Sm interaction and is an excellent tool for comparison, here from contamination with different Sm concentrations. Distinct patterns of Sm fractionation were obtained, denoting that the sorption mechanisms and soil phases controlling Sm sorption hinged on the characteristics of each soil sample (see section 3.2.1, **Table 3.1** and **Table 3.2**).

Almost 100% of the Sm sorbed in DELTA2 at low and high Sm concentrations remained in the final residual fraction, showing that this soil boasts a large number of high-affinity sorption sites for Sm. Considering the DELTA2 properties such as basic pH, high clay and OM contents (33.5% and 23%, respectively) the high and linear Sm sorption (K_d always > 10^4 L kg^{-1}) previously observed in the isotherm can be attributed to complexation reactions of Sm with high-affinity sites such as hydroxyl groups present in clay minerals and/or carboxylic and phenolic groups present in insoluble OM (humin) fraction (Pourret et al., 2009; Ye et al., 2014). Moreover, from the moderate DOC content it is expected that only a small fraction of Sm will be forming complexes with dissolved organic compounds (soluble Sm-humate

complexes) that are weakly sorbed due to coulombic repulsion with the soil surface (Shan et al., 2002; Takahashi et al., 1998).

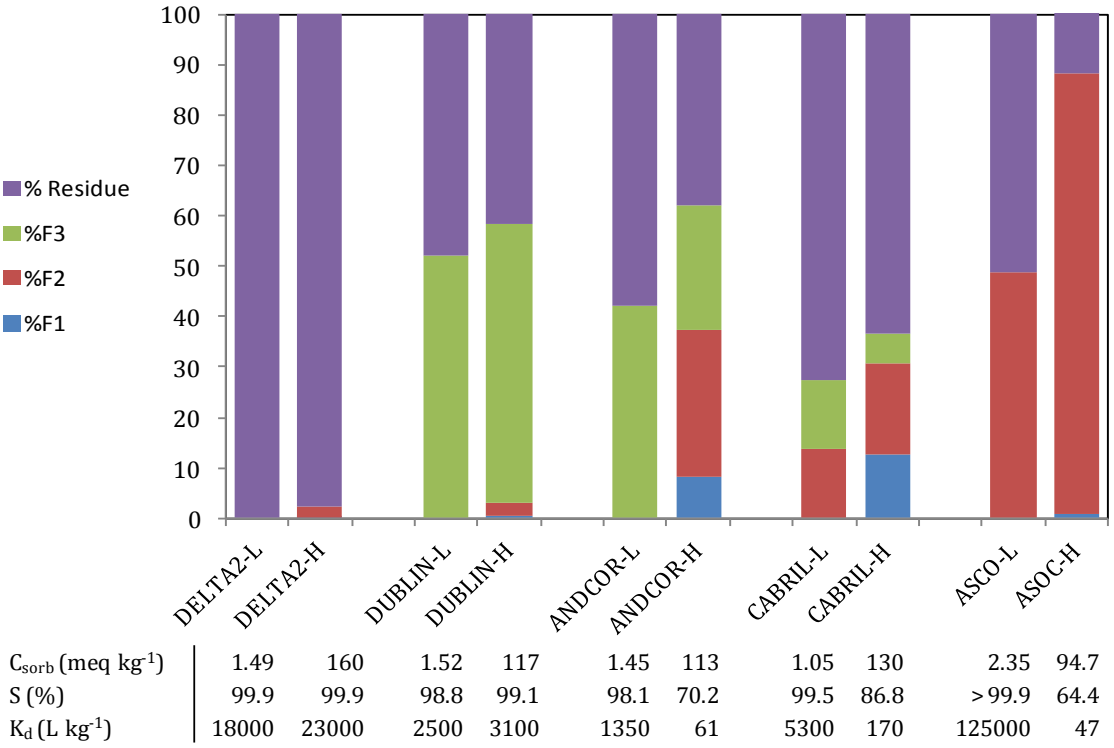

	DELTA2-L	DELTA2-H	DUBLIN-L	DUBLIN-H	ANDCOR-L	ANDCOR-H	CABRIL-L	CABRIL-H	ASCO-L	ASOC-H
C_{sorb} (meq kg^{-1})	1.49	160	1.52	117	1.45	113	1.05	130	2.35	94.7
S (%)	99.9	99.9	98.8	99.1	98.1	70.2	99.5	86.8	> 99.9	64.4
K_d (L kg^{-1})	18000	23000	2500	3100	1350	61	5300	170	125000	47

Figure 3.14 *Fractionation of Sm sorbed in soil residues originated from sorption tests with low (-L) and high (-H) initial concentrations of Sm.*

Alike DELTA2, the fractionation of Sm sorbed in DUBLIN at low Sm concentrations was similar to that at high Sm concentrations. However, in this case only around 40% of Sm remained in the residue fraction and the majority of Sm was found in the non-residual fraction corresponding to soluble OM at alkaline pH. According to DUBLIN properties (extremely high LOI and negligible clay content), this Sm fractionation points to a Sm sorption namely controlled by complexation reactions with more labile (humic and fulvic acids) or insoluble (humin) OM fractions, rather than with clay minerals. The lower residual fraction of Sm in DUBLIN agrees with its considerably lower K_d(Sm) in comparison with that of DELTA2.

Although the high OM content seems to provide enough high-affinity sorption sites to ensure linear sorption in the entire Sm concentration range tested, the Sm sorption in DUBLIN ($K_{d,linear}$ = 2400 L kg^{-1}) was lower than in DELTA2 ($K_{d,linear}$ = 17000 L kg^{-1}). This difference can be explained by the high DOC in DUBLIN (290 mg kg^{-1}) as a result

of the different nature of DUBLIN OM and its acid pH, which suggests that formation of negative charged Sm-humate complexes that remain in solution due to electrostatic repulsion with soil surfaces, may play a key role in this type of soils (Xiangke et al., 2000; Ye et al., 2014).

The Sm fractionation patterns for the rest of soil samples varied according to the Sm concentration and showed an increase in the Sm solubilised in F2 (sensitive to acidification) and/or in F1 (exchangeable) fractions at high Sm concentrations. These results indicate that significant fractions of Sm were sorbed in low affinity sorption sites, which is in agreement with the concentration dependency of Sm sorption (*i.e.*, remarkably decrease in sorption capacity at high Sm concentrations) previously evidenced in the sorption isotherms (**Figure 3.12**). ANDCOR soil, despite having moderate clay and OM contents (18% and 19%, respectively), presented the lowest Sm sorption capacity because its acid pH limits the amount of sorption sites available (low net negative surface charge) and because a significant fraction of Sm is expected to be, alike the case of DUBLIN, slightly reactive with the soil surface due to the formation of highly soluble Sm-humate species (DOC = 78 mg kg^{-1}). In contrast, the relative moderate Sm sorption capacity of CABRIL can be straightforwardly ascribed to not having enough high-affinity sorption sites as a result of its low OM and clay mineral contents. Finally, ASCO soil exhibited the highest Sm sorption capacity at low Sm concentrations and the lowest at high Sm concentrations, thus denoting the presence of a very limited number of extremely high-affinity sites. The Sm fractionation obtained in ASCO at low Sm concentrations revealed that Sm was equally associated to the residual and to the F2 fractions, whereas at high Sm concentrations the majority of Sm was related to F2, which can be considered as Sm bound to carbonate minerals since ASCO has a very low OM content (LOI = 1.6%) and high carbonate content (38%). This behaviour agrees with some authors that pointed out the extremely high affinity of Ln(III) and Ac(III) for certain carbonate minerals such as aragonite, that are present in much lesser extent in soils than other carbonate-like minerals, for instance calcite or dolomite (Sutton, 2009; Zhong et al., 1995). Taking into account that ASCO has the lowest clay content among the soils tested (with the exception of the peat soil DUBLIN), the presence of different types of carbonates in ASCO, appears more likely to be responsible for the Sm sorption behaviour in this soil.

3.4 REFERENCES

Ali, H.A., 2014. Social and environmental impact of the rare earth industries. Resources 3, 123-134.

Awual, M.R., Kobayashi, T., Miyazaki, Y., Motokawa, R., Shiwaku, H., Suzuki, S., Okamoto, Y., Yaita, T., 2013. Selective lanthanide sorption and mechanism using novel hybrid Lewis base (N-methyl-N-phenyl-1,10-phenanthroline-2-carboxamide) ligand modified adsorbent. J. Hazard. Mater. 252-253, 313-320.

Burt, R., 2004. Investigation report No 42, Version 4.0 - Soil survey laboratory methods manual. Natural Resources Conservation Service, USDA, Washington, USA.

Cao, X., Wang, X., Zhao, G., 2000. Assessment of the bioavailability of rare earth elements in soils by chemical fractionation and multiple regression analysis. Chemosphere 40, 23-28.

Cao, X., Chen, Y., Wang, X., Deng, X., 2001. Effect of redox potential and pH value on the release of rare earth elements from soil. Chemosphere 44, 655-661.

Carter, M.R., Gregorich, E.G., 2006. Extractable Al, Fe, Mn and Si. From: Soil Sampling and Methods of Analysis, second ed. Canadian Society of Soil Science, CRC Press, Boca Ratón, USA.

Cheng, H., Hao, F., Ouyang, W., Liu, S., Lin, C., Yang, W., 2012. Vertical distribution of rare earth elements in a wetland soil core from Senjiang Plain in China. J. Rare Earth 30 (7), 731-738.

Choppin, G.R., 2007. Actinide speciation in the environment. J. Radioanal. Nucl. Ch. 273 (3), 695-703.

Das, D.K., Pathak, P.N., Kumar, S., Manchanda, V.K., 2009. Sorption behavior of Am^{3+} on suspended pyrite. J. Radioanal. Nucl. Ch. 281, 449-455.

Degueldre, C., Ulrich, H.J., Silby, H., 1994. Sorption of 241Am onto montmorillonite, illite and hematite colloids. Radiochim. Acta 95, 173-179.

Do, D., 1998. In Adsorption Analysis: Equilibria and Kinetics, vol.2. Imperial College Press-ICP, London.

Echevarría, J.C., Morera, M.T., Mazkiarán, C., Garrido, J.J., 1998. Competitive sorption of heavy metals by soils. Isotherms and factorial experiments. Environ. Pollut. 101, 275-284.

Elbaz-Pulichet, F., Depuy, C., 1999. Behaviour of rare earth elements at the freshwater-seawater interface of two acid mine rivers: the Tinto and Odiel (Andalucia, Spain). Appl. Geochem. 14, 1063-1072.

EPA, 1999. EPA 402-R-99-004A Understanding variation in partition coefficient, K_d, values. Volume I: The Kd model, methods of measurement, and application of chemical reaction codes, United States Environmental Protection Agency, USA.

Esbensen, K.H., 2004. Multivariate data analysis - in practice, fifth ed. CAMO Process AS, Oslo, Norway.

Fagerlund, G., 1973. Determination of specific surface by the BET method. Mater. Struct. 6 (3), 239-245.

Fan, Q.H., Zhang, M.L., Zhang, Y.Y., Ding, K.F., Yang, Z.Q., Wu, W.S., 2010. Sorption of Eu(III) and Am(III) on attapulgite: effect of pH, ionic strength and fulvic acid. Radiochim. Acta 98, 19-25.

Galunin. E., Alba, M.D., Avilés, M.A., Santos, M.J., Vidal, M., 2009. Reversibility of La and Lu sorption onto smectites: implications for the design of engineered barriers in deep geological repositories. J. Hazard. Mater. 172, 1198-1205.

Galunin. E., Alba, M.D., Santos, M.J., Abrão, T., Vidal, M., 2010. Lanthanide sorption on smectitic clays in presence of cement leachates. Geochim. Cosmochim. Ac. 74, 862-875.

Gil-García, C., Rigol, A., Rauret, G., Vidal, M., 2008. Radionuclide sorption-desorption pattern in soils from Spain. Appl. Radiat. Isotopes 66, 126-138.

Gil-García, C., Rigol, A., Vidal, M., 2009a. New best estimates for radionuclide solid-liquid distribution coefficients in soils. Part 1: radiostrontium and radiocaesium. J. Environ. Radioactiv. 100, 690-696.

Gil-García, C.J., Tagami, K., Uchida, S., Rigol, A., Vidal, M., 2009b. New best estimates for radionuclide solid-liquid distribution coefficients in soils. Part 3: miscellany of radionuclides (Cd, Co, Ni, Zn, I, Se, Sb, Pu, Am and others). J. Environ. Radioactiv. 100, 704-715.

Gil-García, C.J., Rigol, A., Vidal, M., 2011a. The use of hard- and soft- modeling to predict radiostrontium solid-liquid distribution coefficients in soils. Chemosphere 85, 1400-1405.

Gil-García, C.J., Rigol, A., Vidal, M., 2011b. Comparison of mechanistic and PLS-based regression models to predict radiocaesium distribution coefficients in soils. J. Hazard. Mater. 197, 11-18.

Gimeno-Serrano, M.J., Auqué, L.F., Nordstrom, D.K., 2000. REE speciation in low-temperature acidic waters and competitive effects of aluminum. Chem. Geol. 165, 167-180.

GRS, 2012. GRS-294 - Radionuclide inventory of vitrified waste after spent nuclear fuel reprocessing at La Hague. Gesellschaft für Anlagen- und Reaktorsicherheit, Germany.

He, J., Lü, C.W., Xue, H.X., Liang, Y., Bai, S., Sun, Y., Shen, L.L., Mi, N., Fan, Q.Y., 2010. Species and distribution of rare earth elements in the Baotou section of the Yellow River in China. Environ. Geochem. Health 32, 45-58.

Higgo. J.J.W., Rees, L.V.C., 1986. Adsorption of actinides by marine sediments: effect of the sediment/seawater ratio on the measured distribution ratio. Environ. Sci. Technol. 20 (5), 483-490.

Hinz, C., 2001. Description of sorption data with isotherm equations. Geoderma 99, 225–243.

Ho Lee, M., Chang, E., Song, K., Hee, Y., Sang, H., 2011. The influence of humic acid on the pH-dependent sorption of americium (III) onto kaolinite. J. Radioanal. Nucl. Ch. 287, 639-645.

Houba, V. J. G., Temminghoff, E. J. M., Gaishorst, G. A., van Wark, W., 2000. Soil analysis procedures using 0.01 M calcium chloride as extraction reagent. Soil Sci. Plant Anal. 31, 1299-1396.

Hu, Z., Haneklaus, S., Sparovek, G., Schnug, E., 2006. Rare earth elements in soils. Commun. Soil Sci. Plan. 37, 1381-1420.

Humsa, T.Z., Srivastava, R.K., 2015. Impact of rare earth mining and processing on soils and water environment at Chavara, Kollam, Kerala: a case study. Proc. Earth Planet. Sci. 11, 566 – 581.

IAEA, 1994. Technical Report Series No 364 - Handbook of parameter values for the prediction of radionuclide transfer in temperate environments. International Atomic Energy Agency, Austria.

IAEA, 2001. Safety Report Series No 19 - Generic models for use in assessing the impact of discharges of radioactive substances to the environment. International Atomic Energy Agency, Austria.

IAEA, 2004. Technical Report Series No 435 - Implications of partitioning and transmutation in radioactive waste management. International Atomic Energy Agency, Austria.

IAEA, 2009. TECDOC-1616 - Quantification of radionuclide transfer in terrestrial and freshwater environments for radiological assessments. International Atomic Energy Agency, Austria.

Ishikawa, N.J., Uchida, S., Tagami, K., 2009. Estimation of soil-soil solution distribution coefficient of strontium using soil properties. Appl. Radiat. Isotopes 67 (2), 319-323.

ISO, 1995. ISO 10694 - Soil quality. Determination of organic and total carbon after dry combustion (elementary analysis). International Organization for Standardization, Switzerland.

Jin, Q., Wang, G., Ge, M., Chen, Z., Wu, W., Guo, Z., 2014. The adsorption of Eu (III) and Am (III) on Beishan granite: XPS, EPMA, batch and modelling study. Appl. Geochem. 47, 17-24.

Jinxia, L., Mei, H., Xiuqin, Y., Jiliang, L., 2010. Effects of the accumulation of the rare earth elements on soil macrofauna community. J. Rare Earth 28 (6), 957-964.

Jones, D.L., 1997. Trivalent metal (Cr, Y, Rh, La, Pr, Gd) sorption in two acid soils and its consequences for bioremediation. Eur. J. Soil Sci. 48, 697-702.

Kitamura, A., Yamamoto, T., Nishikawa, S., Moriyama, H., 1999. Sorption behavior of Am (III) onto granite. J. Radioanal. Nucl. Ch. 239 (3), 449-453.

Kotska, J.E., Luther III, G.W., 1994. Partitioning and speciation of solid phase Fe in saltmarsh sediments. Geocim. Cosmochim. Ac. 58 (7), 1701-1710.

Krauskopf, K.B., 1986. Thorium and rare earth metals as analogues for actinide elements. Chem. Geol. 55, 323-335.

Lee, S.G., Lee, K.Y., Cho, S.Y., Yoon, Y.L., Kim, Y., 2006. Sorption properties of ^{152}Eu and ^{241}Am in geological materials: Eu as an analogue for monitoring the Am behaviour in heterogeneous geological environments. Geosci. J. 10 (2), 103-114.

Li, D., Huang, S., Wang, D., Wang, W., Peng, A., 2000. Transfer characteristics of rare earth elements applied in agricultural soils. J. Environ. Sci. Health A 35 (10), 1869-1881.

Li, D., Huang, S., Wang, W., Peng, A., 2001. Study on the kinetics of cerium (III) adsorption-desorption on different soils of China. Chemosphere 44, 663-669.

Li, X., Chen, Z., Chen, Z., Zhang, Y., 2013. A human health risk assessment of rare earth elements in soil and vegetables from a mining area in Fujian Province, Southeast China. Chemosphere 93, 1240-1246.

Liang, T., Li, K., Wang, L., 2014. State of rare earth elements in different environmental components in mining areas of China. Environ. Monit. Assess. 186, 1499-1513.

Lujaniene, G., Plukis, A., Kimtys, E., Remeikis, V., Jankünaite, D., Ogorodnikov, B.I., 2002. Study of ^{137}Cs, ^{90}Sr, ^{239,240}Pu, ^{238}Pu and ^{241}Am behavior in the Chernobyl soil. J. Radioanal. Nucl. Ch. 251 (1), 59-68.

Lujaniene, G., Motiejunas, S., Sapolaite, J., 2007. Sorption of Cs, Pu and Am on clay minerals. J. Radioanal. Nucl. Ch. 274 (2), 345-353.

Magill, J., Berthou, V., Haas, D., Galy, J., Schenkel, R., Wiese, H.W., Heusener, G., Tommasi, J., Youinou, G., 2003. Impact limits of partitioning and transmutation scenarios on the radiotoxicity of actinides in radioactive waste. Nucl. Energy 42 (5), 263-277.

McCarthy, J.F., Sanford, W.E., Stafford, P.L., 1998. Lanthanide field tracers demonstrate enhanced transport of transuranic radionuclides by natural organic matter. Environ. Sci. Technol. 32, 3901-3906.

Migaszewski, Z., Galuszka, A., Migaszdewski, A., 2014. The study of rare earth elements in farmer's well waters of the Podwisniowka acid mine drainage area (south-central Poland). Environ. Monit. Assess. 186, 1609-1622.

Milinovic, J., Lacorte, S., Vidal, M., Rigol, A., 2015. Sorption behaviour of perfluoroalkyl substances in soils. Sci. Total Environ. 511, 63-71.

Moikin, G.Y., 1993. The establishment of the hygienic standard for the samarium content of water. Gig. Sanit. Jan. 1, 24-5.

Moulin, V., Ouzounian, G., 1992. Role of colloids and humic substances in the transport of radioelements through the geosphere. Appl. Geochem. Suppl. Issue (1), 179-186.

Mueller, G., Gastner, M., 1971. The "Karbonate-bomber", a simple device for the determination of the carbonate content in sediments, soils, and other materials. Neues Jb. Miner. Monat. 10, 466-469.

NAGRA, 1988. NTB 89-05 - Review of HLW disposal concepts in sediments. Swiss National Cooperative for the Disposal of Radioactive Waste, Switzerland.

National Research Council, 1999. Nuclear Physics: The core of matter, the fuel of stars, first ed. National Academies Press, Washington, USA.

NEA, 2000. Geological disposal of radioactive waste: review of developments in the last decades. Organization for Economic Co-operation and Development- Nuclear Energy Agency (OECD-NEA), France.

NEA, 2008. Report No 6433 - Moving forward with geological disposal of radioactive waste. Organization for Economic Co-operation and Development- Nuclear Energy Agency (OECD-NEA), France.

Novikov, A.P., Kalmykov, S.N., Goryachenkova, T.A., Myasoedov, B.F., 2011. Colloid transport of radionuclides in soils. Russ. J. Gen. Chem.+ 81 (9), 2018-2028.

OECD/NEA, 1995. The Environmental and Ethical Basis of Geological Disposal of Long-Lived Radioactive Wastes. A Collective Opinion of the Radioactive Waste Management Committee of the OECD Nuclear Energy Agency, OECD Nuclear Energy Agency, France.

OECD/NEA 2003. Effluent release options from nuclear installations. Technical background and regulatory aspects. OECD Nuclear Energy Agency, France.

Pang, X., Li, D., Peng, A., 2001. Application of rare-earth elements in the agriculture of China and its environmental behavior in soil. J. Soils Sediments 1(2), 124-129.

Pathak, P.N., Choppin, G.R., 2007. Sorption of Am^{3+} cations on suspended silicate: effects of pH, ionic strength, complexing anions, humic acids and metal ions. J. Radioanal. Nucl. Ch. 274 (3), 517-523.

Pavlotskaya, F.I., Goryachenkova, T.A., Kazinskaya, I.E., Novikov, A.P., Myasoedov, B.F., Kuznetsov, Y., Legin, V.K., Shishkunova, L.V., 2003. Speciation and migration behavior of Pu and Am in floodplain soils and bottom sediments of the Yenisei river. Radiochemistry+ 45 (5), 524-531.

Pourret, O., Martinez, R.E., 2009. Modeling lanthanide series binding sites on humic acid. J. Colloid Interf. Sci. 330, 45-50.

Quevauviller, P., Rauret, G., Ure, A., Bacon, J., Muntau, H., 1997. Report EUR 17127 EN - The certification of the EDTA and acetic acid-extractable contents (mass fractions) of Cd, Cr, Cu, Pb and Zn in sewage sludge amended soils CRMs 483 and 484. European Commision, BCR information, Reference materials, Belgium.

Rego, M.E., Vicente, R., Hiromoto, G., 2011. Temporal evolution of activities in wastes from Mo-99 production. In: Proceedings of International Nuclear Atlantic Conference – INAC (2011).

Reid, M.K., Spencer, K.L., 2009. Use of principal components analysis (PCA) on estuarine sediment datasets: The effect of data pre-treatment. Environ. Pollut. 157, 2275-2281.

Righuetto, L., Bidoglio, G., Azimonti, G., Bellobono, I.R., 1991. Competitive actinide interactions in colloidal humic acid-mineral oxide systems. Environ. Sci. Technol. 25 (11), 1913-1919.

Rigol, A., Camps, M., De Juan, A., Rauret, G., Vidal, M., 2008. Multivariate soft-modelling to predict radiocesium soil-to-plant transfer. Environ. Sci. Technol. 42 (11), 4029-4036.

Roussel-Debet, S., 2005. Experimental values for ^{241}Am and $^{239+240}$Pu K_d's in French agricultural soils. J. Environ. Radioactiv. 79, 171-185.

Schott, J., Acker, M, Barkleit, A., Brendler, V, Taut, S., Bernhard, G., 2012. The influence of temperature and small organic ligands on the sorption of Eu (III) on Opalinus Clay. Radiochim. Acta 100, 315-324.

Shan, X.Q., Lian, J., Wen, B., 2002. Effect of organic acids on adsorption and desorption of rare earth elements. Chemosphere 47, 701-710.

Shanbhag, P.M., Morse, J.W., 1981. Americium interaction with calcite and aragonite surfaces in seawater. Geocim. Cosmochim. Ac. 46, 241-246.

Shand, C.A., Cheshire, M.V., Smith, S.; Vidal, M., Rauret, G., 1994. Distribution of radiocaesium in organic soils. J. Environ. Radioactiv. 23, 285-302.

Sheppard, S.C., 2011. Robust prediction of Kd from soil properties for environmental assessment. Hum. Ecol. Risk Assess. 17, 263-279.

SKB, 1995. R-95-13 - Interactions of trace elements with fracture filling minerals from the Aspö Hard Rock Laboratory. Swedish Nuclear Fuel and Management Co., Sweden.

SKB, 1997. R-97-17 - Compilation of radionuclide sorption coefficients for performance assessment. Swedish Nuclear Fuel and Management Co., Sweden.

Sovacool, B.K., 2010. A critical evaluation of Nuclear Power and renewable electricity in Asia. J. Contemp. Asia 40 (3), 393-400.

Sutton, M., 2009. LLNL-SR-415700 - Review of distribution coefficients for radionuclides in carbonate materials. Lawrence Livermore National Laboratory, USA.

Tanaka, T., Muraoka, S., 1999. Sorption characteristics of 237Np, 238Pu and 241Am in sedimentary materials. J. Radioanal. Nucl. Ch. 240 (1), 177-182.

Takahashi, Y., Minai, Y., Kimura, T., Tominaga, T., 1998. Adsorption of europium (III) on kaolinite and montmorillonite in the presence of humic acid. J. Radioanal. Nucl. Ch. 237 (1-2), 277-282.

Tipping, E., Woof, C., Kelly, M., Bradshaw, K., Rowe, J.E., 1995. Solid-solution distributions of radionuclides in acid soils: application of the WHAM chemical speciation model. Environ. Sci. Technol. 29, 1365-1372.

Tyler, G., 2004. Rare earth elements in soil and plant systems-A review. Plant Soil 267, 191-206.

Vandenhove, H., Gil-García, C.J., Rigol, A., Vidal, M., 2009a. New best estimates for radionuclide solid-liquid distribution coefficients in soils. Part 2: naturally occurring radionuclides. J. Environ. Radioactiv. 100, 697-703.

Wang, L., Liang, T., Chong, Z., Zhang, C., 2011. Effects of soil type on leaching and runoff transport of rare earth elements and phosphorous in laboratory experiments. Environ. Sci. Pollut. Res. 18, 38-45.

Wang. L., Liang, T., 2015. Geochemical fractionation of rare earth elements in soil around a mine tailing in Baotou, China. Sci. Rep. 5, 12483.

Venegas, A., Rigol, A., Vidal, M., 2015. Viability of organic wastes and biochars as amendments for the remediation of heavy metal-contaminated soils. Chemosphere 119, 190-198.

Wetje, L., Heidenreich, H., Zhu, W., Wolterbeek, H.T., Korhammer, S., de Goeij, J., 2002. Lanthanide concentrations in freshwater plants and molluscs, related to those in surface water, pore water and sediment. A case study in The Netherlands. Sci. Total Environ. 286, 191-214.

Wold, S., Sjöström, M., Eriksson, L., 2001. PLS-regression: a basic tool of chemometrics. Chemometr. Intell. Lab. 58, 109-130.

Wood, S.A., Gammons, C.H., Parker, S.R., 2006. The behaviour of rare earth elements in naturally and anthropogenically acidified waters. J. Alloy Compd. 418, 161-165.

Xiangke, W., Wenming, D., Xiongxin, D., Aixia, W., Jinzhou, D., Zuyi, T., 2000. Sorption and desorption of Eu and Yb on alumina: mechanisms and effect of fulvic acid. Appl. Radiat. Isotopes. 52, 165-173.

Ye, Y., Chen, Z., Montavon, G., Jin, Q., Guo, Z., Wu, W., 2014. Surface complexation modeling of Eu(III) adsorption on silica in the presence of fulvic acid. Sci. China. Chem. 57 (9), 1276-1282.

Zhang, S., Shan, X.Q., Li, F., 2000. Low-molecular-weight organic-acids as extractant to predict plant bioavailability of rare earth elements. Int. J. Environ. An. Ch. 76 (4), 283-294.

Zhao, Y., Yu, R., Hu, G., Lin, X., Liu, X., 2017. Characteristics and environmental significance of rare earth elements in $PM_{2.5}$ of Nanchang, China. J. Rare Earth 35 (1), 98-106.

Zhong, S., Mucci, A., 1995. Partitioning of rare earth elements (REEs) between calcite and seawater solutions at 25°C and 1atm, and high dissolved REE concentrations. Geochim. Cosmochim. Ac. 59, 443-453.

Zhu, J. G., Xing, G. X., Yamasaki, S., & Tsumura, A., 1993. Adsorption and desorption of exogenous rare earth elements in soils: I. Rate of forms of rare earth elements sorbed. Pedosphere 3, 299–308.

Zhu, W.F., Xu, S.Q., Shao, P.P., Zhang, H., Feng, J., Wu, D.L., Yang, W.J., 1997. Investigation on intake allowance of rare earth – a study on bio-effect of rare earth in South Jiangxi. Chin. Environ. Sci. 1, 63–65.

Zhu, J. H., Yuan, Z. K., Wang, X. Y., & Yan, S. M., 2002. Investigation on the contents of rare earth elements in environment of rare earth ore area in Jiangxi. J. Environ. Health 19, 443–448.

Zhu, Z.Z., Wang, Z.L., Li, J., Li, Y., Zhang, Z.G., Zhang, P., 2012. Distribution of rare earth elements in sewage-irrigated soil profiles in Tianjin, China. J. Rare Earth 30, 609–613.

CHAPTER 4. STRATEGY TO PROPOSE RELIABLE K_D (RN) DATA IN SOILS FROM COMPILATIONS

4.1 INTRODUCTION

4.1.1 K_d variability sources in compilations arising uncertainty in prediction

For a given RN there is not a single K_d value but a series of values that may vary within several orders of magnitude. When this happens, the suitability of any derived K_d best estimate value to assess the RN fate and transport in soils, for instance by using models that require a specific K_d value as input data, is jeopardised. Consequently, generic K_d data derived from compilations are frequently not useful or recommended to perform site-specific assessments, and just used for preliminary or screening analyses. The soil K_d variability frequently observed for RNs arises from different sources (see **Figure 4.1**) that are not neither univariant nor independent among them, which makes it difficult to identify and reduce the relative weight of each one.

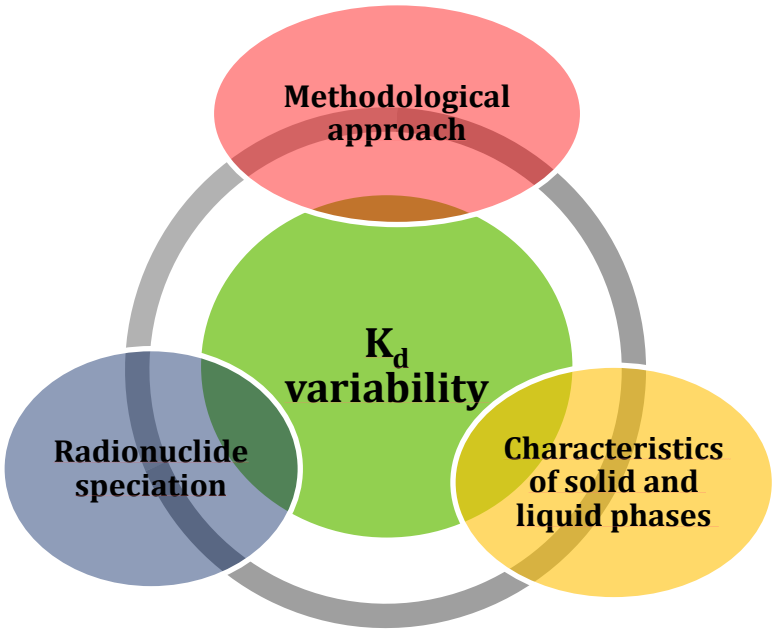

Figure 4.1 *Interlinked sources of variability for soil Kd data.*

Firstly, the geochemical processes governing the RN interaction with soil matrices can be very contrasting depending on the properties of the solid and liquid phases involved, since they determine the availability of potential sorption sites as well as the RN speciation and affinity for these sorption sites. Therefore, changes on those properties of the soil and contact solution that plays a key role on the RN-soil

sorption mechanisms always leads to a variability regarding the extent to which a RN is sorbed into a soil matrix. Although such fact is inherently in the nature of the scenarios under assessment and cannot be avoided, a better understanding of all these processes affecting the interaction of a given element in soils can be achieved through studies like that presented for Ac(III) and Ln(III) elements in previous Chapter 3.

Besides this, depending on the method used and the experimental conditions applied to determine K_d data different geochemical processes may be captured, which may also affect the overall RN interaction with soils (sorption enhancement, partially suppression or inhibition). This "experimental approach effect" can be of special importance for those elements that may undergo sorption dynamics phenomena, *i.e.*, elements whose interaction with a given matrix remarkably varies (increase or decrease) with time.

In order to make the K_d data derived from compilations suitable for risk assessment purposes it must be ensured their representativeness for the contamination scenario under study. Such aim requires to identify the factors controlling the RN-soil interaction in order to propose not a single value but a series of K_d data as much site-specific as possible and, on the other, to explain (and when possible to reduce) the variability within the datasets used for their derivation.

4.1.2 The Cumulative Distribution Function statistical approach to describe K_d variability

End-users of radiological assessment models requiring K_d data of RNs in soils as an input parameter increasingly demand not only single K_d best estimate values, but also information about their uncertainty in order to make a sensitive analysis of the model's performance. A suitable method to describe the population and variability of K_d values for a certain RN-material combination is the construction of Cumulative Distribution Functions (CDF).

In short, CDFs are equations describing the different values of a real-valued variable, in this case K_d, and their related accumulated frequency, which means that the probability that K_d takes a value less than or equal to a certain value can be explained

in a continuous form with a function. CDFs are built with the statistical parameters (*e.g.*, arithmetical mean, geometric mean, mode, variance, etc.) of the underlying frequency distribution (*e.g.*, normal, lognormal, exponential, etc.), that better explains the individual values of a certain dataset of the modelled variable. Thus, in order to construct reliable CDFs it is necessary to unequivocally ascertain the statistical distribution describing the best the data population, as well as to properly derive the corresponding statistical parameters. To reach this goal datasets must have sufficient number of entries so as to ensure the total representativeness of data, which may be a major limitation when applying this statistical approach for the case of K_d parameter as large datasets are not always available for all RNs.

Since the K_d parameter is a ratio of concentrations, K_d data are constricted to positive values and, thus, according to the central limit theorem K_d datasets are expected to follow a lognormal (hereinafter, logN) distribution (Sheppard et al., 2011). If a K_d dataset is lognormally distributed inherently implies that the log-transformed K_d values of this dataset, hereinafter log K_d, follows a Normal or Gaussian distribution. The statistical parameters describing a logN distribution are: the location parameter (μ), which can be considered as the most probable log K_d value since its corresponds to the 50^{th} percentile of the log K_d distribution, and the scale paramater (σ), which gives an estimation of the dispersion among log K_d values. Both statistical parameters (μ and σ) can be determined either by calculating the arithmetic mean (AM) and standard deviation (SD), respectively, of the experimental log K_d values comprising a given dataset; or by fitting the experimental cumulative distribution of the log K_d dataset to the theoretical CDF equation for the normal distribution. It is possible that the best statistical distribution to describe a K_d dataset, especially when it contains few data, may be others than logN, such as loguniform, logtriangular or exponential. In these cases the K_d CDF are constructed on the basis of a statistical distribution that is not fully coherent with the K_d parameter. **Figure 4.2** shows, as an example, the graphical representation of the CDF of an ideal lognormally distributed dataset that contains K_d values ranging from 1 to 10^6 L kg^{-1}.

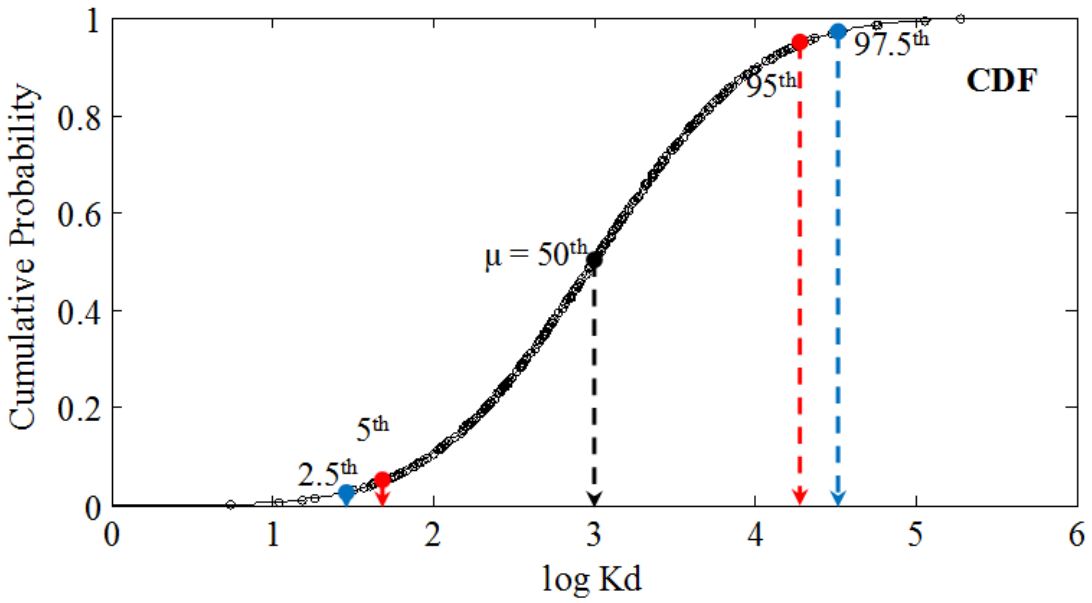

Figure 4.2 *Graphical representation of the CDF of an ideal lognormally distributed K_d dataset.*

CDFs not only give information on the most probable K_d value, corresponding to the 50th percentile of the CDF, but also account for all the range of potential values, with an indication of their probability of occurrence (Ciffroy et al., 2009). Thus, confidence intervals of K_d values can also be established from a CDF constructed with a K_d dataset by calculating the corresponding percentile ranges (*e.g.*, the 90% and 95% confidence intervals correspond to the 5th - 95th and 2.5th - 97.5th ranges, respectively). This statistical approach was previously used, for instance, to propose K_d (RN) data suitable to foresee the partitioning of RNs between liquid and solid phases in freshwater ecosystems (IAEA, 2010), but never applied to propose sorption data in soils. Taken into account that K_d variability in soils is especially large for most of RNs due to the contrasting scenarios regarding terrestrial contamination episodes (soil properties and contact solutions compositions), the application of the CDF approach may allow proposing data more useful for certain risk assessments.

4.1.3 Background to the proposal of soil K_d (RN) data from compilations

The International Atomic Energy Agency (IAEA) launched the international research programme called 'Environmental Modelling for Radiation Safety' (EMRAS) (2003-2007) whose main activities were focused on areas where uncertainties remained in the predictive capability of environmental models, notably in relation to the consequences of releases of RNs to particular types of environment (*e.g.* urban and aquatic environments), restoration of sites with radioactive residues and impact of environmental radioactivity on non-human species. In the frame of the EMRAS Programme, the Technical Report Series (TRS) No. 472 document (IAEA, 2010) and related TECDOC 1616 (IAEA, 2009) were elaborated which summarised the main descriptors of a new soil K_d data compilation that was a major update of the previous one used for the elaboration of the 'Handbook of Parameter Values for the Prediction of Radionuclide Transfer in Temperate Environments', TRS 364 (IAEA, 1994).

Data in that compilation came from field and laboratory experiments, with various contamination sources, considering mainly the scenario of soils contaminated by RNs, and from references mostly from 1990 onwards, including the data from the former TRS 364 and related reports (AECL, 1990; Sheppard and Thibault, 1990), reviewed papers, and grey literature (PhD theses; reports). Data from experiments using other materials than soils (*e.g.* sediments; rock materials or pure soil phases like clays or Fe-Mn-Al oxides) as well as from stable isotopes were not considered. Besides this, data from radioisotopes of the same radioelement were pooled in the same dataset, *i.e.* datasets were created on the basis of the different element without distinguishing among isotopes. That K_d data compilation contained around 2900 records for 67 elements. Caesium and strontium datasets had the highest number of observations (469 and 255, respectively), and those for a few elements had more than 100 entries each, such as iodine, uranium, cobalt, potassium, antimony and selenium.

One of the main outcomes resulting from the analyses of this compilation was the proposal of K_d best estimate values (as a GM value) and the related variability (expressed as a GSD value along with a minimum and maximum K_d values range) on the basis of different soil-types created according to the organic matter, clay and sand (textural) content of the soil samples, the so-called Texture/OM criterion. This approach was straightforwardly applied to all RNs provided that their datasets had

enough data to enable such analysis, regardless of the sorption behaviour or characteristics of the target RN. In addition to this, K_d datasets of a few elements (Cs, Sr, U, Cd, Co, Ni, Zn and I), for which a large number of data were available and their sorption mechanisms in soils were known, were also grouped according to specific factors based on soil properties responsible for the soil-element interaction, *i.e.* soils factors, such as Radiocaesium Interception Potential (RIP) (Wauters et al., 1996) and concentration of K in the soil solution, for caesium; CEC and concentration of Ca and Mg in the soil solution, for Sr; or soil pH, for uranium and heavy metal elements.

A few conclusions from the TRS-472 soil K_d compilation could be drawn, suggesting further work to do. First of all, it was assumed that the K_d datasets followed a lognormal distribution and the derived GM and GSD values were suggested to describe the K_d data analysed rather than the corresponding AM and SD values. However, the underlying statistical distribution describing the datasets was never checked, and thus, no CDFs were proposed. Consequently, the proposed data (GM and GSD values), despite providing K_d end-users with best estimates values and with an estimation of the K_d data variability, were unsuitable to perform sensitivity analyses of radiological models.

Secondly, albeit significant amount of new data was included in the TRS-472 dataset, comparing with the former TRS 364 dataset, there were still evident gaps of values of K_d for a substantial number of radioelements. For instance, K_d datasets of up to 31 elements had less than 10 entries, and when K_d data were grouped according to the above mentioned criteria to reduce the data variability, some originated groups contained a single entry or even some groups could not be proposed due to the lack of data. This fact restricted the possibility of proposing reliable best estimates in many cases, and it was claimed to consider the derived GMs or the single values proposed only as approximate estimates, suitable for screening purposes, but not for conclusive assessments. For the data gaps, it was suggested, as a next step, to explore the use of analogue data, either from other elements or from geological materials other than soils, but it was never tested. Indeed, it was highlighted that this approach should be undertaken with care, taking into account that the analogue and the radionuclide of interest may differ in their chemical form and affinity for the various types of binding sites, and that a quantitative validation of this strategy had never been performed.

And last, but not least, for most of those elements for which only the Texture/OM criterion could be applied, K_d data varied within more than 4 orders of magnitude within the created soil-type categories, thus jeopardising the usefulness and reliability of the calculated GM values, even when gathered from large datasets. This large variability was attributed on the one hand, to the fact that the soil-radionuclide interactions are governed by multiple factors that depend on the radionuclide and on various soil properties, which may not be, directly o indirectly, covered when the Texture/OM criterion is applied, and on the other, to the large number of methodological approaches and experimental conditions used to quantify K_d values. Thus, for a better estimation of K_d values and to decrease their variability, it was recommended to seek additional soil and radionuclide properties (soil factors) for an increased number of radioelements, as well as it was suggested to consider the experimental approach as an additional factor, when possible, for a better grouping of K_d data.

4.1.4 The MODARIA Programme: Towards proposing reliable K_d (RN) data from compilations

The Modelling and Data for Radiological Impact Assessments (MODARIA) Programme was an international research project hosted by IAEA during the period within 2012 and 2015, aiming at improving capabilities in the field of environmental radiation dose assessment by means of acquisition of improved data for model testing and comparison, reaching consensus on modelling philosophies, approaches and parameter values, development of improved methods and exchange of information.

The activities within the frame of the MODARIA Programme dwelt on the improvement of environmental transfer models for reducing associated uncertainties or developing new approaches to strengthen the evaluation of the radiological impact to man, as well as to flora and fauna, arising from radionuclides in the environment. The main goal of MODARIA Programme was to gain information leading to an enhancement of the capabilities of Member States to simulate radionuclide transfer in the environment and, thereby, to assess exposure levels of the public and in the environment in order to ensure an appropriate level of protection from the effects of

ionising radiation, associated with radionuclide releases and from existing radionuclides in the environment.

Since not all parameter values are generically representative as they vary significantly due to variations in ecosystems, agricultural practices, climate, physicochemical form of the radionuclide in question, soil characteristics, life cycle stages of the relevant biota, and data quality and quantity, it would be useful to the scientific community to identify which parameter values need more attention, and which may be of use for generic purposes in order to address such variability. To shed light on this issue, a working group was established (WG4: 'Analysis of radiological data in IAEA Technical Reports Series publications to identify key radionuclides and associated parameter values for human and wildlife assessment') whose main goal was to analyse radiological data quantity and quality, using freely available tools and/or other models, aiming at:

- Ascertaining those radioisotopes which are key dose contributors for different transfer pathways, selected source terms and different exposure situations.
- Identifying the data gaps of those parameters relevant for the radiological assessments associated to the key radioisotopes by comparing the list of high priority radioisotopes with parameter data provided to the community via the TRS documents.
- Filling the priority data gaps by updating previous parameter data compilations with recently available data, or by exploring the viability of applying approaches based on the extrapolation of the current existing data to foresee other scenarios lacking of data, *i.e.*, analogue approach.
- Developing strategies for handling of variability of parameter values associated to key radioisotopes in order to provide end-users with more reliable data (less uncertainty) for radiological assessment purposes.

In this chapter it is presented the strategy developed in the frame of the MODARIA Programme aiming at providing end-users with reliable soil-type specific K_d CDFs by means of decreasing and explaining K_d data variability in soil K_d (RN) datasets created from an updated soil compilation. Concretely, the results obtained for Cs, U and Am,

three case studies of special interest in radioecology and very contrasting with respect to the data availability, soil interaction complexity and knowledge, are extensively discussed.

4.2 MATERIALS AND METHODS

4.2.1 Soil K_d (RN) compilation update and revision of data acceptance criteria

Taking the former soil K_d data compilation (TRS-472) as a starting point, an updating process was done by examining more than 100 documents (reviewed papers and grey literature, such as PhD thesis or reports), most of references being from 2004 onwards. The K_d values available, along with ancillary information regarding both the characterisation data of the matrix they were gathered from and information about the experimental approach applied to quantify the K_d data, were incorporated into the K_d compilation. The criteria for data acceptance or rejection were critically reviewed in order to ensure both data quality and maximum data availability to as many elements as possible, which implied remarkably changes in the content and structure of the former data compilation.

Unlike the case of the former TRS-472 compilation, any kind of K_d value not directly quantified as the ratio between concentrations of the target element measured in a liquid and a solid phase was rejected. Consequently, the current compilation does not include data neither derived from parametric equations, nor deduced from mass-transport experiments such as column tests or diffusion experiments, nor proposed K_d reference values in former K_d data compilations, like K_d best estimates for soil types. Besides this, K_d data originated from the same element-sample combination by applying a set of tests at varying operational variables related to the experimental approach used for their quantification (*e.g.*, contact time or solid-to-liquid ratio in batch experiments) after being critically reviewed were pooled to become a single entry, calculated as a GM value. "Critically reviewed" here refers to check that the conditions applied may lead to the quantification of K_d data relevant for environmental scenarios (*i.e.*, only those K_d data obtained at reasonably experimental conditions were accepted and subsequently pooled in a single entry as mentioned before). Moreover, it is frequent to find in the literature several K_d data gathered from the same RN and material sample but at varying the aqueous phase of the system under study (*i.e.,* contact solutions with different characteristics, such as pH, ionic strength or composition, may be used). All the available K_d data gathered from the same RN-material combination were not pooled in a single entry but introduced as

individual entries since any of them may be relevant for further analysis, as it will be explained in following section 4.2.2. As well as that, in the TRS-472 compilation only K_d data of RNs gathered from soils were accepted, whereas in the current compilation K_d data for stable isotopes were also accepted as far as they were obtained using concentration of the target elements low enough to ensure linear sorption and, thus, being suitable to assess the RN-soil interaction in radioactive contamination scenarios. For instance, K_d data derived from the low concentration (linear sorption) region of sorption isotherms obtained for stable isotopes or K_d data of indigenous elements gathered from desorption tests were included. In line with the previous compilation, currently K_d data from pure (soil) phases, such as clay minerals or metal (hydro)oxides, were not accepted. However, K_d data and ancillary information gathered from a few environmental solid materials were accepted due to their relevance for radiological risk assessment in terrestrial ecosystems and because of the potential analogy of these materials with soils. Thereupon, a brief description of the different materials included in the compilation is provided.

4.2.1.1 Environmental solid materials accepted in the K_d compilation

Soils and subsoils

Soil samples refer mostly to the soil profile within the unsaturated zone, which is characterised by the fact that pore spaces are incompletely filled with water. The soil zone, generally a meter or two thick, contains living roots and supports plant growth. The porosity and permeability under the topsoil, that is the soil subzone or subsoil, which varies in thickness from place to place and is often referred to as the intermediate zone, is generally higher than that of underlying material, and consists of sediments or rocks that have not been exposed to extensive pedogenic (soil-forming) processes. Therefore, albeit some subsoil layers, especially those of the bottom, can be enriched with smaller particles (clay minerals) due to percolation from upper layers, the particle size of subsoils constituents is expected to be on average higher than those corresponding to topsoils and, thus, subsoil texture may be more similar to a sandy soil rather than to a clayey one.

Gyttja

It is a mud formed from organic and mineral matter, which can be found at the bottom or near the shore of certain lakes. Aerobic digestion of the organic matter by bacteria forms humic acids, and reduces the organic matter content in the oxygenated horizon. Due to new organic matter loads or subsequent soil formation processes at upper layers, the preceding decomposed organic matter is engulfed, the oxygen concentration is reduced, often by water logging, and further degradation by anaerobic microbes is favoured, thus producing the gyttja material.

Till

It is an unsorted and non-stratified material deposited directly by glacial ice, which consists of a mixture of clay, silt, sand, gravel, stones, and boulders in any proportion. Consequently, it is expected that the sorption of RNs in tills resemble to that in soils inasmuch tills and soils only differ from their origin.

Surface sediment

A sediment is a naturally occurring material formed by deposition and subsequent cementation of minerals and organic particles originated in a source area that are transported to the sedimentation point by the action of wind, water, or ice, and/or by the force of gravity acting on the particles. The boundary between a surface sediment sample, the upper layer of that material, and a sedimentary soil is somewhat difficult to establish, especially when surface sediments are in unsaturated conditions (*i.e.* not permanently logged by water) and directly exposed to the effect of weathering and erosion processes for a long period of time. The properties of surface sediments (mineralogy, texture, organic matter content, pH, etc.) are the result of the originally particles they are made of by deposition and subsequent weathering and erosion processes, and thus, they can be very contrasting among sediments samples.

4.2.1.2 Structure of the updated soil K_d (RN) compilation

The current soil K_d (RN) compilation consist in a spreadsheet-type document in which K_d and ancillary data are organised on element basis in independent sheets. The structure of the current compilation is similar to that of the previous TRS-472 inasmuch each data entry is placed in independent rows within the corresponding element-sheet and each contemplated field corresponds to columns. The vast majority of the fields considered in the current soil K_d data compilation are those already used in the former one, which are listed thereupon:

- Data source traceability: a series of fields are contemplated in order to properly reference each accepted, which includes the type of data source (*e.g.*, journal, PhD Thesis, technical report, etc.) and typical related reference information (*e.g.*, name of journal or report, title, language, authors, volume, pages, year, etc.).

- Target element and sample identification: isotope analysed, soil code used by authors, country where the soils is originated and related climate zone, soil FAO classification.

- Soil system characterisation: a series of fields are considered regardless of the element studied to summarise the characteristics of each soil system. These are: soil pH, contact solution pH, soil texture classification, organic matter content (OM%), CEC, sand and clay percentage and K_d. Additionally, extra soil characterisation fields are contemplated on element basis. For instance, Ca and Mg concentration in solution, for Sr; carbonate content, for U or Am; or redox potential, for I.

- Experimental approach information: any relevant remark regarding the experimental approach applied to quantify the compiled Kd data is summarised in a specific field.

A major advance achieved in the updated data compilation lies on the fact that 4 fields for tagging each entry in the compilation (K_d data and ancillary information) were created so as to enable the proper data selection aiming at creating subdatasets containing only part of the total number of entries of a given RN dataset that fulfils a series of requirements (hereinafter, partial datasets). As it will be explained in

following section 4.2.2, such fact is crucial in order to properly perform the analyses required to reliably derive probabilistic soil K_d data. Concretely, four selection data fields were created, one referred to the identification of the solid matrix from which K_d data are determined, two referred to the identification of the type of experimental approach followed to determine each K_d value and the last one related to soil factors. Thereupon, each data selection field is briefly described.

Material

Since K_d data gathered from a series of environmental solid materials other than soils have been accepted in the current compilation, the field "Material" was created so as to properly tag each entry according to the material from which a given K_d value is gathered (*i.e.*, soil, subsoil, gittya, till or surface sediment). The aim was to enable the creation of partial datasets on material basis that may be necessary for further data analyses.

Experimental approach

Two new fields, "Methodology-Dynamics" and "Methodology-Test", were created so as to tag each K_d entry on the basis of the experimental approach (at field or at the laboratory) followed for their quantification at two different levels. The first field (Methodology-Dynamics) is used to distinguish between those K_d data that may be representative of a recently contamination scenario (tagged as short-term) from those K_d data gathered from materials in which the target element has been incorporated for a period of time long enough to consider that sorption dynamics may have a significant effect in the RN-material interaction (tagged as long-term). The second field (Methodology-Test) is used to distinguish among the different K_d types that can be determined depending on the interaction processes that may be captured by the method applied to quantify a given K_d value. Thus, K_d entries are also tagged by using this field as sorption, desorption or *in-situ*. **Table 4.1** summarises a series of experimental approaches that may lead to the quantification of the abovementioned types of K_d data.

Table 4.1 Summary of different types of K_d according to the experimental approach applied for their quantification.

Experimental approach K_d-types		Examples of scenarios leading to each experimental approach type of K_d data
Short-term	In-situ	- K_d of anthropogenic elements derived by determining their concentration in water and soil samples collected in areas recently contaminated with radioisotopes or low-concentrations of stable isotopes of the target element. - K_d of indigenous elements (radioisotopes or trace stable isotopes) derived by determining their concentration in water and soil samples collected in non-contaminated areas when only the reversible fraction of the indigenous element sorbed at the solid matrix is quantified (*e.g.* using mild extract agents such as HAc 0.43M).
	Sorption	- K_d of elements derived by applying a sorption test based on putting in contact, usually for a few hours to few days stint, clean soils (initially non-contaminated) with a solution spiked with radioisotopes or low-concentration of stable isotopes of the target element.
	Desorption	- K_d of anthropogenic elements derived by applying an extraction to soils recently contaminated with radioisotopes or low-concentration of stable isotopes of the target element (*e.g.*, soil residues coming from a previous sorption test or soils sampled from recently contaminated areas). - K_d of indigenous elements (radioisotopes or stable isotopes) derived by applying an extraction to contaminated solid materials when only the reversible fraction of the indigenous element sorbed at the solid matrix is quantified (*e.g.*, using mild extract agents such as HAc 0.43M).
Long-term	In-situ	- K_d of anthropogenic elements derived by determining their concentration in water and soil samples collected in areas contaminated long-time ago with radioisotopes or low-concentrations of stable isotopes of the target element. - K_d of indigenous elements (radioisotopes or trace stable isotopes) derived by determining their concentration in water and soil samples collected in non contaminated areas when the total content of the indigenous element at the solid matrix is quantified (*e.g.,* total or pseudo-total digestion using HNO_3+HF conc. acids or *aqua regia*, respectively).
	Desorption	- K_d of anthropogenic elements by applying an extraction to solid materials long-term contaminated with radioisotopes or low-concentration of stable isotopes (*e.g.*, sorption test residues with accelerated interaction dynamics by performing dry-wet cycles, samples from areas contaminated long time ago). - K_d of indigenous elements (radioisotopes or trace stable isotopes) derived by performing an extraction to non-contaminated samples when the total content of the indigenous element at the solid matrix is quantified (*e.g.,* total or pseudo-total digestion using HNO_3+HF conc. acids or *aqua regia*, respectively).

Soil factor

In order to enable the proper data selection according to key soil characteristics the "Soil factor" field was created aiming at tagging each soil entry according to the different soil properties that may be relevant for further analysis (*e.g.*, texture, pH, OM content, etc.). This fact is of special importance when partial datasets are created on the basis of soil factor-based criteria, since it allows to obtain datasets without redundant data that may distort the K_d population distribution, which, in turn, may affect to the eventually derivation of probabilistic K_d data from a given dataset (see following section 4.2.2). In order to exemplify how K_d data will be selected to perform subsequent analyses **Figure 4.3** illustrates, as an example, the selection of K_d (Am) entries from a dataset according to different soil factors (Texture and pH).

Isotope	Soil Texture	Soil pH	Suspension pH	Sand (%)	Clay (%)	Grouping factor	K_d ($L\,Kg^{-1}$)
^{238}U	Loam	7	2	50	30	pH	60
^{238}U	Loam	7	3	50	30	pH	220
^{238}U	Loam	7	4	50	30	pH	500
^{238}U	Loam	7	5	50	30	pH	1300
^{238}U	Loam	7	6	50	30	pH	2000
^{238}U	Loam	7	7	50	30	Texture, pH	5000
^{238}U	Loam	7	8	50	30	pH	35
^{238}U	Loam	7	9	50	30	pH	40
^{238}U	Loam	7	10	50	30	pH	15

Figure 4.3 *Example of soil K_d data selection from a dataset for further K_d grouping. K_d values selected on the basis of soil texture (in green) and on the basis of pH (in red).*

In this case, the K_d (Am) data gathered from the literature correspond to a study where the role of changing pH on K_d (Am) was evaluated for a single soil sample. Thus, when willing to group the K_d (Am) data with respect to soil texture, only one entry should be considered from this study, which corresponds to the K_d value determined in the soil sample with its original pH (in green). Conversely, when willing to group the K_d (Am) data with respect to pH, all entries from this soil sample (in red) can be included in the dataset since all of them correspond to independent pH values.

4.2.2 Development of grouping criteria based on element-soil interaction factors to decrease K_d (Cs), K_d (U) and K_d (Am) data variability

An strategy, similar to that followed in former K_d compilation analyses (IAEA, 2009; IAEA, 2010), was developed and applied to the updated K_d datasets of Cs, U and Am to create partial datasets with less variability. This strategy is based on grouping the K_d data of a given element according to different established and optimised criteria that take into account factors related to the soil characteristics (hereinafter, soil factors), and the experimental approach applied to determine K_d values (hereinafter, experimental approach factors), that are relevant in the RN-soil interaction.

The aim was to identify for each element the soil properties more relevant in their interaction with soils; to select those obtained on routine analyses and, thus, more likely to be available; to establish a series of criteria to properly create different categories or groups of K_d data according to them, enabling the creation of partial datasets with K_d values varying less than in the overall dataset; and to construct CDFs or, at least, to derive best estimate values. From this approach it is expected to obtain a series of soil-type K_d data that may enable the assessment of the interaction of the target elements in a given soil with less uncertainty just by selecting the probabilistic K_d data (best estimate value or CDF) of the soil-type group that matches better with the properties of the soil and the characteristics of the scenario under assessment.

Moreover, as explained in Chapter 1, K_d values can be determined by a great variety of experimental approaches. Depending on the method followed and the experimental conditions applied, K_d values determined for the same RN-soil combination may vary significantly since different sorption processes may be captured. According to this, experimental approach factors were also used simultaneously with soil factors to develop K_d grouping criteria when the effect of the experimental approach on the K_d values was demonstrated to be statistically significant for a given element.

4.2.2.1 Soil factors and developed criteria to group K_d (Cs) data

The Cs interaction with soils and other materials like clays has been thoroughly studied in the last decades, which has led to a good understanding of the sorption mechanisms governing the Cs sorption in soils and to the identification of the physicochemical properties affecting the most the Cs interaction as well as the soil phases involved (Comans et al., 1989; Cremers et al., 1990; Rigol et al., 1998; Vidal et al., 1995). Unlike the forthcoming cases of U and Am, Cs speciation in solution is very simple. The predominant Cs species in solution are hydrolysed cations with scant tendency to form covalent bounds or stable complexes. The Cs-soil interaction (graphically depicted in **Figure 4.4**) is namely based on cation exchange reactions involving two main types of sorption sites with contrasting affinity for Cs and selectivity for monovalent and divalent cations.

In those soils with really high organic matter content and absence of 2:1 phyllosilicates, the Cs sorption is namely caused by the interaction with the regular exchange sites (RES) (Rigol et al., 1998 and 2002). RES are originated in organic matter and clay minerals as a result of deprotonation of certain functional groups and isomorphic substitutions, respectively, and they can be roughly estimated with soil CEC. Since RES present low affinity and selectivity coefficients close to unity for monovalent cations (*e.g.*, Cs^+/K^+ or Cs^+/NH_4^+), Cs sorption in RES is considered as a weak and non-specific interaction (Vidal et al., 1995) that can be highly inhibited by the presence in solution of other monovalent cations and, specially, divalent cations presenting a higher electrostatic affinity, due to sorption competition processes (Comans et al., 1989; Cremers et al., 1990). In soils with relevant contents of 2:1 phyllosilicates, the Cs sorption is namely controlled by its interaction with sorption sites located in the interlayer space of 2:1 phyllosilicates such as illite, vermiculite or smectite and, particularly, in the frayed edge sites (FES). FES present extremely high-affinity for monovalent cations, especially those located in the inner part of the interlayer space present a high affinity for Cs (Cremers et al., 1988).

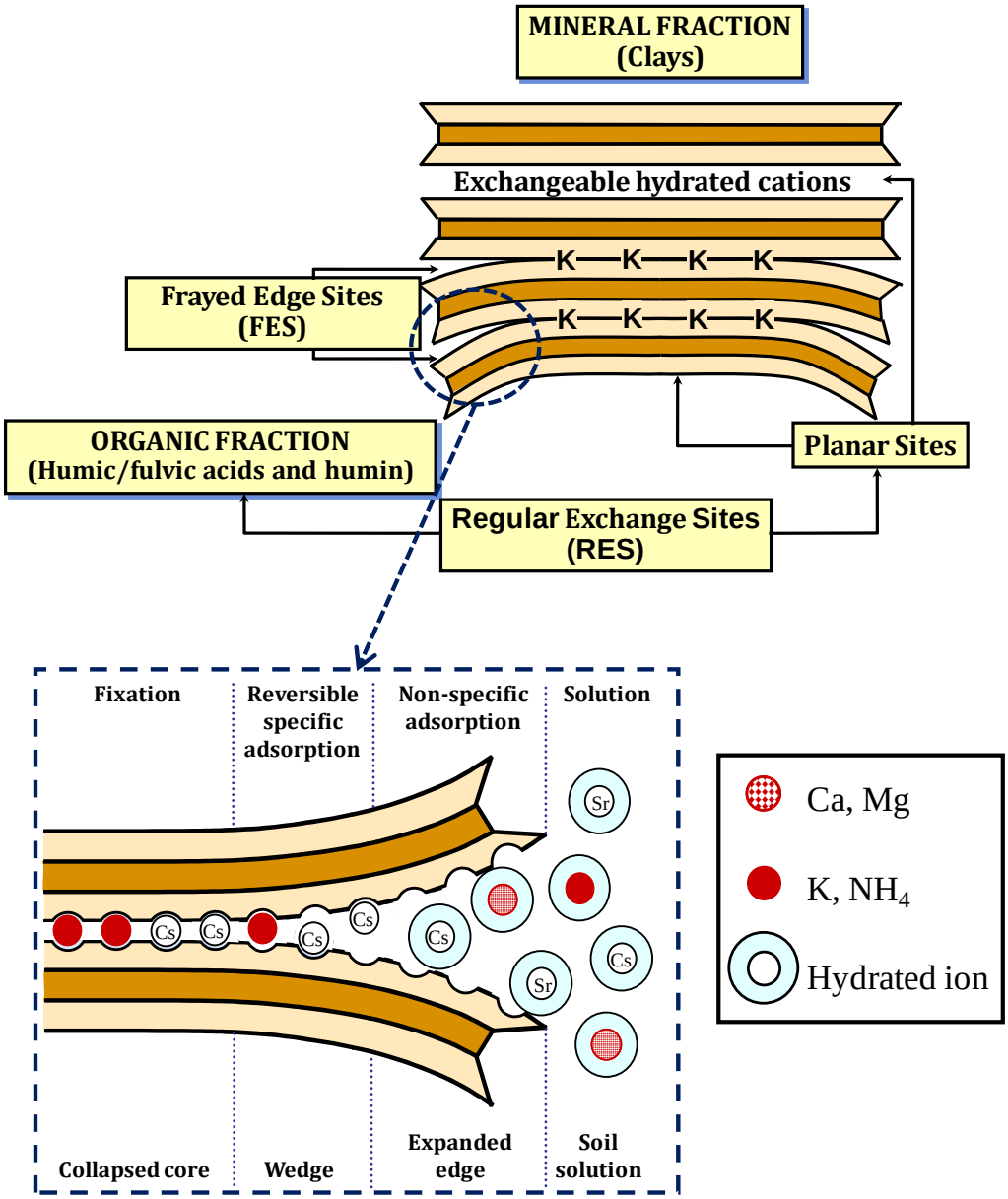

Figure 4.4 *Cs sorption sites in soils.*

This latter specific Cs sorption is crucial for the understanding of the long-term Cs-soil interaction. At a given time since Cs incorporation to internal FES, sorbed Cs species undergo a progressive dehydration reaction which cause the so-called clay interlayer spacing collapse and implies that the dehydrated sorbed Cs get trapped in the clay bulk. As a result of this Cs sorption dynamic process, the fraction of sorbed Cs that no longer participates in the partition between the solid and liquid phases increases with time, which involves an enhancement of the Cs sorption irreversibility, a process known as sorption aging (Absalom et al., 1995; Roig et al., 2007). Therefore,

an important issue that must be tackled when analysing K_d (Cs) data in compilations is to properly distinguish between those data corresponding to short and long elapsed times since Cs incorporation in soils.

According to the Cs sorption mechanisms described above, the proposal of a soil factor based on the soil mineralogy, enabling to create K_d (Cs) data categories on the basis of the soil content of those clay minerals presenting high affinity for Cs, would be of special interest. However, its use is hindered by the fact that few mineralogy characterisation data are usually available for soils, thus making any mineralogy-based grouping criteria of a limited application. Alternatively, a combined K_d grouping criterion based on the texture and organic matter (OM) content of the soils from which the K_d (Cs) values were gathered, the so-called Texture/OM criterion previously agreed (IAEA, 2010), can be applied to group K_d (Cs) data, which is schematically summarised in **Figure 4.5**. In short, a K_d (Cs) value was initially included in the Organic group if the soil from which it was gathered had an OM content ≥ 20%, whereas it was included in the Mineral group if OM was lower than 20%. Secondly, the K_d data contained in the latter group (Mineral) whose clay and sand contents of the mineral fraction were also available were split in three textural groups (Sand, Loam and Clay).

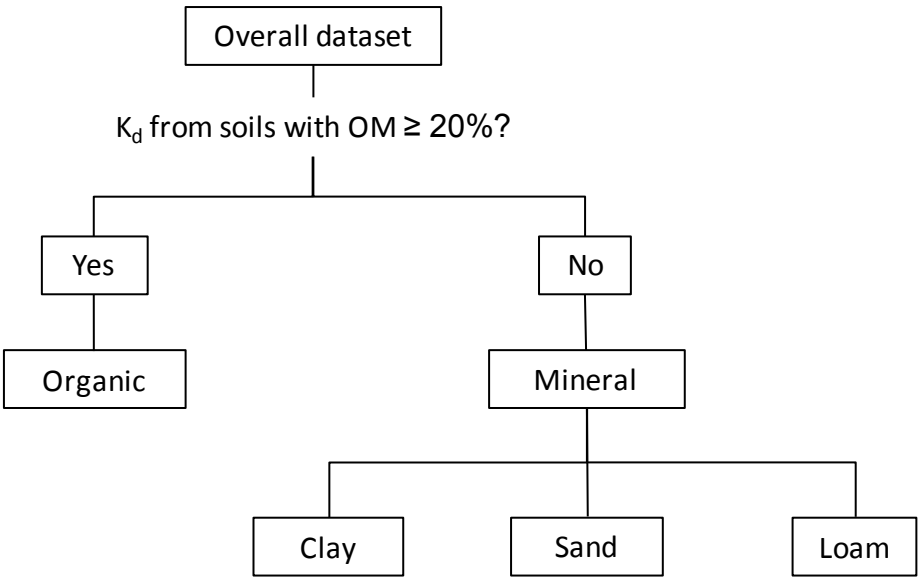

Figure 4.5 *Diagram of K_d (Cs) data grouping according to the Texture/OM criterion.*

The suitability of the Texture/OM K_d grouping criterion to propose soil-type K_d (Cs) data lies on the fact that the soil characterisation data required to group K_d values (OM, clay and sand percentages) are usually available, since they are determined on routine analysis. Besides this, despite the fact that the Texture/OM criterion is not based on the fundamental description of the underlying sorption processes of Cs in soils, it partially captures some of the soil properties that can play a key role in the Cs-soil interaction. On the one hand, K_d (Cs) data corresponding to soils with higher organic matter content (Organic) and, thus, with much lower clay mineral content and lower expected Cs sorption capability are distinguished from those gathered from soils with low OM content (Mineral). On the other, the creation of the different textural K_d groups by taking into account the soil clay content (texture Clay%) may also allow to indirectly distinguish between those "Mineral" soils presenting a higher (Clay group) or a lower (Sand group) amount of specific sorption sites and, thus, with different capability to sorb Cs.

Notwithstanding the advantages of using the Texture/OM criterion to group K_d (Cs) data, the OM threshold used to discern between an organic and a mineral soil may not be the most appropriate to distinguish between those soils presenting high Cs sorption capacity due to their mineral fraction and those soils presenting low capacity to sorb Cs by means of non-specific mechanisms. Therefore, as a second approach, the OM threshold was analysed in order to redefine the Texture/OM criterion. To this end, the optimal OM threshold was firstly ascertained by means of applying increasing OM% from 20% to 90% to split the overall dataset into the respective Organic and Mineral partial datasets. Then, the Texture/OM criterion was applied with the redefined OM%.

Finally, K_d (Cs) were also grouped according to soil factors specific to the Cs sorption mechanisms. To this end, the ratio between the Radiocaesium Interception Potential (RIP), that accounts for the soil capacity to specifically sorb Cs (Sweeck et al., 1990; Wauters et al., 1996), and the potassium in soil solution (K_{ss}), that captures the major competition process for sorption sites with other monovalent cations, was used to split the K_d (Cs) dataset into 4 groups comprising different RIP/K_{ss} ranges ($RIP/K_{ss} < 10^2$; $10^2 \leq RIP/K_{ss} < 10^3$; $10^3 \leq RIP/K_{ss} < 10^4$; and $RIP/K_{ss} > 10^4$), as previously agreed in IAEA, 2010.

4.2.2.2 Soil factors and developed criteria to group K_d (U) data

Uranium sorption in soils is known to be very complex and affected by several soil properties and phases, mainly pH, soil texture, specific surface area (SSA), cation exchange capacity (CEC), carbonate, amorphous iron oxides (Fe_{amorph}) and OM matter contents (EPA, 1999; Payne et al., 2011).

EPA (1999) reported an extensive review of K_d (U) values for soils, crushed rock material and single-mineral phases, which indicated that pH and dissolved carbonate concentration were the two most important factors influencing the sorption behaviour of U(VI), the dominant U species in top soils. At pH below 5, U(VI) is present as the uranyl ion, UO_2^{2+}. At a higher pH, the uranyl ion hydrolyses, forming a number of aqueous hydroxide complexes, which dominate U(VI) speciation in the absence of dissolved inorganic ligands (*e.g.*, carbonate, sulphate or phosphate). At the pH range of 5–10, highly soluble carbonate complexes dominate the U speciation (Langmuir, 1978). In general, the sorption of uranium by soils is low at pH values less than 3, increases rapidly with increasing pH from 3 to 5, reaches a maximum in the pH range from 5 to 7, and then decreases with increasing pH at pH values greater than 7 (EPA, 1999). Thus, U sorption in soils frequently shows a kind of inverted-U shape trend in relation to the pH.

Echevarria et al. (2001) explored the effect of soil characteristics on U sorption for a reduced soil dataset and deduced a significant linear relationship between soil K_d (U) and pH that evidenced that K_d (U) values decreased when increasing pH in the 5.5–8.8 pH range ($R^2 = 0.76$). A similar pattern was also observed by Vandenhove et al. (2007) for a controlled dataset comprising soils with pH ≥ 6, which was explained by the increased amount of soluble uranyl–carbonate complexes at increasing basic pH. However, Sheppard et al. (2006) found that, when considering an heterogeneous dataset composed by soils with pH ranging from 5.5 to 8.8 and data from varying sources, a relative low percentage of K_d (U) variance could be explained by the K_d (U)–pH correlations obtained ($R^2 = 0.41$), indicating that the K_d (U) cannot be univariantly predicted from pH variation and that other soil properties should be taken into account.

Related to this latter point, significant sources of variability in the relationship between K_d (U) and pH are postulated to be, besides the experimental approach used for their determination, the heterogeneity in the organic matter content and soil mineralogy (*i.e.*, soils containing larger percentages of iron oxide minerals and mineral coatings, and/or clay minerals, exhibit higher sorption than soils dominated by quartz and feldspar minerals). Organic matter and clay minerals provide exchange sites that are expected to increase sorption of UO_2^{2+} and other positively-valent U-forms. The influence of organic matter on U interaction is twofold: an increased sorption through exchange mechanisms and a decreased sorption due to formation of soluble organic complexes, for those samples having large amounts of dissolved organic matter content and colloids. The role of humic substances in the mobility of U(VI) was investigated, and uranium was found to be strongly retained by the soil solid phase mainly due to organic aggregates and organic coatings on quartz minerals (Crançon and Van der Lee, 2003), whereas a large fraction of U(VI) was also found to be associated to humic colloids in soil, thus forming a potential mobile uranium phase. Regarding the role of clay minerals, Sheppard (2011) recently suggested updated K_d *vs.* pH and clay correlations, based on a dataset enriched with a significant contribution of field data with indigenous uranium.

Other soil properties could be considered by also affecting K_d (U) variability. Many studies also highlight the importance of iron oxides/hydroxides for the sorption of U (Hsi and Langmuir, 1985; Waite et al., 1994; Duff and Amrhein, 1996; Payne et al., 1996). The positively charged U-species are sorbed to the negatively charged surfaces of the sesquioxides or U-species become structurally incorporated in the iron-oxides (coatings) over the many dissolution–precipitation cycles of these amorphous or poorly crystalline iron oxides (Sowder et al., 2003). The soil SSA is also meant to play a significant role in uranium sorption, as shown for pure mineral phases (Payne et al., 2011). SSA values for soils vary across an extremely wide range, with reported values between 1 and 1000 $m^2\ g^{-1}$. Soils containing large fractions of amorphous or clay minerals are expected to have very large SSA values. Thus, this might be a key soil factor to efficiently group K_d (U) data since it may indirectly account for the total U sorption sites, especially when soils do not have large amounts of specific high-affinity sites, like the above mentioned iron hydro(oxides).

To group K_d (U) values on the basis of soil carbonate content, or more specifically the CO_3^{2-} and HCO_3^- concentration in soil solution, or based on iron hydro(oxides) content or soil SSA, was not considered due to the lack of characterisation data in the current compilation. Instead, K_d (U) data were firstly grouped according to the Texture/OM criterion, previously explained. Alike the case of Cs, this approach partially covers some soil factors that may be relevant to the U sorption in soils. Firstly, by taking into account the OM% to create the Organic and Mineral K_d groups it is distinguished the K_d (U) data corresponding to those soils rich in organic matter, which are expected to be on average higher than those gathered from mineral soils, since OM provides U specific sorption sites. Besides this, by grouping the K_d (U) data gathered from mineral soils according to their clay and sand percentages to create the different textural groups, it is expected that those K_d (U) data corresponding to soils with higher SSA and, thus, with higher U sorption capacity may be classified in different categories (Clay or Loam) than those coming from soils with lower SSA (Sand). Consequently, partial datasets corresponding to textural categories (Clay, Loam and Sand) are expected to contain K_d (U) values varying less than when mixed up in the Mineral group partial dataset and on the overall dataset.

As explained before, pH strongly affects the uranium species present in the soil solution. Consequently, the pH at which the sorption takes place can be considered a soil factor directly related to the U sorption mechanisms in soils. Therefore, the U overall dataset was also split into three pH groups ($pH < 5$; $5 \leq pH < 7$; and $7 \leq pH < 9$) defined according to the U speciation (Vandenhove et al., 2009), which defines the pH criterion.

Finally, for the first time it was evaluated the hierarchical application of K_d (U) grouping criteria based on soil factors both related to the U speciation/sorption in soils (pH) and to the U sorption sites of the soil matrices (OM, clay and sand %) aiming at improving the creation of partial datasets with less variability. As a summary, **Figure 4.6** shows the K_d (U) groups created according to the hierarchical application of the different grouping criteria.

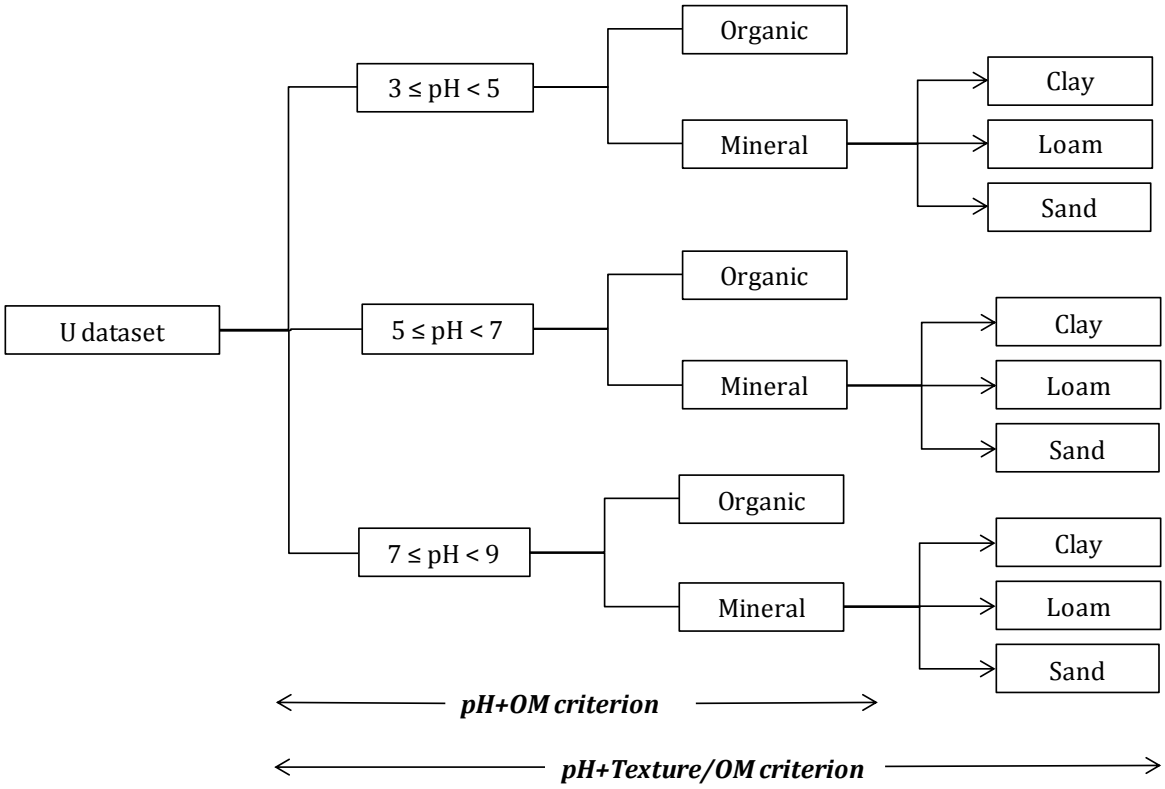

Figure 4.6 *Diagram of hierarchical application of K_d (U) data grouping criteria (pH + OM and pH + Texture/OM).*

Concretely, the U overall dataset was split according to the pH criterion and subsequently, the K_d (U) data of each pH group were split according to the OM content of the soils from they were gathered to create Mineral and Organic groups (pH + OM criterion). In a further step, K_d (U) data in the pH-Mineral groups were also split according to the soil texture into the three textural groups (pH + Texture/OM criterion).

4.2.2.3 Soil factors and developed criteria to group K_d (Am) data

In the preceding section 3.3.2 the influence of the soil properties on the Am interaction was extensively analysed and discussed and it was pointed out the key role of soil dissolved organic matter (DOM), pH and SSA. From that previously explained, first of all it must be recalled that the Am sorption in soils can be strongly inhibited by the formation of stable and anionic Am-DOM complexes that remains in solution because of their low affinity (electrostatic repulsions) with the soil solid

phases. In line with this, it would be desirable to develop any grouping criterion allowing to distinguish between those soils in which Am sorption is namely controlled by the organic matter fraction, presenting a low capacity to sorb Am, from those soils in which the Am sorption is controlled by the mineral fraction, presenting a high capacity to sorb Am.

The Dissolved Organic Carbon (DOC) parameter, an estimator of the amount of dissolved organic compounds coming from the soils would be a suitable soil factor for K_d (Am) data grouping. However, the scarcity of DOC data available hampered to use it for grouping K_d values. Instead of this, since DOC is strongly correlated with the soil organic matter content (OM), K_d data grouping on the basis of the soil OM could also succeed in reaching this goal. Therefore, alike the cases of Cs and U, as a first approach the Texture/OM K_d grouping criterion was once again applied to separate K_d (Am) into two different partial datasets.

The results obtained from the Am sorption studies in soils performed in the present Thesis suggest that the Am-DOM speciation in solution can be dominant even at low concentration of DOM. Therefore, alike the case of Cs, the OM threshold to classify soils as mineral or organic (20%) may not be the most suitable when K_d (Am) data are grouped. According to this, as a second analysis the Texture/OM criterion was redefined by establishing a new OM threshold. Unlike the case of Cs, the current K_d (Am) dataset lacked of data to statistically optimise the OM threshold. Instead of this, according to the results described in section 3.3.2, an OM threshold of 8% was established on the basis of the relationship between OM and DOC parameters and between DOC and K_d (Am) obtained in our controlled scenario of 20 contrasting soils.

Alike the case of U, it was also explored the application of a pH criterion specific for the Am-soil interaction. The K_d (Am) dataset was split into four partial datasets containing each one only those K_d (Am) values gathered within the following pH ranges, established according to the pH-dependent Am speciation in solution and affinity for sorption sites (Choppin, 2007):

- $3 \leq pH < 6$: presence of positively-charged sorption sites and cationic Am species (primarily as Am^{3+}) and lower K_d (Am) are expected due to electrostatic repulsions.

- $6 \leq pH < 7.5$: presence of deprotonated sorption sites, leading to an increase in the sorption of cationic Am species (primarily as $Am(OH)^{2+}$ and $AmCO_3^{+}$).

- $7.5 \leq pH < 9$: increase of sorption sites due to increase in negative charge resulting from progressive deprotonation of functional groups. High K_d (Am) values are expected, excepting for soil-water systems with high content of dissolved carbonate with predominance of the anionic $Am(CO_3)_2^{-}$ species.

- $pH \geq 9$: unless Am precipitation or co-precipitation occurs, much lower K_d (Am) are generally expected since anionic and neutral Am species (primarily $Am(CO_3)_3^{-3}$ and $Am(OH)_3$) are predominant.

In chapter 3 it was already mentioned that the Am-soil interaction cannot be explained univarianty. Thus, a series of grouping criteria were developed by combining different relevant soil factors, which are schematically summarised in **Figure 4.7**. Since the pH-dependency of the Am sorption in soils still remains unclear when DOM is present in the soil solution at concentrations high enough to control Am speciation, a combined grouping criterion involving OM and pH was also tested (OM/pH criterion). That is, the overall K_d (Am) dataset was firstly split into the Mineral and Organic groups by applying the OM% threshold previously established. Secondly, only the K_d data of the Mineral group were subsequently split into the four pH groups previously defined. Finally, since the Am sorption in soils is influenced by the soil SSA, a final attempt was done to improve K_d (Am) data grouping by further splitting the previous Mineral-pH partial datasets containing K_d data at $pH < 9$ according to the soil texture (sand, loam and clay), thus leading to partial datasets containing K_d (Am) data only from a given soil texture (OM/pH/Texture grouping criterion).

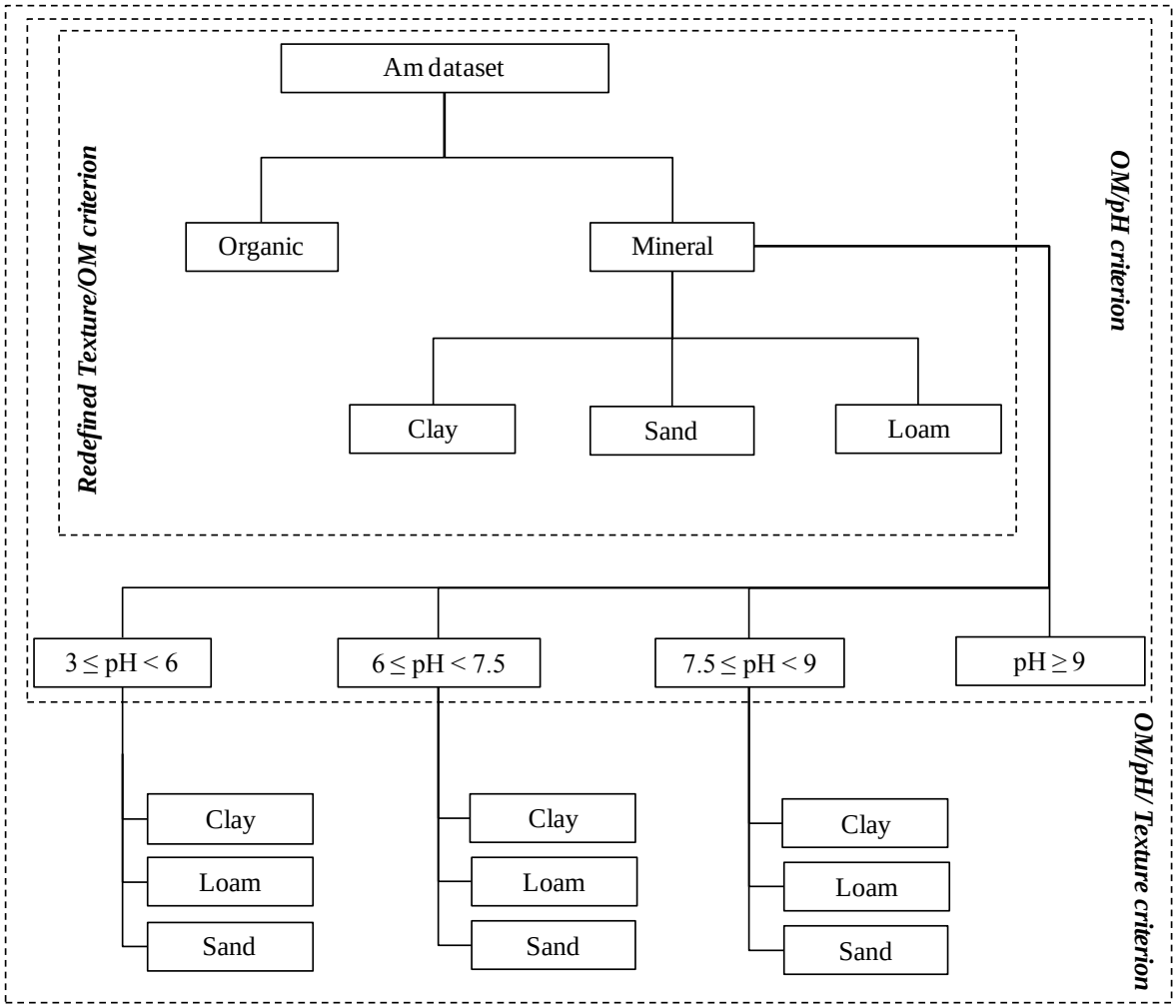

Figure 4.7 *Diagram of application of K_d (Am) data grouping criteria based on combining soil factors (OM/pH and OM/pH/Texture).*

The reason for not splitting the Mineral – pH ≥ 9 partial dataset according to soil texture lies on the fact that K_d variability over pH basically explained by Am precipitation due to the presence of high concentration of carbonate species in solution. Since such process cannot be captured by texture factor, it is not justified to apply of the OM/pH/Texture criterion for this specific soil-type K_d (Am) data.

4.2.3 Analysis of the influence of the experimental approach on K_d (RN) data variability

For the first time factors based on the experimental approach applied to determine the K_d values were used to group K_d (RN) data in soils. This allow the evaluation, on

the one hand, whether sorption dynamics may have an influence on the K_d best estimates, which may entail the necessity of distinguishing between those K_d data suitable to foresee short-term and long-term contamination scenarios, and on the other, whether the different methods applied to quantify K_d values may be a source of K_d variability. However, taking into account that K_d variability is the result of multiple factors the evaluation of the influence experimental approach factors cannot be directly performed.

Before applying the grouping criteria based on experimental approach factors, a data treatment based on group mean centring (GMC) was carried out in order to discard the effect of soil factors identified as relevant to the interaction of the target elements in soils. In short, the GMC consisted in log-transforming the overall dataset of the target element, grouping the K_d data according to the criteria previously established on the basis of different key soil factors, calculating the AM of log K_d values of each "soil-type" group created and correcting each single log K_d value within a given group by subtracting the AM log K_d value of the respective soil-type group.

Secondly, a series of experimental approach factors were applied to split the GMC-corrected log K_d datasets into different categories. To this end, a first factor related to the time elapsed since the target elements were sorbed to soils (Methodology-Dynamics) was considered to split the datasets into two groups, one containing K_d data representative of scenarios in which the target elements interaction in soils may have undergone aging processes (long-term category), and the other containing K_d data representative of recently-contaminated scenarios (short-term category). Moreover, a second factor related to the experimental approach followed to the K_d quantification (Methodology-Test)) was also considered to split each dataset previously created into sorption, desorption or *in-situ* categories. It must be noticed that for the specific cases here studied (Cs, U and Am) there were no in-situ data in their datasets and, thus, it was only necessary to split the created short-term datasets into sorption and desorption categories. Then, statistical tests (F-tests and paired samples t-tests) were performed to check whether the K_d data in the experimental approach datasets significantly differed among them or not. **Figure 4.8** illustrates this approach for the case of considering the Texture/OM criterion for the GMC treatment.

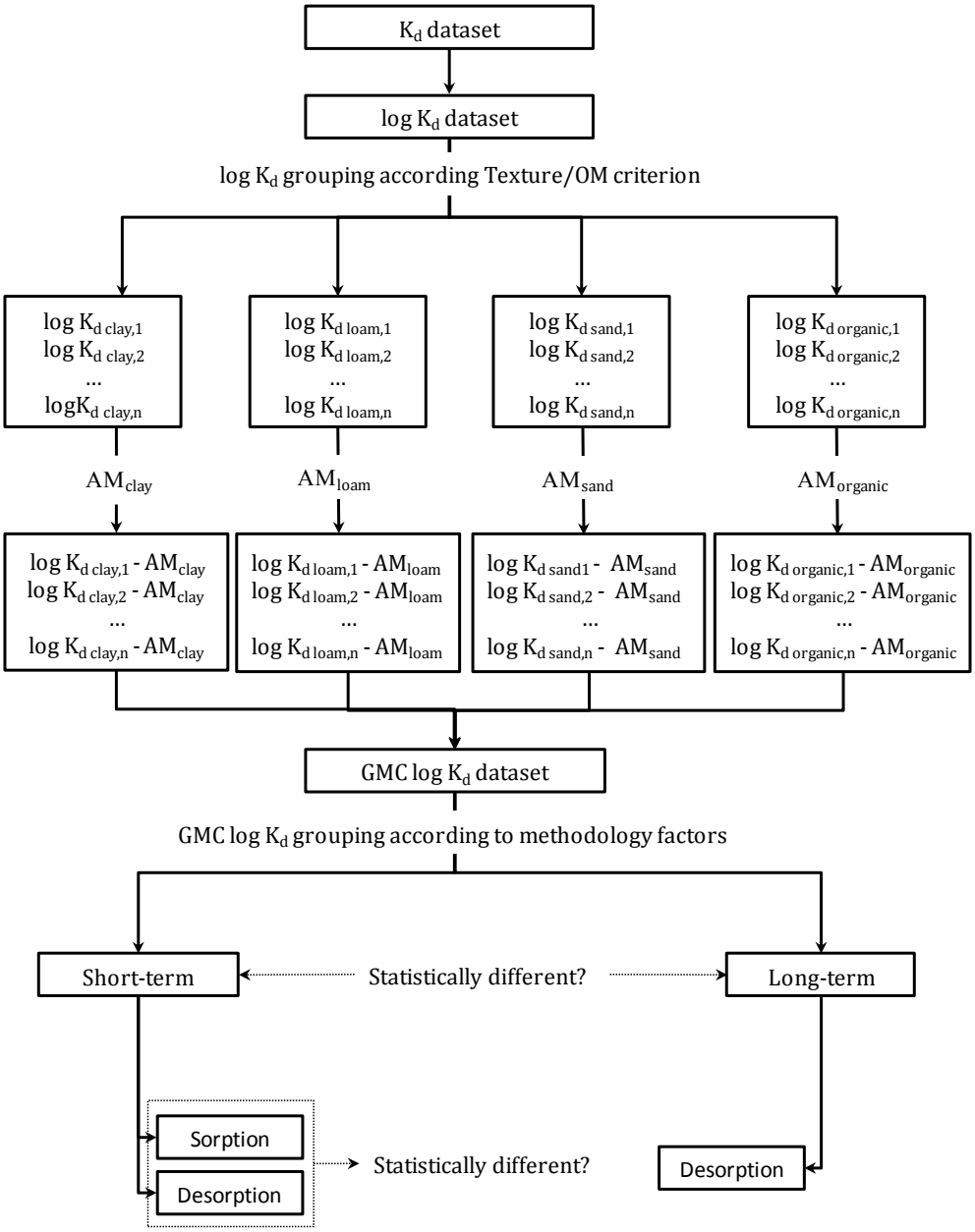

Figure 4.8 *Strategy applied to evaluate the influence of the experimental approaches on K_d data. Group Mean Centring performed according to Texture/OM criterion.*

For the cases of Cs, U and Am several analyses were needed by performing the GMC with the different grouping criteria developed in order to avoid misleading conclusions regarding the experimental approach influence, for instance caused by relevant soil factors others than those covered in each GMC analysis.

4.2.4 Construction of CDFs from soil K_d datasets to explain K_d data variability

The overall and partial datasets of Cs, U and Am were used to construct Cumulative Distribution Functions (CDFs) following the procedure that is schematically shown in **Figure 4.9**. In all cases, K_d data were log-transformed and the presence of possible outlier values in the datasets, which may distort the intrinsic data distribution, was examined by performing an exploratory analysis based on box-and-whisker plots. A threshold of three times the interquartile range was established to decide if a log (K_d) values was an outlier and to remove it from the datasets.

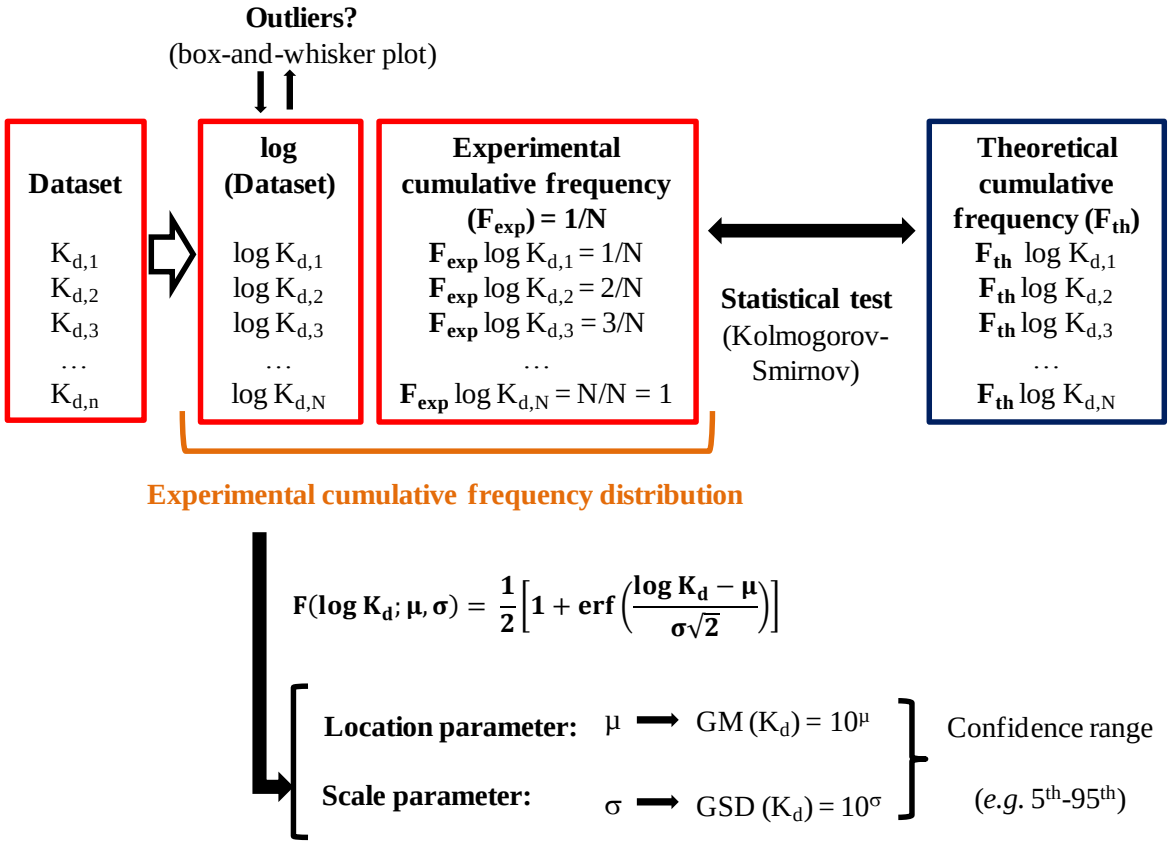

Figure 4.9 *Schematic process to construct CDFs and to derive best estimates values and related confidence intervals from K_d datasets.*

The log K_d data within every dataset were sorted by increasing value and an empirical frequency ($f_{exp,i}$) equal to 1/N (where N is the total number of K_d entries in the respective dataset) was assigned to each entry. Experimental cumulative frequency distributions were constructed by assigning to each sorted log K_d value their corresponding cumulative frequency ($F_{exp,i}$), *i.e.*, the sum of the preceding frequencies

$\left(F(K_{d,j}) = \sum_{i=0}^{j} f(K_{d,i})\right)$. Following to this, a Kolmogorov-Smirnov test, which statistically compares an experimental cumulative distribution with an ideal one, was applied to ascertain the underlying frequency distribution in each K_d dataset. As expected, it was found that all the K_d datasets analysed followed a log-normal (hereinafter, logN) distribution. Consequently, the experimental cumulative frequency distributions constructed with the log K_d data were fitted to the theoretical Normal CDF equation (Eq. 4.1) and the location and scale parameters (μ and σ, respectively) were derived to construct CDFs.

$$P\left(\log K_{d,i} \leq \log K_{d,j}\right) = \sum_{\log K_{d,i} \leq \log K_{d,j}} p\left(\log K_{d,i}\right) = \frac{1}{2} + \frac{1}{2}\,\mathrm{erf}\left(\frac{\log(K_{d,i}) - \mu}{\sigma\sqrt{2}}\right);\ K_{d,i} > 0. \quad [4.1]$$

where

P stands for cumulative probability;

erf is the error function.

A best estimate K_d value (the most likelihood value) was derived as the 50th percentile and the 5th and 95th percentiles (corresponding to the 90% confidence interval) were calculated from each partial dataset with the aim of comparing among the K_d data of the groups created according to the different criteria. However, since the statistical parameters determined in a lognormally distributed K_d dataset (μ, σ and percentiles) are in log-scale, the derived best estimate value and confidence range are also in log-scale. So as to ease the use and understanding of these data, the corresponding antilog parameters were preferred, that is, the geometric mean (GM) and geometric standard deviation (GSD) instead of the μ and σ parameters (see Eq.(4.2) and Eq.(4.3) for the relationship between the two set of parameters), as well as confidence intervals (percentile ranges) of K_d values instead of those of log K_d values will be used.

$$GM\left(K_d\right) = \left(\prod_{i=1}^{N} K_{d_i}\right)^{\frac{1}{N}} = e^{\left(\frac{1}{N}\sum_{i=1}^{N} \log\left(K_{d_i}\right)\right)} = e^{\mu} = \text{antilog}\,(\mu) \quad [4.2]$$

$$GSD\left(K_d\right) = e^{\left(\sqrt{\frac{\sum_{i=1}^{N} \left(\log \frac{K_{d_i}}{GM}\right)^2}{n}}\right)} = e^{\sigma} = \text{antilog}\,(\sigma) \quad [4.3]$$

It is worth noting that to properly derive a reliable CDF from a given K_d dataset it is necessary that it contains a minimum number of entries ($N > 10$), namely because two reasons. Firstly, it is crucial that the underlying statistical distribution of a K_d population could be reliably ascertained in order to properly construct CDFs and to do this, the K_d values comprising a given dataset may pose a high representativeness and lead to well-defined experimental cumulative frequency distributions. Secondly, it is required to ensure a reliable fitting of the K_d data, that is, to derive the descriptor parameters of the CDF with low uncertainty. Exceptionally, from those datasets containing between 6 and 10 entries, CDFs were constructed as far as the datasets presented clear experimental cumulative distributions allowing deriving parameters with low uncertainty, *i.e.* if a good fitting of data could be done. For the rest of cases only GM values were calculated directly from the dataset, assuming that they followed a logN distribution, to propose K_d best estimate values at least useful for screening purposes.

4.3 RESULTS AND DISCUSSION

4.3.1 Current status of the K_d data compilation

Besides data published in peer-reviewed journal or accessible in reports (references of literature used for the compilation updating are listed in ANNEX I), a high amount of data was incorporated from studies made available by personnel and/or research groups of SKB (Sweden), NIRS (Japan), Savannah River National Laboratory (US), Saanio & Riekkola (Finland) and NRSC (China). **Table 4.2** summarises the currently available K_d data in the compilation for each element, and gives information on the data entries that were already available in the former TRS-472 dataset for the sake of comparison. Elements with priority RNs due to their relevance in the context of radiological protection (ICRP, 2008), labelled as ICRP, and management of radioactive waste resulted from the operating times and decommissioning of the nuclear power plants (SKB, 2014), labelled as Radwaste, are also listed to show the associated decrease in relevant data gaps and the related improvement on available information on soil K_d. Moreover, the number of available K_d data coming from solid environmental materials potentially homologous to soils is also indicated in brackets.

Currently, the compilation contains more than 5000 entries of soil K_d for 83 elements, 54 of them with RNs in the priority list, which is a significant improvement with respect to the previous dataset (TRS-472). Compilation also contains around 2000 entries of K_d data for 75 elements gathered from a selection of other solid materials. There has been significant relative increase in the number of entries for elements such as Am, Sm, Eu, Ni, Cs, Sr, U, Ru and Co, whereas soil K_d values were not updated for Ac, C, Cf, Cm, H, In, Pa, Pm and Rh. It is important to point out that the number of elements with more than 10 entries in soils has remarkably increased (from 36 in the TRS-472 compilation to 55 in the current compilation, 73 if K_d data from materials other than soils are also considered), which makes it possible to construct for the first time, at least, a general K_d CDF of the vast majority of elements with relevant RNs. Conversely, for these elements with less than 10 entries (Ac, Gd, H, In, La, Pa, Pd, Pm, Pr, S, Te and Tl), a single best estimate (GM) K_d value only for screening purposes can be derived, since their data distribution generally cannot be properly checked. Therefore, it remains a future challenge to fill these data gaps or, alternatively, to seek analogies with other elements with enough data to construct a CDF.

Table 4.2 Summary of the number of soil K_d entries in the updated compilation. Comparison with element priority lists and with the number of entries in the TRS-472 compilation. Priority elements whose mobility is not predicted with K_d values but with specific activity (*e.g.*, C or H) are not included. In brackets additional K_d entries from materials other than soils.

Element	ICRP	Radwaste	TRS-472	Current compilation	Element	ICRP	Radwaste	TRS-472	Current compilation
Ac		X	4	4 (2)	Dy			2	10 (9)
Ag	X	X	9	22 (30)	Er			-	7 (9)
Al			-	7 (23)	Eu	X	X	-	32 (12)
Am	X	X	62	108 (29)	Fe		X	23	35 (36)
As			7	22 (28)	Ga			2	10 (9)
B			-	7 (17)	Gd		X	-	8 (9)
Ba	X	X	1	20 (29)	Ge			-	7 (9)
Be		X	5	24 (17)	Hf			6	13 (9)
Bi		X	6	18 (5)	Hg			1	7 (10)
Br			4	17 (21)	Ho		X	4	11 (9)
Ca	X	X	34	56 (26)	I	X	X	250	571 (71)
Cd	X	X	61	75 (32)	In		X	2	2
Ce	X		11	19 (19)	Ir	X		15	18
Cf	X		-	-	K	X		237	231 (27)
Cl	X	X	22	30 (35)	La	X	X	1	9 (9)
Cm	X	X	18	18	Li			-	7 (16)
Co	X	X	118	119 (153)	Lu			1	8 (8)
Cr	X		31	38 (38)	Mg			30	53 (26)
Cs	X	X	469	770 (123)	Mn	X	X	83	94 (32)
Cu			11	26 (31)	Mo		X	9	26 (31)

Table 4.2 Summary of the number of soil K_d entries in the updated compilation. Comparison with element priority lists and with the number of entries in the TRS-472 compilation. Priority elements whose mobility is not predicted with K_d values but with specific activity (*e.g.*, C or H) are not included. In brackets additional K_d entries from materials other than soils (Cont'd).

Element	ICRP	Radwaste	TRS-472	Current compilation	Element	ICRP	Radwaste	TRS-472	Current compilation
Na			30	45 (26)	Sb	X	X	152	165 (13)
Nb	X	X	11	23 (42)	Sc			2	8 (6)
Nd			-	8 (9)	Se	X	X	172	269 (59)
Ni	X	X	64	308 (48)	Si			4	11 (17)
Np		X	26	40 (31)	Sm		X	4	38 (9)
Os			-	6 (3)	Sn		X	12	95 (13)
P	X		6	19 (21)	Sr	X	X	255	645 (56)
Pa	X	X	4	4	Ta			5	11 (4)
Pb	X	X	23	44 (38)	Tb			2	9 (8)
Pd		X	6	7 (2)	Tc	X	X	33	48 (55)
Pm		X	2	2	Te	X	X	2	8 (4)
Po		X	44	49 (1)	Th	X	X	46	54 (22)
Pr		X	-	8 (9)	Ti			-	6 (4)
Pt			15	16 (1)	Tl		X	-	8 (7)
Pu	X	X	62	59 (5)	Tm			1	8 (7)
Ra	X	X	51	103 (37)	U	X	X	178	197 (86)
Rb			4	12 (9)	V			2	17 (25)
Re			-	7 (6)	Y		X	7	18 (14)
Rh			12	12	Yb			-	8 (9)
Ru	X	X	15	21 (4)	Zn	X		92	123 (26)
S	X		-	7 (17)	Zr	X	X	11	26 (26)

4.3.2 The case of radiocesium

The updated Cs dataset contains 770 entries with related soil characteristics and details regarding the experimental approach applied. With respect to the former K_d compilation (TRS-472), a significant set of data gathered from desorption experiments of indigenous Cs has been integrated as a result of the changes introduced in data acceptance criteria. The soil K_d (Cs) overall dataset contained values ranging within up to 5 orders of magnitude (Min-Max range of 4×10^{0} - 4.5×10^{5} L kg^{-1}). The large K_d (Cs) variability of the dataset denotes a strong influence of having soils with contrasting key properties (*e.g.*, OM or clay content, K in soil solution, etc.) and/or of the different experimental approaches applied to quantify K_d (Cs) values. Therefore, a single CDF constructed with the overall dataset may be unsuitable for risk assessment purposes since it may pose a high uncertainty and it would not be suitable for most of contamination scenarios.

4.3.2.1 Influence of the experimental approach on K_d (Cs) data

The overall K_d (Cs) dataset contained K_d data gathered by applying sorption and desorption experiments to recent contaminated soils, or under experimental conditions representing a short-term contamination scenario (ST-S and ST-D), as well as by applying desorption tests to long-term contaminated soils, or under experimental conditions representing a long-term contamination scenario (LT-D). In order to test the effect of the experimental approach on the K_d (Cs) data (short-term *vs.* long-term data and sorption *vs.* desorption data), the strategy described in section 4.2.3 was applied. **Table 4.3** summarises the paired sample t-tests performed to the experimental approach partial datasets created by means of GMC data treatments according to the grouping criteria that will be evaluated for Cs (Texture/OM; and RIP/K_{ss}), as explained in previous section 3.2.2.4.

Table 4.3 Analysis of the experimental approach influence on K_d (Cs) data.

Grouping criteria for GMC	K_d (Cs)-types	Comparison	Probability (p)*
Texture/OM	Short-term sorption (ST-S) Short-term desorption (ST-D) Long-term (LT)	ST-S *vs.* ST-D ST *vs.* LT	0.73 < 0.05
RIP/K_{ss}	Short-term sorption (ST-S) Short-term desorption (ST-D)	ST-S *vs.* ST-D	<0.05

*Probability of considering that the K_d datasets do not differ among them.

When the GMC analysis was performed by controlling texture and OM soil factors, no significant differences ($p > 0.05$) existed between K_d (Cs) values obtained from sorption and desorption tests with short-term incorporated Cs, whereas sorption and desorption partial datasets significantly differed when controlling RIP and potassium in solution soil factors, this divergences regarding the effect of the test applied to quantify K_d (Cs) suggests that the variability on K_d (Cs) values due to the method applied (sorption or desorption test) is negligible compared to that caused by the contrasting properties of the soils. Conversely, when sorption and desorption short-term data were pooled and compared with long-term data it was evidenced that K_d (Cs) data values originated for short-term and long-term incorporated Cs were significantly different ($p < 0.05$). According to this, different probabilistic K_d (Cs) data should be derived to assess the Cs interaction in soils depending on the contamination scenario under study. Thus, it is not necessary to separate sorption and desorption K_d (Cs) data for further analyses, whereas short-term and long-term K_d (Cs) data will be distinguished before applying any grouping criteria. **Table 4.4** summarises the K_d (Cs) data obtained from the short-term and long-term partial datasets.

Table 4.4 K_d (Cs) (L kg^{-1}) for soils grouped according to the Methodology-Dynamics factor.

Partial dataset	N	Min	Max	GM	5th	95th
Short-term	601	4.3	3.8×10^{5}	1.5×10^{3}	8.8×10^{1}	2.6×10^{4}
Long-term	169	1.1×10^{1}	4.5×10^{5}	2.5×10^{4}	4.2×10^{3}	1.4×10^{5}

The K_d (Cs) data for long-term incorporated Cs (GM and 5^{th} – 95^{th} percentile range values) were an one order of magnitude or more higher than those of short-term incorporated Cs which made that the long-term CDF (depicted below in **Figure 4.10**) was clearly shifted to higher K_d (Cs) values. The difference between "short-term" and "long-term" data can be attributed to the previously explained changes in Cs sorption with time, that is, long-term incorporated Cs may have undergone an aging process which led to an increase in the Cs sorption irreversibility.

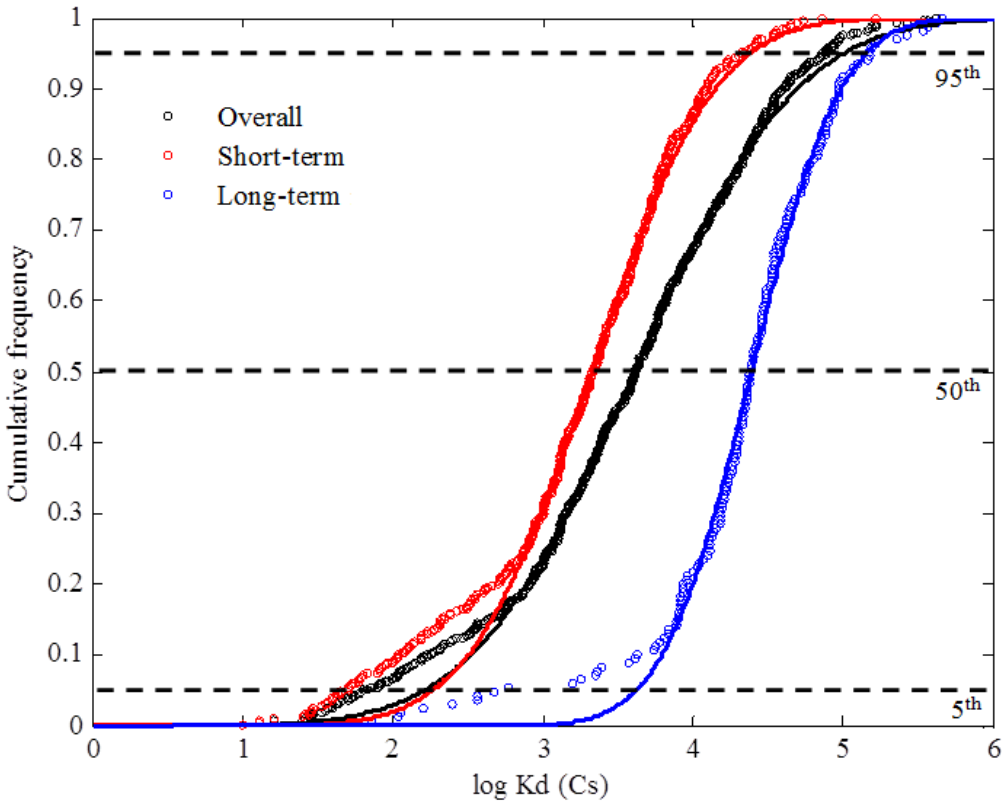

Figure 4.10 *CDFs of K_d (Cs) data in soils according to the time elapsed since Cs incorporation to soils. For the sake of comparison the CDF of the overall dataset is also shown.*

Therefore, from this exploratory analysis it can be suggested avoiding the use of "long-term" K_d (Cs) data to foresee recently contamination episodes of Cs in soils as far as the sorption grade of Cs in the soil matrix would be overestimated, and *vice versa*. According to this, it is therefore recommended to separate, when possible, the K_d (Cs) data representative of the short-term Cs interaction from those being representative of the long-term Cs interaction so as to propose more reliable K_d (Cs) best estimates or to construct CDFs from compilations. Consequently, special care

must be taken when desorption K_d (Cs) data of indigenous Cs are included in compilations since these K_d data can be representative either of the Cs interaction behaviour in the short-term, or in the long-term, depending on the experimental conditions under which the K_d (Cs) values were quantified.

4.3.2.2 K_d (Cs) best estimates and CDFs on the basis of the Texture/OM criterion

The current Cs dataset, when refined on the basis of the Texture/OM criterion (K_d (Cs) data gathered from the same soil sample at varying any factor not contemplated in this grouping criterion was rejected from the dataset, see "*Soil factor field"* in section 4.2.1.2), contained 578 entries of K_d (Cs) data, which means 109 additional entries with respect to the TRS-472 dataset. **Table 4.5** summarises the K_d (Cs) data obtained from the CDFs constructed by applying the Texture/OM criterion to the short-term and long-term partial datasets.

Table 4.5 K_d (Cs) (L kg^{-1}) data grouped according to the Texture/OM criterion.

Partial dataset	N	Min	Max	GM	5th	95th
Short-term						
Clay	32	5.7×10^{2}	1.7×10^{5}	5.8×10^{3}	1.2×10^{3}	2.8×10^{4}
Loam	193	6.2×10^{1}	5.0×10^{4}	3.4×10^{3}	5.4×10^{2}	2.2×10^{4}
Sand	106	1.0×10^{1}	2.6×10^{4}	1.2×10^{3}	7.6×10^{1}	1.8×10^{4}
Organic	64	1.3×10^{1}	7.2×10^{4}	1.8×10^{2}	7.4	4.5×10^{3}
Long-term						
Mineral	148	2.3×10^{3}	4.5×10^{5}	2.9×10^{4}	6.7×10^{3}	1.2×10^{5}
Organic	21	7.3×10^{1}	1.5×10^{5}	1.3×10^{3}	3.1×10^{1}	5.4×10^{4}

The GMs derived from the CDFs created with the "Short-term" data evidenced that K_d (Cs) values increased along with the soil clay content ($GM_{organic} << GM_{sand} < GM_{loam} < GM_{clay}$) and that the lowest GM corresponded to the Organic group. This pattern is consistent with Cs sorption mechanisms, namely that Cs sorption is strongly influenced by the greater binding affinities of clay minerals and the relatively weak sorption of Cs to natural organic matter (Rigol et al., 2002). On the other, whilst no statistical differences were observed ($p > 0.05$) among the textural groups created

from the long-term partial dataset, the same conclusions concerning the relationship between the soil clay content and the K_d (Cs) values can be drawn since the GM derived for the Mineral group was again one order of magnitude higher than that of the Organic group. Moreover, the GMs values derived from the soil groups created from the long-term K (Cs) partial datasets were systematically higher (one order of magnitude) than those derived from the short-term partial datasets and the 5^{th}-95^{th} intervals of the long-term partial datasets were shifted to higher K_d (Cs) values, which corroborates the influence of the sorption dynamics on the K_d (Cs) values.

Comparing the 5^{th}-95^{th} percentile ranges of K_d (Cs) values obtained from the different soil-type partial datasets with that of the overall Cs dataset, the application of the Texture/OM criterion either to the "short-term "or to the "long-term" data allowed us to create K_d groups related to mineral soils whose datasets comprised K_d (Cs) values generally varying much less than those of the Cs overall dataset. This decrease of the K_d variability was especially significant for the Clay and Loam partial datasets of the "short-term" data and the Mineral partial dataset of the "long-term" data, in which K_d (Cs) values varied only within one-to-two orders of magnitude. Conversely, the short-term and long-term Organic partial datasets contained K_d (Cs) with values still ranging within several orders of magnitude. These results suggests that, as expected, the classical Texture/OM criterion only accounts for some of the natural variability and that more specific grouping criteria are necessary.

4.3.2.3 K_d (Cs) best estimates and CDFs on the basis of the redefined Texture/OM criterion

Since it is known that Cs interaction in soils is controlled by the clay fraction unless its content is negligible, a further step was done to redefine the Texture/OM criterion by means of establishing a more restrictive OM threshold to define an “organic soil”, which may enable to differentiate between textural-types of K_d (Cs) data. To this end, K_d data in each of the two partial datasets created on the basis of the Methodology-Dynamics factor (short-term and long-term) were then split into two partial datasets, Mineral and Organic, according to different percentages of OM content of the soils from which the K_d data were gathered. Soils were grouped by increasing OM thresholds, *i.e.* from ≥ 20% of OM, the threshold used in the classical Texture/OM

criterion, to ≥ 90% of OM, and the K_d (Cs) GM values and related 5^{th}-95^{th} intervals were calculated in each case.

In the case of the "short-term" K_d (Cs) data it was observed that the GMs and related 5^{th}-95^{th} intervals (K_d data variability) obtained from the Organic partial datasets progressively decreased by increasing the OM threshold up to 70%, and remained almost constant for higher OM thresholds, whereas the K_d (Cs) variability in the Mineral partial datasets started to increase at OM thresholds higher than 50%. On the other hand, for the "long-term" K_d (Cs) data (GM values and related variability) of the created Organic partial datasets decreased when increasing the OM threshold in all the OM range tested. The decrease was especially significant when the 90% OM was applied, since it led to an Organic partial dataset with the narrowest 5^{th}-95^{th} percentile range (lowest variability). Such fact is in agreement with the Cs sorption dynamics mentioned before, since only in those soils with extremely low mineral content the long-term Cs sorption is unlikely to undergo aging processes.

From these results, it was concluded that when "short-term" and "long-term" K_d (Cs) data are grouped according to the Texture/OM criterion, an OM threshold of 50% and 90%, should be taken, respectively, to create the Organic and Mineral partial datasets since it entailed a better distinction of the K_d (Cs) data for these two types of soils. That is, more contrasting GM values were obtained without increasing the K_d variability within these soil-types partial datasets. The fact that the optimal OM% to distinguish between Organic and Mineral soil-types of K_d (Cs) data is in agreement with the Cs interaction mechanisms in soils. Due to the key role of the sorption dynamics that undergo Cs species interacting with FES sites, only the long-term interaction of those soils with extremely low 2:1 phyllosilicate content (*i.e.*, peat soils with OM > 90%) may be devoid of aging effects. **Table 4.6** summarises the K_d (Cs) data obtained from the CDFs constructed by applying the redefined Texture/OM criteria to the short-term and long-term partial datasets, whereas the CDF graphical representations are depicted in **Figure 4.11**.

The distinction between "short-term" and long-term K_d (Cs) data and the changes introduced concerning the OM thresholds resulted in partial datasets with much lower variability than when using solely the classical Texture/OM criterion, that significantly differed among them ($p < 0.05$), with the exception of the Loam and Clay

texture K_d (Cs) partial datasets. The derived K_d (Cs) best estimates increased with increasing clay content leading to well-defined CDFs among textural groups. Besides, for a given textural soil group, the long-term K_d (Cs) data were systematically much higher (around one order of magnitude) than those corresponding to the "short-term" data.

Table 4.6 K_d (Cs) (L kg^{-1}) data grouped according to the redefined Texture/OM criterion.

Partial dataset	N	Min	Max	GM	5th	95th
Short-term						
Mineral (OM < 50%)	371	9.6	1.7×10^{5}	2.6×10^{3}	2.9×10^{2}	2.3×10^{4}
Clay+Loam[a]	230	6.0×10^{1}	1.7×10^{5}	3.7×10^{3}	5.7×10^{2}	2.4×10^{4}
Sand	108	9.6	7.2×10^{4}	1.2×10^{3}	8.6×10^{1}	1.7×10^{4}
Organic (OM ≥ 50%)	38	1.3×10^{1}	1.9×10^{3}	7.1×10^{1}	1.3×10^{1}	3.8×10^{2}
Long-term						
Mineral (OM < 90%)	161	1.1×10^{2}	4.5×10^{5}	2.7×10^{4}	5.2×10^{3}	1.4×10^{5}
Clay+Loam[a]	116	4.2×10^{3}	4.5×10^{5}	3.2×10^{4}	7.6×10^{3}	1.4×10^{5}
Sand	33	2.3×10^{3}	9.4×10^{4}	1.8×10^{4}	4.0×10^{3}	8.2×10^{4}
Organic (OM ≥ 90%)[*]	8	7.3×10^{1}	1.6×10^{3}	2.4×10^{2}	4.5×10^{1}	1.2×10^{3}

[a] Clay+Loam group contained K_d (Cs) data from clayey and loamy soils.
[*] K_d (Cs) data derived from a CDF constructed with a dataset containing scarce data (N < 10).

It therefore appears that albeit soil texture can be a relevant factor to further decrease K_d (Cs) variability for providing better input data for radiological assessments, it is crucial to firstly decide whether the scenario under study corresponds to a short-term contamination episode (immediate impact of a radioactive contamination) or to a long-term one (for instance, in the context of safety and performance assessment of deep geological repositories or long-term impact assessment of contamination episodes) and, for each scenario, to properly distinguish between organic and mineral soils with the established OM thresholds.

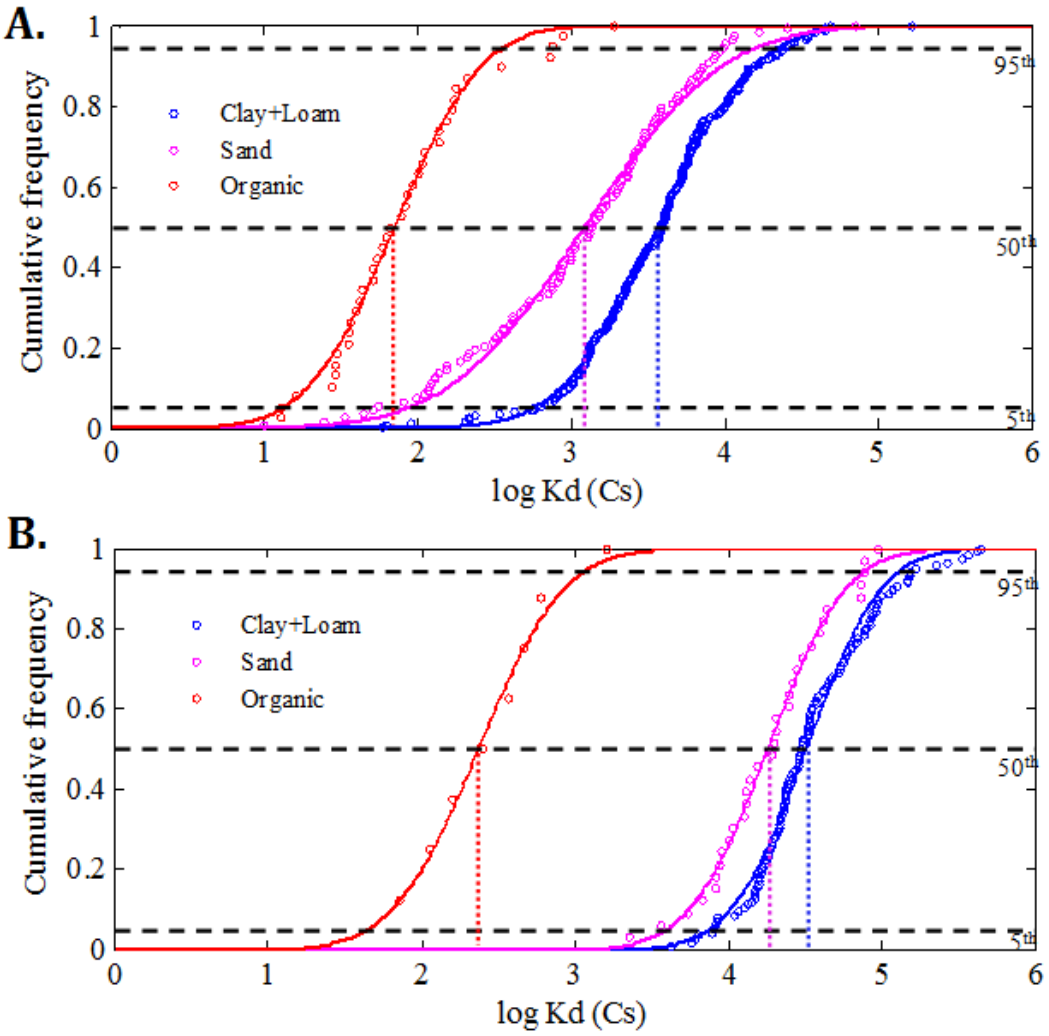

Figure 4.11 *CDFs of K_d (Cs) on the basis of the redefined Texture/OM criterion within the short-term (A.) and long-term (B.) partial datasets. Vertical dashed-lines indicate log K_d (Cs) best estimate values.*

4.3.2.4 K_d (Cs) best estimates and CDFs on the basis of the RIP/K_{ss} criterion

The mechanisms governing radiocaesium interaction in soils have been well identified and validated in past studies (see for instance Gil-García et al., 2011). Sorption tests carried out in laboratory, controlled conditions have elucidated that two sorption contributions are expected for the total K_d (Cs) in soils, those at RES and FES. The relative weight of each contribution depends on the soil type (Vidal et al., 1995), although even for minor clay contents in soils FES would govern Cs sorption. Therefore, the K and NH_4^+ (and even Na for highly saline soils) status in the exchangeable complex and soil solution, as well as the quantity and quality of FES

(which is estimated with the Radiocesium Interception Potential (RIP) parameter) are the key soil factors to be taken into account to predict K_d (Cs) for a specific risk assessment, as illustrated in the following equation (Gil-García et al., 2011):

$$K_d(Cs) = K_d^{FES}(Cs) + K_d^{RES}(Cs) = \frac{RIP_K}{K_{ss} + K_C^{FES}(NH_4/K)\cdot NH_{4,ss} + K_C^{FES}(Na/K)\cdot Na_{ss}} + \frac{K_{exch} + NH_{4,exch} + Na_{exch}}{K_{ss} + NH_{4,ss} + Na_{ss}} \quad [4.4]$$

in which K_c^{FES} stands for the monovalent trace selectivity coefficients at FES. K_C^{FES} (Na/K) takes a value around 0.02, whereas K_C^{FES} (NH_4/K) roughly varies within a 4-8 range.

Therefore, the large K_d (Cs) variability in soils is due to the high range of values that RIP may take in soils as well as due to changes in, basically, NH_4^+ and K status. From the knowledge and application of this equation, the calculation of neither K_d best estimates nor 5^{th}-95^{th} percentiles from the CDF construction is, in principle, not required, as the end-user could calculate straightforwardly a K_d (Cs) value from the values of the variables included in the former equation. However, a few of the variables and parameters of the former equation are not always available. For instance, the NH_4^+ concentration in the exchangeable complex and soil solution is often not determined. Therefore, the quality of the predictions may decrease drastically when all the required information is not available.

As a simplification of the former equation, the ratio between the RIP and the K concentration in soil solution (K_{ss}), RIP/K_{ss}, may be taken as a good predictor of the K_d (Cs)). Therefore, it was decided in this work to test the prediction capacity of this simplified approach taking into consideration how diverse are the data included in the present Cs dataset, as the prediction tests carried out in the past made use of smaller, more homogeneous datasets (Gil-Garcia et al, 2011). The dataset, once properly refined, *i.e.*, it can contain various K_d (Cs) values gathered from the same soil sample as long as they were quantified by changing K_{ss} since this leads to different RIP/K_{ss} values (the soil factor analysed), had a number of K_d values (N = 328) much larger than that used in the TRS-472 (N = 257). It is important to point out that the dataset only contained K_d data obtained by applying sorption and desorption tests to recently-added Cs radioisotopes (representative only of the short-term Cs-soil interaction) and, thus, the RIP/K_{ss} was directly applied without being necessary to

distinguish between the experimental approach followed to determine the K_d (Cs) data.

Table 4.7 summarises the main outcomes from the correlation analyses between log K_d(Cs) and log (RIP/K_{ss}). The correlations tested were based on considering the global refined Cs dataset, as well as partial datasets split according to ranges of the K_d (Cs) values.

Table 4.7 Analyses of the log K_d(Cs) *vs.* log RIP/K_{ss} correlations.

Groups of experimental K_d (L kg^{-1})	N	Interception (standard error)	Slope (standard error)	Regression coefficient, r
< 10^2	68	1.42 (0.09)	0.13 (0.04)	0.36
10^2 – 10^3	105	2.0 (0.1)	0.19 (0.04)	0.42
10^3 – 10^4	117	3.0 (0.1)	0.12 (0.04)	0.29
< 10^4	38	3.1 (0.5)	0.3 (0.1)	0.43
Global	328	0.76 (0.09)	0.73 (0.03)	0.80

Correlations were statistically significant for all cases tested, although correlations for partial datasets had a poorer quality than that for the global refined dataset, which succeeded in explaining more than 60% of the total variance, which is an excellent result considering the degree of the variability of the dataset. However, it is obvious the fact that the prediction equations explained only a small proportion of the variance when dealing with partial K_d (Cs) datasets (which could be anticipated, as for instance the RES contribution is not considered, although it can be significant for K_d (Cs) < 10^2), that they had a significant bias, and that their slope significantly differed from one, indicating the limitations of the prediction exercise. A closer look of the correlations also evidenced that a large variability was associated with the predicted values, as for a given RIP/K_{ss} value the range of experimental K_d varied within more than two orders of magnitude. In this context, the construction of the CDFs may shed some light about the variability associated with the use of the RIP/K_{ss} ratio, as well as to quantify the uncertainty associated with the K_d best estimates (that is, with the calculated RIP/K_{ss} ratios) for every defined range of K_d (Cs) values.

Figure 4.12 depicts the graphical representation of the CDFs constructed from each partial dataset created by applying the RIP/K_{ss} criterion and **Table 4.8** summarises the main quantitative outcomes from the CDF construction. As could be expected, the K_d (Cs) GMs and related 5^{th}-95^{th} percentile ranges increased when increasing each RIP/K_{ss} group.

Table 4.8 K_d (Cs) (L kg^{-1}) data grouped according to RIP/K_{ss} criterion.

Partial dataset	N	Min	Max	GM	5^{th}	95^{th}
RIP/K_{ss} < 10^2	106	9.6	1.7×10^3	1.0×10^2	1.3×10^1	8.1×10^2
10^2 ≤ RIP/K_{ss} < 10^3	72	2.9×10^1	2.9×10^3	3.8×10^2	2.3×10^1	6.3×10^3
10^3 ≤ RIP/K_{ss} < 10^4	79	5.9×10^1	9.2×10^3	1.5×10^3	3.0×10^2	7.1×10^3
RIP/K_{ss} ≥ 10^4	71	7.3×10^2	3.8×10^5	1.0×10^4	1.5×10^3	7.2×10^4

Whereas the examination of the K_d (Cs) GM is of a lesser importance in this case (as an end-user with available RIP and K_{ss} data does not need to use the K_d(Cs) best estimates, because the RIP/K_{ss} ratio can be straightforwardly calculated instead), the 5^{th}-95^{th} percentiles permit to quantify and describe the K_d (Cs) variability within each dataset, in a much better way than with the previous correlations. Thus, the variability in the partial datasets of the soil-type groups created on the basis of the RIP/K_{ss} criterion was of one-to-two orders of magnitude, lower than that of the short-term partial datasets previously created based on the texture/OM criterion. The goodness of using the RIP/K_{ss} ratio was again confirmed as the constructed CDFs curves did not overlap among them (see **Figure 4.12**). Therefore, the calculation of the RIP/K_{ss} ratios permits a rapid estimation of the K_d (Cs), with an associated uncertainty calculated from the corresponding CDF. It should also be reminded that as these CDFs were constructed from datasets containing only short-term data, and the influence of the sorption dynamics effects on the K_d (Cs) values was clearly evidenced from previous analyses, it is recommended to use them in radiological assessments only aiming at foreseeing the short-term interaction of Cs in soils.

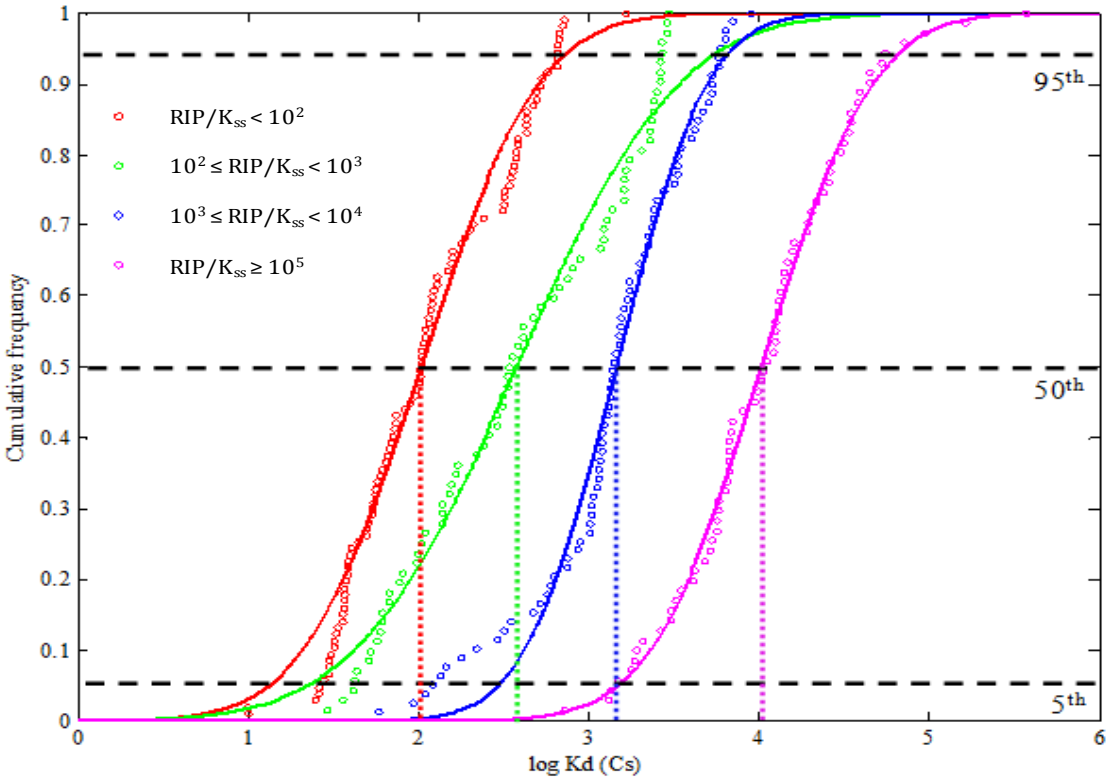

Figure 4.12 *CDFs of K_d (Cs) for soils grouped according to RIP/K_{ss} criterion. Vertical dashed-lines indicate log K_d best estimate values.*

A major limitation of this approach lies on the fact that in order to ascertain the CDF of that soil-type group representative of the soil under assessment, it is necessary to have the soil RIP value, a parameter that albeit being more and more frequently determined it is not characterised on routine. Therefore, end-users may find useful an equation enabling the prediction of soil RIP values from soil properties often available or, at least, much easier to determine than the RIP parameter. Previous studies demonstrated that RIP values can be roughly predicted from soil clay and silt contents (Waegeneers et al. 1999; Gil-García et al., 2011). Here, we provide a multiple linear regression (Eq. 4.5) created from the current compilation (N = 75) that captured 60% of total RIP variability and reliably correlates RIP values of soils with OM < 20% with their clay and silt contents (referred to total soil weight):

$$\log RIP = 1.4\ (\pm 0.2) + 0.9\ (\pm 0.1) \log Clay + 0.5\ (\pm 0.2) \log Silt;\ [r = 0.8] \qquad [4.5]$$

It is worth noting that when the RIP dataset was enlarged with RIP and texture data from soils available in the literature (that had not been included in the compilation

because lack of K_d data), the correlation worsened and only 47% of the total RIP variance was captured. Since most of these extra RIP data came from Andosols, as those present in references Vandebroek et al., 2012; Nakao et al., 2015; Uematsu et al., 2015, the lower capability to predict RIP values from the total clay and silt contents in the extended correlation could be explained by the fact that the clay fraction of Andosols contains much less 2:1 phyllosilicates than other soils with similar clay content (Matus et al., 2014). Thus, Eq. 4.5 is not recommended to predict RIP values neither for Andosols nor for soils with OM > 20%. The development of an equation to predict RIP values not only from clay content but better from clay mineralogy remains a future challenge.

4.3.2.5 Exploring K_d (Cs) data analogy among environmental solid materials

The number of K_d (Cs) data in soils available in the literature was high enough to successfully apply different grouping criteria, which decreased the initial variability of the overall K_d (Cs) data from 4-5 orders of magnitude to 1-2 orders of magnitude. Therefore, the use of data from other environmental solid materials is, in principle, not required for Cs. However, it may be of high interest in radioecology to gain knowledge of the Cs interaction in other environmental samples such as gyttja, tills or subsoils, relevant in specific studies, like the performance assessment and the long-term impact assessment of radioactive waste repositories (SKB, 2011; POSIVA, 2014). Consequently, it would be worth to explore whether the K_d (Cs) data may be suitable to assess the interaction of Cs in the above mentioned environmental samples.

The K_d (Cs) values for surface sediment, subsoil, gyttja and till samples collected in the compilation were split into "short-term" and "long-term" data and, when possible, they were grouped according to the Texture/OM criterion redefined for the case of Cs (section 4.3.2.3). **Table 4.9** summarises the K_d (Cs) data derived for the different groups created from the dataset containing K_d (Cs) values determined in environmental materials other than soils. The partial datasets were then compared with the respective ones previously created for soil K_d (Cs) data. With the exception of the K_d (Cs) data for surface sediments and those of long-term incorporated Cs for tills, the statistical tests revealed that no significant differences ($p > 0.05$) existed

between the K_d data for soils and for the rest of samples, although conclusions drawn should be taken with care due to the reduced number or lack of observations in some of the textural groups.

Table 4.9 Summary of K_d (Cs) data available for other solid environmental materials than soils.

Material	Type of K_d (Cs) data	N	GM	5th	95th
Surface sediment	Short-term*	22	1.9×10^{1}	6	6.5×10^{1}
	Short-term - Sand	8	7.4×10^{1}	n.a.	n.a.
Subsoil	Short-term*	12	2.3×10^{2}	1	1.2×10^{5}
	Short-term - Sand	7	2.7×10^{3}	n.a.	n.a.
Gyttja	Long-term*	16	2.1×10^{4}	3.1×10^{3}	1.4×10^{5}
	Long-term - Mineral*	15	2.4×10^{4}	4.8×10^{3}	1.2×10^{5}
	Long-term - Clay+Loam	6	3.4×10^{4}	n.a.	n.a.
	Long-term - Sand	1	6.5×10^{5}	n.a.	n.a.
	Long-term - Organic	1	3.4×10^{3}	n.a.	n.a.
Till	Short-term*	28	2.0×10^{3}	3.1×10^{2}	1.3×10^{4}
	Short-term - Mineral*	23	2.3×10^{3}	3.8×10^{2}	1.4×10^{4}
	Short-term - Clay+Loam	2	1.2×10^{4}	n.a.	n.a.
	Short-term - Sand*	18	2.0×10^{3}	4.3×10^{2}	9.4×10^{3}
	Long-term*	17	5.3×10^{4}	2.4×10^{2}	1.2×10^{6}
	Long-term - Clay+Loam*	9	2.0×10^{5}	1.6×10^{4}	2.5×10^{6}
	Long-term - Sand*	8	1.6×10^{4}	3.7×10^{3}	6.9×10^{4}

*K_d (Cs) partial datasets of materials that could be statistically compared with the respective soil ones.

This exploratory analysis suggests that the short-term Cs interaction in subsoils and tills as well as the long-term Cs interaction in gyttjas can be estimated with the short-term and long-term K_d (Cs) data attained for soil-types according to key properties (Texture and OM) in previous sections.

4.3.2.6 Key messages from the analyses of the K_d (Cs) dataset and summary of CDFs K_d (Cs) for radiological assessments

From the analyses performed to the K_d (Cs) dataset, it was found that sorption dynamics effects had a strong impact on the K_d (Cs) values. This fact should be taken into consideration when dealing with risk assessment exercises in which K_d (Cs) data are required. Besides, it was also evidenced that soil properties either directly related to the mechanisms governing Cs sorption in soils, like soil RIP and potassium concentration in soil solution, or indirectly related, such as the soil organic matter and to a lesser extent the soil texture, dramatically affected the K_d (Cs) values.

Consequently, a single K_d (Cs) best estimate and/or CDF has little practical value for modelling because it is fraught with variability and it lacks of representativeness to the vast majority of soil-types and contamination scenarios. Alternatively, it is highly recommended to end-users to select the CDF, as summarised in **Table 4.10**, that suits better with the scenario of interest and the type of soil under assessment.

First of all, it is crucial to identify if the assessment is made for a recent contamination episode (short-term scenario) or, on the contrary, for a post-contamination episode that occurred enough time ago to consider that Cs sorption is affected by dynamics effects (long-term scenario). Secondly, if soil organic matter content of the target soil is known, it is suggested to use the CDF that also suits the soil type (Organic or Mineral), whereas if soil texture data is also available it is suggested to refine the CDF election also according to the textural group, if necessary.

Finally, only if the radiological assessment exercise is done for a short-term scenario and the RIP and K_{ss} data are available for the studied soil, it is recommended to use a K_d (Cs) value based on the direct calculation of the RIP/K_{ss} ratio, associated with the uncertainty derived from the constructed CDF for the corresponding RIP/K_{ss} group. For those soils with OM ≥ 20% lacking of the RIP value, with the exception of Andosols RIP can be predicted directly from the clay and silt contents of the soil with Eq. 4.5.

Table 4.10 K_d (Cs) CDFs for specific scenarios and soil-types according to ancillary data available.

Which information is available?	K_d (Cs) group according to sorption dynamics effects and soil-types		Proposed CDF	GM (L kg^{-1})	5th (L kg^{-1})	95th (L kg^{-1})
None	All		logN (μ: 3.3; σ: 0.6)	2.6×10^{3}	7.6×10^{1}	9.2×10^{4}
Elapsed time since contamination	Short-term		logN (μ: 3.2; σ: 0.7)	1.5×10^{3}	8.8×10^{1}	2.6×10^{4}
	Long-term		logN (μ: 4.4; σ: 0.5)	2.5×10^{4}	4.2×10^{3}	1.4×10^{5}
Elapsed time since contamination; OM%	Short-term	Organic (OM ≥ 50%)	logN (μ: 1.9; σ: 0.4)	7.1×10^{1}	1.3×10^{1}	3.8×10^{2}
		Mineral (OM < 50%)	logN (μ: 3.4; σ: 0.6)	2.6×10^{3}	2.9×10^{2}	2.3×10^{4}
	Long-term	Organic (OM ≥ 90%)*	logN (μ: 2.4; σ: 0.4)	2.6×10^{3}	4.5×10^{1}	1.2×10^{3}
		Mineral (OM < 90%)	logN (μ: 4.4; σ: 0.4)	2.7×10^{4}	5.2×10^{3}	1.4×10^{5}
Elapsed time since contamination; OM%; soil texture	Short-term	Clay+Loam[a]	logN (μ: 3.6; σ: 0.5)	3.7×10^{3}	5.7×10^{2}	2.2×10^{4}
		Sand[b]	logN (μ: 3.1; σ: 0.7)	1.2×10^{3}	8.6×10^{1}	1.7×10^{4}
	Long-term	Clay+Loam[c]	logN (μ: 4.5; σ: 0.4)	3.2×10^{4}	7.6×10^{3}	1.4×10^{5}
		Sand[d]	logN (μ: 4.3; σ: 0.4)	1.8×10^{4}	4.0×10^{3}	8.2×10^{4}
Radiocaesium Interception Potential (RIP)**; potassium in soil solution (K_{ss})	Short-term	$RIP/K_{ss} < 10^{2}$	logN (μ: 2.0; σ: 0.5)	1.0×10^{2}	1.3×10^{1}	8.1×10^{2}
		$10^{2} \le RIP/K_{ss} < 10^{3}$	logN (μ: 2.6; σ: 0.7)	3.8×10^{2}	2.3×10^{1}	6.3×10^{3}
		$10^{3} \le RIP/K_{ss} < 10^{4}$	logN (μ: 3.2; σ: 0.4)	1.5×10^{3}	3.0×10^{2}	7.1×10^{3}
		$RIP/K_{ss} \ge 10^{4}$	logN (μ: 4.0; σ: 0.4)	1.0×10^{4}	1.5×10^{3}	7.2×10^{4}

* K_d (Cs) data derived from a CDF constructed with dataset containing scarce data (N < 10).
** For soils with OM < 20%; RIP can be estimated as: log RIP = 1.4 (±0.2) + 0.9 (±0.1) log $Clay_{wt}$ + 0.5 (±0.2) log $Silt_{wt}$.
[a] Short-term – Clay+Loam: OM content < 50%; mineral fraction with < 65% of sand content or with > 65% sand and > 18% clay contents.
[b] Short-term - Sand: OM content < 50%; mineral fraction with < 18% of clay and > 65% of sand contents.
[c] Long-term - Clay+Loam: OM content < 90%; mineral fraction with < 65% of sand contents or with > 65% sand and > 18% clay contents.
[d] Long-term - Sand: OM content < 90%; mineral fraction with < 18% of clay and > 65% of sand contents.

4.3.3 The case of uranium

The overall K_d (U) dataset contained 197 entries (19 more than in the former compilation) with K_d (U) values varying more than 4 orders of magnitude. The derived GM value was 310 L kg^{-1}, in agreement with previous reported values (Sheppard et al. 2006; Vandenhove et al., 2009). However, the GM or CDF that could be derived from the dataset are pointless data since they are fraught with uncertainty (the 5^{th}-95^{th} percentile range was 8×10^{0} -1.2×10^{4} L kg^{-1}) and they may be not suitable to assess the risk in all types of scenarios. In further sections the decrease and explanation of K_d (U) variability in soils is analysed in deep in order to provide end-users with the possibility to ascertain more suitable K_d (U) input data for radiological assessments.

4.3.3.1 Influence of experimental approach on K_d (U) data

The overall U dataset contained entries of short-term sorption (ST-S), short-term desorption (ST-D) and long-term desorption (LT-D) K_d values. Thus, the possible effect of the experimental approach followed for the K_d values quantification (sorption and desorption tests) and/or the sorption dynamics on the K_d (U) data was examined (short- and long-term). For the case of U the Group Mean Centring data treatment was done by taking into account different soil factors, solely or combined (*i.e.*, Texture/OM, pH and pH + OM), relevant to the U sorption.

The statistical analyses performed are summarised in **Table 4.11**. No statistical differences were observed between sorption and desorption data when pH as well as pH and OM soil factors were under control. Conversely, erratic results were obtained regarding the statistical differences among the ST and LT partial datasets depending on the soil factors taken into consideration for the GMC analysis. These results indicated that the effect of the different experimental approaches followed for K_d (U) data quantification on the K_d (U) values of the dataset was negligible compared to that stemmed from the contrasting properties of the soil samples. Therefore, unlike the case of Cs, for further analyses K_d (U) data are not distinguished with regards to any experimental approach factor.

Table 4.11 Experimental approach influence on K_d (U) data.

Grouping criteria for GMC	K_d (U)-types	Comparison	Probability (p)*
Texture/OM	Short-term sorption (ST-S) Long-term (LT-S)	ST *vs.* LT	< 0.05
pH	Short-term sorption (ST-S) Short-term desorption (ST-D) Long-term (LT)	ST-S *vs.* ST-D ST *vs.* LT	0.53 < 0.05
pH + OM	Short-term sorption (ST-S) Short-term desorption (ST-D) Long-term desorption (LT)	ST-S *vs.* ST-D ST *vs.* LT	0.99 0.06

*Probability of considering that K_d datasets do not differ among them.

4.3.3.2 K_d (U) best estimates and CDFs on the basis of the Texture/OM criterion

The current U dataset when refined for applying the Texture/OM criterion contained 161 entries (8 more than in the previous TRS-472) varying in the same range of K_d (U) values than the overall dataset. The data obtained when applying the Texture/OM criterion are presented in **Table 4.12** and, in **Figure 4.13**, the graphical representation of the CDFs that could be constructed from the partial datasets created and from the overall dataset (Overall) is shown.

Whereas the K_d (U) data in the Mineral and Organic partial datasets were significantly different ($p < 0.05$), no differences ($p > 0.05$) were observed in K_d (U) data among textural (Clay, Loam and Sand) groups. Thus, the first criterion to group soils on the basis of soil properties for the case of U should be considered as an OM criterion rather than Texture/OM criterion, since only information of the organic matter content is necessary. Such results denote that soil texture is not a soil factor relevant enough to control the U-soil interaction and, thus, it cannot be used to distinguish between textural soil-types, at least, as previously reported. Besides, the GM of the Organic group was around one order higher than that of Mineral group, which confirmed the role observed in previous studies regarding the enhancement of the uranium sorption due to its interaction with the soil organic matter (Crançon and Van der Lee, 2003).

Table 4.12 K_d (U) (L kg^{-1}) data grouped on the basis of the OM criterion.

Partial dataset	N	Min	Max	GM	5th	95th
Mineral (OM < 20%)	132	1	6.7×10^{4}	2.2×10^{2}	1.0×10^{1}	5.3×10^{3}
Organic (OM ≥ 20%)	18	3.3×10^{1}	1.9×10^{4}	1.4×10^{3}	4.5×10^{1}	4.4×10^{4}

The application of the OM criterion allowed proposing CDFs for the Mineral and Organic groups, which comprised K_d values varying within a narrower range than in the case of the CDF constructed from the overall dataset. Despite this improvement, the usefulness of these CDFs for performing radiological assessments may still be limited since they are constructed from datasets with large variability, especially that for the Organic group.

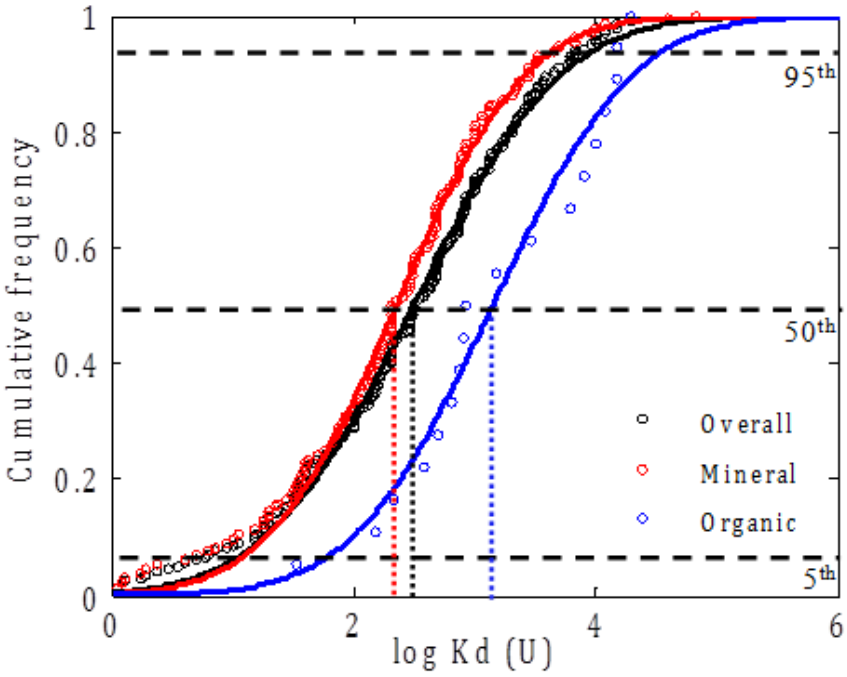

Figure 4.13 *CDFs of K_d (U) for Mineral and Organic soil-types. Vertical dashed-lines indicate log K_d (U) best estimate values.*

The soil organic matter provides sorption sites of higher affinity for U than the minerals present in soils, which entails a higher U sorption capacity of those soils rich in OM. Since it was corroborated that soil OM content has a strong influence on the U sorption behaviour, alike the case of Cs, an exercise to optimise the threshold of OM content to consider a given soil as "organic" was done. The aim of such exercise was to explore the possibility of obtaining partial datasets with less variability, allowing a

better distinction of those soils in which the OM fraction really controls the U-soil interaction and, in turn, to succeed in distinguishing K_d (U) data of mineral soils among textural groups. Therefore, for U it was explored the possibility to decrease the classical OM threshold, from 20% up to 5%, by performing a similar analysis to that previously performed for Cs (section 4.3.2.3), *i.e.*, partial datasets were created according to different OM% thresholds and the K_d (U) best estimate values (GMs) along with related variability (5^{th}-95^{th} percentile ranges) were compared. **Figure 4.15** displays the results obtained.

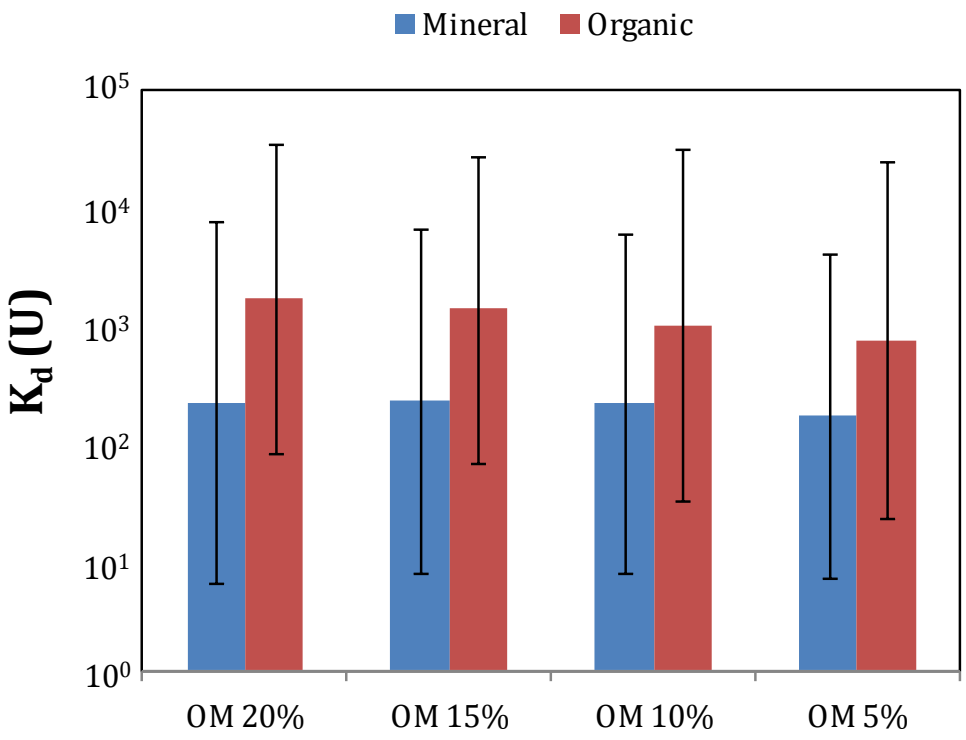

Figure 4.15 *Optimisation of the OM% threshold to define organic and mineral soils for K_d (U). Bars correspond to GM values and error bars to the 5^{th}-95^{th} confidence ranges.*

Unlike the case of Cs, no improvement neither in terms of decreasing the K_d (U) variability nor deriving more contrasting GMs from the partial datasets of the Mineral and Organic groups was obtained by varying the OM threshold. Therefore, concerning the interaction of U in soils, the classical 20% threshold of OM is maintained to consider whether a soil is organic or mineral.

4.3.3.3 K_d (U) best estimates and CDFs on the basis of soil factors related to U sorption mechanisms

The pH criterion

As a first attempt, K_d (U) values were grouped according to the pH at which the U sorption took place into three pH categories (pH < 5, 5 ≤ pH < 7 and 7 ≤ pH) created on the basis of the U speciation, as explained before. **Table 4.13**, presents the K_d (U) data derived, and **Figure 4.14** illustrates the graphical representation of the CDFs, created by applying the pH criterion.

Table 4.13 K_d (U) (L kg^{-1}) data grouped on the basis of the pH criterion.

Partial dataset	N	Min	Max	GM	5th	95th
pH < 5	53	1	1.2×10^{4}	2.0×10^{2}	1.1×10^{1}	3.3×10^{3}
5≤ pH <7	69	6	6.7×10^{4}	1.1×10^{3}	6.4×10^{1}	2.0×10^{4}
pH ≥ 7	75	1	6.1×10^{3}	1.1×10^{2}	2	5.1×10^{3}

The application of the pH criterion led to the creation of partial datasets for pH groups that were significantly different ($p < 0.05$) among them and contained K_d (U) values varying less than in the overall dataset, as the 5th-95th interval of K_d (U) values was decreased down to two-three orders of magnitude. The derived K_d (U) best estimates and related confidence ranges indicated a significant increase in K_d (U) values when increasing pH, reaching a maximum within the 5-7 pH range, and at higher pH, K_d (U) values decreased. This pH-dependent U sorption is in agreement with that previously reported (Dalvi et al., 2014; Payne et al., 2011; Vandenhove et al, 2009). At low pH values (pH < 5) the U sorption in soils is decreased due to the competition of the uranyl cation with protonated sites whereas at pH > 7 the decrease in U sorption is caused by the formation of stable, weakly sorbing uranyl carbonate complexes.

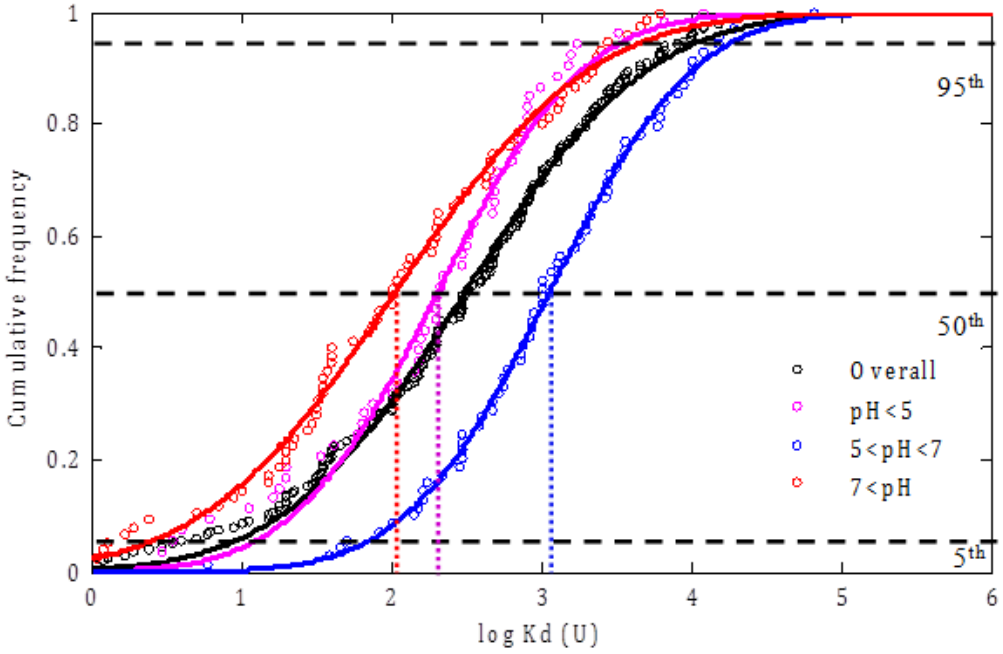

Figure 4.14 *CDFs of K_d (U) for pH groups. Vertical dashed-lines indicate log K_d (U) best estimate values.*

Whereas the K_d (U) CDF of the pH**< 5** partial dataset was clearly shifted to higher values, the 5th-95th percentile CDF region of the 5 ≤ pH < 7 and pH ≥ 7 partial datasets partially overlapped (see **Figure 4.14**, above). This fact, in conjunction with the large K_d (U) variability still existing within the pH groups from which the CDF were constructed, suggested that it was still necessary to seek a better K_d (U) grouping by means of taking into consideration several soil factors altogether. the simultaneous consideration of the two factors (OM and pH) could lead to a better prediction of the K_d (U) since it may properly differentiate pH-OM soil-types.

Hierarchical application of pH and OM criteria: the pH + OM criterion

Table 4.14 summarises the K_d (U) data obtained from the datasets created on the basis of hierarchical application of the pH and OM soil factors (hereinafter pH + OM criterion), whereas **Figure 4.15** depicts the related CDFs.

Table 4.14 K_d (U) (L kg^{-1}) data grouped on the basis of the pH + OM criterion.

Partial dataset		N	Min	Max	GM	5th	95th
pH < 5	Mineral	31	4	6.7×10^{3}	1.4×10^{2}	9	2.1×10^{3}
	Organic*	9	1.5×10^{2}	1.2×10^{4}	5.8×10^{2}	1.2×10^{2}	2.6×10^{3}
5 ≤ pH < 7	Mineral	51	3.8×10^{1}	6.7×10^{4}	8.0×10^{2}	4.1×10^{1}	9.9×10^{3}
	Organic*	9	3.8×10^{2}	1.9×10^{4}	6.2×10^{3}	1.6×10^{3}	2.2×10^{4}
pH ≥ 7	Mineral	64	1	2.2×10^{3}	7.9×10^{1}	3	2.4×10^{3}
	Organic**	2	3.3×10^{1}	6.2×10^{3}	4.5×10^{2}	n.a.	n.a.

*K_d (U) data derived from a CDF constructed with a dataset containing scarce data (N < 10).
**No CDF was constructed due to lack of data (N << 10).

The simultaneous use of pH and OM factors led to the creation of significantly different ($p < 0.05$) partial datasets. The main trends observed when applying solely the OM and the pH criterion were confirmed, *i.e.* for a given pH group, organic soils always had higher GMs and 5th-95th percentile ranges than the respective mineral group, whereas K_d (U) values for the slightly acid - pH group (5 ≤ pH < 7) were always the highest. The variability of K_d data in the pH + OM partial datasets was slightly decreased in comparison to the pH partial datasets.

Besides this, neither the 5th-95th percentile regions of the CDFs constructed from the three pH-Mineral partial datasets nor those from the two pH-Organic partial datasets overlapped (see **Figure 4.15**). Such fact denotes the suitability of using two soil factors for K_d (U) grouping, which are relevant for the U-soil interaction as affects the U speciation in solution and, the potential availability of sorption sites with labile protons, whereas the soil OM content relates to the total amount of sorption sites with high-affinity for U coming from the organic matter phases present in soils.

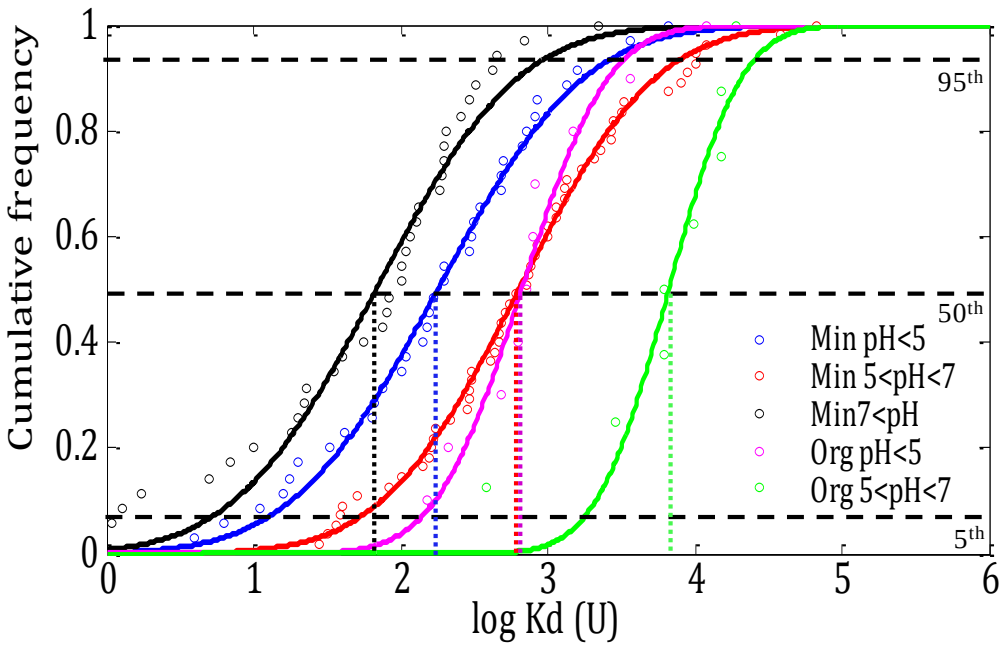

Figure 4.15 *CDFs of K_d (U) for soil-types according to the pH + OM criterion. Vertical dashed-lines indicate the log K_d (U) best estimate values.*

It is worth noting that, albeit the K_d (U) overall dataset contained a large number of entries, only two K_d (U) values at pH ≥ 7 were available. This lack of data thwarted the construction of the CDF for the basic pH - Organic group and, consequently, it jeopardises the reliably assessment of the U sorption in soils rich in organic matter at alkali conditions. The scarcity of such data is not surprising at any stage since K_d values are usually determined (at laboratory or at field) under such conditions representative of environmental scenarios rather than mimicking extreme conditions. Since most of the organic soils has acid-to-neutral pH values, and pH of natural water sources commonly are neutral-to-slightly basic, K_d (RN) data are hardly ever gathered from OM-rich soils under conditions leading to pH ≥ 7.

Hierarchical application of pH and the combined Texture/OM criteria: the pH + Texture/OM criterion

A final step was done to refine the K_d (U) data of the pH-Mineral groups previously created by splitting them into different textural groups according to the clay and sand content of the soils. Then, the pH and the Texture/OM criteria were evaluated simultaneously. However, as can be seen in **Table 4.15**, the majority of the pH-Textural groups had scarce data (N < 10), which hindered the proper evaluation of the data derived.

Table 4.15 K_d (U) (L kg^{-1}) data grouped on the basis of the pH + Texture/OM criterion for mineral soils.

Partial dataset		N	Min	Max	GM	5th	95th
pH < 5	Clay*	1	n.a.	n.a.	4.8×10^{2}	n.a.	n.a.
	Loam**	6	16×10^{1}	1.6×10^{3}	2.8×10^{2}	5	1.8×10^{3}
	Sand**	8	4	6.7×10^{3}	4.3×10^{1}	1	4.9×10^{3}
5 ≤ pH < 7	Clay*	n.a.	n.a.	n.a.	n.a.	n.a.	n.a.
	Loam	33	1.0×10^{2}	3.9×10^{4}	1.2×10^{3}	9.6×10^{1}	1.4×10^{4}
	Sand	13	8.3×10^{1}	6.7×10^{4}	5.6×10^{2}	9.1×10^{1}	3.4×10^{3}
pH ≥ 7	Clay**	7	5	4.7×10^{2}	3.5×10^{1}	1	1.8×10^{3}
	Loam	33	1	5.0×10^{3}	5.8×10^{1}	2	1.4×10^{3}
	Sand	11	7	1.3×10^{3}	3.6×10^{1}	4	3.6×10^{2}

*No CDF was constructed due to lack of data (N << 10).
**K_d (U) data derived from a CDF constructed with a dataset containing scarce data (N < 10).

So as to overcome this issue, the possibility of using K_d (U) data from solid environmental materials other than soils to enhance the datasets was explored, which is explained in the following section.

4.3.3.4 Exploring K_d (U) data analogy among environmental solid materials

With the aim at filling the gaps of K_d (U) data in soils observed in the previous section, an evaluation of the analogy between soils and other solid environmental materials (till, subsoil and gyttja) with respect to their capacity to sorb U was performed. For each material, all K_d (U) data available were pooled in an overall dataset per material and partial datasets were created according to the pH + OM criterion, as previously done for the case of soil K_d (U) data. It must be said that all K_d data corresponded to materials with OM < 20% and, thus, partial datasets only for pH-types of mineral soils (*i.e.*, pH-Mineral groups) could be created. The K_d (U) data derived from each dataset are summarised in **Table 4.16**, which includes data obtained from the respective soil datasets for the sake of comparison.

Table 4.16 Comparison of K_d (U) (L kg^{-1}) data derived from environmental materials other than soils.

Dataset	Material	N	Min	Max	GM	5th	95th
Overall	Soil	197	1	6.7×10^{4}	3.1×10^{2}	8	1.2×10^{4}
	Till	22	1	5.1×10^{3}	2.2×10^{2}	9	5.6×10^{3}
	Subsoil	49	1	1.0×10^{4}	1.2×10^{2}	1	1.4×10^{4}
	Gyttja	15	5.6×10^{2}	4.4×10^{4}	2.0×10^{3}	1.9×10^{2}	2.0×10^{4}
pH < 5 - Mineral	Soil	53	1	1.2×10^{4}	2.0×10^{2}	1.1×10^{1}	3.3×10^{3}
	Till*	9	3	3.6×10^{3}	2.9×10^{2}	4.0×10^{1}	2.1×10^{3}
	Subsoil*	9	2.6×10^{1}	6.2×10^{3}	9.4×10^{1}	1.2×10^{1}	7.4×10^{2}
	Gyttja	11	8.0×10^{2}	4.4×10^{4}	3.1×10^{3}	3.2×10^{2}	3.0×10^{4}
5 ≤ pH < 7 - Mineral	Soil	69	6	6.7×10^{4}	1.1×10^{3}	6.4×10^{1}	2.0×10^{4}
	Till*	6	3	5.1×10^{3}	7.3×10^{2}	3.8×10^{2}	1.4×10^{3}
	Subsoil	16	1	1.0×10^{4}	4.2×10^{2}	1	1.8×10^{4}
	Gyttja	1	n.a.	n.a.	n.a.	n.a.	n.a.
pH ≥ 7- Mineral	Soil	75	1	6.1×10^{3}	1.1×10^{2}	2	5.1×10^{3}
	Till*	7	1	3.7×10^{2}	1.8×10^{1}	0	2.1×10^{3}
	Subsoil	24	1	3.0×10^{3}	5.2×10^{1}	1	2.5×10^{3}
	Gyttja	n.a.	n.a.	n.a.	n.a.	n.a.	n.a.

*K_d (U) data derived from a CDF constructed with a dataset containing scarce data (N < 10).

Whereas all K_d (U) data for gyttja were significantly higher than for soils ($p < 0.05$), the statistical tests revealed that neither the K_d (U) data in the overall datasets nor those in the pH-Mineral partial datasets for till and subsoil were not significantly different ($p > 0.05$) than the soil K_d (U) data. The analogy between soil K_d (U) data and those gathered from subsoils and tills is also evidenced when comparing their CDFs (see **Figure 4.16** below). The pH-mineral CDFs for till and subsoil generally overlapped with those of soils and the vast majority of K_d data of these materials were comprised within the 5th-95th percentile range of soil K_d (U) CDFs, only with the exception of the till basic - pH group, whose CDF was slightly shifted to lower K_d (U) values.

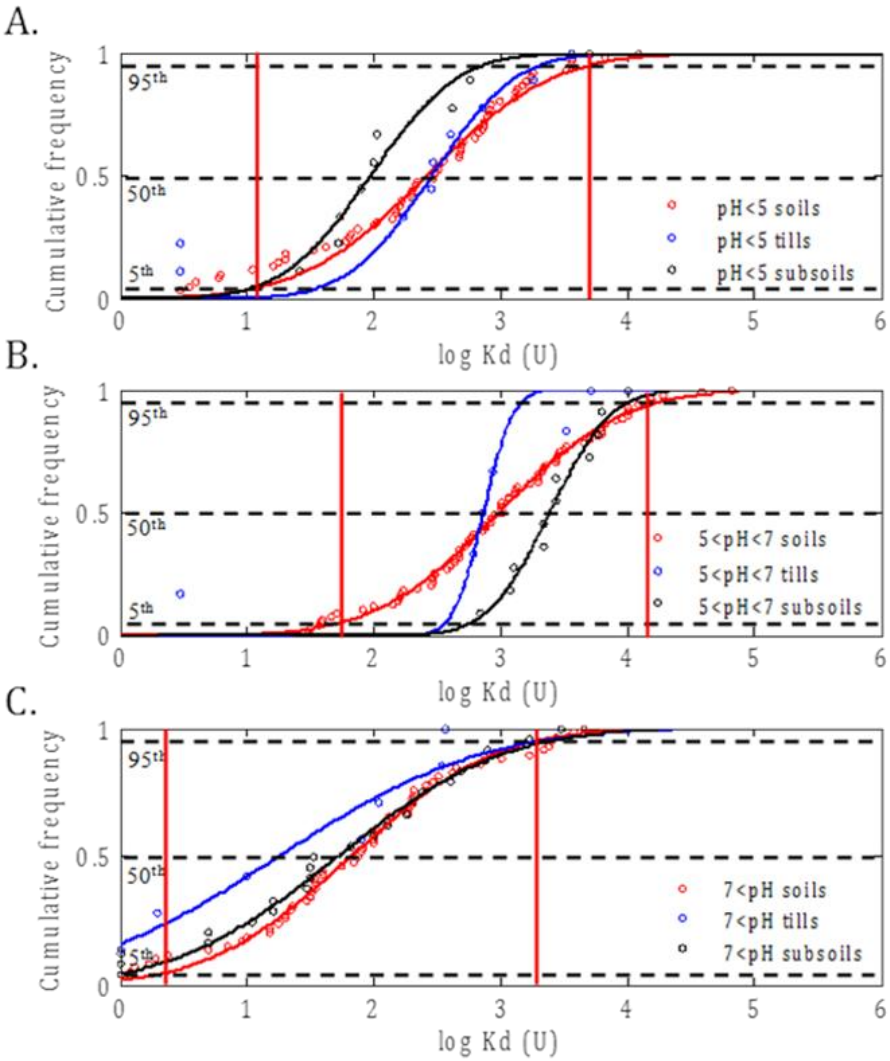

Figure 4.16 *Comparison of K_d (U) CDFs for different materials constructed from partial datasets created according to the pH + OM criterion. A. pH < 5-Mineral groups; B. 5 ≤ pH < 7-Mineral groups; C. pH ≥ 7 -Mineral groups. Vertical solid-lines in red indicate the 5th and 95th percentile of soil log K_d (U) values.*

From this analysis it seems that any K_d (U) value gathered from gyttja samples were unsuitable to fill soil data gaps. Conversely, till and subsoils can be considered analogous to soils in terms of U sorption capacity and behaviour and, thus, all the available data for these materials were used to enhance the soil pH-Textural partial datasets. **Table 4.17** summarises the data derived from the datasets in which soil and analogous materials K_d (U) values were pooled.

Table 4.17 K_d (U) (L kg^{-1}) data on the basis of the pH + Texture/OM criterion by including data gathered from solid materials homologous to soils (subsoils and tills).

Partial dataset		N	Min	Max	GM	5th	95th
pH < 5	Clay*	1	n.a.	n.a.	4.8×10^{2}	n.a.	n.a.
	Loam	10	16×10^{1}	1.6×10^{3}	1.6×10^{2}	1.1×10^{1}	2.1×10^{3}
	Sand	10	4	6.7×10^{3}	5.1×10^{1}	1	3.7×10^{3}
5 ≤ pH < 7	Clay*	n.a.	n.a.	n.a.	n.a.	n.a.	n.a.
	Loam	42	1.0×10^{2}	3.9×10^{4}	1.3×10^{3}	1.3×10^{2}	1.3×10^{4}
	Sand	16	8.3×10^{1}	6.7×10^{4}	7.3×10^{2}	1.1×10^{2}	5.0×10^{3}
7 ≤ pH	Clay**	7	5	4.7×10^{2}	3.5×10^{1}	1	1.8×10^{3}
	Loam	42	1	5.0×10^{3}	8.1×10^{1}	4	1.7×10^{3}
	Sand	13	7	1.3×10^{3}	3.9×10^{1}	3	4.6×10^{2}

*No CDF was constructed due to lack of data (N << 10).
**K_d (U) data derived from a CDF constructed with a dataset containing scarce data (N < 10).

The inclusion of subsoil and till K_d (U) data on the pH-Texture partial datasets allowed constructing CDFs for a few more pH-Textural groups. Although some pH-Textural groups still present lack of data, the GMs and 5th-95th percentile ranges that could be derived are consistent with the U mechanisms. That is, K_d (U) values of sandy soils (with lower SSA, on average) were significantly ($p < 0.05$) lower than those of loamy soils ($GM_{Sand} < GM_{Loam}$) for all the pH groups. Besides this, the K_d variability in the different pH-Loam and pH-Sand groups was generally lower than in the respective pH-Mineral ones (see **Table 4.14**). According to this, the proposal of K_d (U) data for soil-type groups on the basis of pH, OM and Texture is a promising approach useful for radiological assessments, whereas its application remains a challenge since the current compilation, even with soil analogue K_d (U) data, does not enable neither the construction of K_d (U) CDF from any pH-Clay partial dataset, nor

the derivation of a reliable K_d (U) best estimate value to assess the U interaction in clayey soils at pH < 7.

4.3.3.5 Key messages from the analyses of the K_d (U) dataset and summary of CDFs K_d (U) for radiological assessments

The analyses performed to the K_d (U) dataset demonstrated that a single K_d (U) best estimate value or CDF should be avoided as input data to model the radiological risk derived from any type of uranium soil contamination episode. Instead, modellers should make an effort to better gather information of the scenario focusing on some key properties of the soils in which the risk is assessed (see **Table 4.18**).

Unlike the case of Cs, it is not necessary to select K_d (U) data taking into account the elapsed time since contamination as it was demonstrated that K_d (U) values were devoid of any major effect caused by aging processes. On the contrary, it is suggested to select data on the basis of both the pH and the soil organic matter content at which the U sorption takes place in soil, that is, to select the pH-Mineral or pH-Organic CDF that suits better with the scenario under study. However, special care must be taken to foresee the U interaction in organic (OM ≥ 20%) soils at basic pHs since no CDF could be derived due to the lack of specific data (K_d (U) values and/or soil physical-chemical characterisation data). Instead, end-users are suggested to select either the Organic CDF or the basic-pH CDF, according to the soil OM content or expected pH, respectively.

In relation to this latter issue, it was evidenced that despite the efforts made to update the K_d (U) compilation there are still evident K_d (U) gaps in certain soil-type and pH combinations, such is the case of the aforementioned organic soils at basic pHs, or that of soils with clay texture at acid pHs, two scenarios of minor environmental relevance. This lack of data hampered the complete evaluation of the efficiency of a grouping criteria based on simultaneously using pH, soil OM and Texture and, thus, the proposal of "more site-specific" data was not fulfilled.

Table 4.18 K_d (U) CDFs for specific soil-types according to soil ancillary data available.

Which information is available?	Soil-types of K_d (U)		Proposed CDF	GM (L kg^{-1})	5^{th} (L kg^{-1})	95^{th} (L kg^{-1})
None	All		logN (μ: 2.5; σ: 1.0)	3.1×10^{2}	8	1.2×10^{4}
OM%	Organic (OM ≥ 20%)		logN (μ: 2.3; σ: 0.8)	1.4×10^{3}	4.5×10^{1}	4.4×10^{4}
	Mineral (OM < 20%)		logN (μ: 3.1; σ: 0.9)	2.2×10^{2}	1.0×10^{1}	5.3×10^{3}
pH	pH < 5		logN (μ: 2.3; σ: 0.8)	2.0×10^{2}	1.1×10^{1}	3.6×10^{3}
	5 ≤ pH < 7		logN (μ: 3.1; σ: 0.8)	1.1×10^{3}	6.4×10^{1}	2.0×10^{4}
	pH ≥ 7		logN (μ: 2.0; σ: 0.9)	1.1×10^{2}	2	5.1×10^{3}
pH; OM%	pH < 5	Mineral	logN (μ: 2.1; σ: 0.7)	1.4×10^{2}	9	2.1×10^{3}
		Organic*	logN (μ: 2.8; σ: 0.6)	5.8×10^{2}	1.2×10^{2}	2.6×10^{3}
	5 ≤ pH < 7	Mineral	logN (μ: 2.9; σ: 0.7)	8.0×10^{2}	4.1×10^{1}	9.9×10^{3}
		Organic*	logN (μ: 3.8; σ: 0.4)	6.2×10^{3}	1.6×10^{3}	2.8×10^{4}
	pH ≥ 7	Mineral	logN (μ: 1.9; σ: 0.9)	7.9×10^{1}	3	2.4×10^{3}

*K_d (U) data derived from a CDF constructed from a dataset containing scarce data (N < 10).

Finally, it was demonstrated that there were no statistical differences between the K_d (U) data gathered from soils and those geological materials as till and subsoil, which opened the door of using data from these analogue materials to enhance the soil datasets lacking of data, as well as to propose the soil K_d (U) CDFs also to assess the U interaction in these materials. However, despite the incorporation of these analogue-material data was insufficient to allow constructing reliable CDFs for some pH-Textural groups. Therefore, further work should be done to fill these data gaps.

4.3.4 The case of americium

The updated overall Am dataset contained 108 entries of K_d (Am) values, 46 more than in the previous K_d compilation (TRS-472), varying within up to 5 orders of magnitude (the Min-Max range was 3.0×10^{0} – 2.8×10^{5} L kg^{-1}). In addition to this, 29 entries for other materials, such as subsoils and surface sediments, were available. The strong dependency demonstrated in chapter 3 of the Am sorption in soils on different soil characteristics makes the proposal of different sorption data (K_d best estimate values or CDFs) based on soil-types a required approach to properly foresee the interaction of this element in different scenarios and, thus, the derived risk for the environment and human health.

4.3.4.1 Influence of experimental approach on K_d (Am) data

The K_d (Am) data available in the current compilation were originated only from sorption and desorption tests of recently-added Am (ST-S and ST-D, respectively). Consequently, the effect of sorption dynamics on K_d (Am) data could not be checked due to a lack of data gathered from long-term incorporated Am (LT), and thus, any K_d (Am) CDF or best estimate value proposed hereinafter could be strictly representative for the short-term interaction of Am in soils. Conversely, the possible influence of the experimental approach applied to quantify the K_d (Am) data (sorption and desorption tests) on the data variability was evaluated though performing the corresponding GMC data treatments, grouping K_d (Am) on the basis of the Methodology-Test factor (ST-S vs. ST-D) and statistically comparing the created

datasets. **Table 4.19** summarises the analyses performed and the main outcomes obtained.

Table 4.19 Experimental approach influence on K_d (Am) data.

Grouping criteria for GMC	K_d (Am)-types	Comparison	Probability (p)*
Texture/OM	Short-term sorption (ST-S) Short-term desorption (ST-D)	ST-S vs. ST-D	0.23
pH	Short-term sorption (ST-S) Short-term desorption (ST-D)	ST-S vs. ST-D	<0.05
OM/pH	Short-term sorption (ST-S) Short-term desorption (ST-D)	ST-S vs. ST-D	<0.05

*Probability of considering that K_d datasets do not differ among them.

The statistical tests applied revealed that there were significant differences between the sorption and desorption partial datasets when the experimental approach partial datasets were created by means of taking into account pH as well as pH and OM soil factors altogether, but not when considering soil texture and OM. Such, unclear effect of the experimental approach (*i.e.*, dependent on the soil factors controlled when performing the GMC analysis) on the K_d (Am) suggests that the variability on K_d (Am) values due to the method applied (sorption or desorption tests) is negligible compared to that caused by the contrasting properties of the soils. Therefore, for further analyses K_d (Am) data are not distinguished with regards to any experimental approach factor.

4.3.4.2 K_d (Am) best estimates and CDFs on the basis of the Texture/OM criterion

Notwithstanding the remarkably increase of entries due to the updating process, the current dataset, after being refined to perform the analysis of the application of the Texture/OM criterion, contained 58 entries of K_d (Am) data (4 less than in the former TRS-472 dataset). This is the result of removing data of the overall dataset for the same soil (and thus, same soil texture), but at different soil pH, or K_d (Am) data gathered from geological materials other than soils, included in the previous K_d data

compilation because they were misclassified as soil data. **Table 4.20** summarises the K_d (Am) data obtained here by applying the Texture/OM criterion.

An unclear effect of the texture or the organic matter content on K_d (Am) values was observed since no statistical differences existed ($p > 0.05$) neither between the K_d data of the different textural (Clay, Loam and Sand) partial datasets, nor between the Organic and Mineral partial datasets. Therefore, it seems that the Texture/OM criterion does not capture the actual mechanisms governing Am sorption and, as expected, other soil factors more specifically related to the Am-soil interaction must be applied to properly and efficiently group K_d (Am) data.

Table 4.20 K_d (Am) (L kg^{-1}) for soil-types according to the Texture/OM criterion.

Partial dataset	N	Min	Max	GM	5th	95th
Mineral (OM < 20%)	50	6.7×10^1	2.8×10^5	8.6×10^3	4.5×10^2	1.6×10^5
Clay*	4	6.7×10^1	7.2×10^4	7.8×10^3	n.a.	n.a.
Loam	33	4.1×10^2	1.8×10^5	9.8×10^3	6.3×10^2	1.6×10^5
Sand	13	6.7×10^1	2.8×10^5	3.8×10^3	2.9×10^2	5.1×10^4
Organic (OM ≥ 20%)**	8	2.1×10^2	8.1×10^3	3.2×10^3	4.2×10^2	2.4×10^4

*CDF not constructed due to lack of K_d (Am) data (N << 10).
**K_d (Am) data derived from a CDF constructed with a dataset containing scarce data (N < 10).

Besides this, it is important to point out that there were evident K_d (Am) data gaps for some soil types, like those rich in organic matter and, especially, for clayey soils. This scarcity of data may hinder the application of combined grouping criteria unless K_d data homologue to that of Am in soils, such as those gathered from other solid environmental materials and/or K_d data of Am chemical analogues, are considered. These issues are covered in the following sections.

4.3.4.3 K_d (Am) best estimates and CDFs on the basis of soil parameters related to Am sorption mechanisms

The redefined Texture-OM criterion

The Texture/OM criterion was reanalysed aiming at establishing a new OM threshold to define an organic soil. Unlike in the previous cases of Cs and U, for which the optimum OM threshold was ascertained by grouping the K_d data according to different OM% and by analysing the derived data (GM and 5th-95th percentile range) in each case, for Am this exercise was not possible to perform due to the few amount of data available. Instead, a new OM threshold of 8% was established according to the results obtained in chapter 3 that evidenced that soils with high OM contents are expected to have concentration of dissolved organic matter (DOM) high enough to control the Am speciation and, thus, its sorption in the soil matrix (section 3.3.2). The number of soils included in this analysis decreased to 49 as some entries lacked information of OM content, which was indispensable to apply the redefined Texture/OM criterion. **Table 4.21** summarises the K_d data derived from the partial datasets created according to the redefined Texture/OM criterion datasets and in **Figure 4.17** are depicted the CDFs that could be constructed.

Table 4.21 K_d (Am) (L kg^{-1}) for soils grouped according to redefined Texture/OM criterion.

Partial dataset	N	Min	Max	GM	5th	95th
Organic (OM ≥ 8%)	12	1.4×10^3	2.2×10^4	4.5×10^3	1.1×10^3	1.8×10^4
Mineral (OM < 8%)	37	6.7×10^1	2.7×10^5	1.1×10^4	7.6×10^2	2.0×10^5
Clay*	2	7.1×10^4	7.2×10^4	7.2×10^4	n.a.	n.a.
Loam	24	4.1×10^2	1.8×10^5	1.7×10^4	1.9×10^3	1.6×10^5
Sand	11	6.7×10^1	2.7×10^5	3.8×10^3	5.4×10^2	2.0×10^4

*CDF not constructed due to lack of K_d (Am) data (N << 10).

The redefinition of the OM threshold led to a better distinction not only among the K_d (Am) data of the Organic and Mineral soil-type groups, but also between the Textural groups, whose partial datasets contained K_d (Am) values that significantly differed ($p < 0.05$) among them. The GM value derived from Mineral soils was close to

one order of magnitude higher than that from Organic soils. Besides this, a much clearer sequence between K_d (Am) data of textural groups was attained since the GM values decreased at decreasing the clay content of soils, which denotes that the ambiguity previously observed was overcome with this new grouping OM threshold. These findings are in agreement with the Am sorption mechanisms, since as explained in chapter 3, Am is sorbed in a lesser extent in soils with higher OM content (potentially leading to higher DOM), whereas those soils with higher SSA (here indirectly represented in the Clay textural group) present higher Am sorption capacity.

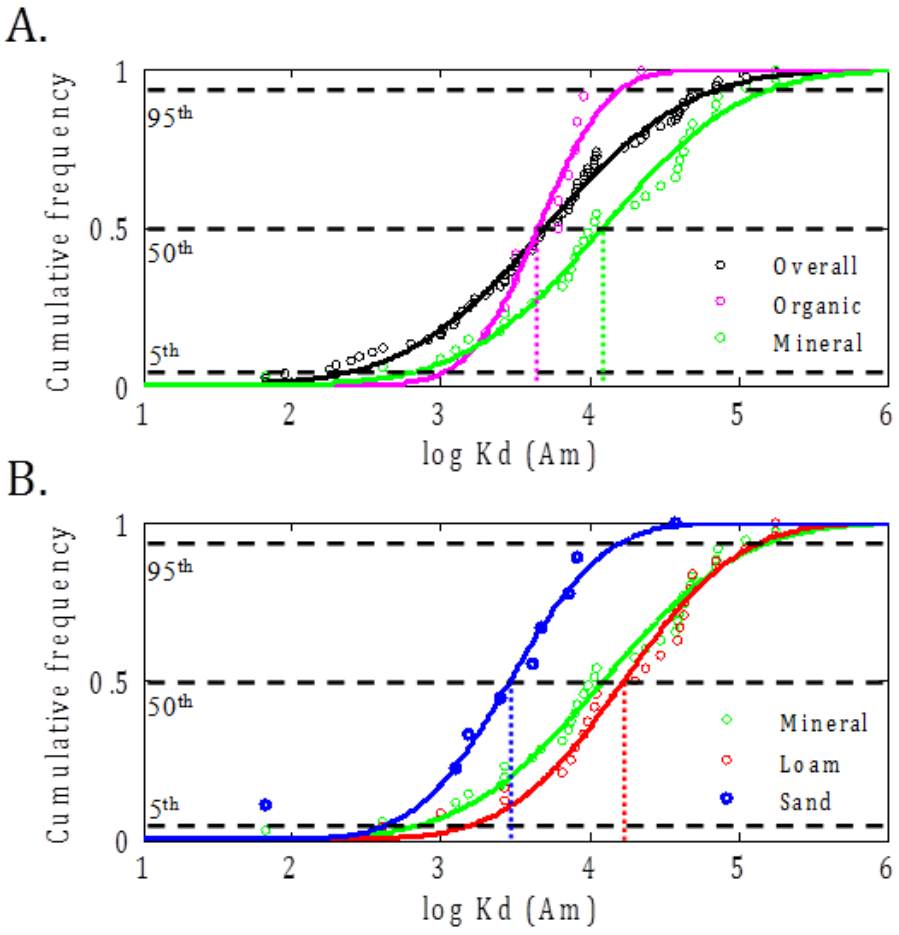

Figure 4.17 *CDFs of K_d (Am) for soil-types according to the redefined Texture/OM criterion. A. Comparison of overall with Mineral and Organic groups. B. Comparison of Mineral with Loam and Sand textural groups. Vertical dashed-lines indicate log K_d (Am) best estimate values.*

In addition, the K_d values comprised within the 5^{th}-95^{th} percentile range for the redefined Organic group only vary within one order of magnitude which evidenced that data variability for this type of soils was lowered with respect to the previous

threshold. Conversely, with the redefined Texture/OM criterion the data variability was still very high for loamy soils, as well as for mineral soils in general, in which K_d data still vary within 3 orders of magnitude in both partial datasets. This fact evidences that for mineral soils the redefined Texture/OM criterion does not capture all the factors relevant to the Am sorption, such as pH. Moreover, it is worth noting that no CDF could be constructed for the Clay group because only two K_d (Am) entries were available for clay soils with OM < 8%.

The pH criterion

As a second approach, the K_d (Am) overall dataset was refined according to pH factor, which contained 86 entries, and it was split on the basis of the pH at which the Am sorption took place in each soil sample (pH criterion) into four categories, each one comprising different pH ranges, as mentioned in previous section 4.2.2.2. **Table 4.22** summarises the K_d (Am) data obtained from the CDFs constructed from the partial datasets created by applying the pH criterion.

Table 4.22 K_d (Am) (L kg^{-1}) for soils grouped according to pH

Partial dataset	N	Min	Max	GM	5th	95th
3 ≤ pH < 6	33	6.7×10^{1}	4.8×10^{4}	2.2×10^{3}	2.3×10^{2}	2.2×10^{4}
6 ≤ pH <7.5	22	6.7×10^{1}	7.1×10^{4}	6.6×10^{3}	1.3×10^{3}	3.2×10^{4}
7.5 ≤ pH < 9	22	9.1×10^{1}	1.8×10^{5}	1.4×10^{4}	7.5×10^{2}	2.6×10^{5}
pH ≥ 9*	9	2.7×10^{1}	2.8×10^{5}	4.4×10^{2}	1.2×10^{1}	1.6×10^{4}

*K_d (Am) data derived from a CDF constructed with a dataset with N < 10.

The four partial datasets created according to the pH criterion presented contrasting GM values showing that K_d (Am) best estimates gradually increased within the 3 – 9 pH range, and decreased at higher pH values, which is consistent with the Am sorption mechanisms. As can be seen in **Figure 4.18,** which plots the resulting CDF for each pH partial dataset, the 5th-95th percentile region of the CDFs constructed on the basis of pH did not overlap among them (only with the exception of the low K_d (Am) region of the CDFs constructed from the 6 ≤ pH <7.5 and 7.5 ≤ pH < 9 partial datasets, which showed a low degree of overlap), thus indicating that the partial

datasets of the four pH groups contained K_d values that clearly differed among them. Besides this, the K_d data variability was significantly lower in the $3 \leq pH < 6$ and $6 \leq pH < 7.5$ partial datasets than in the overall dataset (see the 5^{th}-95^{th} percentile ranges of the constructed CDFs, which comprised K_d values only varying within one and two orders of magnitude, respectively), whereas in the rest of pH-type partial datasets the K_d (Am) variability was still around three orders of magnitude.

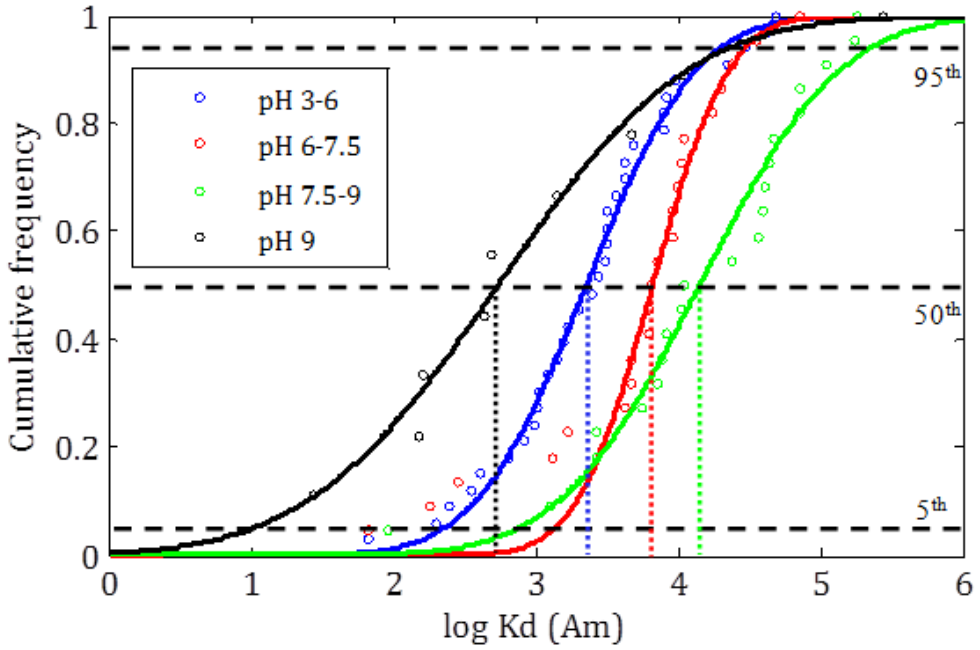

Figure 4.18 *CDFs of K_d (Am) for soil-types according to the pH criterion.*

These results denote that the pH criterion was suitable to propose K_d (Am) data for different relevant scenarios, namely because it directly takes into account one of the parameters with greater relevance to the Am sorption in soils, but on the other, they suggest that other factors than pH should be taken into account to efficiently describe the K_d variability in soils at basic pH conditions.

Application of OM and pH factors: the combined OM/pH criterion

From the previous analyses it was evidenced that the solely application of a grouping criterion based either on the soil OM, or pH, successfully decreased the K_d variability. As a further step, a combined grouping criterion taking into account simultaneously the soil OM and pH for Mineral soils (the OM/pH criterion) was applied. So that, the Am dataset, after excluding data gathered from Organic soils (N = 52), was subsequently split according the pH criterion. **Table 4.23** summarises the K_d (Am) data obtained from the CDFs constructed by applying the OM/pH criterion.

Table 4.23 K_d (Am) (L kg^{-1}) for soils grouped according to OM/pH.

Partial dataset	N	Min	Max	GM	5^{th}	95^{th}
Mineral - 3 ≤ pH < 6	20	6.7×10^{1}	4.8×10^{4}	1.7×10^{3}	7.8×10^{1}	3.6×10^{4}
Mineral - 6 ≤ pH < 7.5	13	1.8×10^{2}	7.1×10^{4}	7.3×10^{3}	1.1×10^{3}	4.9×10^{4}
Mineral - 7.5 ≤ pH < 9	19	1.3×10^{3}	1.8×10^{5}	2.0×10^{4}	1.4×10^{3}	2.7×10^{5}
Mineral - pH ≥ 9*	8	2.7×10^{1}	2.8×10^{5}	5.9×10^{2}	7.1	4.8×10^{4}

The application of the OM/pH criterion led to Mineral - pH partial datasets that did not significantly differ ($p > 0.05$) from the respective pH partial datasets including Organic soils data, which confirms the key role of the pH factor in the Am sorption in soils, albeit slightly more contrasting K_d (Am) CDFs were evidenced as can be seen from the 5^{th}-95^{th} percentile region of the CDFs that totally did not overlap among them (see **Figure 4.19,** below).

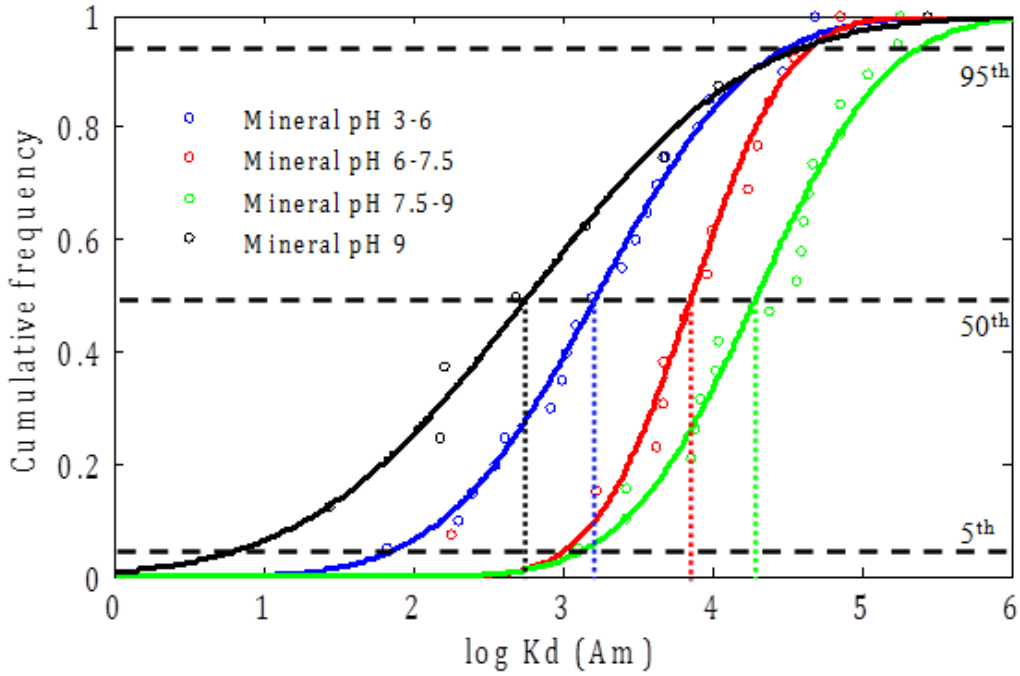

Figure 4.19 *CDFs of K_d (Am) for soil-types according to OM/pH.*

Concerning the K_d variability, it can be said that the inclusion of the OM factor did not lead to an improvement for Mineral soils in terms of variability reduction. However, the K_d (Am) CDF for the redefined Organic group (OM ≥ 8%) created solely on the basis of OM was constructed from a dataset with extreme low data variability. Therefore, the proposal of K_d (Am) CDFs on the basis of both OM and pH is preferred so as to allow, at least, assessing with less uncertainty the Am interaction in organic soils.

The OM/pH/Texture criterion

Although for mineral soils, pH was a key factor to describe and decrease the K_d (Am) variability, it was also evidenced that for mineral soils different values of GM K_d (Am) and CDFs can be proposed depending on their texture (as proven in the redefined Texture/OM criterion section). Thus, a final attempt was made to propose more suitable K_d (Am) data by analysing the simultaneous use of all the previously examined factors (OM, pH and Texture) for K_d (Am) grouping. **Table 4.24** summarises the K_d (Am) data obtained by applying the OM/pH/Texture criterion.

Table 4.24 K_d (Am) (L kg^{-1}) for mineral soils (OM ≤ 8%) grouped according to the OM/pH/Texture criterion.

Partial datasets		N	Min	Max	GM	5th	95th
	Clay	n.a.	n.a.	n.a.	n.a.	n.a.	n.a.
3 ≤ pH < 6	Loam	13	2.0×10^{2}	4.8×10^{4}	2.2×10^{3}	6.6×10^{1}	7.5×10^{4}
	Sand*	6	6.7×10^{1}	4.8×10^{3}	1.3×10^{3}	n.a.	n.a.
	Clay	n.a.	n.a.	n.a.	n.a.	n.a.	n.a.
6 ≤ pH <7.5	Loam	10	1.7×10^{3}	7.1×10^{4}	1.0×10^{4}	2.1×10^{3}	5.3×10^{4}
	Sand*	3	1.8×10^{2}	6.5×10^{3}	1.7×10^{3}	n.a.	n.a.
	Clay*	2	7.1×10^{4}	7.2×10^{4}	7.2×10^{4}	n.a.	n.a.
7.5 ≤ pH < 9	Loam	13	2.7×10^{3}	1.8×10^{5}	2.2×10^{4}	1.9×10^{3}	2.6×10^{5}
	Sand*	4	1.3×10^{2}	3.7×10^{4}	7.2×10^{3}	n.a.	n.a.

*CDF not constructed due to lack of K_d (Am) data (N << 10).

As expected from the analyses previously performed, most of the created pH-Textural partial datasets generally did contain neither enough data (N << 10) to construct CDFs, nor even a single entry was available. Only the pH - Loam datasets had sufficient data to reliably construct a CDF. This fact denotes that it is required the inclusion of analogue data in order to properly evaluate this approach. Analogue data may be gathered either from other solid materials homologous to soils or from other elements demonstrated in chapter 3 to be Am chemical analogues, *i.e.*, Ac(III) and Ln(III)), to fill the gaps and increase the relative number of entries at each dataset.

4.3.4.4 Exploring K_d data potentially analogous to soil K_d (Am) data: consideration of Am chemical analogues and environmental solid materials homologous to soils

All entries available in the updated soil K_d compilation corresponding to K_d (Am) data gathered from environmental solid materials other than soils (subsoils and surface sediments) lacked of the soil characterisation required to be used for enhancing the pH-Textural partial datasets and, thus, these type of data were not considered in the present analysis. Conversely, K_d data of La, Sm, Eu, Gd, Er, Lu and Cm, *i.e.*, Ln(III) and Ac(III) elements analogous to Am with regards to the soil interaction, gathered both

from soils and other environmental solid materials (gyttjas, tills and subsoils) were considered to check their analogy with soil K_d (Am) data.

All the available K_d data for Ln(III) and Ac(III) elements other than Am were pooled to create a common dataset (K_d (Analogue) dataset) and it was split into partial datasets on the basis of the environmental material they were quantified (soil, till and gyttja). Subsequently, each material partial dataset was refined and grouped according to the OM/pH criterion in order to create partial datasets that could be straightforwardly compared with the respective ones of soil K_d (Am) data. **Table 4.25** summarises the K_d (Analogue) data derived from each material - OM/pH group combination.

Table 4.25 K_d (Analogue) data from soils and other materials (L kg^{-1}) grouped according to the OM/pH criterion.

Material	Partial dataset	N	GM	5th	95th
Soil	Organic (OM ≥ 8%)	56	5.6×10^{3}	9.7×10^{2}	3.2×10^{4}
	Mineral (OM < 8%)	33	1.4×10^{4}	1.1×10^{3}	1.7×10^{5}
	Mineral - 3 ≤ pH < 6*	7	6.2×10^{3}	n.a.	n.a.
	Mineral - 6 ≤ pH < 7.5	12	9.0×10^{3}	1.9×10^{3}	4.2×10^{4}
	Mineral - 7.5 ≤ pH < 9	14	3.1×10^{4}	2.6×10^{3}	3.8×10^{5}
Till	Mineral (OM < 8%)	22	1.3×10^{4}	6.4×10^{2}	6.1×10^{4}
	Mineral - 3 ≤ pH < 6	11	3.6×10^{3}	2.1×10^{2}	6.1×10^{4}
	Mineral - 6 ≤ pH < 7.5*	6	2.1×10^{4}	n.a.	n.a.
	Mineral - 7.5 ≤ pH < 9*	5	5.0×10^{4}	n.a.	n.a.
Gyttja	Organic (OM ≥ 8%)	24	2.6×10^{3}	8.9×10^{2}	7.8×10^{3}

*K_d (Analogue) OM/pH partial dataset with sufficient entries to be statistically compared with the respective soil K_d (Am) partial dataset.

The statistical tests revealed that soil K_d (Am) data for the OM/pH groups did not significantly differ ($p > 0.05$) from those of the different combinations of analogue elements and materials. Besides this, the K_d (Analogue) GMs, as well as the 5th-95th percentile ranges of the CDFs that could be constructed, followed the same trend and were very similar to those derived from the corresponding soil K_d (Am) CDFs (compare with data in previous **Table 4.23**). Provided that the analogy between K_d (Analogue) data and soil K_d (Am) data was demonstrated, it was deemed all these data to be suitable for enhancing soil K_d (Am) partial datasets. According to this, all

the available K_d (Am) data and the K_d (Analogue) data were pooled in the same dataset and the OM/pH/Texture criterion was applied to split it. **Table 4.26** summarises the K_d data derived from the partial datasets created on the basis of the OM/pH/Texture criterion.

Table 4.26 K_d (Am+Analogue) (L kg^{-1}) for mineral samples grouped according to the OM/pH/Texture criterion.

Partial datasets		N	Min	Max	GM	5th	95th
	Clay*	-	-	-	-	-	-
3 ≤ pH < 6	Loam	23	2.0×10^{2}	8.0×10^{4}	6.1×10^{3}	2.2×10^{2}	1.7×10^{5}
	Sand	14	6.7×10^{1}	4.8×10^{3}	1.6×10^{3}	7.4×10^{2}	3.5×10^{3}
	Clay*	1	-	-	4.0×10^{4}	-	-
6 ≤ pH < 7.5	Loam	23	1.7×10^{3}	7.1×10^{4}	1.5×10^{4}	3.7×10^{3}	5.8×10^{4}
	Sand**	7	1.8×10^{2}	6.5×10^{3}	2.0×10^{3}	1.4×10^{2}	3.0×10^{4}
	Clay**	9	4.5×10^{3}	1.2×10^{5}	6.7×10^{4}	3.2×10^{4}	1.4×10^{5}
7.5 ≤ pH < 9	Loam	25	2.7×10^{3}	2.6×10^{5}	2.7×10^{4}	2.9×10^{3}	2.5×10^{5}
	Sand*	4	1.3×10^{3}	3.7×10^{4}	7.2×10^{3}	-	-

*CDF not constructed due to lack of K_d (Am) data (N << 10).
** K_d (Am) data derived from a CDF constructed with a dataset containing scarce data (N < 10).

The inclusion of K_d (Analogue) data succeeded in enhancing some of the pH - Textural partial datasets. However, alike the case of U, there were some data gaps for certain pH - Textural combinations (*i.e.*, 3 ≤ pH < 6 - Clay; 6 ≤ pH < 7.5 - Clay and 7.5 ≤ pH < 9 - Sand partial datasets), which hinder the proper evaluation of the combined use of the pH, OM and Texture groups to efficiently group K_d (Am) data. When the pH - Textural partial datasets were compared with the respective Mineral - pH ones of soil K_d (Am) data (see **Table 4.23**), only the 3 ≤ pH < 6 - Sand and the 7.5 ≤ pH < 9 - Clay partial datasets were significantly different ($p < 0.05$). The K_d variability in these pH - Textural groups (one-to-two orders of magnitude) was much less than in the previous Mineral-pH partial datasets. Such results suggest that the texture factor in conjunction with pH and OM may be only relevant to propose probabilistic K_d (Am) data in soils whose texture corresponds to really high or low clay content, and thus, with remarkably high or low SSA, respectively.

4.3.4.5 Key messages from the analyses of the K_d (Am) dataset and summary of CDFs of K_d (Am) for radiological assessments

The K_d (Am) values in soils in the current compilation varied within more than 4 orders of magnitude namely as a consequence of the contrasting properties of the soils. From the analyses performed here it has been demonstrated that when soils are grouped on the basis of soil properties relevant to the Am sorption in soils, statistically different probabilistic K_d (Am) data are obtained for different soil-types, and generally, with much less uncertainty than when soils are considered all together. Therefore, to perform radiological assessments related to soils contaminated with Am it is not recommended the use of a single K_d (Am) best estimate or CDF since it may be not representative of numerous scenarios. Instead of this, the CDFs summarised in **Table 4.27** are proposed so as to provide end-users with different alternatives.

The organic matter content was found to be one of the properties affecting the most the K_d (Am) data, up to the point that those soils containing OM ≥ 8% (organic soils) are distinguished only according to OM and, thus, a single CDF (Organic) is proposed for this type of soils. On the other hand, for those soils containing OM < 8% (Mineral) it was crucial to take into account the pH at which the Am sorption occurs, and to a lesser extent, the soil texture. Currently, only pH - Textural CDFs for loamy soils could be constructed from the soil K_d (Am) compilation, due to the lack of data for other soil textures. For those pH and texture combinations missing of CDF the respective Mineral - pH CDFs are proposed.

In this context, K_d data available of Am chemical analogues gathered from soils and solid materials homologous to soils were successfully used to fill some of the K_d (Am) data gaps, which allowed to propose CDFs for other pH and soil texture combinations. However, there are still scarce K_d data of Am (or chemical analogues) gathered from materials with OM < 8%, in particular from those with clayey and sandy texture determined at acid and basic pHs, respectively. Besides, it was found that the Texture factor do not allow obtaining more specific K_d (Am) data when dealing with loamy soils.

Table 4.27 K_d (Am) CDFs for specific soil-types according to soil ancillary data available.

Which information is available?	Soil-types of K_d (Am)	Proposed CDF	GM (L kg^{-1})	5th (L kg^{-1})	95th (L kg^{-1})
None	All	logN (μ: 3.6; σ: 0.8)	4.2×10^{3}	1.7×10^{2}	1.1×10^{5}
OM%	Organic[a]	logN (μ: 3.7; σ: 0.4)	4.5×10^{3}	1.1×10^{3}	1.8×10^{4}
	Mineral[b]	logN (μ: 4.1; σ: 0.7)	1.1×10^{4}	7.6×10^{2}	2.0×10^{5}
OM%; Texture	Loam[c]	logN (μ: 4.2; σ: 0.6)	1.7×10^{4}	1.9×10^{3}	1.6×10^{5}
	Sand[d]	logN (μ: 3.6; σ: 0.5)	3.8×10^{3}	5.4×10^{2}	2.0×10^{4}
pH	3 ≤ pH < 6	logN (μ: 3.3; σ: 0.6)	2.2×10^{3}	2.3×10^{2}	2.2×10^{4}
	6 ≤ pH <7.5	logN (μ: 3.9; σ: 0.4)	6.6×10^{3}	1.3×10^{3}	3.2×10^{4}
	7.5 ≤ pH < 9	logN (μ: 4.3; σ: 0.8)	1.4×10^{4}	7.5×10^{2}	2.6×10^{5}
	pH ≥ 9*	logN (μ: 2.7; σ: 1.0)	5.4×10^{2}	1.0×10^{1}	2.9×10^{4}
OM%; pH	Mineral - 3 ≤ pH < 6	logN (μ: 3.2; σ: 0.8)	1.7×10^{3}	7.8×10^{1}	3.6×10^{4}
	Mineral - 6 ≤ pH <7.5	logN (μ: 3.9; σ: 0.5)	7.3×10^{3}	1.1×10^{3}	4.9×10^{4}
	Mineral - 7.5 ≤ pH < 9	logN (μ: 4.3; σ: 0.7)	2.0×10^{4}	1.4×10^{3}	2.7×10^{5}
	Mineral - pH ≥ 9	logN (μ: 2.8; σ: 1.2)	5.9×10^{2}	7.0	4.8×10^{4}
	Sand - 3 ≤ pH < 6	logN (μ: 3.2; σ: 0.2)	1.6×10^{3}	7.4×10^{2}	3.5×10^{3}
	Clay[e,*] - 7.5 ≤ pH < 9	logN (μ: 4.8; σ: 0.2)	6.7×10^{4}	3.2×10^{4}	1.4×10^{5}

*CDF constructed with a dataset containing scarce data (N < 10).
[a]Organic: OM ≥ 8%.
[b]Mineral: OM < 8%
[c]Loam: OM content < 8%; mineral fraction with clay content within 18-35%, or with < 18% clay and < 65% sand contents.
[d] Sand: OM content < 8%; mineral fraction with < 18% of clay and > 65% of sand contents.
[e] Clay: OM content < 8%; mineral fraction with clay content > 35%.

When neither soil OM nor texture data are available, the CDFs constructed solely on the basis of pH should be considered, whereas when soil OM and texture data are available, but pH is missing, the Texture CDFs (Organic, Loam or Sand CDFs) can be used to foresee the interaction of Am in soils. Notice that for the particular case of dealing with an assessment in a clayey soil and missing pH data, only the more general Mineral CDF can be used since no Clay CDF could be proposed due to a lack of data. It is worth noting that since Texture CDFs do not capture the effect of pH on K_d (Am) data, these CDFs are appropriate just to perform screening exercises rather than specific radiological assessments.

Moreover, all the above mentioned K_d (Am) CDFs were constructed from K_d datasets containing K_d (Am) values that were quantified by applying sorption and desorption experiments (either spiked or from recent-contaminated soil samples) representative of short-term sorption. Consequently, strictly speaking these CDFs may be only applied to assess the short-term interaction of this element in soils since the effect of sorption dynamics on the K_d (Am) values could not be evaluated. Despite this fact, it is well known that Am sorption in soils, alike those of other trivalent lanthanides in mineral matrices, is highly irreversible (see section 3.3.1) and thus, it is expected that the sorption dynamic effects in the Am-soil interaction may be negligible.

Finally, it is important to point out that from the analysis performed it was demonstrated the suitability of interchangeably using soil, subsoil and till K_d data of any Ac(III) (*e.g.,* Ac or Cm) and Ln(III) (*e.g.,* La, Eu, Gd or Lu) to foresee the interaction in soils of Am. Thus, by the same token, the CDFs proposed here for Am can be applied not only in radiological assessments concerning this element but also for contamination episodes involving any of the solid materials and/or elements aforementioned.

4.4 REFERENCES

Absalom, J.P., Young, S.D., Crout, N.M., 1995. Radio-caesium fixation dynamics: measurement in six Cumbrian soils. Eur. J. Soil Sci. 46, 461-469.

AECL, 1990. AECL 10125 A critical compilation and review of default soil solid/liquid partition coefficients, Kd, for use in environmental assessments. Atomic Energy of Canada Limited, Canada.

Ciffroy, P., Durrieu, G., Garnier, J. M., 2009. Probabilistic distribution coefficients (Kds) in freshwater for radioisotopes of Ag, Am, Ba, Be, Ce, Co, Cs, I, Mn, Pu Ra, Ru, Sb, Sr and Th. Implications for uncertainty analysis of models simulating the transport of radionuclides in rivers, J. Environ. Radioact. 100, 785-794.

Choppin, G.R., 2007. Actinide speciation in the environment. J. Radioanal. Nucl. Ch. 273 (3), 695-703.

Comans, R.N., Middelburg, J.J., Zonderhuis, J., Woittiez, J.R., De Lange, G.J., Das, H.A., Van der Weijden, C.H., 1989. Mobilization of radiocesium in pore water of lake sediments. Nature 339, 367-369.

Cotton, F.A., Wilkinson, G., 1986. Química inorgánica avanzada, fourth ed. Limusa, Mexico.

Crançon, P., Van der Lee, J., 2003. Speciation and mobility of uranium (VI) in humic-contain soils. Radiochim. Acta, 91 (11), 673–679.

Cremers, A., Elsen, A., De Preter, P., Maes, A., 1988. Quantitative analysis of radiocesium retention in soils. Nature 335, 247-249.

Cremers, A., Elsen, A., Valcke, E., Wauters, J., Sandalls, F.J., Gaudern, S.L., 1990. In: Transfer of radionuclides in natural and semi-natural environments, Desmet, G., Nassibeni, P., Belli, M. Eds. Elsevier Applied Science Publishers, London and New York, pp. 238-248.

Dalvi A.A., Kumar A.V., Reddy V.R. 2014. A site specific study on the measurement of sorption coefficients for radionuclides. Int. J. Environ. Sci. Technol. 11, 617-622.

Duff, M.C., Amrhein, C., 1996. U(VI) sorption on goethite and soil in carbonate solutions. Soil Sci. Soc. Am. J. 60, 1393–1400.

Echevarria, G., Sheppard, M., Morel, J.L., 2001. Effect of pH on the sorption of uranium in soils. J. Environ. Radioactiv. 53, 257–264.

EPA, 1999. EPA 402-R-99-004B Understanding Variation in Partitioning Coefficients, Kd, Values: Volume II: Review of Geochemistry and Available Kd Values for Cadmium, Caesium, Chromium, Lead, Plutonium, Radon, Strontium, Thorium, Tritium and Uranium. Environmental Protection Agency, USA.

Gil-García, C. J. , Rigol, A., Vidal, M., 2011. Comparison of mechanistic and PLS-based regression models to predict radiocaesium distribution coefficients in soils. J. Hazard. Mat. 197, 11– 18.

Hsi, C.K.D., Langmuir, D., 1985. Adsorption of uranyl onto ferric oxy-hydroxides: application of the surface complexation site-binding model. Geochim. Cosmochim. Acta 49, 1931–1941.

IAEA, 1994. TRS-364 Handbook of Parameter Values for the Prediction of Radionuclide Transfer in Temperate Environments, International Atomic Energy Agency, Austria .

IAEA, 2009. TECDOC-1616 Quantification of radionuclide transfer in terrestrial and freshwater environments for radiological assessments. International Atomic Energy Agency, Austria.

IAEA, 2010. TRS-472 Handbook of Parameter Values for the Prediction of Radionuclide Transfer in Terrestrial and Freshwater Environments. International Atomic Energy Agency, Austria.

ICRP, 2008. ICRP Publication 107 Nuclear Decay Data for Dosimetric Calculations. Ann. ICRP 38 (3).

Langmuir, D., 1978. Uranium solution–mineral equilibria at low temperature with applications to sedimentary ore deposits. Geochim. Cosmochim. Acta 42, 547–569.

Matus, F., Rumpel, C., Neculman, R., Panichini, M., Mora, M.L., 2014. Soil carbon storage and stabilisation in andic soils: a review, Catena 120 102–110.

Nakao, A., Takeda, A., Ogasawara, S., Yanai, J., Ito, T., 2015. Relationship between paddy soil Radiocesium Interception Potentials and physicochemical properties in Fukushima, Japan. J. Environ. Qual. 44, 780-788.

Payne, T.E., Davis, J.A., Waite, T.D., 1996. U sorption on ferrihydrite – effects of phosphate and humic acid. Radiochim. Acta 74, 239–243.

Payne, T.E., Brendler, V., Comarmond, M.J., Nebelung, C., 2011. Assessment of surface area normalisation for interpreting distribution coefficients (Kd) for uranium sorption. J. Environ. Radioactiv. 102, 888-895.

POSIVA, 2014. Working Report 2013-66: Geochemical and physical properties, distribution coefficients of soils and sediments at the Olkiluoto Island and in the reference area in 2010-2011. POSIVA, Finland.

Rigol, A., Vidal, M., Rauret, G., 1998. Competition of organic and mineral phases in radiocesium partitioning in organic soils of Scotland and the area near Chernobyl. Environ. Sci. Technol. 32, 663-669.

Rigol, A., Vidal., M., Rauret, G., 2002. An overview of the effect of organic matter on soil-radiocaesium interaction: implications in root uptake. J. Environ. Radioactiv. 58, 191-216.

Roig, M., Vidal, M., Rauret, G., Rigol, A., 2007. Prediction of radionuclide aging in soils from the Chernobyl and Mediterranean areas. J. Environ. Qual. 36, 943-952.

Sheppard, M.I., Thibault, D.H., 1990. Default soil solid/liquid partition coefficients, Kds, for four major soil types: a compendium. Health Phys. 59, 471.

Sheppard, S.C., Sheppard, M.I., Tait, J.C., Sanipelli, B.L., 2006. Revision and metaanalysis of selected biosphere parameter values for chlorine, iodine, neptunium, radium, radon and uranium. J. Environ. Radioactiv. 89, 115–137.

Sheppard, S.C., 2011. Robust Prediction of Kd from Soil Properties for Environmental Assessment. Hum. Ecol. Risk Assess. 17(1), 263-279.

SKB, 2011. R-11-24 Solid/liquid partition coefficients (Kd) and plant/soil concentration ratios (CR) for selected soils, tills and sediments at Forsmark. Svensk Kämbränslehantering AB-Swedish Nuclear Fuel and Waste Management Co, Sweden.

SKB, 2014. TR-14-002 Initial state report for the safety assessment SR-PSU. Svensk Kämbränslehantering AB-Swedish Nuclear Fuel and Waste Management Co, Sweden.

Sowder, A.G., Bertsch, P.M., Morris, P.J., 2003. Partitioning and availability of uranium and nickel in contaminated riparian sediments. J. Environ. Qual. 32, 885–898.

Sweeck, L., Wauters, J., Valcke, E., CRemers, A., 1990. In: Transfer of radionuclides in natural and semi-natural environments, Desmet, G., Nassibeni, P., Belli, M. Eds. Elsevier Applied Science Publishers, London and New York, pp. 249-258.

Uematsu, S., Smolders, E., Sweeck, L., Wannijn, J, Van Hees, M., Vandenhove, H., 2015. Predicting radiocaesium sorption characteristics with soil chemical properties for Japanese soils, Sci. Total Environ. 524-525, 148-156.

Vandebroek, L., Van Hees, M., Delvaux, B., Spaargaren, O., Thiry, Y., 2012. Relevance of Radiocaesium Interception Potential (RIP) on a worldwide scale to assess soil vulnerability to 137Cs contamination. J. Environ. Radioactiv. 102, 87-93.

Vandenhove, H., Van Hees, M.,Wouters, K.,Wannijn, J., 2007. Can we predict uranium bioavailability based on soil parameters? Part 1: Effect of soil parameters on soil solution uranium concentration. Environ. Pollut. 145, 587–595.

Vandenhove, H., Gil-García, C., Rigol, A., Vidal, M. 2009. New best estimates for radionuclide solid-liquid distribution coefficients in soils. Part 2. Naturally occurring radionuclides. J. Environ. Radioactiv. 100, 697-703.

Vidal, M., Roig, M., Rigol, A., Llauradó, M., Rauret, G., Wauters, J., Elsen, A., Cremers, A., 1995. Two approaches to the study of radiocaesium partitioning and mobility in agricultural soils from the Chernobyl area. Analyst 120, 1785-1791.

Waegeneers, N., Smolders, E., Merckx, R., 1999. A statistical approach for estimating the radiocaesium interception potential of soils. J. Environ. Qual. 28, 1005–1011.

Waite, T.D., Davis, J.A., Payne, T.E., Waychunas, G.A., Xu, N., 1994. U(VI) sorption to ferrihydrite: application of the surface complexation model. Geochim. Cosmochim. Acta 58, 5465–5478.

Wauters, J., Elsen, A., Cremers, A., Konoplev, A.V., Bulgakov, A.A., Comans, R.N.J., 1996. Prediction of solid liquid distribution coefficients of radiocaesium in soils and sediments. Part 1: A simplified procedure for the solid characterisation, Appl. Geochem. 11, 589–594.

CHAPTER 5. CONCLUSIONS

Regarding the examination of the main factors controlling the interaction of trivalent actinides and lanthanides in soils, the main conclusions drawn are:

- The systematic determination of sorption and desorption parameters of Am and Sm in a large number of soil samples presenting very contrasting properties has contributed to a deep understanding of the interaction of these two elements in soils.

- The Am and Sm sorption-desorption patterns evidenced that, in general, these elements were highly and very irreversibly sorbed by soils (K_d were always $>10^3$ L kg^{-1} and desorption percentages were always <2%). According to this, in case of soil contamination at radioactive concentration levels, it is expected a remarkably retention of Am and Sm in the soil solid phase, which may reduce their mobility and limit their incorporation into the food chain, thus posing a moderate radiological risk to humans in radioactive exposure scenarios namely involving food ingestion and water consumption pathways.

- The performed statistical analyses succeeded in identifying the key soil characteristics best explaining the variability of K_d values of Am and Sm. These were: pH, dissolved organic carbon, BET (specific surface area), organic carbon and carbonate contents.

- The knowledge gained regarding the Am and Sm interaction in soils permitted to hypothesise that the cationic species of these elements are sorbed by surface complexation reactions involving high-affinity negatively-charged sorption sites. According to this, Am and Sm are sorbed in a greater extent in alkaline soils, since the species of these elements are predominantly cationic at basic pH; in soils with large contents of carbonates, since these minerals present extremely high affinity for Am and Sm; in soils with a high specific surface area, since the pool of sorption sites is increased; and also in soils with a low content of soluble organic compounds, since the formation of stable, non-reactive humate complexes is decreased.

- Parametric K_d models based on multiple linear regressions (MLRs) and partial least square regressions (PLS) are proposed to predict Am and Sm K_d values, based on soil characteristics representative for the hypothesised sorption

mechanisms, with relative low uncertainty. However, MLR-based models are recommended over the PLS-based ones since they require less characterisation data.

- The analogy between the interaction of Am and Sm in soils has been largely demonstrated in the present thesis since, for both elements, similar sorption and desorption K_d data were obtained for the soil set. Moreover, comparable soil characteristics governing their sorption were identified and non-significantly different prediction models were obtained. In light of this, it is assumed that the soil-to-solution partitioning of Ac(III) and Ln(III) might be comparable in a given soil-water system and, thus, in case there is a restriction in accessing to K_d data for a target Ac(III) or Ln(III), K_d data of any Ac(III) and Ln(III) can be used indistinctly to assess the soil interaction of the target element.

- The sorption and desorption data gathered at low concentrations of stable Sm is similar to those of Sm radioisotopes, which evidences that the capacity of soils to retain Sm is comparable in both cases. Consequently, it is demonstrated that the interaction data gathered from the stable Sm would be suitable to assess the risk derived from radioactive releases to the environment involving Sm radioisotopes. This finding might be also extended to radioisotopes of other Ac(III) or Ln(III) relevant to the radioactive waste management and nuclear safety.

- It has been evidenced, from the Sm isotherms, that the capacity of some soils to sorb Sm decreased when increasing Sm concentration, due to the saturation of sites. According to this Ac(III) and Ln(III) radionuclides might be significantly mobile in soil contamination events involving high concentrations of these elements.

- The fractionation experiments of the Sm sorbed in soils at low and high concentrations allowed us to confirm that only those soils presenting a large pool of sorption sites of high-affinity for Sm (*i.e.*, slightly acid peat soils or alkaline soils rich in clay and organic matter content) may present a constant,

high capacity to sorb Sm regardless of the Sm concentration in solution. For the rest of soils, sorption occurs at low-affinity sites at high Sm concentrations.

- According to the latter two conclusions, different sorption isotherms models are proposed to properly foresee the soil interaction of Ac(III) and Ln(III) elements in a wide range of concentrations (up to 10 meq L^{-1}). A linear model is proposed al low Sm concentrations, whereas Langmuir or Freundlich models are required for those soils that undergo saturation of sorption sites at high Sm concentrations.

Regarding the development of a strategy to derive probabilistic K_d data from compilations, with low uncertainty and suitable to perform reliable risk assessments, the following conclusions are drawn:

- A critically reviewed compilation that contains more than 5000 entries of soil K_d and ancillary information for 83 elements is now available. This compilation has enough entries to enable, for the first time, the construction of cumulative distribution functions (CDF) of soil K_d data for the vast majority of radionuclides relevant from the standpoint of radiological protection and/or radioactive waste management. Besides this, the compilation also contains more than 2000 entries of K_d data gathered from solid materials potentially analogous to soils that could be used in case of scarcity of soil K_d data.

- The establishment of a series of acceptance and data treatment criteria guarantees the quality of data and, thus, permits to derive reliable probabilistic K_d data after a proper analysis of the dataset.

- The application of grouping criteria customised on element basis by elucidating relevant soil factors directly or indirectly controlling the target element interaction in soils has been demonstrated to be a suitable strategy to efficiently decrease the K_d variability, in most cases up to a few orders of magnitude, especially when various soil factors are simultaneously taken into consideration to develop grouping criteria either by means of hierarchically applying different soil factors or by simultaneously combining them.

- A given soil factor may be used in a different way to group K_d data depending on the target element and the sorption mechanisms governing its interaction in soils. For instance, pH and OM can be hierarchically applied to obtain pH-Mineral and pH-Organic K_d (U) partial datasets with less variability, since pH is the most relevant parameter controlling U interaction in soils. In contrast, for Am these factors must be combined differently in order to take into account the effect of dissolved organic matter (DOM), which is highly relevant for the Am speciation in solution and interaction with the solid phase.

- Much better probabilistic K_d data can be proposed for Cs when K_d (Cs) values representative of short-term and long-term Cs-soil interaction are treated separately. According to this, it has been demonstrated that the effect of the experimental approach must also be evaluated to ensure the representativeness of the proposed data for different contamination scenarios and, thus, their suitability to properly assess the interaction of a target element. This issue is of paramount importance when dealing with the risk assessment in case of contamination episodes involving radioisotopes of elements that may undergo sorption dynamics processes.

- It is recommended to apply a holistic statistical approach to correctly and individually evaluate all sources of variability. As an example, the strategy based on performing a Group Mean Centring, is required when K_d values can be simultaneously influenced by different sources of variability, such as in the case of K_d (Cs), for which the possible effects on the K_d data variability arisen from the contrasting soil characteristics and those that may result from the different experimental approaches used for the K_d data quantification may simultaneously appear.

- From the analyses of the U and Am datasets it is noticed that there are still evident gaps in K_d values for a few types of soil, despite the significant increase in the number of entries in the updated K_d compilation. This may jeopardise the proper estimation of the soil sorption of these elements in some scenarios since no reliable probabilistic K_d data could be derived. This is the case of soils with a high clay content and, thus, there is a clear need to obtain new experimental K_d values in this type of soil.

- The suitability of using K_d data either gathered from certain solid environmental materials analogous to soils and/or from other chemical analogue elements to enhance those datasets with insufficient data to construct CDFs has been demonstrated for the case of Am and U. Whether it is suitable or not to enhance partial datasets by using analogue K_d data must be always checked by statistically comparing the candidate analogue K_d data with the soil K_d data of the target element.

- In order to assist modelers and end-users in properly selecting the K_d data that fit better with the scenario under assessment, it is necessary not only to make available K_d best estimates or CDFs for the different radionuclides but also to provide enough information about how the K_d values of a target element depend on the soil properties and the characteristics of the contamination scenario. It is also recommended to gather relevant characteristics of both the soils and the type of contamination under study so as to be able to select the most suitable probabilistic K_d data.

- The establishment of grouping criteria on the basis of key factors governing radionuclide interaction to create partial datasets and subsequently derive probabilistic K_d data, represents a relevant and user-friendly strategy to propose input data for risk assessment models with lower uncertainty and more representative for a given contamination event.

ANNEX I: REFERENCES OF LITERATURE USED TO UPDATE THE SOIL K_D (RN) COMPILATION

Bakkaus, E., Collins, R. N., Morel, J. L., Gouget, B., 2008. Potential phytoavailability of anthropogenic cobalt in soils as measured by isotope dilution technique. Sci. Total Environ. 406, 108-115.

Cantrell, K. J., Serne, R. J., Last, G. V., 2003. PNNL-13895 Hanford contaminant distribution coefficient database and users guide. Pacific Northwest National Laboratory, USA.

Chon, J. K., Lee, K-J., Yun, J-I., 2012. Sorption of cobalt (II) on soils:_effects of birnessite and humic acid. J. Radioanal. Nucl. Chem. 293, 511-517.

EPA, 2004. EPA 402-R-04-002C Understanding variation in partition coefficient, Kd, values. Vol III: Review of geochemistry and available Kd values for americium, arsenic, curium, iodine, neptunium, radium and technetium. Environmental Protection Agency, USA.

Grogan, K. P., 2008. MsC Thesis 'Spatial variability of radionuclide distribution coefficients at the Savannah River Site and the sub-surface transport implications'. Clemson University. All Theses. Paper 385, USA.

Grogan, K. P., Fjeld, R. A., Kaplan, D., DeVol T. A., Coates, J. T., 2010. Distributions of radionuclide sorption coefficients (Kd) in sub-surface sediments and the implications for transport calculations. J. Environ. Radioactiv. 101, 847-853.

Hormann, V., Fischer, W., 2013. Estimating the distribution of radionuclides in agricultural soils – Dependence of soil parameters. J. Environ. Radioactiv. 124, 278-286.

Ishikawa, N. K., Uchida, S., Tagami, K., 2009. Estimation of soil-soil solution distribution coefficient of radiostrontium using soil properties. Appl. Radiat. Isotopes 67, 319-323.

Ishikawa, N. K., Uchida, S., Tagami, K., 2011. Iodide sorption and partitioning in solid, liquid and gas phases in soil samples collected from Japanese paddy fields. Radiat. Prot. Dosim. 146 (1), 155-158.

Ishikawa, N. K., Uchida, S., Tagami, K., Satta, N., 2011. Soil solution Ni concentrations over which K_d is constant in Japanese agricultural soils. J. Nucl. Sci. Technol. 48 (3), 337-343.

Ishikawa, N. K., Tagami, K., Uchida, S., 2013. Effect of biological activity due to different temperatures on iodine partitioning in solid, liquid, and gas phases in Japanese agricultural soils. J. Radioanal. Nucl. Chem. 295, 1763-1768.

Kamel, N. H. M., 2010. Adsorption models of ^{137}Cs radionuclide and Sr (II) on some Egyptian soils. J. Environ. Radioactiv. 101, 297-303.

Kaplan, D. I., Millings, M. R., 2006. WSRC-TC-2006-00246 Distribution coefficients for the Vogtle early site permit. Washington Savannah River Company, USA.

Kaplan, D. I., Parker, K. E., Kutynakov, I. V., 1998. PNNL-11966 Radionuclide distribution coefficients for sediments collected from Borehole 299-E17-21: Final Report for subtask 1a. Pacific Northwest National Laboratory, USA.

Kaplan, D. I., Serkiz, S. M., 2000. WSRC-TR-99-00488 In-situ Kd values and geochemical behavior for inorganic and organic constitutents of concern at the TNX Outfall Delta (U). Westinghouse Savannah River Company, USA.

Kaplan, D. I., Serne, R. J., 1995. PNL-10379 Distribution coefficient values describing iodine, neptunium, selenium, technetium, and uranium sorption to Hanford sediments. Pacific Northwest Laboratory, USA.

Kaplan, D. I., Serne, R. J., Owen, A. T., Conca, J., Wietsma, T. W., Gervais T. L., 1996. PNNL-11485 Radionuclide adsorption distribution coefficients measured in Hanford sediments for the low level waste performance assessment project. Pacific Northwest national Laboratory, USA.

Loffredo, N., Mounier, S., Thiry, Y., Coppin, F., 2011. Sorption of selenate on soils and pure phases: kinetic parameters and stabilisation. J. Environ. Radioactiv. 102, 843-851.

Maity, S., Sahu, S. K., Pandit, G. G., 2015. Estimation of distribution coefficient of radium around a uranium mining site. Radioprotection 50 (2), 129-134.

Meier, H., Zimmerhackl, E., Zeitler, G., Menge, P., 1994. Parameter studies of radionuclide sorption in site-specific sediment/groundwater systems. Radiochim. Acta 66/67, 277-284.

Mishra, S., Maity, S., Pandit, G. G., 2012. Estimation of distribution coefficient of natural radionuclides in soil around uranium mines and its effect with ionic strength of water. Radiat. Prot. Dosim. 152 (1-3), 229-233.

Palágyi, S., Vodicková, H., 2009. Sorption and desorption of $^{125}I^{-}$, $^{137}Cs^{+}$, $^{85}Sr^{2+}$ and $^{152+153}Eu^{3+}$ on disturbed soils under dynamic flow and static batch conditions. J. Radioanal. Nucl. Ch. 280 (1), 3-14.

Payne, T.E., Harris, J.R., 2000. Adsorption of Cs and U(VI) on soils of the Australian arid zone. Radiochim. Acta 88, 799-802.

Payne, T. E., Itakura, T., Comarmond, M. J., Harrison, J. J., 2009. Environmental mobility of cobalt - Influence of solid phase characteristics and groundwater chemistry. Appl. Radiat. Isotopes 67, 1269-1276.

Perrier, T., 2004. PhD Thesis 'Étude théorique et expérimentale du comportement biogéochimique de l'Américium-241 en conditions rhizosphériques simplifiées. Application dans un sol agricole calcaire. Université Henri Poincaré Nancy I, France.

Peters, R. W., Shem, L., 1992. Adsorption/desorption characteristics of lead on various types of soil. Environ. Prog. 11 (3), 234-240.

POSIVA, 2013. Working Report 2012-102: Studies on reference mires: 1. Lastensuo and Pesänsuo in 2010-2011. POSIVA, Finland.

POSIVA, 2014. Working Report 2013-66: Geochemical and physical properties, distribution coefficients of soils and sediments at the Olkiluoto Island and in the reference area in 2010-2011. POSIVA, Finland.

POSIVA, 2014. Working Report 2013-68: Distribution coefficients of caesium, chlorine, iodine, niobium, selenium and technetium on Olkiluoto soils. POSIVA, Finland.

Powell, B. A., Lilly, M. A., Miller, T. J., Kaplan, D. I., 2010. SRNL-STI-2010-00527 Iodine, neptunium, radium, and strontium sorption to Savannah River Site sediments. Savannah River National Laboratory, USA.

Ramírez-Guinart, O., Vidal, M., Rigol, A., 2016. Univariate and multivariate analysis to elucidate soil properties governing americium sorption in soils. Geoderma 269, 19-26.

Ramírez-Guinart, O., Rigol, A., Vidal, M., 2017. Assessing soil properties governing radiosamarium sorption in soils: can trivalent lanthanides and actinides be considered as analogues**?** Geoderma 290, 33-39.

Roussel-Debet, S., Colle, C., Hurtevent, P., Morello, M., 2000. Influence d'acides organiques sur la désorption de l'américium 241 et du neptunium 237 à partir d'un sol cultivé acide. Radioprotection 35 (4), 505-518.

Salbu, B., Burkitdaev, M., Stromman, G., Shishkov, I., Kayukov, P., Uralbekov, B., 2013. Environmental impact assessment of radionuclides and trace elements at the Kurday U mining site, Kazakhstan. J. Environ. Radioactiv. 123, 14-27.

Serne, R. J., Conca, J. L., LeGore, V. L., Cantrell, K. J., Lindenmeier, C. W., Campbell, J. A., Amorette, J. E., Wood, M. I., 1993. PNL-8889 Vol.1 Solid-waste leach characteristics and contaminant-sediment interactions. Volume 1: batch leach and adsorption tests and sediment characterisation. Pacific Northwest Laboratory, USA.

Seymour, A. H., Nevissi, A., Schell, W. R., Sanchez, A., 1976. Annual Report NUREG/CR-0801 Distribution coefficient for radionuclides in aquatic environments. I. Development of methods and results for plutonium and americium in fresh and marine water-sediment systems. U.S. Nuclear Regulatory Commission, USA.

SKB, 2009. R-09-27 Solid/liquid partition coefficients (Kd) for selected soils and sediments at Forsmark and Laxemar-Simpevarp. Svensk Kämbränslehantering AB-Swedish Nuclear Fuel and Waste Management Co, Sweden.

SKB, 2010. TR-10-07 Element-specific and constant parameters used for dose calculations in SR-Site. Svensk Kämbränslehantering AB-Swedish Nuclear Fuel and Waste Management Co, Sweden.

SKB, 2011. R-11-24 Solid/liquid partition coefficients (Kd) and plant/soil concentration ratios (CR) for selected soils, tills and sediments at Forsmark. Svensk Kämbränslehantering AB-Swedish Nuclear Fuel and Waste Management Co, Sweden.

Solecki, J., 2005. Investigation of 85Sr adsorption on selected soils of different horizons. J. Environ. Radioactiv. 85, 303-320.

Tserenpil, S., Maslov, O. D., Norov, N., Liu, Q. C., Filipov, M. F., Theng, B. K. G., Belov, A. G., 2013. Chemical and mineralogical composition of the Mongolian rural soils and their uranium sorption behavior. J. Environ. Radioactiv. 118, 105-112.

Twining, J. R., Payne, T. E., Itakura, T., 2004. Soil-water distribution coefficients and plant transfer factors for ^{134}Cs, ^{85}Sr and ^{65}Zn under field conditions in tropical Australia. J. Environ. Radioactiv. 71, 71-87.

Vogler, E., 2008. PhD Thesis term paper 'Biogeochemistry of Radioselenium in soils. Term paper'. Institute of Biogeochemistry and Pollutant Dynamics, ETH Zurich, Switzerland.

Wang, X., Liu, X., 2005. Sorption and desorption of radioselenium on calcareous soil and its solid components studied by batch and column experiments. Appl. Radiat. isotopes 62, 1-9.

Wang, Y. Q., Fan, Q. H., Li, P., Zheng, X. B., Xu, J. Z., Jin, Y. R., Wu, W. S., 2011. The sorption of Eu (III) on calcareous soil: effects of pH, ionic strength, temperature, foreign ions and humic acids. J. Radional. Nucl. Ch. 287, 231-237.

Whicker, J. J., Pinder III, J. E., Ibrahim, S. A., Stone, J. M., Breshears, D. D., Baker, K. N., 2007. Uranium partition coefficient (Kd) in forest surface soil reveal long equilibrium times and vary by site and soil size fraction. Health Physics 93 (1), 36-46.

Zhang, M. I., Ren, A., Shao, D., Wang, X., 2006. Effect of fulvic acid and ionic strength on the sorption of radiostrontium on Chinese calcareous soil and its components. J. Radional. Nucl. Ch. 268, 33-36.

ANNEX II: LIST OF SYMBOLS AND ABBREVIATION

Ac(III): Trivalent actinide elements.

Al_{amorph}: Amorphous aluminium content.

ALARA: As low as reasonably achievable.

BET: Brunauer-Emmett-Teller method.

CDF: Cumulative distribution function.

CEC: Cation exchange capacity.

CIEMAT: *Centro de Investigaciones Energéticas, Medioambientales y Tecnológicas;* Energy, environment and technology research centre.

C_{org}: Organic carbon.

CROM: *Código de cRiba para EvaluaciÓn de IMpacto* (Screening model for environmental assessment*).*

DCAL: Dose and risk calculation model.

DGR: Deep geological repository.

DIC: Dissolved inorganic carbon.

DOC: Dissolved organic carbon.

DOM: Dissolved organic matter.

EMRAS: Environmental Modelling for Radiation Safety.

ERICA: Environmental Risk from Ionising Contaminants: Assessment and Management.

EV: External validation.

Fe_{amorph}: Amorphous iron content.

FES: Frayed edge site.

GM: Geometric mean.

GSD: Geometric standard deviation.

HA: Humic acid.

HLRW: High level radioactive waste.

IAEA: International Atomic Energy Agency.

ICRP: International Commission on Radiological Protection.

ICP-MS: Inductively coupled plasma – mass spectrometry.

ICP-OES: Inductively coupled plasma – optical emission spectrometry.

IRSN: *Institut de Radioprotection et de Sûreté Nucléaire*; French Institute for radioprotection and Nuclear Safety.

K_d: Solid-liquid distribution coefficient.

LET: Linear energy transfer.

LILRW: Low and intermediate level radioactive waste.

Ln(III): Trivalent lanthanide elements.

LOI: Loss on ignition.

LOOCV: Leave-one-out cross-validation.

LSC: Liquid scintillation counting.

LV: Latent variable.

MLR: Multiple linear regression.

Mn_{amorph}: Amorphous manganese content.

MODARIA: Modelling and Data for Radiological Impact Assessments.

OM: Organic matter.

PC: Principal component.

PCA: Principal component analysis.

PDF: Probability density function.

PLS: Partial least square.

RSm: Radiosamarium.

RES: Regular exchange site.

RESRAD: Residual radioactivity materials code.

RIP: Radiocaesium Interception Potential.

RMSECV: Root mean square error in cross-validation.

RMSEP: Root mean square error in prediction.

RN: Radionuclide.

RWMD: Radioactive Waste Management Directorate.

RODOS: Real-Time On-Line Decision Support System for Off-site Emergency Management in Europe.

SKB: *Svensk Kärnbränslehantering AB*; Swedish Nuclear Fuel and Waste Management Company.

SOM: Soil organic matter.

SNF: Spent nuclear fuel.

SSA: Specific surface area.

TENORM: Technologically enhanced naturally occurring radioactive materials.

TRS: Technical report series.

ULR: Univariate linear regression.

UNSCEAR: United Nations Scientific Committee on the Effects of Atomic Radiation.

VIP: Variable importance in projection.

WHAM: Windermere Humic Aqueous Model.

ANNEX III: THESIS SUMMARY IN CATALAN

Atesa la creixent quantitat de residus radioactius generats principalment a conseqüència de la proliferació de la indústria nuclear i atès el potencial risc que poden comportar aquests residus per al medi ambient i la salut humana, l'estimació del risc radiològic que eventualment podria comportar un escenari de contaminació radioactiva ha esdevingut un desafiament científic d'especial interès en l'actualitat. L'estimació del risc radiològic és una tasca complexa que requereix tenir en compte un gran nombre de processos i interaccions que succeeixen entre els diferents compartiments mediambiental i que regeixen el transport dels radionúclids emesos des de la font de contaminació fins a un possible receptor. Quan el medi terrestre es pot veure afectat per un episodi de contaminació radioactiva, un dels processos clau a tenir en compte per tal de poder estimar l'exposició humana a radiacions ionitzants és la predicció de la distribució dels radionúclids emesos entre les fases sòlides i líquides dels sòls contaminats, ja que aquest procés controla, en cert grau, el posterior transport de radionúclids a zones no contaminades adjacents, així com la introducció d'aquestos en la cadena tròfica. Aquest procés de partició és pot estimar a partir del coeficient de distribució sòlid-líquid (K_d) de radionúclids en sòls, el qual pot variar significativament per a un mateix radionúclid depenent les característiques del sòl estudiat. D'acord amb aquests fets, la present tesi s'emmarca en el desenvolupament d'estratègies que permetin derivar valors fiables de K_d de radionúclids en sòls que puguin ser emprats per a la predicció del risc radiològic en cas de contaminació radioactiva**.** Per tal d'assolir aquest objectiu, es van explorar dues estratègies basades en adquirir coneixement sobre la interacció radionúclid-sòl per tal de poder disminuir i descriure la variabilitat intrínseca d'aquest paràmetre.

Per una banda, la present tesi s'ha centrat en l'estudi sistemàtic de la interacció de dos radioelements, l'americi (Am) i el samari (Sm), que representen dues famílies d'elements, actínids trivalents (Ac(III)) i lantànids trivalents (Ln(III)), respectivament, que tot i ser d'especial rellevància en el context de la gestió dels residus radioactius i seguretat nuclear, poc es sap sobre el seu comportament de sorció en sòls. En concret, els esforços es van centrar en:

1. Determinar paràmetres de sorció i desorció de Am i Sm (K_d i percentatges de desorció) en una col·lecció de sòls de característiques edàfiques contrastades

per avaluar les seves capacitats d' incorporar i retenir aquests dos radioelements.

2. Examinar la relació existent entre els comportaments de sorció-desorció observats en els sòls i les seves característiques per tal de comprendre els processos claus que regeixen la interacció Am-sòl i Sm-sòl i identificar aquelles propietats de sòl més rellevants en la sorció d'aquests elements en sòls.
3. Desenvolupar models paramètrics que permetin la predicció de valors de K_d de Am i Sm en sòls a partir de propietats de sòl fàcilment disponibles.
4. Comprovar l'analogia entre Am i Sm respecte a la seva interacció en sòls per tal demostrar que paràmetres de sorció i desorció de qualsevol Ac(III) i Ln(III) es poden emprar indistintament per a estimar la interacció en sòls de qualsevol element d'aquestes dues famílies.
5. Avaluar el comportament de sorció de Sm en sòls en funció de la concentració de Sm en solució mitjançant la construcció d'isotermes de sorció i l'anàlisi del fraccionament de Sm sorbit a través de l'aplicació d'extraccions seqüencials.

Els resultats obtinguts evidencien que la capacitat del sòls per retenir Am i Sm en cas contaminació és generalment molt elevada, atesa la gran sorció i l'alt grau d'irreversibilitat observat en els sòls estudiats. Per tant, la mobilitat d'aquests elements, així com la seva incorporació a la cadena tròfica, serà bastant limitada. De les anàlisis estadístiques realitzades s'ha deduït que la sorció d'aquests dos elements en sòls està governada per múltiples característiques dels sòls, entre les quals les més rellevants són el pH, l'àrea de superfície específica, així com el contingut de matèria orgànica soluble i de carbonats. Totes elles són característiques dels sòls relacionades amb l'especiació d'aquests elements en solució, així com amb l'existència de setis de sorció d'elevada afinitat per aquests elements. També s'ha demostrat que aquestes propietats dels sòls es poden emprar per predir satisfactòriament valors de K_d de Am i Sm en sòls mitjançant models paramètrics basats en regressions múltiples lineals o mínims quadrats parcials. L'alt grau d'analogia entre el comportament de sorció de Am i Sm observat en els sòls estudiats ha permès deduir que en cas de mancança de valors de K_d per a un determinat Ac(III) o Ln(III), la sorció d'aquest en sòls és pot estimar a partir de dades de K_d de qualsevol altre element pertanyent a aquestes famílies d'elements o bé a partir dels models paramètrics de predicció construïts per

Am i Sm. Finalment, dels estudis de sorció de Sm en funció de la seva concentració en solució s'ha demostrat que en escenaris on hi hagi elevades concentracions de Ac(III) o Ln(III), la capacitat per retenir Am i Sm dels sòls es pot veure compromesa. Atesa la existent dependència de la sorció d'aquests elements amb la concentració en solució dels mateixos, s'han construït models basats en isotermes de sorció que permeten predir la interacció de Ac(III) i Ln(III) en sòls en funció de la concentració esperada de Am i Sm en cada escenari de contaminació.

D'altra banda, quan no existeixen dades de K_d específiques d'un l'emplaçament donat o quan es vol abastar un ventall ampli d'escenaris de contaminació possibles, els models d'estimació de risc radiològic acostumen a emprar dades genèriques de K_d en sòls, sovint en forma de funcions de densitat de probabilitat (FDP). Aquest tipus de dades sovint es dedueixen estadísticament de compilacions de dades on els valors de K_d inclosos poden variar molts ordres de magnitud ja que són representatius de molt tipus de sòls. Conseqüentment, aquest tipus de K_d probabilístiques tenen un alt grau de incertesa, el que limita la seva aplicabilitat i idoneïtat per estimar de manera fiable el risc radiològic. Per tal de donar una millor resposta en aquest escenari concret de K_d probabilístiques, en la present tesi s'ha treballat en el desenvolupament d'una estratègia que permeti la derivació d'aquest tipus de dades amb menys incertesa. Per tal d'assolir aquest objectiu va ser necessari:

1. Construir una compilació de dades de RNs en sòls actualitzada i críticament revisada per assegurar la qualitat de les dades incloses en ella.

2. Establir i optimitzar criteris basats en factors clau de la interacció RN-sòl (característiques dels sòls i metodologia emprada en la quantificació de valors de K_d) per tal de seleccionar i agrupar valors de K_d en sets amb menys variabilitat.

3. Comprovar la viabilitat d'emprar valors de K_d determinats en matrius mediambientals anàlogues als sòls, així com de anàlegs químics d'un element d'interès donat per augmentar el nombre de dades en certs sets de dades i per tant, per poder deduir K_d probabilístiques de més qualitat.

Fruit del treball realitzat, actualment es disposa d'una compilació de K_d de radionúclids en sòls i informació auxiliar (relativa a la caracterització dels sòls i de la

metodologia emprada per obtenir els valors de K_d) que conté més de 5000 entrades per 83 elements diferents, així com entrades 2000 extres corresponents a altres matrius sòlides potencialment anàlogues als sòls. Les dades incloses en la compilació fan possible que per primera vegada es pugui derivar una FDP per a la gran majoria de radioelements considerats prioritaris des de el punt de vista de protecció radiològica i de gestió de residus radioactius. L'anàlisi dels sets de dades de tres radionúclids rellevants en el camp de la radioecologia (Cs, U i Am) ha permès demostrar que l'aplicació de criteris d'agrupament de dades basats en la interacció específica del radionúclid estudiat permet disminuir diversos ordres de magnitud la variabilitat intrínseca dels valors de K_d i, per tant, proposar millors K_d probabilístics. Resultats especialment satisfactoris es van obtenir quan diversos criteris es van aplicar jeràrquicament o quan diverses característiques del sòls es van emprar per definir els criteris d'agrupament. Un altre factor rellevant, especialment quan K_d probabilístiques es volen derivar per elements que presenten una sorció en sòls depenent del temps (dinàmiques de sorció), és l'agrupament de valors de K_d d'acord a l'aproximació de laboratori emprat per tal de poder proposar diferent valors de K_d en funció de si es vol predir la interacció a curt o a llarg termini. Un altre tret important és el fet que es va demostrar la idoneïtat d'emprar valors de K_d determinats en matrius ambientals similars als sòls, tals com sediments o subsòls, per augmentar les entrades en certs sets de dades. També s'ha pogut comprovar que valors de K_d probabilístics derivats per certs elements, tals com Am, es poden emprar per estimar la interacció de famílies d'elements (Ac(III) i Ln(III)). D'acord als resultats satisfactoris obtinguts pels tres casos estudiats (Cs, U i Am), es pot dir que l'estratègia basada en l'establiment de criteris d'agrupament de valors de K_d, definits en base al coneixement de les propietats de sòls que governen la interacció específica de radionúclids en sòls, per tal de crear set de dades parcials amb molta menys variabilitat i la posterior construcció de funcions de densitat de probabilitat de valors de K_d per diferents tipus de sòls i escenaris de contaminació, presenta un clara millora en la proposta de valors de K_d probabilístics, ja que poden ser emprats per estimar amb menys incertesa el risc radiològic derivat de diversos episodis de contaminació radioactiva.